WRPS-66073
Revision 0

FY2020 Long-Term PCT of ILAW Glasses

Final Report VSL-20R4820-1, Rev. 0, 09/30/2020

Prepared for the U.S. Department of Energy
Assistant Secretary for Environmental Management

Contractor for the U.S. Department of Energy
Office of River Protection under Contract DE-AC27-08RV14800

P.O. Box 850
Richland, Washington 99352

FY2020 Long-Term PCT of ILAW Glasses

Final Report VSL-20R4820-1, Rev. 0, 09/30/2020

I. L. Pegg
The Catholic University of America

I. S. Muller
The Catholic University of America

R. S. Skeen
Washington River Protection Solutions

Date Published
February 2021

Department of Energy

Prepared for the U.S. Department of Energy
Assistant Secretary for Environmental Management

Contractor for the U.S. Department of Energy
Office of River Protection under Contract DE-AC27-08RV14800

washingtonriver protectionsolutions
P.O. Box 850
Richland, Washington 99352

APPROVED
By Lynn M Ayers at 12:41 pm, May 25, 2021

Release Approval Date

VSL-20R4820-1

Final Report

FY2020 Long-Term PCT of ILAW Glasses

prepared by

Isabelle S. Muller and Ian L. Pegg

Vitreous State Laboratory
The Catholic University of America
Washington, DC 20064

for

Atkins Energy Federal EPC, Inc.
Columbia, MD 21046

and

Washington River Protection *Solutions*, LLC
Richland, WA

August 4, 2020

Rev. 0, 9/30/20

Completeness of Testing:

This report describes the results of work and testing specified by WRPS. The work and any associated testing followed established quality assurance requirements. The descriptions provided in this test report are an accurate account of both the conduct of the work and the data collected. Results required by the test program are reported. Also reported are any unusual or anomalous occurrences that are different from the starting hypotheses. The test results and this report have been reviewed and verified.

I. L. Pegg: _____ **Date:** 9/30/20
VSL Program Director/Principal Investigator

I. Joseph: Innocent Joseph **Date:** 9/30/2020
Atkins Sub-Contract Manager

TABLE OF CONTENTS

List of Tables

List of Figures

List of Abbreviations

ANL-LRM	Argonne National Laboratory – Low-Activity Waste Reference Material
ASME	American Society of Mechanical Engineers
ASTM	ASTM International (formerly the American Society for Testing and Materials)
CCC	Canister Centerline Cooling
CERCLA	Comprehensive Environmental Response, Compensation, and Liability Act
C-S-H	Calcium Silicate Hydrate
CUA	The Catholic University of America
DCP-AES	Direct Current Plasma Atomic Emission Spectroscopy
DOE	Department of Energy
EDS	Energy Dispersive X-Ray Spectroscopy
HLW	High Level Waste
IDF	Integrated Disposal Facility
ILAW	Immobilized Low Activity Waste
IHLW	Immobilized High Level Waste
LAW	Low Activity Waste
LFRG	Low Level Waste Disposal Facility Federal Review Group
ORP	Office of River Protection
PCT	Product Consistency Test
PA	Performance Assessment
PFT	Pulsed Flow Test
PNNL	Pacific Northwest National Laboratory
PUF	Pressurized Unsaturated Flow Test
NIST	National Institute of Standards and Technology
NQA	Nuclear Quality Assurance
QA	Quality Assurance
QAPP	Quality Assurance Project Plan
QARD	Quality Assurance Requirements and Description
RCRA	Resource Conservation and Recovery Act
ROD	Record of Decision
RSD	Relative Standard Deviation
S/V	Surface to Volume Ratio
SEM	Scanning Electron Microscopy
SPFT	Single-Pass Flow-Through (Test)
TC&WM EIS	Tank Closure & Waste Management Environmental Impact Statement
TST	Transition State Theory
VHT	Vapor Hydration Test
VSL	Vitreous State Laboratory
WRPS	Washington River Protection *Solutions*, LLC
WTP	Hanford Tank Waste Treatment and Immobilization Plant
XRD	X-Ray Diffraction
XRF	X-Ray Fluorescence Spectroscopy

SECTION 1.0
INTRODUCTION

1.1 Background

About 50 million gallons of high-level mixed waste is currently stored in underground tanks at The United States Department of Energy's (DOE's) Hanford site in the State of Washington. The Hanford Tank Waste Treatment and Immobilization Plant (WTP) will provide DOE's Office of River Protection (ORP) with a means of treating this waste by vitrification for subsequent disposal. The tank waste will be separated into low- and high-activity waste fractions, which will then be vitrified respectively into Immobilized Low Activity Waste (ILAW) and Immobilized High Level Waste (IHLW) products. The ILAW product will be disposed in a near-surface engineered facility – the Integrated Disposal Facility (IDF) – on the Hanford site, while the IHLW product is designed for deep geological disposal in a national facility for high-level nuclear waste. The ILAW and IHLW products must meet a variety of requirements with respect to protection of the environment before they can be accepted for disposal. The objective of the work described in this report is to perform testing, data collection, and analyses for the ILAW glass product for subsequent use in the performance assessment (PA) of the IDF to assess potential environmental risks associated with long-term storage.

The Record of Decision (ROD) from the Tank Closure & Waste Management Environmental Impact Statement (TC&WM EIS) establishes the current waste streams to be disposed of at the IDF to be located in the 200 East Area which include ILAW, secondary waste associated with ILAW production, and other on-site Hanford Non-Comprehensive Environmental Response, Compensation, and Liability Act (CERCLA) waste. In accordance with the DOE order on radioactive waste management (DOE Order 435.1), the IDF PA is intended to analyze the long-term impacts on human health and the environment of the disposition of waste placed into the facility. Evaluation of the impact of disposed waste requires the ability to predict the long-term release of key radionuclides from the engineered system. In the case of IDF, the engineered system includes a number of components including the proposed Resource Conservation and Recovery Act (RCRA) cap, back fill material, ILAW glass, leachate collection system, and the like.

Since 1998, the IDF PA (formerly the ILAW PA) has been supported by a PA maintenance plan focused on collecting the critical data needed to predict long-term performance: site geology, recharge, hydrology, geochemistry (measurement of site specific K_d values for key contaminants of concern), and waste form release. The purpose of the PA maintenance plan is to allow PA revisions to reflect new scientific information that reduces the technical uncertainty associated with critical aspects of the PA. Although many of the components contained in the engineered system, and addressed in previous IDF Pas, are important in minimizing radionuclide release, arguably one of the most important aspects of the engineered system is the long-term performance of the ILAW glass. The ILAW glass serves as a primary barrier that controls radionuclide release and the glass is expected to have the highest inventories of radionuclides that pose the greatest

potential impact, such as Tc-99 and I-129. Therefore, developing robust, scientifically defensible predictions of long-term glass performance for the IDF PA is critical. The technical approach that is currently used to predict long-term release from ILAW glass for the IDF PA previously gained acceptance from the Low-Level Waste Disposal Facility Federal Review Group (LFRG) and the international community evaluating the long-term corrosion of waste glasses [1-8]. It was also peer reviewed and approved by a panel of independent experts during development of the 1998 IDF PA.

In the early IDF PAs, three prototypic glasses that spanned the range of glass compositions expected to be produced by the WTP (LAWA44, LAWB45, and LAWC22) were selected based upon specific processing constraints and composition projections that were current at the time [7]. However, subsequent work has expanded the range of glass compositions that may be produced at the WTP and this type of composition range expansion is likely to continue through the life of the project. Thus, while the basic technical approach is well developed, there is a need to expand the range of glasses tested in order to span the composition range expected to be disposed in the IDF and to develop an understanding of the dependence of the underlying model parameters and reaction network on the ILAW glass composition. Washington River Protection *Solutions*, LLC (WRPS) is leading the work to address this need and contracted with Atkins and the Vitreous State Laboratory (VSL) of The Catholic University of America (CUA) to provide scientific and technical support. The work initiated in 2010 includes long-term Product Consistency Tests (PCT-Bs[1]) and Single Pass Flow Through (SPFT) tests. Many of the long-term PCTs started in prior years are on-going, with periodic sampling and analysis of the leachates to collect longer-term leach data. Continued sampling and analysis of on-going long-term PCTs were part of the FY2020 work scope for WRPS [9]. The present report provides results from that work, started in FY2018 according to a Test Plan [10] that was responsive to the corresponding FY2018 WRPS scope of work [11], and continued in FY2019 and FY2020. An overarching objective of the present work was to review the accumulated data and perform additional analyses on selected ongoing tests in order to characterize the secondary phases that have formed.

1.2 ILAW Release Approach for the IDF PA

The technical approach that is currently used to predict long-term release from ILAW glass for the IDF PA has been developed, refined, and updated over the past decade or so. The approach and the supporting test data for ILAW glasses have been extensively documented [1, 3-7, 12 - 15]. A brief summary is presented in this section.

The underlying premise of the IDF PA is that the source term for radionuclide release is

[1] The PCT method (ASTM C1285) offers two procedures: (1) PCT-A requires testing at 7-day ± 2%, at a temperature of 90 ± 2 °C, in static condition in a 304L stainless steel vessel, using -100 to +200 mesh particles in ASTM Type 1 water and a leachant volume of 10 ± 0.5 cm^3/g sample; and (2) PCT-B offers wide flexibility of varying sampling time, size of sample, temperature, and ratio of sample mass to volume of leachant. In the VSL procedure for PCT-Bs used in the present work the 4 mL of leachant taken for liquid analyses at each sampling time is replaced with 4 mL of deionized water.

controlled by the long-term weathering of the glass matrix. This engineering-based approach has been used in previous PAs to provide the defense-in-depth required to defend the above premise and demonstrate through computer simulations that the proposed glass waste form will meet the regulatory requirements for which LFRG provides oversight. The focus of this engineering-based approach is on estimating the model parameters and chemical reaction network needed to provide a robust simulation of glass weathering and the corresponding release of radionuclides over the period of performance (~10,000 years). The overall model incorporates the effects of chemical affinity and ion exchange as discussed below. The model parameters $\vec{k}_o$, η, E_a, and K_g are used to populate a chemical affinity-based kinetic rate law that is based upon Transition State Theory (TST) [16]:

$$r = \vec{k}_0 10^{\eta pH} exp\left(\frac{-E_a}{RT}\right)\left[1 - \left(\frac{Q}{K_g}\right)\right]^{\sigma} \tag{1.1}$$

where r is the dissolution rate [g/(m^2 d)], $\vec{k}_o$ is the forward rate constant [g /(m^2 d)], pH is the negative of the logarithm to base 10 of the hydrogen ion activity, η is the power law coefficient, E_a is the apparent activation energy (kJ/mol), R is the gas constant [kJ/(mo1 K)], T is the temperature (K), Q is the ion activity product (unitless), K_g is the pseudo-equilibrium constant for the rate controlling phase or phases (unitless), and σ is the Temkin coefficient which has been theoretically shown to equal one. Equation (1.1) relates the effect of: (1) pH, (2) temperature, and (3) the activities of species that affect the rate of glass dissolution via Q. Equation (1.1) is based on the kinetic rate equation developed by Åagaard and Helgeson [17], as applied to glass by Grambow [18] wherein orthosilicic acid (H_4SiO_4) is the only rate controlling species in Q.

In addition to the dissolution rate equation (1.1), a term is included in the IDF PA calculations to account for the ion-exchange rate (r_{IEX}) between sodium in the glass and hydrogen ions in the aqueous phase, as the glass-water reaction proceeds. In general, the ion exchange rate is thought to be a function of temperature, glass composition, and reaction progress (stage of the glass-water reaction). The potential importance of the contribution from ion exchange in the long-term corrosion mechanism had been emphasized previously by Feng and Pegg [19-21]. In previous glass testing work in support of the IDF PA, the standard approach to estimate this parameter has been that of McGrail et al. [5] and Pierce et al. [7] whereby r_{IEX} is obtained by subtraction of the boron dissolution rate from the sodium dissolution rate (and subsequently converted to moles-Na released per time and unit surface area); measurement of its temperature dependence also permits estimation of the activation energy of the Na ion exchange reaction E_{IEX}. More recently, various issues with this approach have been identified [22, 23] including: (i) the reliability of this subtraction approach in view of the apparent diffusive release of boron [13, 15]; (ii) an error in the calculation of r_{IEX} that has been propagated through previous work [23]; and (iii) the use of an r_{IEX} that is independent of time and solution composition [22, 23]. In view of these issues, WRPS has commissioned studies of potential alternative approaches for incorporation of ion exchange into the rate law [22, 23]; some of the recommendations from those studies have been implemented in FY2019 and FY2020 testing at VSL [9, 10, 24].

The use of Equation (1.1) with suitably estimated parameters allows for the source-term to be estimated within a reactive chemical transport modeling framework that takes into account the coupled effects of fluid flow and glass-water reactions on the chemistry of fluids percolating through the disposal facility. Coupling the fluid chemistry with a kinetic rate equation allows the simulations to describe the response of the glass corrosion rate to changes in fluid composition as a function of time and space.

In previous work, the model parameters for Equation (1.1) have been obtained from the analysis of data produced using a variety of experimental techniques. The SPFT test has been the primary technique used to estimate the coefficients of Equation (1.1). The results of the recent work at VSL [24] show that pulsed flow tests can also be used to obtain the parameters of Equation (1.1). Other tests used to evaluate glass durability are long-term high surface to volume ratio (S/V) product consistency test (PCT-B), vapor hydration test (VHT), and pressurized unsaturated flow test (PUF) [1, 3-7, 12-14, 25, 26]. This suite of tests evaluates different aspects of the glass-water reaction over the course of the various regimes of glass weathering: the initial forward rate regime; the decreasing rate regime; the residual rate regime; and the alteration rate renewal regime. These regimes are described below and illustrated in Figure 1.1 [8].

The initial forward rate consists of both ion-exchange and hydrolysis reactions. In dilute to near-saturated solutions, the TST-based model (without the ion-exchange term) successfully accounts for silicate dissolution in terms of temperature, pH, and reactive surface area when hydrolysis is the controlling reaction. However, as the glass-water reaction proceeds and the concentration of glass components (particularly the dissolved silicic acid concentration) increases in solution, the rate of dissolution decreases. For ILAW glasses tested under alkaline conditions, it has been observed that ion exchange becomes the dominant process controlling glass weathering under these near-saturated conditions, as was pointed out earlier for high-level waste (HLW) glasses [21].

As the glass continues to dissolve, the aqueous concentrations of dissolved components approach saturation with respect to the formation of a hydrated surface layer [36]. The combined H^+/Na^+ ion-exchange and hydrolysis of the silicate network lead to the formation of a multi-layered reaction zone including a hydrated layer, a porous gel layer, and possibly, crystalline phases that precipitate on the surface. Increasing the ratio of surface area of glass to volume of leachant (S/V) (as is possible in PCT-B) is one method to explore higher reaction progresses and identify the secondary phases that are associated with the alteration rate renewal regime, also referred to as resumption.

Layers within the reacted glass forms either as a reorganization of the hydrated layer (phyllosilicates) or when relatively insoluble glass components (e.g., Al, Fe, and Si) accumulate in the bulk solution and precipitate at the glass-water interface (tectosilicate) [25, 26]. The water-glass interface is a multi-layer system that includes phases in which the less soluble components left behind are organized into a hydrated layer of phyllosilicates and tectosilicates from the precipitation of components in solution that exceed their solubility limits [25]. The rate of dissolution then continues at a relatively constant residual rate that has been shown in some cases to be consistent with a process controlled by diffusion through the hydrated surface layer. The key

alteration phase is often a clay mineral, such as a smectite or chlorite. The precipitation kinetics associated with these phases can be complex, but in general, the rate of secondary phase growth increases in response to an increase in the magnitude of supersaturation [27, 28].

Finally, depending on the type of alteration phases that form, the glass-water reaction rate can increase from the residual rate and return to an elevated rate usually different from the initial rate, which is termed resumption. This type of behavior has been observed in accelerated testing, with high temperatures and high solid surface area to volume ratios, for various glasses including US HLW glasses [29-33], other HLW glasses [34-44], as well as Hanford low-activity waste (LAW) glasses [15, 32, 45, 46].

The data collected from VHT, PCT-B, and PUF experiments along with geochemical modeling and solid-phase characterization are used to identify the key alteration phases formed as the glass weathers. The results from these tests provide the additional confirmatory information needed to identify and constrain the appropriate chemical reaction network required for model simulations.

1.3 Test Objectives

One of the mechanisms that affect glass dissolution is the formation of secondary phases, which can either decelerate or accelerate the dissolution process. To be able to analyze the long-term effects of secondary phases, the phases involved in long-term PCT leaching of LAW glasses need to be identified. In FY2020, monitoring and testing continued for the glasses that have very recently reached resumption or that had not yet reached resumption. In addition, a set of higher waste loading LAW glasses, which were selected for PCT-B in FY2018, have now reached two-year sampling duration. Leachate samples, solid precipitates, and reacted glass surfaces have been analyzed. Thus, the objectives of the present work are:

- Compile and review the long-term PCT data on the IDF glasses.
- Based on the above review identify and analyze additional PCT leachates.
- Based on the review (first bullet above) and additional PCT leachates analyses, identify PCTs for altered glass and secondary phase analysis.
- Open selected vessels and remove and analyze small amounts of the solids by Scanning Electron Microscopy (SEM)/ Energy Dispersive X-Ray Spectroscopy (EDS) and X-Ray Diffraction (XRD).
- Use results from the above analysis to identify, in particular, the onset of leach rate resumption, and associated secondary phase formation.
- Analyze replicates of Argonne National Laboratory – Low-Activity Waste Reference Material (ANL-LRM) standard glass samples that were included in the test sets to assess the long-term reproducibility of PCT results.

- Continue sampling of the fifteen FY2018 PCT-B on glasses selected from those formulated to develop the Enhanced LAW Glass Correlation for high waste loading glasses.

1.4 Previous Testing at VSL

A large data set of results from long-term PCT-B performed at VSL on WTP LAW glasses was compiled and reported previously [15]. The data set includes glass compositions, leachate compositions, and pH at each sampling interval, sampling time, test condition (leachant, temperature, S/V, test protocol, and the like), and associated secondary phase information. Data for a total of 253 LAW glass compositions are included in the data set, which extended up to 3982 days of PCT-B leaching. These glass formulations were developed at VSL in support of the WTP and provided the basis for the present WTP baseline formulations. These glasses, presented in a 2011 report [15], span a composition range that is much more extensive than those used in previous performance assessment glass testing work [7]. Selected tests were sampled and analyzed to characterize the secondary phases, which included zeolites such as analcime and phillipsite and phyllosilicates of the smectite group, stevensite and swinefordite [15]. Glasses in the later stages of the reaction progress were included in this secondary phase analysis.

In addition to the development of the baseline operating envelope for the WTP, since 2003, VSL has been developing a wide range of LAW formulations that achieve considerably higher waste loadings than the WTP baseline formulations [47-49]. As a result, the range of glass compositions that may be produced at the WTP is expanding toward higher sodium and sulfate contents and new glass components such as V_2O_5 (for improved sulfate solubility), SnO_2 (for leach resistance at high alkali concentrations), and Cr_2O_3 (for resistance to K-3 refractory corrosion) that are added as glass former additives, and this type of composition range expansion is likely to continue through the life of the project. The IDF glass sets that are the subject of the present report include 27 high waste loading glasses, which complement the earlier set of 253 WTP glasses, as follows:

- In an initial effort to encompass the composition range expected to be disposed at the IDF, a total of ten glasses, referred to as IDF Phase 1 glasses, were selected as representative bounding glasses for this composition expansion [15]. These tests have now reached 10 years of continuous leaching at 90°C and 40°C.

- A second set of ten IDF Phase 2 glasses were added in FY2015 to expand the population of glasses at high alkali contents and fill gaps among lower Na_2O glasses with higher SO_3 contents [50-52].

- Seven more glasses selected from those formulated to support development of an Enhanced LAW Glass Correlation for high waste loading glasses [53-55] were added to the test set in FY2018 [56] and the testing continued [57]. These are designated as IDF Phase 3 glasses.

The compositions of IDF Phase 1 and Phase 2 glasses are presented in Tables 1.1 and 1.2 respectively, and shown in Figure 1.2. The selection was based on an analysis of the compositions and properties of the large number of LAW glasses that have been developed for the WTP at VSL. Multiple batches of these ten selected IDF Phase 1 glasses were prepared for testing at VSL. Samples of three of these glasses were also shipped to Pacific Northwest National Laboratory (PNNL) to support complementary PUF testing (IDF1-B2, IDF2-G9, and IDF3-F7). Long-term PCT-Bs at VSL were conducted under accelerated conditions compared to the IDF in which the glass will be stored at 15 °C. The first ten of these glasses were subjected to PCT-B at VSL at three temperatures (40 °C, 90 °C, and 120 °C) and two S/V (2,000 m^{-1} and 20,000 m^{-1}), all in triplicate. IDF Phase 2 glasses were subjected to long-term PCT-B at 90 °C and S/V of 20,000 m^{-1} in triplicate. The results showed that although the LAW glasses selected for this evaluation are compositions that have higher waste loadings than those developed for the WTP baseline, they follow generally similar leaching behavior. It is also evident that an increase in total alkali content alone is not necessarily detrimental to long-term PCT leaching. Furthermore, glass IDF1-B2, which has the highest alkali content of all glasses, and which fails the WTP VHT requirement by a significant margin, is actually one of the better performing glasses over the range of PCT-B conditions investigated. This indicates that the WTP VHT requirement (testing at 200°C) may be conservative with respect to the long-term robustness of the vitrified waste forms under disposal conditions (IDF at 15 °C). Glass IDF1-B2 showed robustness with respect to rate resumption despite increases in test temperature and S/V, both of which promote more reactive leaching conditions that drive the system towards secondary phase formation. This glass was deliberately included in the study to provide such a bounding case, together with the other IDF Phase 1 glasses described above; the rationale for the selection of these glasses has been described previously [15].

Four of the ten selected IDF Phase 1 glasses were also subjected to SPFT testing at VSL; the results were reported earlier [15, 58]. Full-suites of SPFT experiments as a function of pH, temperature, and silicic acid concentration (48 tests) were performed on the selected bounding glass, IDF1-B2. Full-suites of SPFT experiments were conducted later on glass IDF7-E12 [58]. More limited SPFT tests as a function of silicic acid concentration and temperature were performed on two other glasses, IDF2-G9 and IDF3-F7 [15]. Subsequently, a full suite of SPFT tests was conducted on glass IDF2-G9 at PNNL [59] as well as on a fifth glass from the IDF Phase 2 set: IDF18-A161. The results of the SPFT tests were analyzed to determine the parameters in the ILAW glass dissolution model.

The selected bounding glass IDF1-B2 has a high Na_2O concentration (25 wt%) that significantly exceeds that of the WTP baseline glasses; it also has properties that challenge but are within the WTP limits except for its VHT response. The rate law parameters were generally similar to those for the previously tested WTP baseline glasses, but a number of deviations from that model were identified and discussed [15, 58]. For example, the model worked well for IDF1-B2 tests performed far from saturation, but under near saturation conditions, the data for glass IDF1-B2 fit the TST rate model with H_4SiO_4 as rate controlling species only at low temperatures. Overall, however, the rate law parameters η, E_a, and K_g determined from the SPFT tests on the five high waste loading glasses (IDF1-B2, IDF2-G9, IDF3-F7, IDF7-E12, IDF18-A161) predict dissolution rates at 15 °C that are of the same order of magnitude as those determined for other

LAW glasses, such as LAWA44, LAWB45, and LAWC22, which are baseline WTP formulations that have generally lower waste loadings and, therefore, lower alkali contents. The fact that the rate law parameters determined for the bounding glass are close to those for the more typical WTP glasses is of practical significance since it suggests that higher waste loading glasses such as IDF1-B2 will likely still meet the requirements of the IDF PA. Establishing the viability of such high waste loading glasses in this regard is important in realizing their potential benefits in terms of reductions in life cycle costs and mission duration.

Other recent and ongoing SPFT tests have been conducted on glasses selected from 52 formulations (termed ORLEC glasses) spanning the range of alkali and sulfur concentrations in Hanford LAW [61]. These were formulated and characterized to support the development of an Enhanced LAW Glass Correlation [53-55] for the higher waste loading LAW glasses (Table 1.3). Glasses ORLEC28 and ORLEC33 were selected for SPFT testing at PNNL in FY2017 [60]. Glasses used in recent SPFT tests at the VSL include IDF21-EC14, representative of the high-alkali, moderate-sulfur (24 wt% Na_2O and 0.60 wt% SO_3) region of the high waste loading LAW formulations [61], IDF22-EC46 (18 wt% Na_2O and 1.37 wt% SO_3) at higher sulfur content, and IDF23-EC52 (23.8 wt% Na_2O and 0.90 wt% SO_3) at intermediate sulfur content [62]. These recent ORLEC glasses were the primary source for the selection of new glass compositions for long-term PCT-B immersed in FY2018 and on which sampling continued this year. A detailed description of the composition algorithm is provided elsewhere [53-55], but a summary of the selection process and its comparison to other LAW glasses is provided in Section 2.

The results from long-term PCT-Bs collected at VSL over the previous nine years for the ten IDF Phase 1 glasses have been reported earlier [50-52, 56, 57]. The data were collected at an S/V of 20,000 m^{-1} at 90 °C and 120 °C, over 272 days, as well as at the nominal PCT S/V of 2000 m^{-1} at temperatures of 90 °C and 40 °C, and reported over ~3300 days, so far. At the lower temperature of 40 °C, no change in alteration has been observed in recent years with the rate of alteration remaining near zero. The greatest extent of reaction based on boron normalized release was for glass IDF8-A125CCC, which reached 10 to 11% reacted glass at 900 days; that glass has stabilized at this level with little further alteration over the past seven years. Very little (0.5% to 3%) of the glass has reacted for the other nine glasses tested at 40 °C, all remaining stable over the last nine years. At 90 °C and S/V of 2000 m^{-1}, seven of the ten IDF Phase 1 glasses were found to be over 50% reacted (IDF9-A187, IDF6-D6, IDF7-E12, IDF8-A125, IDF4-A15, IDF3-F7 and IDF1-B2) and one (IDF5-A20) showed a rising leach rate over the past years, which then plateaued at ~25% reacted. However, one of the two high-alkali glasses, IDF2-G9, and the high zirconia glass IDF10-Zr6, are still showing low extent of reaction of 9% and 6% reacted, respectively.

Among the IDF Phase 2 glasses tested at 90 °C and S/V of 20,000 m^{-1}, two reached resumption within the first six months, two others and the reference glass ANL-LRM2 [63] reached resumption within the first year, and two more reached resumption in the second year and have plateaued at around 50% reacted glass. These are generally low-zirconia glasses (less than 2 cation% Zr) with high alumina (above 9 cation% Al) [56, 57]. The remaining four glasses (IDF11-G27CCC, IDF12-A38CCC, IDF16-A58CCC, and IDF17-A60CCC) showed the least altered glass (~5% to 15%) based on normalized boron release. All four are glasses containing higher than 2.75 wt% SnO_2, and, among these, three glasses are high in silica and low in alumina, which is

consistent with the observations from the IDF Phase 1 set (resumption delayed for glasses with Al/Si ratio lower than 1/3).

During FY18, PCT-Bs were started on seven IDF Phase 3 glasses selected from those formulated to develop the Enhanced LAW Glass Correlation for high waste loading glasses [53-55]. All seven glasses are being tested at 90 °C and S/V of 20,000 m^{-1}. Two of the glasses are also being tested at 90°C and S/V of 1000, 2000, 5000, 10,000 and 20,000 m^{-1}. Results from 7-day to 365-day samplings of the tests at different S/V [57] showed that the PCT releases follow a power law function of S/V, which was suggested by earlier observations on various HLW glasses [21].

Extensive SEM/EDS evaluation of solid samples taken from the leach tests of IDF Phase 1 and Phase 2 glasses were reported in FY2019 [57]. These confirmed and enhanced XRD analyses previously reported [56]. XRD permitted identification of phases present on the glass surface, for the most part, tecto- and sorosilicates crystallizing on top of phyllosilicates covering the gel layer of glass alteration. The phyllosilicate phases observed are members of the smectite clay mineral family and encompass a broad range of compositions. Although both are aluminosilicate minerals, smectites and zeolites have very distinguishable features. Smectites are anhedral and zeolites are euhedral. SEM cross-sectional evaluation primarily defines smectites by their Si/Al elemental ratio in the range of 4 to 7, much higher than is found in zeolites, typically ~2. In smectites, SEM/EDS revealed an evolution of elemental profiles with enrichments in Fe, Zn, and Mg in layers closest to the solution and higher Zr close to the hydration front towards the pristine glass. Ca, Sn, and Ti were also found in significant amounts in smectites. The phyllosilicate tobermorite was identified in previous XRD analyses of Hanford LAW glass alteration products. SEM micrographs also revealed that the phase was abundant in severely altered samples rich in CaO (8 to 10 wt%) .

Analcime is the zeolite identified most frequently but others commonly observed are chabazite, phillipsite, and gmelinite, in which sodium is the dominant extra framework cation. The morphology of some of these zeolite crystals identified in earlier samplings of the altered glasses [50] had not been observed before in Hanford LAW glass alteration products (long-term PCT, VHT). However, more of the same morphology seen in samples of IDF Phase 1 and Phase 2 altered glasses were previously identified in alteration of basaltic glass formed from volcanic activity 15 to 20 million years ago, as discussed previously [52]. These were identified on the altered glass when resumption was observed, but also when it is incipient based on leachate analysis.

It must be noted also that based on previous XRD evaluation [56], none of the glasses tested at 40 °C showed any sign of alteration phases having developed after eight years of PCT-B. High magnification SEM micrographs [57] revealed a sub-micron size gel layer where compositional changes point to nascent formation of a smectite, but no zeolites.

Overall, the PCT-B results reported so far show that although the LAW glasses selected for this evaluation have higher waste loadings than those developed for the WTP baseline, they follow generally similar leaching behavior to that observed with the lower waste loading WTP baseline LAW glasses and the increase in total alkali content alone is not necessarily detrimental to long-term PCT leaching.

1.5 Summary of FY20 Testing

This report provides an update on the PCT-B data for the 27 IDF Phase 1 (10 years), IDF Phase 2 (5 years), and IDF Phase 3 glasses. The long-term tests were subjected to additional leachate sampling and analysis in order to bring the data set up to date. The frequency of testing for IDF Phase 3 glasses was increased in comparison to earlier tests to better define the time when glasses reach resumption. Samples of reacted glass were recovered from selected test vessels for analysis of the secondary phases. This year, solids analysis focused on IDF Phase 3 glasses. Selected tests are being continued in order to extend the data set to longer times.

SECTION 2.0
DESCRIPTION OF THE 27 IDF GLASSES IN COMPOSITIONAL SPACE

The target compositions of the IDF Phase 1 and Phase 2 glasses are given in Tables 1.1 and 1.2, respectively. They were selected from higher waste loading LAW glasses and the majority of them have been tested for processability at VSL in the DM10 melter, as shown in Figure 1.2 (thirteen larger red circles). A few glasses that have been tested only at crucible scale were included to better cover the compositional space for LAW glass compositions (red triangles in the figure). Target compositions of the seven IDF Phase 3 glasses selected for PCT-B from the Enhanced LAW Glass Correlation for high waste loading glasses are given in Table 1.3. Their compositions in elemental percentage along with a summary of their properties are given in Table 2.1. They are marked in red squares in Figure 2.1, which plots the two alkalis from LAW as ALK (Na_2O + 0.66 × K_2O) and SO_3 concentrations, and in Figure 2.2 where the Na_2O concentration is shown on the y-axis. The two glasses tested at various S/V are highlighted in yellow.

All IDF glass batches included a rhenium spike targeted at 0.1 wt% Re_2O_7 if all of it were retained in the glass. To differentiate the IDF glasses from similar glasses formulated earlier without a rhenium spike, they are renamed as "IDFx-y" (e.g., ORLPLB2 is renamed IDF1-B2). To accommodate the rhenium addition, 0.1 wt% SiO_2 was removed in comparison to the original composition. X-Ray fluorescence spectroscopy (XRF) measured rhenium and SO_3 values from the crucible glass melts prepared for IDF tests [50, 56] are used to define the respective Re and SO_3 content of these glasses.

All 27 IDF glasses included in long-term PCTs that are the subject of the present work are presented in Figure 2.3 in terms of their alkali and sodium contents; the higher alkali glasses are found at the upper right corner and the high sulfate-lower sodium glasses at the lower left.

A short compositional description of these glasses is given below and illustrated in Figures 2.3 to 2.7 in cation percent[2] for some key constituents, as discussed below.

Phase 1 IDF glasses:

- IDF1-B2 (top right in Figure 2.3), based on ORPLB2 (25.0 wt% Na_2O, 0.1 wt% K_2O, 0.5 wt% SO_3) has the highest mol% alkali oxide content among the selected glasses. This glass shows K-3 refractory corrosion neck loss close to the limit of 0.04 inches and VHT alteration rate slightly more than double the WTP limit. Other glasses evaluated for selection at the highest Na_2O content were rejected as they have viscosity values outside of the acceptable WTP upper limit of 150 poise at 1100 °C or include 3 vol% crystals after

[2] Percentage of glass constituents calculated without oxygen.

heat treatment for 20 hours at 950 °C. Of candidate glasses containing 25 wt% Na_2O, ORPLB2 is one for which properties relevant to processing are close to but within the WTP limits, PCT releases are within the WTP limits, and only the VHT response is above the WTP limit; it was therefore selected as the bounding glass composition for the full suite of SPFT testing and for long-term PCT-B.

- IDF2-G9, based on ORPLG9 (21.0 wt% Na_2O, 5.8 wt% K_2O), was selected from the high alkali-high potassium glasses. This glass shows K-3 corrosion neck loss and VHT alteration rate close to, but within WTP limits. This glass was selected for SPFT testing and PCT-B. The sample had not reached resumption based on PCT-B results up to nine years at 90 °C and S/V of 20,00 m^{-1} (see Section 5.2).
- IDF3-F7, based on ORPLF7 has the highest SO_3 and lowest Na_2O concentrations (12.0 wt% Na_2O, 1.5 wt% SO_3) among the glasses selected for IDF Phase 1 testing. This glass also contains the highest lithium concentration of 4.37 wt% Li_2O.
- IDF4-A15 and IDF5-A20, based on ORPLA15 and ORPLA20, respectively, are two glasses with high alkali content (24.0 wt% Na_2O, 0.5 wt% K_2O) that have been used in melter tests at VSL [64, 65]. These compositions meet all of the WTP contract specifications for LAW glass. These glasses have the second highest sodium concentration (after IDF1-B2), as can be seen in Table 2.1.
- IDF6-D6 (22.0 wt% Na_2O, 0.2 wt% K_2O, 1.2 wt% SO_3) was selected from glasses with intermediate sodium content where waste sodium loading is decreased to accommodate higher sulfate content. The alumina content also is high in this glass (10.1 wt% Al_2O_3) with Al/Si atomic ratio close to $^1/_3$ (see Table 2.1).
- IDF7-E12, based on ORPLE12 (16.0 wt% Na_2O, 0.6 wt% K_2O, 1.5 wt% SO_3), was selected from glasses that could accommodate the highest SO_3 concentration of 1.5 wt%. This glass contains 2.5 wt% Li_2O and 10 wt% CaO to improve sulfate solubility (Figures 2.5 - 2.6). This glass was selected for the full suite of SPFT testing and PCT-B.
- IDF8-A125 based on LAWA125 (20.0 wt% Na_2O, 4.2 wt% K_2O) was selected from high alkali-high potassium glasses with VHT alteration rate and K-3 refractory corrosion neck loss well within the WTP limits. This is a glass with one of the lowest combined alumina and zirconia contents (5.64 wt% Al_2O_3 and 2.91 wt% ZrO_2) but high silica content (42.81 wt% SiO_2), as is evident in Figures 2.4 and 2.5.
- IDF9-A187 (23.0 wt% Na_2O, 0.5 wt% K_2O) was selected from glasses with Na_2O concentrations ranging from 23.0 to 23.5 wt% but with high VHT alteration rate. This glass, as with IDF6-D6, has high Al_2O_3 content and Al/Si ratio close to $^1/_3$ (see Table 2.1).
- IDF10-Zr6 is based on glass LE4H-Zr6 and contains 9.50 wt% ZrO_2 (highest Zr content in Figure 2.4). This glass was formulated by increasing the ZrO_2 concentration in the WTP baseline glass LAWE4H by 6 wt%. This glass was included in the set for PCT-B because higher ZrO_2 decreases VHT alteration rate and K-3 neck corrosion, which makes high zirconia of interest for high waste loading LAW glasses. Tests conducted for WRPS [66] to improve technetium retention in LAW glasses showed that ZrO_2 also may be beneficial

in this regard. Accordingly, this glass was selected for PCT-B because none of the other glasses have such high ZrO_2 concentration. Note that this glass has the lowest alumina content (4.95 wt% Al_2O_3), as evident in Figure 2.5.

Among these IDF Phase 1 glasses for which long-term leach tests were initiated in 2010, glasses IDF9-A187CCC and IDF6-D6CCC showed resumption at the earliest, with both showing the formation of analcime and gobbinsite in the alteration products [50]. As noted above, these two glasses have the highest Al_2O_3 content and Al/Si ratio very close to $^1/_3$ (Table 2.1). Zirconium is also relatively low in these two glasses, and in IDF8-A125CCC, which also showed analcime formation in long-term leach test results, as reported earlier [50].

For the IDF Phase 2 glasses, seven were selected from the high-alkali region:

- IDF11-G27, based on ORPLG27 (21.0 wt% Na_2O, 5.8 wt% K_2O); this glass has one of the highest alkali oxide concentrations among all of the glasses selected for testing.
- IDF12-A38, based on ORPLA38-1 (24.0 wt% Na_2O, 0.5 wt% K_2O) includes V_2O_5 as an additive for high alkali glasses to accommodate higher concentrations of SO_3 (0.8 wt%).
- IDF13-A51 based on ORPLA51 (24.0 wt% Na_2O, 0.5 wt% K_2O) investigates the effect of higher TiO_2 concentration.
- IDF14-A59 (24.0 wt% Na_2O, 0.5 wt% K_2O) is a new formulation prepared for the IDF Phase 2 tests; it is based on ORPLA51 but at lower Cl and SO_3 concentrations. Comparison of the long-term PCT responses for IDF13-A51 and IDF14-A59 can therefore show the effect of Cl and SO_3 concentrations.
- IDF15-A57 (24.0 wt% Na_2O, 0.5 wt% K_2O) is also a new formulation prepared for the IDF Phase 2 tests. This glass is based on ORPLA57 and, as with the previous two glasses, was formulated with high alumina, titania, and zinc to control K-3 corrosion in high alkali glasses without adding Cr_2O_3. IDF15-A57 contains 10.65 wt% Al_2O_3, 3.0 wt% TiO_2, 4.0 wt% ZnO, but no MgO.
- IDF16-A58 is based on ORPLA58 (24.0 wt% Na_2O, 0.5 wt% K_2O) and is similar in composition to the previous four glasses (10.65 wt% Al_2O_3, 3.0 wt% TiO_2, 3.0 wt% ZnO) but without CaO.
- IDF17-A60 is based on ORPLA20 with high Na_2O content but with Cl decreased to 0.1 wt% and SO_3 decreased to 0.3 wt%. In this way, the results from PCT-B of this glass can be compared to those from ORPLA20 because the alkali content in both are fixed at 24.0 wt% Na_2O and 0.53 wt% K_2O.

Three Phase 2 glasses were included to fill the composition gaps amongst the lower Na_2O glasses.

- IDF18-A161 is based on LAWA161, which was the enhanced formulation for LAW from Tank AN-105 when the waste definition included higher chlorine content. As a result, the

formulation was designed at 20.66 wt% Na_2O and included 1.17 wt% Cl. This formulation was further tested in a melter at progressively increasing sulfate levels up to 1.10 wt% SO_3 without the formation of secondary sulfate phases [67]. It is also a low zirconium glass (Figure 2.4).

- IDF19-C100 is based on LAWC100 (for Tank AN-102). This formulation is close to LAWA161 in composition but is higher in SO_3 content (1.2 wt%) and lower in Cl content (0.65 wt%). Among the IDF glasses selected for testing, this glass has the highest boron content (13.68 wt%).
- IDF20-F6 is based on ORPLF6, an enhanced formulation for LAW from Tank AZ-101 for which a sodium loading of 13.0 wt% Na_2O would require a sulfate loading of 2.09 wt% SO_3 based on the waste composition [65]. The selected formulation at 13 wt% Na_2O was prepared with a sulfate content of 1.25 wt% SO_3 since that is the sulfate content that was previously evaluated in sulfate oversaturation tests.

The seven IDF Phase 3 glasses were selected from 52 high waste loading LAW glasses, termed "ORLEC" glasses, spanning the range of alkali and sulfur concentrations in Hanford LAW formulated and characterized to support the development of an Enhanced LAW Glass Correlation for high waste loading glasses [53-55]. The strategy for the development of this Enhanced LAW Glass Correlation is similar to the one used in the development of the WTP Baseline LAW Glass Correlation [68]. The selection has been described in a previous report [56] and the glass distribution in composition space can be seen in Figure 2.1. The glasses span the range of alkali and sulfate concentrations for the high waste loading Hanford LAW glasses and are marked in Figure 2.1 by a red box around the sample number. Another consideration in making the selection of these ORLEC glasses for long-term PCT in FY2018 is that eight of the ORLEC compositions have already been recommended for SPFT testing in FY2017. The seven glasses selected for long-term PCT are as described below and their elemental compositions along with a summary of their properties are given in Table 2.1.

- IDF24-EC28 (originally ORLEC28) is at the high potassium (3.36 wt% K_2O) and medium SO_3 (0.4 wt%) part of the *Alkali Limited Region (AL)*[3] range where the alkali content of the glass limits waste loading. It bridges the gap between IDF2-G9 (highest K_2O content) and other high alkali glasses with lower K_2O contents.

[3] ORLEC formulations are defined in the range of alkali and sulfate concentrations of Hanford tank wastes as either *Alkali Limited Region (AL)* where ALK = Na_2O (wt%) + 0.66 K_2O (wt%) is limited to 24.33 wt% or as *Alkali & Sulfate Limited Region (ASL)* where both Na_2O and SO_3 concentrations need to be managed to optimize waste loading (curved section in Figure 2.1). If the sulfate concentration in the LAW increases further, waste loading in the glass is limited by sulfate alone at a value of 1.5 wt% SO_3 in a region termed *Sulfate Limited Region (SL)*.

- IDF28-EC50 (originally ORLEC50) is a high sodium (24 wt% Na_2O) glass at the high SO_3 (0.6 wt%) concentration part of the *AL* region. The plot of Na_2O vs. SO_3 in Figure 2.2 provides another view of the difference between ORLEC28 and ORLEC50 with different sodium and potassium contents.

- IDF23-EC52 (ORLEC52), IDF25-EC34 (ORLEC34), IDF26-EC64 (ORLEC44), IDF22-EC46 (ORLEC46), and IDF27-EC48 (ORLEC48) are glasses selected at decreasing Na_2O and increasing SO_3 concentrations in the *ASL* region.

Although some overlap appears in Figure 2.3 with some of the earlier IDF glasses and the new selections (e.g., IDF9-A187 and ORLEC34, IDF7-E12 and ORLEC48), the glasses have differences when considering all of the other glass constituents.

Two of these seven glasses were selected to be tested at five different S/V, to total 15 PCTs initiated in FY2018. These are divided into three sets of five glasses: two sets for the S/V variation study and one set for the remaining five glasses.

Glass preparation, compositional analyses, evaluation and preparation of the glass powders for long-term PCT have been described in earlier reports for IDF Phase 1 [15], IDF Phase 2 [50], and IDF Phase 3 [56] glasses. All glasses were subjected to canister centerline cooling (CCC) heat treatment [69] before PCT-B, with the suffix CCC added to their name. The ORP LAW Enhanced Correlation (ORLEC) glasses were prepared for PCT-B in the same manner as earlier glasses, and with the same sample nomenclature as given below:

IDF22-EC46CCC for formulation ORLEC46
IDF23-EC52CCC for formulation ORLEC52
IDF24-EC28CCC for formulation ORLEC28
IDF25-EC34CCC for formulation ORLEC34
IDF26-EC44CCC for formulation ORLEC44
IDF27-EC48CCC for formulation ORLEC48
IDF28-EC50CCC for formulation ORLEC50

In the data discussion that follows, some of these sample names have been simplified to "ECxx".

2.1 Summary of Test Parameters: Temperature and Variation in S/V

Long-term PCT-Bs on LAW IDF Phase 1 and Phase 2 glasses have been conducted at three temperatures (40 °C, 90 °C, and 120 °C) and two S/V (2,000 m^{-1} and 20,000 m^{-1}). Tests conducted at room temperature on early WTP glasses [70] showed very low alteration, well below 1 g/L, likely requiring decades before the reacted surface would show measurable alteration in SEM. Similarly, little alteration has been observed in the long-term PCTs conducted at 40 °C, as described in Section 1.4. In contrast, resumption was reached in many of the tests conducted at 90

°C and 120 °C. At 90 °C, the reacted glass sampled could be well characterized, and phases were identified. At the higher temperature of 120 °C, the reacted glass and leachate quickly became difficult to sample because the entire system gelled together [52]. A test temperature of 90 °C was therefore selected for the IDF Phase 3 tests.

Variation in S/V has been investigated on Phase 1 glasses at two S/V of 2,000 m^{-1} and 20,000 m^{-1}, while Phase 2 glasses were all tested at 20,000 m^{-1}. The same single S/V of 20,000 m^{-1} was selected for the tests initiated in FY2018 on IDF Phase 3 glasses, along with a more comprehensive study of the impact of the S/V on glass leaching. In Phase 1 glasses, resumption was observed at both S/V values, but it also affected greatly the resulting solution pH, as reported earlier [15]. Matrix dissolution, ion exchange, and secondary phase formation are intricate mechanisms of the long-term glass leaching, which are all highly affected by the leachate pH [17-21, 25-30, 33, 71, 72]. The contribution from ion exchange and the corresponding pH rise is further enhanced by making more surface area of the glass available to the leaching reaction by increasing the surface area of glass per unit volume of leachant. In the IDF Phase 3 work, the effect of systematic changes in S/V on leachate composition, pH, and on the reacted glass layer and secondary phases are also studied by testing glasses ORLEC28 and ORLEC52 at five different S/V. Extensive studies on the impact of S/V on pH and resumption were previously conducted at VSL on multiple HLW glasses [21].

The selections of the five different S/V were made based on results from long-term PCT of Phase 1 and Phase 2 glasses at 90°C, which showed that resumption was reached within months to two years at S/V of 20,000 m^{-1} and as early as one year at 2000 m^{-1}. The range selected is from 1000 m^{-1} to 20,000 m^{-1}.

SECTION 3.0
LONG-TERM PCT-B DATA

Long-term PCTs were initiated on ten high waste loading IDF Phase 1 glasses under a test program for WRPS in 2010 [15]. Although funding for that program ended in 2011, most of the long-term PCTs were maintained at VSL's expense and then continued under the 2015 IDF Phase 2 program. Also in IDF Phase 2, tests on ten additional glasses were initiated and are continuing. Finally, in FY2018, PCTs were initiated on seven more IDF Phase 3 glasses selected from those formulated to support development of the Enhanced LAW Glass Correlation for high waste loading glasses [53-55], including variations in S/V on two of the glasses. This section provides an update on the PCT-B data for the 27 IDF Phase 1 (10 years), IDF Phase 2 (5 years), and IDF Phase 3 glasses. The long-term tests were subjected to additional leachate sampling and analysis in order to bring the data set up to date. The frequency of testing for IDF Phase 3 glasses was also increased in comparison to earlier tests to better define the time when glasses reach corrosion resumption. In addition, samples of reacted glass were recovered from selected test vessels for analysis of the secondary phases. This year, solids analysis focused on IDF Phase 3 glasses. Selected tests are being continued (maintenance, sampling, and analysis) in order to further extend the data set to yet longer times. Note that in the figures presented in association with the discussion below, the sample label is often shortened and does not include the "-" separating the IDF number and the original glass code, nor the suffix "CCC," which is part of the sample ID and which denotes the heat treatment that has been imposed on all IDF samples tested herein. It is also noted that ANL-LRM is the PCT reference glass that has undergone PCT-A round robin testing [63]; that glass was tested without the CCC heat treatment.

The product consistency test [73] is used to evaluate the relative chemical durability of glasses by measuring the concentrations of the chemical species released from 100-200 mesh crushed glass (75-149 μm) to the test solution (de-ionized water in this case). PCT-A (90 ºC, 2000 m^{-1} and 7-day) had been performed previously on most of the selected LAW glasses in standard 60-mL 304L stainless steel leach vessels. PCT-B conducted in IDF Phase 1 and Phase 2 work used leach vessels of 150 mL capacity (also 304L stainless steel). These vessels have a bottom plug and a top plug assembly that screw on to each end permitting regular leachate sampling through a laminated three-layer silicone top septum without breaking the seal of the vessel, and, if needed, sampling of the glass by dismounting the bottom plug. The vessels are placed on their side in the oven and are returned to the upright position for sampling. A new type of dome-base stainless steel vessel with sampling port integrated into the wide mouth lid was used for IDF Phase 3 glasses. This further facilitated the sampling of the reacted glass, as described in Section 4.

The PCT-B was performed in triplicate on all of the glasses [15, 50, 56] in parallel with the ANL-LRM reference glass, which was included in each test set. The tests are generally divided into sub-sets to keep the PCT sets at a manageable size of 20 vessels (five glass tests in triplicate, plus three standard glass samples, and two blanks). IDF Phase 1 tests include PCT at S/V of 2000

m^{-1}, with 10 g of glass powder in 100 ml of deionized water per vessel. The 20 IDF Phase 1 and Phase 2 glasses have been tested at 90 °C and the high S/V of 20,000 m^{-1}; this was selected in order to investigate as early as possible the secondary phases that are formed. In this case, 40 g of glass powder is placed in 40 ml of deionized water. The IDF Phase 3 PCTs included seven glasses at S/V of 20,000 m^{-1}, as well as two of these glasses at four additional S/V of 1000 m^{-1}, 2000 m^{-1}, 5000 m^{-1}, and 10,000 m^{-1}. The mass of glass powder and the respective volume of deionized water per vessel for these tests are provided in Table 3.1.

The sampling protocol consisted of removing an aliquot of 4 mL of the leachate at 7, 28, 56, 120, 181, 270, 365, 547 days, and yearly thereafter; however, the sampling frequency during the second year of testing was increased to approximately every 90 days for IDF Phase 3 sample sets ILHE, ILHF, and ILHG to better identify the onset of resumption. After sampling, the solution that is removed for analysis is replaced with 4 mL of deionized water. As noted in the data provided below, the effect of the minor dilution (4% at 2000 m^{-1}, or 10% at 20,000 m^{-1}) due to this solution exchange is not detectable between successive samplings unless some of the phases crystallizing absorb a significant fraction of the leachant. In addition to the effects of glass composition at 90 ºC and S/V of 20,000 m^{-1}, variations in test temperature (40 °C and 90 °C) and S/V (2000 m^{-1} and 20,000 m^{-1}) are represented in the dataset for IDF Phase 1 glasses. The data for the IDF Phase 1 glasses now extend to ten years at S/V of 2000 m^{-1}. PCTs on IDF Phase 2 glasses (90 °C and S/V of 20,000 m^{-1}) have just passed five years of testing, and IDF Phase 3 glasses have reached two full years of testing. Sampling and analysis of all of the PCTs that have not reached resumption[4] are continuing. In some cases, sampling continued beyond resumption to allow further growth of secondary phases before sample collection in order to facilitate their identification.

In addition to the leachate concentrations, it is convenient and conventional to also consider the normalized leachate concentrations, which are used in discussions in this section. The normalization is performed by dividing the concentration measured in the leachate for any given component by its mass fraction in the glass. Thus, the *normalized concentration* C_i of element i (in g/L) is calculated from the elemental concentration c_i measured in the leachate (in g/L) as:

$$C_i = \frac{c_i}{f_i} \ , \tag{3.1}$$

where f_i is the mass fraction of element i in the glass. The normalized concentrations are a measure of the mass of glass reacted based on the specific element and provides a useful insight into which of the glass constituents contribute to new phase formation. If species are found in solution in proportion to their stoichiometry in the glass, dissolution is congruent. This is usually the case for boron for which the rate of release from the glass is proportional to the glass dissolution rate because it is typically not retained in any reaction product formed during leaching. When alkali and boron in the leachate have similar normalized concentrations, their release is congruent. On the contrary, a strong deviation from congruency likely indicates that the constituent is involved

[4] Leachate analysis is used to identify resumption: it is identified as a sharp increase in leach rate, after a succession of stable lower leach rates, the latter corresponding to the Residual Rate regime (illustrated in Figure 1.1).

in surface crystallization, or otherwise is retained in the altered glass. Under the PCT conditions employed in tests at S/V of 2000 m^{-1} (10 g glass per 100 ml water), a normalized boron release nearing 100 g/L corresponds to 100% reacted glass since it is equivalent to the full glass boron content being released to the solution. At S/V of 20,000 m^{-1}, 1000 g/L corresponds to 100% reacted glass.

Since each leachate concentration for the i^{th} element $c_i(n)$ is measured in triplicate (n=1,2,3), c_i(average), the corresponding arithmetic average of the triplicate measurements, is calculated prior to normalization. Based on percent relative standard deviations (%RSDs) given in Appendix A1-A3, triplicate results are in good agreement and resumption, when it occurs, takes place for the three replicates at about the same time. The spread of triplicate measurements increases (%RSD up to 100%) when leachate sampling happens to coincide with the sharp rise in resumption (see illustration A-1 at the end of Appendix A) but the %RSD decreases again in later samplings.

3.1 Long-Term PCT-B at 90 °C and S/V of 20,000 m^{-1}

PCT-B at 90 °C and S/V 20,000 m^{-1} was performed on the ten IDF Phase 1 glasses, as reported previously [50] and summarized in Section 1.4, and on ten IDF Phase 2 Glasses. No new data for these conditions were collected on IDF Phase 1 glasses since the tests were terminated, but the results are combined in summary Table 3.2 for comparison to other results presented below. As pointed out earlier, the glasses that showed resumption early in that set have the lowest zirconia (such as IDF9-A187), as well as the highest Al_2O_3 contents and Al/Si ratio very close to 1/3 (IDF6-D6). Sampling of the reacted glass samples showed heavy formation of analcime and gobbinsite in the alteration products [50].

The leachate sampling duration for the IDF Phase 2 glasses has now reached five years. The results from sampling of the two PCT sets (designated ILHC and ILHD) are summarized in Table 3.3. IDF18-A161CCC and IDF19-C100CCC were the first two glasses to reach resumption shortly after the 119-day sampling (Figure 3.1). Next to reach resumption were IDF14-A59CCC and IDF20-F6CCC, at 1-year sampling, along with the reference glass ANL-LRM. IDF14-A59CCC reached 100% altered glass (1087 g/L) but IDF20-F6CCC, IDF18-A161CCC, and IDF19-C100CCC stabilized at around 55-70% altered glass (544 to 702 g/L), staying in the range of 450 to 700 g/L for the last three years. As reported last year [57] for these three glasses, the normalized boron release in the leachate indicated that resumption was reached within the first year of testing, after which the release plateaued. SEM images showed abundant calcium silicate gel that developed around the reacted particles [57]. This gel layer also seemed responsible for collecting the boron and some of the other leachate constituents as well as some of the water in the crystals. The leach tests were terminated and only around half of the leachate could be collected, confirming substantial hydration of calcium silicate crystals around the highly altered glass.

In contrast, resumption started for IDF14-A59CCC at later sampling dates (after the 273-day sampling) but the boron release continued to rise sharply over the following two years.

Leachate sampling for IDF14-A59CCC at 913 days shows that all available boron has been released (1087 g/L with 1.7% RSD among triplicates). This is a glass with lower Cl and SO_3 concentrations (both targeted at 0.1 wt%), and therefore considerably less calcium was required as a glass former. The absence of calcium silicate crystallization (only phillipsite was observed in SEM [57]) may explain why, in this case, resumption leads to the release of all available boron.

The reference glass ANL-LRM2 also reached resumption around the 1-year sampling period with excellent agreement between both sets of triplicates from sets ILHC and ILHD. The reason for the drop in boron release observed in Figure 3.1 after reaching 100% altered glass can be partially explained by the 10% dilution brought about at sampling and which cannot be compensated for after all the boron from the glass is released. At such large extents of alteration, most of the sample has converted into a gelled mass, which might retain some of the leached constituents. Sampling becomes difficult, and in some cases, the amount of free liquid available for sampling in the vessel is very small. Test vessels containing this glass, as well as IDF14-A59, were sampled and the tests were terminated.

Between 300 and 900 days, the leach rates for glasses IDF13-A51CCC and IDF15-A57CCC increase at much slower rates (see Figure 3.1). These are two glasses for which higher amounts of TiO_2 and ZnO and high alumina content were tested to prevent excessive K-3 refractory corrosion; they have low CaO content because the SO_3 concentration is not very high (0.7 wt%). However, IDF13-A51 was almost fully reacted at around 1300 days and was terminated in the past year after reaching 870 g/L boron release. IDF15-A57, the formulation without MgO, but with 1.5 wt% CaO, stabilized at around 300 g/L normalized boron and remained at that level at the 5th year of sampling.

Removing calcium entirely in IDF16-A58CCC delayed the time to resumption as compared to IDF15-A57CCC (no MgO) and IDF14-A59CCC (with CaO, and MgO). A relative increase of 150% in normalized boron release is observed in IDF16-A58CCC during the last year (Figure 3.1), indicating resumption. The increase, rather than a plateau in normalized release, is also consistent with the absence of calcium preventing the formation of a calcium silicate gel. Sampling and analysis of solids from this test will be performed next year to identify the secondary phases.

The remaining three glasses (IDF11-G27CCC, IDF12-A38CCC, and IDF17-A60CCC) still show the least altered glass (~5% to 15%) based on normalized boron release, with very little change in the last sampling. These three glasses are high in silica and low in alumina, which is consistent with the observations from the IDF Phase 1 set (resumption delayed for glasses at Al/Si ratio lower than 1/3). In addition, all three are glasses containing higher than 2.75 wt% SnO_2 and 6.0 wt% or more ZrO_2. In the case of glass IDF12-A38, a larger spread between triplicate tests (66 %RSD) than generally observed indicates that resumption is probably ongoing, showing a larger rise in normalized release in one of the samples.

At this high S/V of 20,000 m^{-1}, liquid sampling became very difficult in most PCT vessels now containing a large fraction of highly hydrated glass/gel, even when the measured boron in

solution remains lower than is available from the glass. Most glasses that reached > 50% reaction based on boron (>500 mg/L), became impossible to sample due to lack of access to any liquid and were terminated. In sets ILHC and ILHD, PCTs on four glasses (twelve vessels) are ongoing: IDF11-G27CCC, IDF12-A38CCC, IDF16-A58CCC, and IDF17-A60CCC.

3.2 Long-Term PCT-B at 90 °C and S/V of 2000 m^{-1} on IDF Phase 1 Glasses

The results from PCT-B at 90 °C and S/V of 2000 m^{-1} on IDF Phase 1 glasses show a similar trend in leach rate to those observed at high S/V [50, 57] but they occur at longer times and in a slightly different order (Table 3.4 and Figure 3.2; note that at this S/V a normalized boron release of 100 g/L corresponds to 100% of the boron content in the glass in solution). In the first six years of the total of ten years of testing, six of the ten glasses exhibited elevated rates indicative of resumption. First was IDF9-A187CCC, followed by IDF6-D6CCC (shortly after samplings at 365 and 545 days, respectively). For these two glasses, the order is the same as in the respective higher S/V tests. Resumption was observed next with IDF8-A125CCC, between 720 and 1800 days, but the alteration rate is not as high. For IDF7-E12CCC, resumption occurred around 1200 days with a sharp rise in rate. Resumption of IDF4-A15CCC was observed between 1200 and 1800 days; it has now reached 80 g/L normalized boron release. Finally, glass IDF3-F7CCC reached resumption with a sharp rise at 1925 days and stabilized at 90 g/L normalized boron release. It had become difficult to obtain a liquid sample from these last four glasses, which were all nearly fully reacted, and these tests were terminated at the same time as when solid samples were collected. As noted in Figure 3.2, tests for these six glasses have been terminated and the solid phases were collected and analyzed previously [50, 57], showing abundance of zeolites phases.

IDF5-A20CCC has reached 3608 days of testing as of the 2020 sampling. It showed an increase in normalized boron release from 8.2 g/L at year 5 to 14.5 g/L at year 6 and 23.5 g/L at year 7 but plateaued at 24.0±0.1 g/L in the past three years. It is not clear what could suppress the increase in release rate, but it is possible that the 4% liquid replenishment is affecting the solution when so much of the liquid is immobilized in the alteration gel. Large solid masses showing agglomeration of glass grains and gels that are likely trapping the solution also were observed in these samples [57].

IDF1-B2CCC, which has the highest sodium content (38.4 cation% Na; see Table 2.1), had reached resumption before the sampling at 3274 days when the normalized boron release had more than doubled in the previous two years. It had reached 58 g/L and had plateaued at this value for the yearly sampling at 3634 days. Here again, it is likely that a large fraction of the liquid is immobilized in the alteration gel. Upcoming solid sampling and analysis will help verify this assumption.

IDF2-G9CCC, the high potassium glass, is actually higher than IDF1-B2 in total alkali content but it remains the most durable among this series of high alkali glasses (Na + K is 38.5 cation% in IDF1-B2 and 38.9 cation% in IDF2-G9 – see Table 2.1). At 3634 days of testing, it remains stable at about 8-10% alteration based on boron.

Finally, the lowest alteration is observed for the high zirconia glass IDF10-Zr6CCC (medium alkali), which remained at 6% altered glass (boron normalized release of 5.6 to 6.4 g/L) in the last fourteen samplings. Although this test was also difficult to sample in 2019, which may be the reason for the slight apparent decrease in normalized release, no difficulty in sampling was encountered this year. Solid evaluation [57] established the presence of zeolite on some grains of glass, but the sample has not yet reached resumption.

The ANL-LRM reference glass [63] continues to show a consistently high rate of alteration, with a higher rise at the last four samplings, with good reproducibility between replicates (now at 50±0.5 g/L boron normalized release, but replicates show larger spreads 15.6% RSD and 9.4% RSD for the two triplicate datasets).

3.3 Long-Term PCT-B at 40 °C and S/V of 2000 m^{-1} on IDF Phase 1 Glasses

At the lower test temperature of 40 °C, all ten IDF Phase 1 glasses and the ANL-LRM2 reference glass show much less alteration and none of the glasses have reached resumption over the period of testing, now reaching 10 years. As shown in Table 3.5 and Figure 3.3, the alterations remain nearly unchanged in the past six years of leach testing. Based on normalized boron release, for nine of the glasses, less than 0.5% to 3% of the glass has reacted, all remaining stable over the last few years. For IDF8-A125CCC, 10 to 11% of the glass had reacted at 900 days and the reaction appears to have stabilized at this level up to 3632 days as of the latest sampling. As shown in Figure 3.4, the normalized releases for the two alkalis (Na and K) follow the same trend but sodium shows a small deviation from congruence with boron (~8.6 g/L on average, unchanged over the last 7 years) and potassium is found at only a third of the boron release. As noted in the figure, the pH increased slowly at each successive sampling but dipped at the last sampling. A drop in pH is generally indicative of ongoing crystallization, likely an increase in the amount of phyllosilicates previously observed [57].

3.4 Long-Term PCT-B on IDF Phase 3 Glasses

3.4.1 Long-Term PCT-B on IDF Phase 3 Glasses at 90 °C and S/V of 20,000 m^{-1}

Five of the seven IDF Phase 3 glasses described in Section 2 were tested together in one PCT-B set at 90 °C and S/V of 20,000 m^{-1} designated ILHE. Glasses ORLEC52 and ORLEC28, in tests designated ILHF and ILHG, respectively, were tested at various S/V, including an S/V of 20,000 m^{-1}; the discussion herein compares the results from all seven glasses tested at S/V of 20,000 m^{-1}.

PCT leachate analyses up to two years are reported for these samples in Table 3.6. At this high temperature and high S/V, the leaching was already well beyond the early stages of alteration (inter-diffusion and hydrolysis) at the 7-day sampling reported shortly after immersion [56]. As

sampling proceeded through the first year, tests for glasses ORLEC46 and ORLEC50 were reduced from triplicate to duplicate after one month because the weight loss from one vessel in each triplicate exceeded 10% of the original leachant weight, the maximum acceptable per VSL procedure.

During the first 56 days [57], all seven glasses followed the "residual rate" regime depicted in Figure 1.1. At this high S/V of 20,000 m^{-1}, none of the ORLEC glasses exhibited early resumption as was the case for the Phase 1 glass IDF6-D6 (at 56 days). Because the IDF Phase 3 formulations are designed to span the range of alkali and sulfate concentrations for the high waste loading Hanford LAW glasses with glass formers defined by systematic functions, trends can be seen in the results of the leach tests. For example, as shown in Figure 2.2, Na_2O decreases as SO_3 increases in the series ORLEC34, ORLEC44, ORLEC46, and ORLEC48 while CaO increases with SO_3. As shown in Figure 3.5, the normalized boron releases for these glasses stabilize at levels that increase with alkali content in the glass. Conversely, the three higher alkali glasses, ORLEC28, ORLEC50, and ORLEC52, have similar CaO concentrations because they have similar ALK values; it is the difference in ZrO_2 and SnO_2 additions that are likely leading to the differences in leaching behavior.

During the following samplings, resumption was detected around 6-months in the four higher SO_3 glasses: ORLEC34, ORLEC44, ORLEC46, and ORLEC48 (Figure 3.6 – the last four characters of the glass names match the last four characters of the sample label). These are glasses in which SnO_2 was not used as a glass former additive and ZrO_2 was kept at relatively low concentrations of between 3.5 and 4 wt% since they are detrimental to sulfate solubility in the glass. Instead, the calcium content was increased with increasing SO_3 in these formulations. Leachates for these four tests reached maximum boron concentrations between 270 and 365 days, and, as previously observed in IDF Phase 1 and Phase 2 glasses with high calcium contents, boron leachate concentrations decreased thereafter. Leach vessels for these four glasses were disassembled to collect and analyze the solid phases present. Only about 20-25 ml out of the 40 ml starting leachate solution volume could be recovered from the vessel even though the total vessel mass remained the same. Glass, secondary phases, and some of the leachates had gelled together into a solid mass that occupied about the same volume as the original glass. The mixture was so hard that a core drill was needed to collect the solids for XRD and SEM analyses.

In contrast, the three high alkali glasses ORLEC28, ORLEC50, and ORLEC52 showed less than 25 g/L normalized boron release (<2.5% reacted per boron release) after a full year of testing, remaining in the residual rate regime at up to 270 days. A slight increase in normalized boron release was detectable at the 365-day sampling and continued throughout the second year. The largest increase was for glass IDF23-EC52 with the highest sodium content and high %RSD between replicates (shown by the arrows in Figure 3.6), indicating that resumption is ongoing at the two-year sampling for this glass. Results from the last sampling show a small increase in normalized release that could indicate that resumption is reached for glass ORLEC28. Sodium release follows a similar trend for all glasses: regardless of resumption, it remains at about 60 to 70% below congruence with boron. At 22 months, samples were taken from one of the leach vessels to identify the secondary phases associated with ongoing resumption.

Finally, as shown in Figure 3.7, pH measurements suggest that crystallization is taking place when resumption occurs. pH measured in the leachates for the four higher SO_3 glasses show drops of approximately half a pH unit, starting from the time of resumption, but the three, higher alkali glasses that did not show resumption continue to show slow increase in pH. The pH drop is an indicator of extensive crystallization during PCT-B [25, 74, 75].

3.4.2 Long-Term PCT-B on IDF Phase 3 Glasses at 90 °C and Various S/V

Glasses IDF23-EC52CCC and IDF24-C28CCC, in tests designated ILHF and ILHG, respectively, were tested at various S/V. All tests are conducted at 90 °C and five S/V of 1000, 2000, 5000, 10,000, and 20,000 m^{-1}, in triplicate. These two glasses are in the high alkali composition range, containing 23.80 wt% Na_2O, 0.50 wt% K_2O, and 0.90 wt% SO_3 for IDF23-EC52CCC, and 22.11 wt% Na_2O, 3.36 wt% K_2O, and 0.40 wt% SO_3 for IDF24-C28CCC. PCT leachate analysis for two years of testing are reported for these samples in Table 3.6, and for the ANL-LRM reference glass in Table 3.7.

The effect of variations in S/V on PCT releases can be seen in Figures 3.8 and 3.9 for glasses IDF23-EC52CCC and IDF24-EC28CCC, respectively. As suggested from previous tests on other waste glass formulations in long-term PCT [21], an increase in S/V produces an increase in leaching for the main glass components. Normalized boron release is shown as a function of time in Figures 3.8 and 3.9; similar trends are observed for Na, K, Re, and Si (see Table 3.6). Boron exhibits the highest release for both glasses, but it is lower in IDF24-EC28CCC, even close to resumption (the 2-year normalized boron release at S/V of 20,000 m^{-1} is 43 g/L in IDF24-EC28CCC versus 157 g/L in IDF23-EC52CCC). In IDF23-EC52CCC, PCT sodium release is about 3/4 of that of boron, potassium about 1/3, and silicon less than 10% of that of boron (Figure 3.10). Because boron leaches less in the higher potassium glass IDF24-EC28CCC, deviations from congruence are slightly lower (sodium release is about 80% of boron release, potassium 45 to 50% of boron, and silicon varies between 25% to 7% of boron (Figure 3.11)). These ratios remain similar throughout the two years of testing, except near resumption in the specific case of rhenium discussed below. The pH increased over the first four samplings (7 days to 120 days) and stabilized after 180 days, with little variation up to the last sampling (0.5% to 0.9%RSD).

Normalized releases of the main glass components and the rhenium spike are shown as a function of S/V in Figures 3.12 and 3.13 for the two glasses IDF23-EC52CCC and IDF24-EC28CCC, respectively. The values used to compile these graphs include data from the residual rate region only. Thus, points excluded from Figure 3.10 for glass IDF23-EC52CCC are the last sampling at 743 days for S/V of 10,000 m^{-1}, which appears to show a possible transition to resumption, and any sampling for S/V of 20,000 m^{-1} after 272 days. For glass IDF24-EC28CCC in Figure 3.11, the last sampling at 743 days for S/V of 20,000 m^{-1} was excluded. The releases show a power law relationship with S/V, which is in agreement with the previously demonstrated dependence with pH [21]. A more direct comparison between the present results and [21] is afforded by the behavior of the leachate pH itself, which is plotted for these two glasses against

log(S/V) in Figure 3.14. Very good linear relationships are evident and the slopes, which correspond to the power law exponent, are close to 2/3, as predicted in [21].

Rhenium is often used as a non-radioactive surrogate for Tc. Because Tc is a major contributor to the overall dose calculations in the IDF PA, it is important to understand the behavior of Tc as it relates to glass corrosion. For this reason, the release behavior of the 0.1 wt% Re_2O_7 spike from IDF23-EC52CCC and IDF24-EC28CCC was evaluated for all samplings between 7-days and 743-days and compared to the release behavior of the other components, as shown in Figures 3.10 and 3.11. Previously reported 7- and 28-day samplings showed that at the lowest S/V and 7-day sampling for IDF24-EC28CCC, rhenium release was nearly congruent to that of boron (0.55 g/L Re and 0.67 g/L B) but it quickly decreases to about 1/3 of that of boron (3.29 g/L Re and 9.47 g/L B), and close to the release of potassium (4.21 g/L) [56, 57]. As shown in the top part of Figure 3.10, these deviations from congruence remain true for all releases in the residual rate region. Similar near-congruence for IDF23-EC52CCC at S/V of 1000 m^{-1} (0.40 g/L Re and 0.58 g/L B) was observed at the 7-day sampling, which decreased to about 1/3 of boron at the 28-day sampling (0.65 g/L Re and 1.85 g/L B), close to the release of potassium (0.64 g/L). Evaluation of all leachates up to the 365-day sampling showed that normalized rhenium release remains well below 5 g/L while boron release rises to above 15 g/L. In this region, on average, rhenium release is 27% that of boron in IDF23-EC52CCC and 22% in IDF24-EC28CCC. Once resumption is reached, rhenium release returns to nearly congruent to that of boron, as shown in the lower part of Figure 3.10. This indicates that rhenium is not held in the phases that crystallized at resumption. However, releases of Na, K, and Si, which are constituents of such crystallized phases, remain low.

3.4.3 Al and Si in IDF Phase 3 Glasses

Al and Si are two constituents essential to the formation of the passivating gel layer and all aluminosilicate phases that crystallize during glass leach tests, . As shown in Figure 3.15, release of Si remains low (less than 18 g/L normalized release at S/V of 20,000 m^{-1} or equivalent to less than 1.8 % altered glass) and release of Al remains much lower (always below 0.8 g/L or 0.08 % altered glass). The low Si release can likely be explained by the reorganization of a reacted leached glass surface to gel layer and, over time, to phyllosilicates, and later by precipitation to zeolites. Al is equally essential to the formation of these phases with elemental fractions of Al much higher in zeolites than in phyllosilicates. The sharp drop in Al releases, at as early as 6-months, is indicative of ongoing aluminosilicate precipitation.

Sampling for evaluation of the glass leached layers after corrosion was conducted simultaneously with the 11th liquid sampling (651 or 652 days) of the seven IDF Phase 3 glasses, at the highest S/V of 20,000 m^{-1}.

SECTION 4.0
SECONDARY PHASE ANALYSIS OF IDF PHASE 3 PCT-B SAMPLES

In recent years, samples of solid phases have been collected from 28 ongoing PCT-Bs on IDF Phase 1 and Phase 2 glasses (8 glasses from tests ILHA and ILHB at 90 °C and S/V of 2,000 m^{-1}, 10 glasses from tests ILLA and ILLB at 40 °C and S/V of 2,000 m^{-1}, and 10 glasses from tests ILHC and ILHD at 90 °C and S/V of 20,000 m^{-1}) [56, 57]. This year, samples of the solid phases developed on IDF Phase 3 glasses were collected from the tests listed below. The sample nomenclature for glass powders after their sampling from a leach vessel is as follows: the glass ID followed by the vessel number and the sampling time. For example, IDF22-EC46 altered glass taken from vessel #4 at the 11^{th} time the leachate was sampled is designated as 22EC46-04-11. The altered glass samples collected and analyzed this year are as follows:

- From test set ILHE: Eleven samples from glasses tested at 90 °C and S/V of 20,000 m^{-1}, all having reached resumption over a year earlier:
    - 22EC46-04-11 and 22EC46-05-11
    - 25EC34-06-11, 25EC34-07-11 and 25EC34-08-11
    - 26EC44-09-11, 26EC44-10-11 and 26EC44-11-11
    - 27EC48-12-11, 27EC48-13-11 and 27EC48-14-11

  In addition, samples were collected of a white powdery deposit on the walls of the vessels, about ½ inch above the solid line in samples 22EC46-04-11 and 27EC48-14-11.

- From test sets ILHE, ILHF, and ILHG: Three small aliquots from glasses tested at 90 °C and S/V of 20,000 m^{-1} but before resumption:
    - 28EC50-16-11
    - 20K23EC52-15-11
    - 20K24EC28-15-11.

For the ILHE test sets, the vessels were disassembled and solids samples were collected. For the other three tests, a small amount of the altered glass was removed from one of the triplicate vessels (which was then so identified) and the tests were continued. Sampling was done in this manner to allow for the possibility that phases developed at the glass surface would be insufficiently crystallized for characterization and, therefore, later sampling would be required to identify the crystals. In the latter case, between 0.45 and 0.50 g of sample was taken out of a total of 40 g of glass per vessel in tests ILHE, ILHF, and ILHG. The powder was triple-rinsed with warm (near 90 °C) de-ionized water and dried prior to preparation for analysis by SEM/EDS and XRD. Evaluations completed and reported previously [56, 57], are provided in Tables 4.1 and 4.2, where earlier evaluations of IDF Phase 1 and Phase 2 glasses are also collected to complement and compare with the XRD and SEM findings described below for IDF Phase 3 glasses.

For low alteration glasses, SEM analyses where conducted following two different sample preparations of each collected altered glass sample: (1) Grains were mounted on a small carbon-impregnated tape to observe the morphology of crystallization; (2) The altered glass was embedded in epoxy and polished to expose a cross-sectional view in SEM. Since all of the most altered glass samples had agglomerated into a single mass, examination was possible only of the cross-section for the core-drilled samples. EDS spectra were acquired under 20 V accelerating voltage, 0.45 nA current, and 10 mm working distance. The data, given in atomic% (at%), are normalized to 100 at% with oxygen calculated by stoichiometry.

For XRD analysis, dried samples of altered glasses were crushed and then deposited onto a sample holder. This was necessary to avoid preferential crystal orientation, which would hinder phase identification by XRD. The amount collected for XRD was very small for some of the samples (due to agglomeration of the reacted glass sample in the leach vessel) and care was taken to avoid loss of material during grinding. Search matches were compared to XRD powder patterns previously reported [56, 57]; typical phases have included nontronite and saponite, smectites of the phyllosilicate mineral group, and, for glasses that have reached resumption, phillipsite, gobbinsite, and analcime (all zeolites of the tectosilicate mineral group) [15, 50].

In prior evaluation of IDF Phase 1 and Phase 2 glasses [50-52, 56, 57] that have reached resumption, the phases identified in the leached glass samples are tecto- or sorosilicates, as identified using XRD by well-defined sharp diffraction peaks. In SEM, structures that developed above the glass surface were observed. Phyllosilicates were less frequently identified in surface evaluation of IDF Phase 2 glasses in earlier samplings [52] but were clearly evident in cross-sectional evaluation of the EDS profiles [57]. In contrast, phyllosilicates were identified in IDF Phase 1 glasses (lower S/V tests), even when alteration remained low, together with tectosilicates in glasses that underwent resumption. One particular phase found in IDF Phase 1 and Phase 2 glass samples associated with severe alteration, and long after resumption, was a calcium silicate identified as tobermorite, classified as a phyllosilicate (2-D sheets) and often found in nature as the product of limestone weathering. This phase acts in the present case as a cementing material, binding together the altered glass grains and the zeolites that may have formed. It was found in altered glass originally containing 8 to 10 wt% CaO, added to improve SO_3 solubility (all with greater than 6 cation% Ca, Table 2.1) [57].

4.1 XRD Results

XRD powder patterns were collected and evaluated on samples from nine leach vessels testing IDF Phase 3 glasses. All were from tests at 90 °C and S/V of 20,000 m^{-1} in sets ILHE, ILHF, and ILHG.

28EC50-16-11, 20K24EC28-15-11, and 23EC52-15-11

The three high alkali glasses ORLEC28 (IDF24-EC28), ORLEC50 (IDF28-EC50), and ORLEC52 (IDF23-EC52) show the least alteration at 90 °C and S/V of 20,000 m^{-1} after 651 days of leaching (normalized boron release of 25 to 133 g/L). From the XRD powder patterns (Figure 4.1), these three glasses for which alterations remain in the range of 2 to 13% of the glass, show no sign of crystallization. No diffraction peak other than the broad feature typical of a borosilicate glass is visible in the three patterns shown in the figure.

25EC34-07-11 and 26EC44-10-11

XRD powder patterns of ORLEC34 (IDF25-EC34) and ORLEC44 (IDF26-EC44) glass alteration products are similar, with slight differences in the relative abundance of the various phases identified. Best matches in the XRD powder patterns of samples IDF25-EC34 (Figure 4.2) and IDF26-EC44 (Figure 4.3) were found for three zeolites: zeolite-SiO_2 (no formula provided), the zeolite $Na_6(Al_6Si_{10}O_{32})(H_2O)_{12}$, and two calcium-rich zeolites such as a chabazite-Ca ($Ca_2Al_4Si_8O_{24}.12H_2O$) in Figure 4.2, or phillipsite ($(Ca_{0.52}Na_{0.54})(K_{0.15}Li_4(Al_{5.92}Si_{10.08}O_{32})((H_2O)_{13.31})$) in Figure 4.3, which also contains lithium. These phases have been identified frequently in IDF Phase 1 and Phase 2 altered glass samples. In the IDF26-EC44 glass sample, a lower intensity pattern for nontronite ($Na_{0.3}Fe_2Si_4O_{10}(OH)_{2.4}H_2O$) is also observed.

22EC46-04-11 and 22EC46-05-11

XRD patterns from the two samples collected from the IDF22-EC46 glass test are compared in Figure 4.4. The plot on top shows the diffraction pattern collected from the white powdery deposit on the walls of vessel 22EC46-04-11. The diffraction pattern shows analcime $Na(AlSi_2O_6)(H_2O)$, a phillipsite, and tobermorite ($Ca_{2.25}(Si_3O_{7.5}(OH)_{1.5})(H_2O)$). The latter is a common calcium-rich hydrothermal alteration product that was also detected at prior samplings [50, 57]. This phase identification was not surprising since this glass is one of two with the highest CaO content among IDF Phase 3 glasses (along with ORLEC48, discussed below). This XRD pattern, which contains little to none of the rounded humps between 20 and 40° typical of the amorphous glass phase, indicates crystallization taking place from components available in solution.

The XRD pattern from the sample core-drilled out of the solid mass of altered material is given in the lower part of Figure 4.4. The two zeolites identified in this XRD powder pattern are identical to those found in the IDF26-EC44 sample: a lithium-rich phillipsite ($(Ca_{0.52}Na_{0.54})(K_{0.15}Li_4(Al_{5.92}Si_{10.08}O_{32})((H_2O)_{13.31})$) and the zeolite $Na_6(Al_6Si_{10}O_{32})(H_2O)_{12}$. In addition, the pattern of the zinc-rich phyllosilicate, sauconite $Na_{0.3}Zn_3(Si,Al)_4O_{10}(OH)_2.4H_2O$, is strong and its characteristic broad peaks indicate possible substitutions (for example Mg^{2+} in place of part of the Zn^{2+}) in the formula given in the match. Such substitutions lead to changes in unit

cell dimensions and the superposition of multiple substitutions gives the appearance of broader peaks for smectites.

27EC48-13-11 and 27EC48-14-11

The two samples collected from altered glass IDF27-EC48 (Figure 4.5) are very similar to those collected from glass IDF22-EC46. The diffraction pattern collected on the white powdery deposit from the walls of vessel 27EC48-14-11 shows analcime, possibly a second zeolite, and tobermorite. The XRD pattern from the core-drilled sample shows tobermorite along with a Ca-Li-phillipsite and the Zn-smectite sauconite.

The similarity in the secondary phases in the samples of the glasses IDF26-EC44, IDF22EC46, and IDF27-EC48 is not surprising since these three glasses are formulated with systematic increases in Ca and Li to accommodate higher SO_3 concentrations in the LAW glass.

4.2 SEM Evaluation

23EC52-15-11

In surface evaluation (Figure 4.6), the altered glass grains of IDF23-EC52 show very little alteration products with no detectable euhedral crystals and an extremely thin anhedral phase. At large magnification (Figure 4.6c), coating of a sub-micron phase can be seen on the glass grains. This coating is too thin to obtain an EDS spectrum but is likely a phyllosilicate based on its morphology.

In cross-section, a small fraction of the grains display an alteration layer, which in some cases (Figure 4.6f), can be as large as 10 μm. A detailed compositional profile was obtained from a line-scan of 62 EDS analyses provided in Figure 4.7. This reveals an uneven alteration layer around the glass grain from ~2-3 μm and up to 12 μm in thickness. In comparison to the core of the grain (the lighter grey in SEM micrograph), the alteration layer is depleted in sodium (14 at% in the glass and ~4 at% in the alteration layer) and enriched in silica and oxygen (oxygen possibly due to hydration). From the lower graph in Figure 4.7, it can be seen that Zr is enriched throughout to ~ 2.2 at% (vs. 1.3 at% in the glass). Ca shows the next largest increase, but in this case, the increase is highest near the interface of the pristine glass and the hydrated gel layer (around 12-13 μm) and slowly decreases towards the edge of the grain. At the outermost edge of the altered grain (last 1 μm), Mg and Zn are enriched. This is accompanied by a small depletion in Zr and a slight increase in Al.

In the unaltered glass, observed in lighter grey color in the SEM, the Al:Si ratio is at the expected ~1:3.3 ratio and the Na concentration remains constant. In the altered zone, Na decreases by about 70 relative percent while Si increases slightly to compensate for the change in Na and the ratio of Al:Si increases to ~1:6, similar to the ratio in many smectites identified by XRD in other

more altered glasses [56, 57]. However, multiple domains are observed in the sodium depleted zone. As described in Aréna *et. al.* [76], the zone closest to the glass defines the hydrated gel layer, which preferentially incorporates Ca. Aréna *et. al.* describe a high Ca gel versus high Mg/Fe crystalline phase but, in the present case, the crystallizing outer layer is enriched in Mg and Zn. Ca^{2+} can participate in gel network formation as a charge compensator for the $[AlO_4]^-$ and $[ZrO_6]^{2-}$ units. The Mg/Zn rich zone corresponds to a more crystallized phase of the smectite group with higher concentrations of M^{2+}, M^{3+}, and M^{4+} metals, which in the present case are Mg, Zn, Zr, and some remaining Ca (Table 4.3). Such metal substitutions, not uncommon in smectites, lead here to the empirical formula $(Na_{1.3},K_{0.1})(Mg_{0.3}Ca_{0.4}Zn_{0.3}Zr_{0.6})Al_{1.1}Si_{6.5}O_{18}$. Mg and Zn are further enriched in the last micron zone at the transition between the smectite and the solution; their role here is not clear but the fact that the Al content also nearly doubles to an Al:Si ratio of ~1:3 could indicate the approaching nucleation of a zeolite, concurrent with the nascent resumption observed in the leach data on glass IDF23-EC52.

28EC50-16-11

The altered glass grains of IDF28-EC50 appear to be relatively free of crystalline material on the surface (Figures 4.8 a-b). At high magnification (Figures 4.8 c-d), coating of the grains with a sub-micron phase with a morphology identifiable as phyllosilicate is observed.

In cross-section (Figures 4.8 e-f), a thin alteration layer of ~2-3 μm thickness (more rarely up to 10-12 μm) is seen at the surface of some glass grains, similar to what was observed in IDF23-EC52. One instance of a darker crystal was found (see left side of Figure 4.8f), which is likely a zeolite based on its EDS analysis (Al:Si ratio of ~1:2 for empirical formula close to $Na(AlSi_2O_6)(H_2O)$). Detailed compositional profiles across one particular grain are given in Figure 4.9. In this case, there appears to be a small half-moon shaped pocket of alteration near the pristine glass (the glass is pale grey in appearance at lower left in the SEM micrograph). In this zone of ~3 μm in thickness, the Na concentration decreases[5] and the Ca and Zr concentrations increase from the glass grain to the alteration gel layer. Ca and the remaining Na act here as preferential charge compensators for hydrated $[AlO_4]^-$ and $[ZrO_6]^{2-}$ in the hydrated gel [77]. A second more uniform alteration layer of ~10 μm thickness shows sodium depletion (62 relative % lower than in the glass) and enrichment in Zr and Ca, as observed in the previous zone, but with enrichments also in Mg and Zn. K, which is a minor constituent in this glass (~0.3 at%), remains unchanged from the glass through the alteration layer. Metals at low concentration in the glass, such as Cr, Ti, Fe, and Sn (~0.15 at%), are all enriched by ~40-55% in the outer most region. Finally, three glass components below detection limit in the altered layer (but clearly measured in the glass) are V, Cl, and S.

[5] Note here that the curvature in the profile for Na at the transition to the gel is probably due to the change in material density, causing a rounding of the polished surface and variation in the thickness of the carbon coating. The normalization of the results can frequently confuse the interpretation of the absolute significance of the concentrations when observing line-scans. The energy of the oxygen line is 0.525 keV, which is about half of the energy of the sodium line, 1.040 keV. Thus, an uneven carbon coating will absorb the oxygen line more strongly than the sodium line and the normalization function will make the sodium appear to increase in concentration even when it remains constant.

24EC28-15-11

Formulation IDF24-EC28 was designed for high-potassium waste and contains 3.36 wt% K_2O in addition to 22.11 wt% Na_2O (vs. 24 wt% Na_2O in IDF28-EC50 and IDF23-EC52). IDF Phase 1 and Phase 2 glasses IDF2-G9 and IDF11-G27, respectively are other glasses that have high K_2O concentrations. As was previously observed for other high-potassium glasses [56, 57], IDF24-EC28 is so far the most leach-resistant among IDF Phase 3 glasses tested under similar conditions (90 °C and S/V of 20,000 m^{-1}).

Altered glass grains of IDF24-EC28 appear relatively free of crystalline material on the surface (Figures 4.10 a-b). The micrographs reveal 70-150 μm glass powder, angular, relatively clean, and with smooth surfaces. Large magnification micrographs (Figures 4.10 c-d), display grains coated with a very thin layer of Na-aluminosilicate that is fibrous/acicular/flaky, likely a phyllosilicate. A few rare euhedral crystals are visible (Figure 4.10 d) but are too thin to obtain reliable EDS analysis, although some Al enrichment is noticeable in the small square crystal at the lower edge of Figure 4.10 d.

In cross-section (Figures 4.10 e-f), some grains show a few sites with alteration, which were analyzed further. First, a rounded pocket of alteration about 10 μm deep was evaluated through an EDS line-scan of 62 spectra, the results of which are given in Figure 4.11. Not shown in the figure are oxygen, calculated by stoichiometry to be around 60 at%, and Si which varies between 18.1 and 21.5 at% in the glass and altered zone, respectively. Silicon variation is likely a result of the 60% depletion in Na (down to 5 at% in the altered zone from 12 at% in the pristine glass). The concave curvature in the concentration profile for Na through the glass (~11.7 to 26 μm) is probably an artifact of polishing and slightly uneven carbon coating. The depleted zone in potassium (to ~8.3 μm) coincides with the depletion in sodium but is less extensive (only 28 relative% depletion). This is consistent with the PCT normalized releases (Figure 3.13) for K found at half that of Na, both indicating preferential retention of potassium in the alteration gel. Concurrent with alkali depletion, Zr and Ca are enriched (by 36% and 20%, respectively, in comparison to the glass concentration) between ~8.3 and 11.7 μm. Sn is also retained and enriched by 22 relative% in the altered area. Conversely, Zn, as well as the other transition metals in minor amounts, Ti, Cr, and Fe, remain unchanged until ~1-2 μm from the outer edge. Although too thin to differentiate clearly, this outermost layer seems to show a decrease in K and Ca, with a slight increase in Mg and some of the transition metals. This may be the sign of the gel evolving to a phyllosilicate in which these elements are frequently observed.

A second EDS line-scan was taken at higher magnification on a thinner layer of the alteration zone, with the results shown in Figure 4.12. The SEM micrograph reveals a gel of varied composition, as evident from the much varied density indicated by the change in the intensity of the gray color in the first 7.5 μm from the edge of the grain. Here again, a concave curvature in the profile for Na in the glass (~7.5 to 20.3 μm) is an artifact of polishing and slightly uneven carbon coating. Na concentration decreases from 12.3 at% in the glass to 6.9 at% in the region

from 1.3 to 5.2 µm where it is stable, before decreasing again towards the edge of the alteration zone. The composition changes indicate three zones in the altered glass:

(1) 5.2 to 7.5µm: The large Na depletion is accompanied by a slower depletion in K but enrichment in Zr and Ca. In this zone, Zn and Mg are also depleted.

(2) 1.3 to 5.2 µm: Na concentration remains constant, K continues to decrease slowly, Zr and Ca also decrease slightly, Zn is stable at a low concentration, and Mg is absent.

(3) 0 to 1.3 µm: Concentrations of Na, K, Zr, Ca, and Zn drop sharply but Al and Mg concentrations increase.

Zone (1) (between the two black dashed lines in Figure 4.12) represents the alteration front where H^+/alkali ion-exchange is taking place with Na, and with K to a lesser extent. The increase in Zr and Ca concentrations is evidence of gel formation incorporating both components and in which K incorporates somewhat better than Na but less so than Ca, as previously seen in other high level waste glasses [77]. The alteration gel extends to 1.3 µm from the surface (Zone (2) starting at the pink solid line) with a slow decrease in Ca and Zr and lower concentration of Zn. In the outermost Zone (3), sharp increases in Al and Mg concentrations indicate the crystallization of a Mg-rich phyllosilicate [74, 76]. This observation could not be confirmed at the present time because the phyllosilicate layer is still undetectable by XRD and, even though visible in SEM surface evaluation, it is too thin to verify its composition by EDS. Future solids samplings and analysis when glass alteration has progressed will allow better identification of the alteration phases.

25EC34-07-11

As shown in the SEM micrograph in cross-section (Figures 4.13 a-c), the core sample drilled from the solidified reacted glass IDF25-EC34 is composed of glass powder grains that are almost completely altered and bound together with other phases. Analcime is the major phase identified between glass grains. The grains seem to retain their original shape but appear to have a hollow core. A rare occurrence of remnant glass is observed in a glass grain shown on the micrograph in Figure 4.13 d. Six EDS analyses taken from this sample are summarized in a bar graph in Figure 4.13 e. Spectra 50, 51, and 52, all taken from the center of the grain, are averaged and are close in composition to the glass. Three very different zones are also observed (Spectra 53, 54, and 55) in which the Na content decreases the most the farther from the core. The striated region (Spectrum 53), which appears very porous, is highest in Al. The thin white region (Spectrum 54) appears denser and is highest in Zr. The outermost layer (Spectrum 55) is enriched in Mg, Ca, and Zn. Some elemental similarity remains in the alteration layer with EDS profiles presented earlier for less altered glasses but it is difficult to identify specific phases. However, it appears that the denser Zr-rich layer permitted retention of the glass grains once alteration proceeded and crystalline phases developed on both sides of this dense layer.

26EC44-10-11

Advanced alteration is seen in the core-drilled sample of IDF26-EC44 (Figure 4.14). Remnants of the glass grains are bound together with a mixture of heavily cracked zeolites and a calcium silicate hydrate (C-S-H) phase shown at the lower right edge of Figure 4.14 c (Spectrum 106).

The SEM micrograph taken in cross-section at the edge of a remnant glass grain (Figure 4.15) shows a multilayer structure. They show two zones, both with high Na and Ca contents, with possibly remnants of the glass structure. The very thin (sub-micron) layer at the outermost edge seems to have the highest Ca concentration but this EDS analysis could be influenced by the neighboring C-S-H phase. Behind this thin layer are various regions that appear denser and where Ca decreases and Zn, Zr, and Mg increase, indicative of a phyllosilicate phase.

22EC46-04-11 and 22EC46-05-11

An SEM micrograph of a white powder collected from the walls of the test vessel for glass IDF22-EC46 is shown in Figure 4.16 a. The SEM micrograph confirms previous XRD findings of analcime and tobermorite in previous samples from this test. Large icosahedral analcime particles of size up to 30-40 μm are inundated with the fibrous Ca-bearing phase. The core-drilled sample observed in cross-section (Figures 4.16 b-d) shows remnant grain shapes surrounded by fibrous crystals. EDS analysis indicates that this crystallization is C-S-H. In this series of formulations, the calcium content in the glass is increased from IDF26-EC44 to IDF22-EC46 to IDF27-EC48 to improve sulfate solubility. Higher Ca appears also to favor early resumption in PCT-B by formation of a large amount of the calcium-bearing phase tobermorite. XRD patterns of tobermorite were identified in IDF Phase 3 glasses sampled this year and for IDF Phase 1 and Phase 2 glasses sampled in 2015 and in 2018. The phases identified show various degrees of hydration and Ca/Si ratios: $(Ca_{2.25}(Si_3O_{7.5}(OH)_{1.5})(H_2O)$, $Ca_4(Si_6O_{15})(OH)_3(H_2O)_5$ [50] or $Ca_{4.9}(Si_{5.5}Al_{0.5}O_{16.3})(OH)_{0.7}(H_2O)_5$ [56, 57].

Figure 4.17 presents the EDS line-scan across the edges of two remnant glass grains and the phase in the middle that holds them together. This shows clear evidence of the Ca-rich phase (darker area in the SEM micrograph at the top of the page) binding the two remnant grains. As was the case with IDF26-EC44, at the edge of the grains, Ca drops sharply with increases in Zn and Mg, which together with Zr, form a shell of phyllosilicate phases with varying compositions.

27EC48-13-11 and 27EC48-14-11

SEM evaluation of IDF27-EC48 shows results very similar to those from IDF22-EC46. Designed for LAW glasses with the highest SO_3 contents, this formulation contains the highest CaO and Li_2O concentrations among the IDF Phase 3 glasses (8.14 wt% CaO and 2.58 wt% Li_2O).

The powder collected from the leach vessel walls (Figure 4.18 a) contains large analcime crystals and fibrous tobermorite. Remnant grains (Figure 4.18 b-d) are solidified with two types of phases identified by their EDS spectra as analcime (Figure 4.18 e) and C-H-S (Figure 4.18 f). The components remaining in the remnants of the glass particles are predominantly Si, Na, and Al, with considerable amounts of Ti, Zr, and Zn and trace amounts of of Cl, Mg, and K.

Zeolites observed in four IDF Phase 3 glasses after resumption remain close in composition, as evident from the EDS analyses summarized in Table 4.4. The compositions average to $Na_{7.1}Al_{9.8}Si_{21.4}O_{61.3}$ with minor contributions of Zn, and possibly Ca and Fe, which could also be contaminations from nearby phases.

PCT normalized boron releases for glasses IDF26-EC44, IDF22-EC46 and IDF27-EC48 indicate that resumption was reached within the first year of testing, after which the release plateaued around 60 to 70% of the total available boron. Although SEM/EDS analyses only show abundant calcium silicate gel that developed around the reacted particles, it is likely that the boron, undetectable in SEM/EDS, could be held within the C-S-H. Although calcium borate hydrates were identified during leaching of borosilicate glasses containing Ca [78, 79], no such phases were detected in the XRD spectra of the glasses from the present study.

4.3 Discussion of Solids Evaluation

The present evaluation of IDF Phase 3 altered glasses after long-term PCTs revealed two distinct zones of alteration and two crystalline phases, as discussed below.

(1) An alteration gel found at the front of hydration (closest to the unreacted glass), in which Na and K concentrations decrease, with Na decreasing much faster than K. This is accompanied by sharp increases in Ca and Zr. Other authors [76, 77] identified this zone as a gel layer in which Zr enhances the passivating role of the gel and Ca acts as a preferential charge compensator. It appears that K is also a preferred charge compensator since the gel is enriched in K as compared to Na in the altered glass sample of IDF24-EC28 with high K content. Similar observations were made for IDF Phase 1 (IDF2-G9) and IDF Phase 2 (IDF11-G27) glasses with high K contents, which are also the most leach resistant.

(2) Phyllosilicates have been observed in the three glasses (IDF24-EC28, IDF28-EC50, and IDF23-EC52), which have not reached resumption and remain in earlier stages of alteration after 2 years of PCT-B at 90 °C and S/V of 20,000 m^{-1}. They are observed in a range from ~2-3 μm and up to 12 μm thickness behind the gel. Even in glasses that have undergone resumption and that have been fully reacted for close to a year, phyllosilicates appear to remain in a thin crust identified in remnants of the glass grains, and XRD patterns indicate their likely presence among other phases. The phyllosilicates identified here for IDF Phase 3 glasses are members of the smectite clay mineral family. Although phases identified by XRD include nontronite ($Na_{0.3}Fe_2Si_4O_{10}(OH)_{2.4}H_2O$) or sauconite ($Na_{0.3}Zn_3(Si,Al)_4O_{10}(OH)_2.4H_2O$), SEM/EDS analyses indicated cation contributions to be mostly from Zr, Zn, Mg, and Ca, with

trace amounts of Cr, Fe, Ti, and Sn. Between the silicate sheets and various open sites that constitute phyllosilicates are present the divalent cations Mg^{2+} and Zn^{2+}. Isomorphic substitution of Zr^{4+}, which has a similar ionic radius to Mg^{2+} (radii of $^{VI}(Zr^{4+})$ = 0.72 Å, $^{VI}(Mg^{2+})$ = 0.72 Å) [80, 81] is observed as well. This is possible when hydration provides the required charge compensation. Swelling with interstitial water also permits accommodation of larger ionic species (K^+ 1.42 Å, Cs^+ 1.81 Å). These phyllosilicates appear to crystallize within the altered gel-layer that is formed during glass leaching, as evident from the progressive changes in composition seen in EDS analyses of glass grain cross-sections. As a result of boron release from the glass (likely replaced by water molecules) and sodium depletion, the layered intergrowth of micron to sub-micron sized smectite crystals is favored and keeps evolving as the hydration front progresses. The variety of interstitial metals, some with strong structural bonds such as Zr, probably contributes to the diffusion barrier and passivating character of the reacted gel layer and phyllosilicates. Ca and Mg often show opposite trends in concentration profiles. These are also signs of rearrangements taking place within the gel, in agreement with observations from natural weathering of igneous silicates into clay minerals by solid-state rearrangement [82-85].

(3) Calcium Silicate Hydrate (C-S-H) are nanocrystals formed in the system CaO-SiO_2-H_2O at variable stoichiometry, particularly at high pH. The calcium present in glass alteration is sourced here from the glass [44, 84] but other authors have shown similar phases may form from calcium in solution, particularly from cementitious water [78]. Ca, added to the glass formulation to improve SO_3 solubility, can play a beneficial role in the formation of the gel layer during early stages of alteration. C-S-H phases were found in high-Ca IDF Phase 3 glasses (IDF26-EC44, IDF22-EC46, and IDF27-EC48) and in multiple cases of IDF Phase 1 and Phase 2 glasses [56, 57]) associated with severe alteration, and long after resumption. Thus, Ca becomes detrimental at advanced stages of leaching since C-S-H was observed so far only in tests at 90 °C and S/V of 20,000 m^{-1}. This phase identified as tobermorite by XRD is classified as a phyllosilicate (2-D sheets) and often found in nature as the product of limestone weathering. It is also known in cement chemistry and indeed acts in the present case as a cementing material, binding together the altered glass grains and the zeolites that may have formed in leach Stage III after resumption.

(4) Zeolites are the crystals found in the glass alteration products in conjunction with leach Stage III (resumption). In contrast with smectite phases, zeolites are clearly identified in XRD by sharp well defined diffraction patterns characteristic of euhedral crystals. Their well-formed crystal faces are also clearly identifiable in SEM. Analcime dominates many of the XRD patterns collected from the most reacted glass samples, and is the main crystal identified in altered IDF Phase 3 glasses. In prior evaluation of IDF Phase 1 and Phase 2 altered glasses, zeolites of different morphologies were identified. These include phillipsite, chabazite, and gmelinite, based on the best phase matches to the XRD powder patterns [15, 52, 56]. However, these latter crystals are smaller, about one-fifth of the size of the analcime icosahedral crystals, which are frequently seen as large as ~50 μm in size. Tectosilicate crystals have been found in large quantities only in glasses that had reached resumption. It is likely that these crystals are concomitant with, and probably responsible for the resumption.

Although many transition metals can be found in site substitutions of phyllosilicates (e.g., Fe, Cr), vanadium is not found in significant quantity, even when its content exceeds that of Mg in glasses IDF25-EC34, IDF26-EC44, IDF22-EC46, and IDF27-EC48. Also, two glass constituents (S and Cl) are notably absent from any type of crystalline phase identified in long-term PCT and are only seen in the pristine glass and the hydrated gel.

SECTION 5.0
SUMMARY AND CONCLUSIONS

This report provides results of work performed to collect information on the corrosion behavior of LAW glasses to support the IDF PA. In addition to the development of the baseline operating envelope for the WTP, since 2003, VSL has been developing a wide range of LAW glass formulations that achieve considerably higher waste loadings than the WTP baseline formulations. As a result, the range of glass compositions that may be produced at the WTP is expanding toward higher sodium and sulfate contents and new glass forming additives, and this type of composition range expansion is likely to continue through the life of the project. In an initial effort (Phase 1), started to encompass the composition range expected to be disposed at the IDF, a total of 10 IDF Phase 1 glasses were selected for this composition expansion [15]. The selection was based on an analysis of the compositions and properties of the large number of LAW glasses that have been developed for the WTP at VSL. Those glasses were subjected to testing using the long-term PCT-B, and selected glasses were tested according to the SPFT method to determine rate law parameters. The Phase 1 program ended in 2011 but most long-term PCTs were maintained at VSL's expense. Work conducted under Phase 2 offered the opportunity to collect leachate data from those tests that were continued and to characterize the alteration phases [50, 57]. A second objective of the Phase 2 work was to extend the Phase 1 study by adding ten new high waste loading glasses in order to further span the expanded glass composition range, taking into consideration more recent high waste loading compositions that have been developed at the VSL. The IDF Phase 1 and Phase 2 glasses include compositions that are bounding with respect to performance on the WTP leach test specifications (PCT and VHT), that are higher in waste loading than the baseline WTP glasses, and that include variations in significant minor components such as sulfate and chlorine, as well as glass constituents that are not present in the baseline glasses. Both the IDF Phase 1 and Phase 2 series also include one glass each (IDF1-B2 and IDF15-A57, respectively) with a VHT response that exceeds the WTP contract limit.

Many of the long-term PCT-Bs initiated on IDF Phase 1 and Phase 2 glasses are ongoing and yet longer-term data will be collected. The most recent data show that among the ten IDF Phase 1 glasses tested at 90 °C and S/V of 2000 m^{-1}, seven are now over 50% reacted, including IDF1-B2, which plateaued at ~60% reacted, and one (IDF5-A20) showed a rising leach rate over the past years, which then plateaued at ~25% reacted. However, one of the two high-alkali glasses, IDF2-G9, and the high zirconia glass IDF10-Zr6 are still showing low leach rates of 9% and 6% reacted, respectively. In contrast, no change in alteration rate has been observed for the IDF Phase 1 glasses being tested at 40 °C and S/V of 2000 m^{-1}. Among the IDF Phase 2 glasses tested at 90 °C and S/V of 20,000 m^{-1}, two reached resumption within the first six months, two others and the reference glass ANL-LRM2 reached resumption within the first year, and two more reached resumption in FY18. Since then, a glass with high TiO_2 is now nearly fully reacted (IDF13-A51) and another, without MgO addition (IDF15-A57), has plateaued at around 30% reacted glass. Most recent to reach resumption was the glass without CaO addition, IDF16-A58.

Glasses reaching resumption at the earliest are generally low-zirconia glasses (less than 2 cation% Zr) with high alumina (above 9 cation% Al). All glasses that have reached resumption at the earliest time in each set of tests are found in the lower section of Figure 2.4, with low Zr concentrations of about 2 cation% or less. Since these are not the glasses with the highest alkali content, high-alkali alone is not the determining factor in the relatively rapid alteration. These are observations that can be used to improve the relative performance of glasses under the test conditions. However, the test conditions with higher temperatures (40 – 90 °C) and higher S/V are expected to lead to much faster glass alteration than under the conditions of storage at the IDF, where both the S/V in the event of water intrusion and the temperature are expected to be lower.

During FY18, PCT-Bs were started on seven glasses selected from those formulated to develop the Enhanced LAW Glass Correlation for high waste loading glasses [53-55]. All seven glasses are being tested at 90 °C and S/V of 20,000 m^{-1}. Two of the glasses are also being tested at 90 °C and S/V of 1000, 2000, 5000, 10,000, and 20,000 m^{-1}. All have now reached two full years of leach testing. The 7-day samplings showed that the PCT release results are consistent with results from prior testing of the same glasses without CCC heat treatment [53-55]. Results from 7-day to 743-day samplings of the tests at different S/V before resumption show that the PCT releases follow a power law function of S/V (see Figures 3.12 and 3.13), which was suggested by earlier observations on various HLW glasses [21]. Furthermore, the leachate pH shows very good linear relationships with log(S/V) and the slopes are in good agreement with the power law exponent of 2/3 as predicted in [21]. Thus, the steady-state pH directly correlates to the diffusion of alkali in Stage II leaching, where the rate is not simply decreasing with S/V by the effect of dilution. It is noted that these observations are for LAW glasses tested at 90 °C. Similar tests with variations in S/V at temperatures between 90 °C and 40 °C are recommended for future work since that would help identify changes in the time for resumption and phases formed on the glass surfaces with S/V and temperature. In particular, it would help identify the conditions that promote zeolite formation as pH and leachate compositions vary.

At S/V of 20,000 m^{-1}, four glasses have reached resumption at about six months of testing. Of the remaining three higher alkali formulations, one is undergoing resumption at the 2-year sampling, one is nearing resumption, and a third has still not shown signs of resumption. As previously seen in IDF Phase 1 and Phase 2 glasses, high-alkali alone is not the determining factor in reaching relatively rapid alteration at earlier time. The planned frequency of sampling after 365 days was at 547 days and yearly thereafter; however, the reaction may advance rapidly to resumption in that interval, particularly at the high S/V of 20,000 m^{-1}. For that reason, additional samplings were included in tests ILHE, ILHF, and ILHG for IDF Phase 3 glasses at 90-day intervals. Sampling every 90 days provided the opportunity to collect some of the altered glass samples for solids analyses at about the same time resumption occurred. For example, for glass IDF23-EC52, solid samples were collected for analysis at the same time as the 652-day sampling, which showed incipient resumption.

XRD and SEM/EDS evaluations of solid samples taken from the leach tests of IDF Phase 3 glasses confirmed and enhanced analyses from last year on IDF Phase 1 and Phase 2 glasses [56,

57], including samples from some of the tests at 40 °C. As before, XRD permitted identification of phases present on the glass surface, for the most part, tecto- and sorosilicates crystallizing on top of phyllosilicates covering the gel layer of glass alteration. The phyllosilicate phases observed are members of the smectite clay mineral family and encompass a broad range of compositions. Although both are aluminosilicate minerals, smectites and zeolites have very distinguishable features. Smectites are anhedral and zeolites are euhedral. SEM cross-sectional evaluation primarily defines smectites by their Si/Al elemental ratio in the range of 4 to 5, much higher than is found in zeolites, typically ~ 2 (see Tables 4.3 and 4.4). In smectites, SEM/EDS revealed an evolution of elemental profiles with enrichments in Zn and Mg in layers closest to the solution and higher Zr close to the hydration front towards the pristine glass. K, Ca, Sn, and Ti are also found in significant amounts in smectites. A parallel can be drawn to chemical weathering of igneous silicates in which solid-state rearrangement forms the clay minerals observed on their surface [74].

The phyllosilicate tobermorite was identified in previous XRD and SEM/EDS analyses of IDF Phase 1 and Phase 2 glass alteration products [56, 57]. Solids evaluation of IDF Phase 3 glasses also show this phase to be abundant in severely altered glass samples with high CaO content (above 5 wt%). This calcium silicate hydrate is also known in cement chemistry as C-S-H and appears in altered LAW glasses after resumption takes place. It acts as a cementing material, binding together the altered glass grains and the zeolites that may have formed while also consuming most of the free leachate.

Analcime is the zeolite identified most frequently in altered glass samples but others commonly observed are chabazite, phillipsite, and gmelinite. The morphology of some of these zeolite crystals identified in earlier samplings of the altered glasses [50, 56, 57] had been observed previously in Hanford LAW glass alteration products (long-term PCT, VHT). Zeolites have not yet been observed in the alteration products of the IDF Phase 3 higher alkali formulations, even though incipient resumption is observed from the PCT normalized releases for two of them. However, analcime of similar composition (Table 4.4) has been identified consistently in the alteration products from the four IDF Phase 3 high sulfate glass formulations. As noted before, the alteration products of IDF Phase 1 and Phase 2 glasses are of similar morphology to those previously identified in alteration of basaltic glass formed from volcanic activity 15 to 20 million years ago [83]. The alteration in these natural analogues results in the formation of various zeolites during hydrothermal alteration (<150 °C) under alkaline conditions and provides a good resource for identification of crystal morphologies observed in the present LAW glass samples.

5.1 Major Observations on Resumption from Leach Test Results

- Boron is generally used as the marker of glass matrix dissolution because it is typically neither retained in the alteration layers of the reacted glass nor forms secondary phases. However, in the case of glass leaching in tests at high pH and high calcium contents (from the glass or added to the solution), the formation of calcium silicates appears to trap a large part of the leachate volume and normalized

boron release plateaus at low release. Calcium borates have been observed in other work [79] but none have been identified in the present tests.

- Alkalis are network modifiers and are charge compensators for sites in the glass structure such as $[AlO_4]^-$ or $[ZrO_6]^{2-}$. Among alkalis, sodium releases show the smallest deviation from congruence with those of boron, while potassium and lithium releases generally remain lower than that of sodium and, in most cases, their releases fall well below that of boron.

- High sodium and/or potassium concentrations in the glass alone are not responsible for the occurrence of early resumption. Other glass constituents play essential roles.

- Aluminum normalized release remains generally low (~0.5 g/L) and stable and might rise to about 0.8 g/L within the first 2-3 months at high S/V but drops as zeolite start forming during resumption. Glasses high in alumina (> 9 cation% or Si/Al atomic ratio ≅ 3) are likely to reach resumption early.

- Glasses with low zirconia content (< 2 cation%) are likely to reach resumption early.

- Silicon, being the major constituent in the glass is easily measurable in leachates but remains much below congruence to boron. It is also the main network former of the gel in the alteration zone, and an essential constituent of most of the secondary phases that are formed.

5.2 Major Observations from Secondary Phase Analysis

Analysis of IDF Phase 3 glass alteration products show results that are similar to those obtained from the analysis of alteration products from IDF Phase 1 and Phase 2 glasses. In summary:

- Tectosilicates of the zeolite group (analcime predominantly, but also chabazite, phillipsite, and gmelinite) in which sodium is the dominant extra framework cation, crystallize on the altered glass when resumption is observed or is incipient, based on leachate analysis. Similar phases are found in samples collected from the walls of the leach vessel.
- High temperature (90°C, and previous tests at 120°C) and high S/V (20,000 m^{-1}) favor zeolite formation and earlier occurrence of resumption.
- No evidence of zeolite formation was observed at 40°C.
- Higher Li_2O and CaO concentrations are used in glasses formulated to accommodate higher sulfate contents because both of these components improve

sulfate solubility in the borosilicate glass. Alteration products from the leach tests of these glasses show a tobermorite gel that agglomerates the altered glass grains and the zeolites.

- Smectites of great diversity were observed to form at 40°C [57] and 90°C. Their compositions vary with glass composition, including in particular Zr, Sn, K, Na, Al, Fe, Zn, Ti, Ca, and Mg. These phases are characterized in LAW glass alteration products by an atomic ratio of Si/Al close to 5±1, with a progressive change in composition from the altered glass to the outer layer, indicating their formation by restructuring of the hydrated altered glass.
- Zr, and to a lesser extent, Sn, and Ti are found to remain in the altered glass gel and are enriched in the smectite layer. When smectites rich in Zr, Sn, and Ti are present in the alteration products, resumption is delayed.
- Fe, Ca, Mg, and Zn are also found in the smectites but only Zn-smectites appear to retard glass leaching. Ca and Mg appear to have similar and even synergistic roles in the smectites. However, Ca and Mg play very different roles in leaching and in alteration phases, as described below.

Contributions from five elements have been identified through evaluation of the alteration products from IDF Phase 3 altered glasses, indicating the role of these glass constituents:

- **Zr** is not present to any significant extent in the leachates. SEM/EDS evaluations show that it is entirely retained in two zones of alteration: (1) in the passivating gel layer where it densifies the gel by creating strong Si–O–Zr bonds [81], and (2) in phyllosilicates where its isomorphic substitution in octahedral sites collects hydration molecules for charge compensation. In both roles, Zr improves long-term leach resistance [30, 44, 81, 84].
- **Ca** is preferentially retained in the alteration gel developed at the interface between the glass and the front of alteration, as charge compensator to $[ZrO_6]^{2-}$ units. Together, Ca and Zr create a denser passivating gel layer in which silica and alumina continue to retain the structure they had in the glass, which delays the progress of hydrolysis. This decreases the residual rate, and this benefit in the early stage of alteration seems to be sustained for longer periods of time if Ca is present in the glass in moderate amounts (~2 wt% CaO). As glass leaching progresses, and with increasing pH, the passivation gel evolves as other elements (Mg, Zn) may take preferential roles in the formation of phyllosilicates. However, for compositions in which the concentration of Ca greatly exceeds that of Zr, precipitation of detrimental C-S-H may take place.
- **K** is retained in the gel and appears to reinforce its passivating properties in three glasses with high K contents that have been subjected to long-term PCT (IDF2-G9, IDF11-G27, and IDF27-EC28). Potassium can act as a charge compensator similar to Ca and since these formulations are low in Ca, some of the potassium can be

accommodated in that manner as well. Potassium can also incorporate into phyllosilicates. However, the beneficial role of potassium probably resides in its ability to stabilize the gel. This is a subject that deserves more attention in future work.

- **Zn and Mg** can be incorporated in the gel but not when competing with Ca. In that case, octahedral sites in phyllosilicates are more favorable for Zn and Mg. Phyllosilicates appear to be fairly stable in leach products, especially in combination with a dense Zr-rich gel; however, over time, phyllosilicates seem to weaken the alteration gel in long-term leaching. Small amounts of Al and Si that become available in solution may induce the growth of zeolites and destabilize the phyllosilicates layers.

Three new glass components added to increase waste loading in LAW glasses are V_2O_5 (for improved sulfate solubility), SnO_2 (for leach resistance at high alkali concentrations), and Cr_2O_3 (for resistance to K-3 refractory corrosion). Vanadium does not appear to contribute to secondary phase formation. Sn, and occasionally traces of Cr, are found in smectites but do not appear to alter the leaching behavior of glasses significantly.

The results from this study highlight the benefits of early investment in the initiation of LAW glass corrosion tests that are continued for long durations. This work has also benefited considerably from the periodic review of LAW compositions and glass testing results, and addition of new glasses and test conditions into the inventory of ongoing tests. The IDF Phase 1, 2, and 3 glasses are prime examples of this strategy. Accordingly, it is recommended that this process is continued and that additional glasses and test conditions are added in the next phase of this work.

SECTION 6.0
QUALITY ASSURANCE

This work was conducted under a quality assurance (QA) program compliant with the applicable criteria of 10 CFR 830.120; the American Society of Mechanical Engineers (ASME) Nuclear Quality Assurance (NQA)-1-2008 including NQA-1a-2009 addenda; and DOE Order 414.1D, Quality Assurance. These QA requirements are implemented through a Quality Assurance Project Plan (QAPP) for WRPS work [86] that is conducted at VSL. Test and procedure requirements by which the testing activities are planned and controlled are also defined in this plan. The program is supported by VSL standard operating procedures that were used for this work [87]. This is LAW work and is not subject to the requirements of DOE/RW-0333P, Office of Civilian Waste Management Quality Assurance Requirements and Description (QARD).

SECTION 7.0
REFERENCES

[1] "Experimentally Determined Dissolution Kinetics of Na-rich Borosilicate Glasses at Far-From-Equilibrium Conditions: Implications for Transition State Theory," J.P. Icenhower, B.P. McGrail, W.J. Shaw, E.M. Pierce, P. Nachimuthu, D.K. Shuh, E.A. Rodriguez, and J.L. Steele, *Geochimica Cosmochimica Acta* **72**, 2767-2788 (2008).

[2] "Measurement of Kinetic Rate Law Parameters on a Na-Ca-Al Borosilicate Glass for Low-Activity Waste," B.P. McGrail, W.L. Ebert, A.J. Bakel, and D.K. Peeler, *J. Nucl. Mater.* **249**, 175-189 (1997).

[3] "A Strategy to Conduct an Analysis of the Long-Term Performance of Low-Activity Waste Glass in a Shallow Subsurface Disposal System at Hanford," B.P. McGrail, W.L. Ebert, D.H. Bacon and D.M. Strachan, PNNL-11834, Pacific Northwest National Laboratory, Richland, WA, (1998).

[4] "Low-Activity Waste Glass Studies: FY2000 Summary Report," B.P. McGrail, J.P. Icenhower, P.F. Martin, D.R. Rector, H.T. Schaef, E.A. Rodriguez, and J.L. Steele, PNNL-13381, Pacific Northwest National Laboratory, Richland, WA (2000).

[5] "Waste Form Release Data Package for the 2001 Immobilized Low-Activity Waste Performance Assessment," B.P. McGrail, J.P. Icenhower, P.F. Martin, H.T. Schaef, M.J. O'Hara, E.A. Rodriguez, and J.L. Steele, PNNL-13043, Rev. 2, Pacific Northwest National Laboratory, Richland, WA (2001).

[6] "Laboratory Testing of Bulk Vitrified Low-Activity Waste Forms to Support the 2005 Integrated Disposal Facility Performance Assessment," E.M. Pierce, B.P. McGrail, L.M. Bagaasen, E.A. Rodriguez, D.M. Wellman, K.N. Geiszler, S.R. Baum, L.R. Reed, J.V. Crum, and H.T. Schaef, PNNL-15126, Rev. 2, Pacific Northwest National Laboratory, Richland, WA (2005).

[7] "Waste Form Release Data Package for the 2005 Integrated Disposal Facility Performance Assessment," E.M. Pierce, B.P. McGrail, E.A. Rodriguez, H.T. Schaef, K.P. Saripalli, R.J. Serne, K.M. Krupka, P.F. Martin, S.R. Baum, K.N. Geiszler, L.R. Reed, and W.J. Shaw, PNNL-14805, Pacific Northwest National Laboratory, Richland, WA (2004).

[8] "An International Initiative on Long-Term Behavior of High-Level Nuclear Waste Glass", S. Gin, A. Abdelouas, L.J. Criscenti, W.L. Ebert, K. Ferrand, T. Geisler, M.T. Harrison, Y. Inagaki, S. Mitsui, K.T. Mueller, J.C. Marra, C.G. Pantano, E.M. Pierce, J.V. Ryan, J.M. Schofield, C.I. Steefel and J.D. Vienna, *Materials Today* **16**(6) 243-248 (2013).

[9] Request for Off-Site Services (Technical) Statement of Work, "Parameterizing an ILAW Glass Ion Exchange Rate Model to Support the IDF PA," Rev. 0, Requisition #331831, Washington River Protection Solutions, LLC (WRPS), 09/17/19.

[10] "FY2018 Long-Term PCT of ILAW Glasses," I.S. Muller and I.L. Pegg, Test Plan, VSL-17T4510-1, Rev. 0, Vitreous State Laboratory, The Catholic University of America, Washington DC, 2/6/18.

[11] Request for Off-Site Services (Technical) Statement of Work, "ILAW Glass Durability Testing to Support the IDF PA - SPFT, PCT, Ion Exchange Model and Technical Support for ILAW Glass," Requisition #305361, Rev. 1, Washington River Protection *Solutions*, LLC (WRPS), 10/11/17.

[12] "An Experimental Study of the Dissolution Rates of Simulated Aluminoborosilicate Waste Glasses as a Function of pH and Temperature under Dilute Conditions," E.M. Pierce, E.A. Rodriguez, L.J. Calligan, W.J. Shaw, and B.P. McGrail, *Applied Geochemistry* **23**, 2559-2573 (2008).

[13] "A Strategy to Conduct an Analysis of the Long-Term Performance of Low-Activity Waste Glass in a Shallow Subsurface Disposal System at Hanford," J.J. Neeway, E.M. Pierce, V.L. Freedman, J.V. Ryan, and N.P. Qafoku, PNNL-23503, Rev. 0, Pacific Northwest National Laboratory, Richland, WA (2014).

[14] "Immobilized Low-Activity Waste Glass Release Data package for the Integrated Disposal Facility Performance Assessment," V.L. Freedman, J.V. Ryan and D.H. Bacon, PNNL-24615, RPT-IGTP-005, Rev. 0, Pacific Northwest National Laboratory, Richland, WA, September, 2015.

[15] "ILAW Glass Testing for Disposal at IDF: Phase 1 Testing," A.E. Papathanassiu, I.S. Muller, M. Brandys, K. Gilbo, A. Barkatt, I. Joseph and I.L. Pegg, VSL-11R2270-1, Rev. 0, Vitreous State Laboratory, The Catholic University of America, Washington, DC, 6/6/11.

[16] "The Activated Complex in Chemical Reactions," H. Eyring, *J. Chem. Phys.* **3**, 107-114 (1935).

[17] "Thermodynamic and Kinetic Constraints on Reaction Rates among Minerals and Aqueous Solutions. I. Theoretical Considerations," P. Åagaard and H.C. Helgeson, *Am. J. Sci.* **282**, 237-285 (1982).

[18] "A General Rate Equation for Nuclear Waste Glass Corrosion," B. Grambow, *Material Research Symposium Proceedings* **44**, 15-27 (1985).

[19] "Kinetic Ion Exchange Salt Effects on Glass Leaching," X. Feng and I.L. Pegg, *Energy, Environment and Information Management*, Eds. H. Wang, S. Chang, and H. Lee, Argonne, IL, p. 7-9, (1992).

[20] "Effects of Salt Solutions on Glass Dissolution," X. Feng and I.L. Pegg, *Phys. Chem. Glasses*, **35**, 1 (1994).

[21] "A Glass Dissolution Model for the Effects of S/V on Leachate pH," X. Feng and I.L. Pegg, J. *Non-Cryst. Solids*, **175**, 281 (1994).

[22] "Survey of Literature on the Role of Ion Exchange in Glass Corrosion," A.E. Papathanassiu, W. Gong, W. Lutze, and I.L. Pegg, Final Report, VSL-17L4320-1, Rev. 0, Vitreous State Laboratory, The Catholic University of America, Washington DC, 8/2/17.

[23] "A Critical Review of Ion Exchange in Nuclear Waste Glasses to Support the Immobilized Low-Activity Waste Integrated Disposal Facility Rate Model," C.E. Lonergan, J.J Neeway, RPT-IGTP-018, Rev 0.0, Pacific Northwest Laboratory, Richland, WA, 09/13/2017.

[24] "FY 2019 ILAW Glass Ion Exchange Rate Testing," I.S. Muller, C. Viragh, K. Gilbo, and I.L. Pegg, Final Report, VSL-20R4820-2, Rev. 0, Vitreous State Laboratory, The Catholic University of America, Washington DC, 4/27/20.

[25] "Characterization of Alteration Phases on HLW Glasses after 15 Years of PCT Leaching," I.S. Muller, S. Ribet, I.L. Pegg, S. Gin, and P. Frugier, *Ceramic Transactions*, Vol. 176, p.191 (2005).

[26] "Long-Term PCT Data for LAW Glasses," I.S. Muller, D.A. McKeown, X. Xie, I.L. Pegg, and I. Joseph, Final Report, VSL-17R4090-1, Rev. 0, Vitreous State Laboratory, The Catholic University of America, Washington, DC, 05/30/17.

[27] "Dissolution and Precipitation Kinetics of Sheet Silicates," K.L. Nagy, *Reviews in Mineralogy and Geochemistry*, **31**, 173-233, Mineralogical Society of America, Chantilly, VA (1995).

[28] "Letter: Simultaneous Precipitation Kinetics of Kaolinite and Gibbsite at 80°C and pH 3," K.L. Nagy, and A.C. Lasaga, *Geochimica et Cosmochimica Acta* **57**, 4329 – 4335 (1993).

[29] "Preliminary Results of Durability Testing with Borosilicate Glass Compositions," M. Adel-Hadadi, R. Adiga, Aa. Barkatt, X. Feng, I.L. Pegg, et al., Tech. Info. Center, Office of Sci. and Tech. Info., USDOE, DOE/NE/44139-34, (1988).

[30] "Compositional Effects on Chemical Durability and Viscosity of Nuclear Waste Glasses – Systematic Studies and Structural Thermodynamic Models," X. Feng, Ph.D. Thesis, The Catholic University of America (1988).

[31] "Leach Rate Excursions in Borosilicate Glasses: Effects of Glass and Leachant Composition," Aa. Barkatt, S.A. Olszowka, W. Sousanpour, M.A. Adel-Hadadi, R. Adiga, Al. Barkatt, G.S. Marbury, and S. Li, Mat. Res. Soc. Symp. Proc., 212, 65 (1991).

[32] "Alteration Layers on Glasses After Long-Term Leaching," A.C. Buechele, S.T.- Lai, and I.L. Pegg, *Ceramic Transactions*, Eds. D.K. Peeler and J.C. Marra, vol. 87, p. 423, American Ceramic Society (1998).

[33] "Compositional Effects on the Long-Term Durability of Nuclear Waste Glasses: A Statistical Approach," S. Ribet, I.S. Muller, I.L. Pegg, S. Gin, and P. Frugier, Mat. Res. Soc. Symp. Proc. Vol. 824 (2004).

[34] "The Long-Term Corrosion and Modeling of Two Simulated Belgian Reference High-Level Waste Glasses – Part II," J. Patyn, P. Van Iseghem, and W. Timmermans, Mat. Res. Symp. Soc. Proc., 176, 299 (1990).

[35] "New Insight into the Residual Rate of Borosilicate Glasses: Effect of S/V and Glass Composition", S. Gin, P. Frugier, P. Jollivet, F. Bruguier, E. Curti, Int. J. Appl. Glass Sci., 4, 371-382 (2013).

[36] "Nuclear Glass Durability: New Insight into Alteration Layer Properties," S. Gin, C. Guittonneau, N. Godon, D. Neff, D. Rebiscoul, M. CabieS. Mostefaoui, J. Phys. Chem. C 115, 18696-18706, (2011).

[37] "Multi-Glass Investigation of Stage III Glass Dissolution Behavior from 22 to 90° C Triggered by the Addition of Zeolite Phases," B. Parruzot, J.V Ryan, J.L. George, R.K. Motkuri, J.F. Bonnett, L.M. Seymour, and M.A. Derewinski, J. Nucl. Mater. 523 (2019) 490–501.

[38] "Origin and Consequences of Silicate Glass Passivation by Surface Layers", S. Gin, P. Jollivet, M. Fournier, F. Angeli, P. Frugier, T. Charpentier, Nat. Commun., 6 (2015).

[39] "The Fate of Silicon During Glass Corrosion Under Alkaline Conditions: A Mechanistic and Kinetic Study with the International Simple Glass," S. Gin, P. Jollivet, M. Fournier, C. Berthon, Z. Wang, A. Mitroshkov, Z. Zhu, J. V. Ryan, Geochim. Cosmochim. Acta, 151, 68–85 (2015).

[40] "Resumption of Nuclear Glass Alteration: State of the art," M. Fournier, S. Gin, P. Frugier, J. Nucl. Mater., 448, 348–363 (2014).

[41] "Open Scientific Questions About Nuclear Glass Corrosion," S. Gin, Procedia Materials Science, 163-171 (2014).

[42] "Current Understanding and Remaining Challenges in Modeling Long-Term Degradation of Borosilicate Nuclear Waste Glasses," J.D. Vienna, J.V. Ryan, S. Gin, and Y. Inagaki, Int. J. Appl. Glass Sci., 4, 283–294 (2013).

[43] "Contribution of Atom-Probe Tomography to a Better Understanding of Glass Alteration Mechanisms: Application to a Nuclear Glass Specimen Altered 25 years in a Granitic Environment," S. Gin, J.V. Ryan, D.K. Schreiber, J. Neeway, and M. Cabie, Chem. Geol. 349, 99–109 (2013).

[44] "Effect of Composition on the Short-Term and Long-Term Dissolution Rates of Ten Borosilicate Glasses of Increasing Complexity from 3 to 30 Oxides", S. Gin, X. Beaudoux, F. Angeli, C. Jegou, N. Godon, J. Non-Cryst. Solids, 358, 2559–2570 (2012).

[45] "Development of the Vitrification Compositional Envelope to Support Complex-Wide Application of MAWS Technology," I.S. Muller, H. Gan, A.C. Buechele, S.T. Lai, and I.L. Pegg, DOE/CH-9601, September 1996.

[46] "Alteration Phases on High Sodium Waste Glasses after Short- and Long-Term Hydration," A.C. Buechele, S.-T. Lai, and I.L. Pegg, *Ceramic Transactions*, vol. 107, p. 251 (2000).

[47] "Waste Loading Enhancements for Hanford LAW Glasses," I.S. Muller, K.S. Matlack, H. Gan, I. Joseph, and I.L. Pegg, Final Report, VSL-10R1790-1, Rev. 0, Vitreous State Laboratory, The Catholic University of America, Washington, DC, 12/01/10.

[48] "Improved High-Alkali Low-Activity Waste Formulations," I.S. Muller, M. Chaudhuri, H. Gan, A. Buechele, X. Xie, I.L. Pegg, and I. Joseph, Final Report, VSL-15R3290-1, Rev. 0, Vitreous State Laboratory, The Catholic University of America, Washington, DC, 08/12/15.

[49] "Enhanced LAW Glass Property-Composition Models – Phase 2," I.S. Muller, K. Gilbo, I. Joseph, and I.L. Pegg, Final Report, VSL-14R3050-1, Rev. 0, Vitreous State Laboratory, The Catholic University of America, Washington, DC, 8/29/14.

[50] "FY15 ILAW Glass Testing for Disposal at IDF," I.S. Muller, and I.L. Pegg, VSL-15R3790-1, Rev. 0, Vitreous State Laboratory, The Catholic University of America, Washington, DC, 4/15/16.

[51] "FY2016 Update on ILAW Glass Testing for Disposal at IDF," I.S. Muller, and I.L. Pegg, VSL-16S4170-1, Rev. 0, Vitreous State Laboratory, The Catholic University of America, Washington, DC, 2/1/17.

[52] "LAW Glass Testing by Long-Perm PCT to Support Disposal at IDF," I.S. Muller, and I.L. Pegg, VSL-17R4320-1, Rev. 0, Vitreous State Laboratory, The Catholic University of America, Washington, DC, 9/28/17.

[53] "Enhanced LAW Glass Correlation – Phase 1," I.S. Muller, K. Matlack, I.L. Pegg and I. Joseph," Final Report, VSL-16R4000-1, Rev. 0, Vitreous State Laboratory, The Catholic University of America, Washington, DC, 12/01/16.

[54] "Enhanced LAW Glass Correlation – Phase 2," I.S. Muller, K. Matlack, I.L. Pegg and I. Joseph," Test Plan, VSL-17R4140-1, Rev. 0, Vitreous State Laboratory, The Catholic University of America, Washington, DC, 6/30/17.

[55] "Enhanced LAW Glass Correlation – Phase 3," I.S. Muller, K. Matlack, I.L. Pegg and I. Joseph," Test Plan, VSL-17R4230-1, Rev. 0, Vitreous State Laboratory, The Catholic University of America, Washington, DC, 11/15/17.

[56] "FY2018 Long-Perm PCT of ILAW Glasses," I.S. Muller, and I.L. Pegg, VSL-18R4510-1, Rev. 0, Vitreous State Laboratory, The Catholic University of America, Washington, DC, 12/19/18.

[57] "FY2019 Long-Perm PCT of ILAW Glasses," I.S. Muller, and I.L. Pegg, VSL-19R4620-1, Rev. 0, Vitreous State Laboratory, The Catholic University of America, Washington, DC, 09/30/19.

[58] "FY2016 ILAW Glass SPFT Testing for Disposal at IDF," A.E. Papathanassiu, C. Viragh, I.S. Muller, and I.L. Pegg, VSL-17R3860-1, Rev. 0, Vitreous State Laboratory, The Catholic University of America, Washington, DC, 7/12/17.

[59] "FY2016 ILAW Glass Corrosion Testing with the Single-Pass Flow-Through Method," J.J. Neeway, R.M. Asmussen, B.P. Parruzot, E.A. Cordova, B.D. Williams, I.L. Leavy, J.R. Stephenson, and E.M. Mcelroy, PNNL-26169, RPT-IGTP-013 Rev. 0.0, Pacific Northwest National Laboratory, Richland, WA (2017).

[60] "FY2017 ILAW Glass Corrosion Testing with the Single-Pass Flow-Through Method," J.J. Neeway, R.M. Asmussen, E.A. Cordova, C.E. Lonergan, B.D. Williams, I.L. Leavy, and E.M. McElroy, PNNL-27098, RPT-IGTP-015, Rev. 0, Pacific Northwest National Laboratory, Richland, WA, February, 2018.

[61] "FY2017 ILAW Glass SPFT Testing for Disposal at IDF: Glass IDF21-EC14," C. Viragh, H. Abramowitz, I.S. Muller, A. E. Papathanassiu, and I.L. Pegg, VSL-17R4320-2, Rev. 0, Vitreous State Laboratory, The Catholic University of America, Washington, DC, 2/27/18.

[62] "FY2018 ILAW Glass SPFT Testing for Disposal at IDF: Glasses ORLEC46 and ORLEC52," C. Viragh, H. Abramowitz, I.S. Muller, A. E. Papathanassiu, and I.L. Pegg, VSL-18R4510-2, Rev. 0, Vitreous State Laboratory, The Catholic University of America, Washington, DC, 12/27/18.

[63] "Round Robin Testing of a Reference Glass for Low-Activity Waste Forms," W.L. Ebert and S.F. Wolf, Department of Energy Report ANL-99/22, Argonne National Laboratory, Argonne, IL (1999).

[64] "Enhanced LAW Glass Formulation Testing," K.S. Matlack, I. Joseph, W. Gong, I.S. Muller, and I.L. Pegg, Final Report, VSL-07R1130-1, Rev. 0, Vitreous State Laboratory, The Catholic University of America, Washington, DC, 10/05/07.

[65] "Glass Formulation Development and DM10 Melter Testing with ORP LAW Glasses," K.S. Matlack, I. Joseph, W. Gong, I.S. Muller, and I.L. Pegg, Final Report, VSL-09R1510-2, Rev. 0, Vitreous State Laboratory, The Catholic University of America, Washington, DC, 6/12/09.

[66] "Improving Technetium Retention in Hanford LAW Glass – Phase 1," K.S. Matlack, I.S. Muller, I. Joseph and I.L. Pegg, Final Report, VSL-10R1920-1, Rev. 0, Vitreous State Laboratory, The Catholic University of America, Washington, DC, 03/19/10.

[67] "Glass Formulation Testing to Increase Sulfate Incorporation," K. S. Matlack, M. Chaudhuri, H. Gan, I.S. Muller, W. Gong, and I.L. Pegg, Final Report, VSL-04R4960-1, Rev. 0, Vitreous State Laboratory, The Catholic University of America, Washington, DC, 2/28/05.

[68] "Proposed Approach for Development of LAW Glass Formulation Correlation," I.S. Muller, G. Diener, I. Joseph, and I.L. Pegg, Letter Report, VSL-04L4460-1, Rev. 2, Vitreous State Laboratory, The Catholic University of America, Washington, DC, 10/29/04.

[69] "LAW Container Centerline Cooling Data," RPP-WTP Memorandum, L. Petkus to C. Musick, CCN# 074181, River Protection Project−Waste Treatment Plant, Richland, WA, 10/16/03.

[70] "Glass Formulation and Testing with TWRS LAW Simulants," I.S. Muller, I.L. Pegg, A.C. Buechele, H. Gan, C. Kim, S.T. Lai, G. Del Rosario and Q. Yan, Final Report, VSL-10R1790-1, Rev. 0, Vitreous State Laboratory, The Catholic University of America, Washington, DC, 1/16/1998.

[71] "Role of Neoformed Phases on the Mechanisms Controlling the Resumption of SON68 Glass Alteration in Alkaline Media", S. Ribet and S. Gin, Journal of Nuclear Materials **324,** 152-164 (2004).

[72] "Aqueous Alteration of Japanese Simulated Waste Glass P0798: Effects of Alteration-Phase Formation on Alteration Rate and Cesium Retention" Y. Inagaki, A. Shinkai, K. Idemistu, T. Arima, H. Yoshikawa, M. Yui, J. Nucl. Mater. 354 (2006) 171–184.

[73] "Standard Test Methods for Determining Chemical Durability of Nuclear, Hazardous, and Mixed Waste Glasses and Multiphase Glass Ceramics: The Product Consistency Test (PCT)," ASTM C 1285-14, American Society for Testing and Materials, West Conshohocken, PA, 2014.

[74] "SON68 glass dissolution driven by magnesium silicate precipitation" B. Fleury, N. Godon, A. Ayral, S. Gin, Journal of Nuclear Materials 442 (2013) 17–28.

[75] "Impact of Zn, Mg, Ni and Co elements on glass alteration: Additive Effects," H. Aréna, N. Godon, D. Rébiscoul, R. Podor, E. Garces, M. Cabie, J.-P. Mestre Journal of Nuclear Materials 470, 55-67 (2016).

[76] "Impact of Fe, Mg and Ca elements on glass alteration: Interconnected process," H. Aréna, D. Rébiscoul, R. Podor, E. Garces, M. Cabie, J.-P. Mestre, N. Godon, Geochim. Cosmochim. Acta, 239, 420–445 (2018).

[77] "Comparative effect of alkaline elements and calcium on alteration of International Simple Glass," H. Aréna, D. Rébiscoul, E. Garces, N. Godon, npj Materials Degradation 3:10 (2019).

[78] "Etude des mécanismes d'altération du verre par des eaux cimentaires," Sara Depierre, Doctoral Dissertation, Montpellier II University, 345 p. (2012).

[79] "Antagonist effects of calcium on borosilicate glass alteration," S. Mercado-Depierre, F. Angeli, F. Frizon, S. Gin, Journal of Nuclear Materials, 441, 402-410 (2013).

[80] "Synthetic Smectite Colloids: Characterization of Nanoparticles after Co-Precipitation in the Presence of Lanthanides and Tetravalent Elements (Zr, Th)," M Bouby, N. Finck and H. Geckeis, *Chromatography* 2015, *2*, 545-566.

[81] "First Investigations of the Influence of IVB Elements (Ti, Zr, and Hf) on the Chemical Durability of Soda-lime Borosilicate Glasses," B. Bergeron, L. Galoisy, P. Jollivet, F. Angeli, T. Charpentier, G. Calas and S.Gin, *Journal of Non-Crystalline Solids*, 356, 2315-2322 (2010).

[82] "Soil and Environmental Chemistry (2nd Edition), Chapter 3: Clay Mineralogy and Chemistry," William Bleam, ISBN 9780128041789, Pages 87-146, Academic Press, 2017.

[83] D. B. Hawkins, "Kinetics of Glass Dissolution and Zeolite Formation Under Hydrothermal Conditions," December 1980 Clays and Clay Minerals 29(5):331-340 (1981).

[84] "Influence of zeolite precipitation on borosilicate glass alteration under hyperalkaline conditions," S. Mercado-Depierre, M. Fournier, S. Gin, F. Angeli, F. Frizon, J. Nuclear Materials, 491, 67-82 (2017).

[85] "Influence de la morphologie du gel sur la cinétique d'altération des verres nucléaires: rôle du calcium et du zirconium," C. Cailleteau, Doctoral Dissertation, Ecole polytechnique de Paris (2008).

[86] "Quality Assurance Project Plan for WRPS Support Activities Conducted by VSL," Vitreous State Laboratory, QAPP-WRPS, Rev. 5, Vitreous State Laboratory, The Catholic University of America, Washington, DC, 9/30/19.

[87] "Master List of Controlled VSL Manuals and Standard Operating Procedures in Use," QA-MLCP, Rev. 174, Vitreous State Laboratory, The Catholic University of America, Washington, DC, 9/28/20.

Table 1.1. Target Compositions of the Ten IDF Phase 1 Glasses (wt%).

Glass ID	IDF1-B2[#]	IDF2-G9[#]	IDF3-F7[#]	IDF4-A15	IDF5-A20	IDF6-D6	IDF7-E12[#]	IDF8-A125	IDF9-A187	IDF10-4HZr
Tank	AN-107	AP-101	AZ-102	AN-105	AN-105	AN-102	AZ-101	AP-101	AN-105	AN-105
Loading	27%	29%	15%	31%	31%	26%	20%	27%	30%	28%
Al_2O_3	10.00	6.76	8.65	9.45	6.65	10.09	7.58	5.64	10.57	4.95
B_2O_3	7.30	8.51	9.53	8.60	8.74	9.85	9.82	9.55	12.77	11.77
CaO	1.10	2.70	9.77	3.32	3.32	7.89	10.02	1.94	6.47	2.43
Cr_2O_3	0.52	0.59	0.56	0.49	0.50	0.50	0.50	0.02	0.52	0.08
Cs_2O spike	0.15	-	-	0.14	-	-	0.15	0.18	-	-
Fe_2O_3	1.10	0.20	0.23	0.92	0.19	0.28	0.24	5.39	0.90	6.70
K_2O	0.12	5.76	0.50	0.54	0.53	0.17	0.55	4.21	0.51	0.54
Li_2O	-	-	4.37	-	-	-	2.49	-	-	-
MgO	1.10	0.96	0.98	0.92	0.92	1.00	1.04	1.44	0.90	1.45
Na_2O	25.00	21.00	12.00	24.00	24.00	22.00	16.00	20.00	23.00	21.27
NiO	0.04	0.01	-	-	-	0.04	-	-	-	0.01
PbO	-	0.01	-	-	-	0.01	-	-	-	0.01
SiO_2	39.88	40.82	42.38	39.17	42.24	37.14	41.19	42.81	34.70	38.89
SnO_2	1.08	2.84	-	2.73	2.74	-	-	-	1.00	-
TiO_2	-	-	-	-	-	-	-	1.94	-	-
V_2O_5	2.00	-	2.50	-	-	1.96	1.74	-	0.97	-
ZnO	3.65	3.40	2.92	2.43	2.74	2.96	3.21	2.88	2.99	1.50
ZrO_2	5.44	5.68	3.92	5.91	5.96	3.98	3.53	2.91	2.99	9.50
Cl	0.11	0.23	0.01	0.68	0.67	0.35	0.02	0.22	0.64	0.20
F	0.49	0.09	0.08	0.00	0.00	0.18	0.20	0.32	-	0.08
P_2O_5	0.23	0.14	0.04	-	-	0.30	0.12	0.08	-	0.12
SO_3	0.52	0.20	1.50	0.60	0.70	1.20	1.50	0.37	0.95	0.41
Re_2O_7 Spike	0.10	0.10	0.10	0.10	0.10	0.10	0.10	0.10	0.10	0.10
MnO_2	0.06	-	-	-	-	-	-	-	-	-
Sum	100.0	100.0	100.0	100.0	100.0	100.0	100.0	100.0	100.0	100.0

- Empty data field
[#] SPFT tested

Table 1.2. Target Compositions of the Ten IDF Phase 2 Glasses (wt%).

Glass ID	IDF11-G27	IDF12-A38	IDF13-A51	IDF14-A59	IDF15-A57	IDF16-A58	IDF17-A60	IDF18-A161[#]	IDF19-C100	IDF20-F6
Tank	AP-101	AN-105	AN-105	AN-105	AN-105	AN-105	AN-105	AN-105	AN-102	AZ-102
Loading	29%	32%	31.52%	31.52%	31.52%	31.52%	31.52%	26%	24%	16.06%
Al_2O_3	6.03	6.94	10.15	10.31	10.65	10.65	6.75	10.04	10.16	8.48
B_2O_3	7.92	8.21	8.02	8.15	8.05	8.75	8.87	13.51	13.68	9.36
CaO	2.69	3.12	1.00	1.02	1.50	-	3.37	7.90	8.02	9.58
Cr_2O_3	0.59	0.49	0.02	0.02	0.02	0.02	0.51	0.02	0.02	0.56
Cs_2O spike	-	-	-	-	-	-	-	0.15	-	-
Fe_2O_3	0.28	0.26	0.19	0.19	0.05	0.25	0.19	0.99	1.00	0.29
K_2O	5.75	0.53	0.530	0.53	0.53	0.53	0.53	0.44	0.15	0.54
Li_2O	-	-	-	-	-	-	-	-	-	3.45
MgO	0.44	0.98	1.93	1.96	-	1.55	0.93	0.99	1.00	0.97
Na_2O	21.00	24.00	24.00	24.00	24.00	24.00	24.00	20.66	20.00	13.00
NiO	0.01	-	-	-	-	-	-	-	0.03	-
PbO	0.01	-	-	-	-	-	-	-	0.01	-
SiO_2	42.00	41.52	38.93	39.55	40.73	40.78	42.75	36.05	36.52	42.28
SnO_2	3.19	2.66	1.00	1.02	-	-	2.78	-	-	0.84
TiO_2	-	-	4.00	4.06	3.00	3.00	-	-	-	-
V_2O_5	-	0.91	-	-	-	-	-	0.99	1.00	2.47
ZnO	2.69	2.80	2.80	2.84	4.00	3.00	2.78	2.95	3.00	2.87
ZrO_2	6.44	6.00	5.96	6.05	6.00	6.00	6.05	2.95	3.00	3.83
Cl	0.23	0.67	0.67	0.10	0.67	0.67	0.10	1.17	0.65	0.01
F	0.09	-	-	-	-	-	-	-	0.190	0.089
P_2O_5	0.14	-	-	-	-	-	-	-	0.27	0.04
SO_3	0.41	0.80	0.70	0.10	0.70	0.70	0.30	1.10	1.20	1.25
Re_2O_7 Spike	0.10	0.10	0.10	0.10	0.10	0.10	0.10	0.10	0.10	0.10
Sum	100.0	100.0	100.0	100.0	100.0	100.0	100.0	100.0	100.0	100.0

- Empty data field
[#] SPFT tested

Table 1.3. Target Composition of the Nine IDF Phase 3 Glasses (wt%).

Glass ID	**ORLEC14**	**ORLEC28**	**ORLEC50**	**ORLEC52**	**ORLEC33**	**ORLEC34**	**ORLEC44**	**ORLEC46**	**ORLEC48**
IDF batching	**IDF21-EC14**	**IDF24-EC28**	**IDF28-EC50**	**IDF23-EC52**	**PNNL Test**	**IDF25-EC34**	**IDF26-EC44**	**IDF22-EC46**	**IDF27-EC48**
Testing for IDF PA	SPFT	SPFT & Long Term PCT	Long Term PCT	SPFT & Long Term PCT	SPFT	Long Term PCT	Long Term PCT & PFT	SPFT & Long Term PCT	Long Term PCT
Al_2O_3	10.00	10.00	10.00	9.92	8.36	8.36	7.60	7.60	7.60
B_2O_3	10.00	10.00	11.00	11.00	11.00	11.00	11.00	11.00	11.00
CaO	1.95	1.95	1.95	1.95	3.64	3.64	5.49	6.94	8.14
Cr_2O_3	0.34	0.44	0.34	0.20	0.08	0.08	0.08	0.08	0.08
Fe_2O_3	0.34	0.60	0.34	0.20	0.20	0.20	0.20	0.20	0.20
K_2O	0.50	**3.36**	0.50	0.50	0.50	0.50	0.50	0.50	0.50
Li_2O	0.00	0.00	0.00	0.00	0.00	0.00	0.99	1.86	2.58
MgO	1.00	1.00	1.00	1.00	1.00	1.00	1.00	1.00	1.00
Na_2O	24.00	22.11	24.00	23.80	22.00	22.00	20.00	18.00	16.00
NiO	0.01	0.01	0.01	0.01	0.01	0.01	0.01	0.01	0.01
PbO	0.01	0.01	0.01	0.01	0.01	0.01	0.01	0.01	0.01
SiO_2*	38.71	37.66	38.49	38.51	42.31	42.31	42.43	41.93	41.91
SnO_2	2.33	2.33	1.00	0.80	0.00	0.00	0.00	0.00	0.00
TiO_2	0.34	0.60	0.34	0.00	0.00	0.00	0.00	0.00	0.00
V_2O_5	0.35	0.00	0.90	1.88	2.27	2.27	2.44	2.50	2.50
ZnO	3.00	3.00	3.00	3.00	3.00	3.00	3.00	3.00	3.00
ZrO_2	6.03	6.03	6.03	5.83	4.03	4.03	3.50	3.50	3.50
Cl	0.20	0.20	0.20	0.20	0.20	0.20	0.20	0.20	0.20
F	0.08	0.08	0.08	0.08	0.08	0.08	0.08	0.08	0.08
P_2O_5	0.12	0.12	0.12	0.12	0.12	0.12	0.12	0.12	0.12
SO_3	0.60	0.40	0.60	0.90	1.10	1.10	1.25	1.37	1.47
Re_2O_7 Spike*	0.10	0.10	0.10	0.10	0.10	0.10	0.10	0.10	0.10
Sum	100.0	100.00	100.00	100.00	100.00	100.00	100.00	100.00	100.00

* Re_2O_7 was not added to the crucible glasses characterized in the ORP Enhanced LAW Glass Correlation tests, but was added at the expense of SiO_2 for long-term PCT samples.

Table 2.1. Elemental Compositions and Properties of the Twenty-Seven IDF Glasses.

Glass ID / Atom %	IDF1-B2	IDF2-G9	IDF3-F7	IDF4-A15	IDF5-A20	IDF6-D6	IDF7-E12	IDF8-A125	IDF9-A187	IDF10-Zr6	IDF11-G27	IDF12-A38	IDF13-A51	IDF14-A59	IDF15-A57	IDF16-A58	IDF17-A60	IDF18-A161	IDF19-C100	IDF20-F6
Al	9.34	6.45	7.84	8.87	6.25	9.37	6.95	5.31	9.57	4.72	5.81	6.56	9.49	9.65	9.97	9.87	6.36	9.13	9.28	7.83
B	9.99	11.89	12.66	11.82	12.04	13.39	13.18	13.17	16.94	16.45	11.18	11.37	10.98	11.17	11.04	11.87	12.24	17.99	18.30	12.66
Ca	0.93	2.34	8.05	2.83	2.84	6.66	8.35	1.66	5.33	2.11	2.36	2.68	0.85	0.87	1.28	0.00	2.89	6.53	6.66	8.05
Fe	0.66	0.12	0.13	0.55	0.11	0.17	0.14	3.24	0.52	4.08	0.17	0.16	0.11	0.11	0.03	0.15	0.11	0.57	0.58	0.17
K	0.12	5.95	0.49	0.55	0.54	0.17	0.55	4.29	0.50	0.56	6.00	0.54	0.54	0.54	0.54	0.53	0.54	0.43	0.15	0.54
Li	0.00	0.00	13.52	0.00	0.00	0.00	7.79	0.00	0.00	0.00	0.00	0.00	0.00	0.00	0.00	0.00	0.00	0.00	0.00	10.88
Mg	1.30	1.16	1.12	1.09	1.09	1.17	1.21	1.72	1.03	1.75	0.54	1.17	2.28	2.32	0.00	1.82	1.11	1.14	1.16	1.13
Na	38.42	32.95	17.90	37.05	37.13	33.60	24.12	30.99	34.27	33.38	33.30	37.32	36.90	36.96	36.98	36.58	37.20	30.90	30.05	19.76
Si	31.61	33.03	32.60	31.18	33.70	29.25	32.02	34.21	26.67	31.48	34.34	33.30	30.87	31.41	32.36	32.05	34.17	27.81	28.30	33.14
Sn	0.34	0.92	0.00	0.87	0.87	0.00	0.00	0.00	0.31	0.00	1.04	0.85	0.32	0.32	0.00	0.00	0.89	0.00	0.00	0.26
Ti	0.00	0.00	0.00	0.00	0.00	0.00	0.00	1.17	0.00	0.00	0.00	0.00	2.39	2.43	1.80	1.78	0.00	0.00	0.00	0.00
V	1.05	0.00	1.27	0.00	0.00	1.02	0.89	0.00	0.49	0.00	0.00	0.48	0.00	0.00	0.00	0.00	0.00	0.50	0.51	1.28
Zn	2.14	2.03	1.66	1.43	1.61	1.72	1.84	1.70	1.70	0.90	1.62	1.66	1.64	1.67	2.35	1.74	1.64	1.68	1.72	1.66
Zr	2.10	2.24	1.47	2.29	2.32	1.53	1.34	1.13	1.12	3.75	2.57	2.35	2.30	2.34	2.32	2.30	2.36	1.11	1.13	1.46
Cl	0.15	0.32	0.01	0.92	0.91	0.47	0.03	0.30	0.83	0.27	0.32	0.91	0.90	0.13	0.90	0.89	0.14	1.53	0.85	0.01
F	1.23	0.23	0.19	0.00	0.00	0.45	0.49	0.81	0.00	0.20	0.23	0.00	0.00	0.00	0.00	0.00	0.00	0.00	0.47	0.22
S	0.31	0.12	0.87	0.36	0.42	0.71	0.88	0.22	0.55	0.25	0.25	0.48	0.42	0.06	0.42	0.41	0.18	0.64	0.70	0.74
Others*	0.32	0.27	0.20	0.19	0.17	0.32	0.24	0.08	0.17	0.10	0.27	0.17	0.02	0.02	0.02	0.02	0.17	0.04	0.15	0.20
Sum**	100.0	100.0	100.0	100.0	100.0	100.0	100.0	100.0	100.0	100.0	100.0	100.0	100.0	100.0	100.0	100.0	100.0	100.0	100.0	100.0
Properties																				
PCT-A (B) (g/m^2)	0.84	0.74	0.17	0.66	0.72	0.56	0.25	0.96	1.71	0.70	0.66	0.73	0.37	–	0.21	0.31	–	0.67	0.52	0.16
PCT-A (Na) (g/m^2)	0.77	0.77	0.36	0.68	0.73	0.67	0.40	0.81	1.46	0.55	0.77	0.68	0.54	–	0.50	0.49	–	0.67	0.43	0.34
VHT 24-day rate ($g/m^2/d$)	110	41 to 50$	18	25	7	5 to 18$	31 to 41$	38	25 to 73$	0.6	13 to 57$	8 to 32$	2 to 32$	22	63 to 75$	25 to 33$	5	25 to 68$	10 to 14$	13 to 17$
Viscosity (P) 1100°C	131	86	32	112	95	48	34	104	33	58	102	98	119	–	150	150	–	44	52	40
Conductivity (S/m) 1100°C	0.644	0.464	0.349	0.598	0.444	0.392	0.457	0.327	0.47	0.433	0.451	0.552	0.568	–	0.504	0.477	–	0.311	0.240	–
K3 Neck Loss (inch)	0.039	0.038	0.01	0.036	0.033	0.0395	0.031	0.0255	0.0325	–	0.034	0.043	0.0315	–	0.027	0.022	–	0.0325	0.036	0.012

*Cs, Cr, Ni, Pb, P, Re; ** Atom % excludes oxygen; - Empty data field; $ Duplicate test results; highlights denote values discussed in the text.

Table 2.1. Elemental Compositions and Properties of the Twenty-Seven IDF Glasses (cont'd).

Glass ID / Atom %	IDF24-EC28	IDF28-EC50	IDF23-EC52	IDF25-EC34	IDF26-EC44	IDF22-EC46	IDF27-EC48	WTP property limits
Al	9.38	9.21	9.15	7.74	6.97	6.92	6.90	
B	13.73	14.83	14.85	14.92	14.77	14.68	14.63	
Ca	1.66	1.63	1.63	3.06	4.57	5.75	6.72	
Fe	0.36	0.20	0.12	0.12	0.12	0.12	0.12	
K	3.41	0.50	0.50	0.50	0.50	0.49	0.49	
Li	0.00	0.00	0.00	0.00	3.11	5.79	8.01	
Mg	1.19	1.16	1.17	1.17	1.16	1.15	1.15	
Na	34.11	36.35	36.10	33.51	30.16	26.98	23.91	
Si	30.04	30.14	30.20	33.32	33.07	32.48	32.37	
Sn	0.74	0.31	0.25	0.00	0.00	0.00	0.00	
Ti	0.36	0.20	0.00	0.00	0.00	0.00	0.00	
V	0.00	0.46	0.97	1.18	1.26	1.28	1.27	
Zn	1.76	1.73	1.73	1.74	1.72	1.71	1.71	
Zr	2.34	2.30	2.22	1.54	1.33	1.32	1.32	
Cl	0.27	0.26	0.27	0.27	0.26	0.26	0.26	
F	0.20	0.20	0.20	0.20	0.20	0.20	0.19	
S	0.24	0.35	0.53	0.65	0.73	0.79	0.85	
Others*	0.20	0.17	0.12	0.08	0.08	0.08	0.08	
Sum**	100.00	100.00	100.00	100.00	100.00	100.00	100.00	
Properties								
PCT-A (B) (g/m^2)	0.51	0.80	0.84	0.90	0.49	0.34	0.27	2.0
PCT-A (Na) (g/m^2)	0.51	0.58	0.71	0.68	0.52	0.41	0.43	2.0
VHT 24-day rate ($g/m^2/d$)	6.5	2.1	17.1	27.1	30.0	26.6	45.8	50
Viscosity (P) 1100°C[&]	113	90	77	90	58	43	36	10 to 150
Conductivity (S/m) 1100°C	0.408	0.509	0.519	0.406	0.363	0.378	0.347	0.1 to 0.7
K3 Neck Loss (inch)	0.0300	0.0180	0.0330	0.0195	0.0350	0.0400	0.0330	≤ 0.035[$]

* Cr, Ni, Pb; ** Atom % excludes oxygen; - Empty data field; [&] The listed viscosity requirements are from [49]. Per another document "Preliminary ILAW Formulation Algorithm Description" 24590-LAW-RPT-RT-04-0003, Rev 1, viscosity requirements are ≤ 150 poise at 1100°C and 20 - 80 poise at 1150°C.

[$]For the Enhanced LAW glass formulation development work for ORP, since higher waste loading compositions are being explored, a slightly higher neck corrosion value of 0.040 inches was used as a guide for acceptable corrosion characteristics.

Table 3.1. Mass of Glass and Volume of Leachant Used in Long-Term PCT at Various S/V.

S/V ratio (m^{-1})	1,000	2,000	5,000	10,000	20,000
Mass of glass (g)	5	10	15	20	40
Volume of leachant (ml)	100	100	60	40	40

Table 3.2. Summary of 90 °C Long-Term PCT on 27 IDF Glasses.

Description	Tests Conditions	90°C and S/V 20,000 m^{-1}			90°C and S/V 2,000 m^{-1}		
	Glass ID	Duration (d)	Resumption (d)	Status*	Duration (d)	Resumption (d)	Status*
Phase 1 Immersed 2010	IDF1-B2	272	Nearing	Terminated	3634	2647	O
	IDF2-G9	272	No		3634	NO	O
	IDF3-F7	272	No		2912	1925	T
	IDF4-A15	272	Nearing		2886	1617	T
	IDF5-A20	272	No		3608	2390	O
	IDF6-D6	180	56		1877	574	T
	IDF7-E12	181	120		2912	1171	T
	IDF8-A125	272	Plateau		2912	963	T
	IDF9-A187	180	56		1877	438	T
	IDF10-Zr6	272	No		3608	NO	O
Phase 2 Immersed 2015	IDF11-G27	1814	No	O			
	IDF12-A38	1814	Nearing	O			
	IDF13-A51	1449	734	T			
	IDF14-A59	1087	318	T			
	IDF15-A57	1814	653	O			
	IDF16-A58	1813	1813	O			
	IDF17-A60	1813	No	O			
	IDF18-A161	1449	179	T			
	IDF19-C100	1449	216	T			
	IDF20-F6	1449	326	T			
Phase 3 Immersed 2018	IDF24-EC28[$]	652	No	O	652	No	O
	IDF28-EC50	651	Nearing	O			
	IDF23-EC52[$]	651	No	O	651	No	O
	IDF25-EC34	651	~170 to 250	T			
	IDF26-EC44	651	~170 to 250	T			
	IDF22-EC46	651	~170 to 250	T			
	IDF27-EC48	651	~170 to 250	T			

* O=Ongoing, T=Terminated (also highlighted); [$] Glasses tested at five S/V

Table 3.3. Long-Term PCT-B Results at 90 °C and S/V of 20,000 m^{-1} (Tests ILHC and ILHD).

Glass ID	Test	Immersion Date	Sampling Date	Period	pH[#]	Norm. Release [g/L]				
						B	K	Li	Na	Si
IDF11-G27CCC	ILHC	6/9/2015	6/16/2015	7	12.31	5.41	4.47	-	7.35	0.91
			7/7/2015	28	12.61	8.25	6.16	-	10.64	1.42
			8/4/2015	56	12.65	9.54	6.84	-	11.09	1.64
			10/6/2015	119	12.71	10.06	7.79	-	12.59	1.66
			12/8/2015	182	12.83	12.41	9.31	-	16.42	2.08
			3/8/2016	273	12.91	13.68	10.19	-	17.03	2.42
			6/7/2016	364	12.93	15.64	10.34	-	23.62	3.00
			12/8/2016	548	13.26	35.67	20.10	-	32.92	10.07
			6/8/2017	730	13.28	41.71	18.98	-	37.71	11.30
			12/8/2017	913	13.32	51.69	26.55	-	57.01	16.93
			2/13/2019	1345	12.67	23.30	13.49	-	20.55	5.50
			5/28/2019	1449	12.68	25.72	13.23	-	24.08	6.79
			5/27/2020	1814	11.82	21.78	14.30	-	23.15	6.76
IDF12-A38CCC	ILHC	6/9/2015	6/16/2015	7	12.16	4.59	3.02	-	5.47	0.90
			7/7/2015	28	12.41	6.85	4.08	-	8.82	1.33
			8/4/2015	56	12.47	7.94	4.97	-	9.11	1.51
			10/6/2015	119	12.53	8.08	4.95	-	9.94	1.48
			12/8/2015	182	12.66	13.96	9.75	-	14.16	2.70
			3/8/2016	273	12.71	20.64	13.01	-	21.47	4.11
			6/7/2016	364	12.75	29.94	12.93	-	26.47	5.02
			12/8/2016	548	12.87	41.59	20.77	-	34.99	6.50
			6/8/2017	730	12.94	58.12	32.69	-	37.55	9.53
			12/8/2017	913	12.97	84.89	38.72	-	63.41	15.26
			5/31/2018	1087	12.87	93.95	39.61	-	60.60	15.60
			2/13/2019	1345	12.86	99.72	49.38	-	58.49	10.77
			5/28/2019	1449	12.93	98.90	38.04	-	77.88	10.33
			5/27/2020	1814	12.23	70-137	43.28	-	51.19	8.33
IDF13-A51CCC	ILHC	6/9/2015	6/16/2015	7	12.05	3.08	2.06	-	4.07	0.61
			7/7/2015	28	12.33	5.61	2.79	-	6.31	0.92
			8/4/2015	56	12.43	6.61	3.55	-	6.87	1.01
			10/6/2015	119	12.50	8.51	3.51	-	8.27	1.08
			12/8/2015	182	12.64	9.97	4.51	-	9.70	1.20
			3/8/2016	273	12.70	11.54	5.08	-	11.94	1.29
			6/7/2016	364	12.73	16.88	7.08	-	19.65	1.79
			12/8/2016	548	12.86	104.36	38.01	-	62.76	5.70
			6/8/2017	730	13.33	197.31	71.53	-	79.53	8.10
			12/8/2017	913	13.37	323.17	133.51	-	180.51	10.28
			2/13/2019	1345	13.37	861.27	377.06	-	324.51	27.03
			5/28/2019	1449	13.43	870.56	261.37	-	347.79	27.78
			Solid sampling and terminated							
IDF14-A59CCC	ILHC	6/9/2015	6/16/2015	7	12.11	2.64	2.09	-	4.25	0.64
			7/7/2015	28	12.37	5.03	2.54	-	7.13	1.05
			8/4/2015	56	12.48	6.39	3.77	-	7.43	1.25
			10/6/2015	119	12.54	9.53	4.88	-	10.38	1.33
			12/8/2015	182	12.77	22.09	9.65	-	17.67	2.37
			3/8/2016	273	12.81	132.61	52.46	-	65.30	6.45
			6/7/2016	364	12.85	268.65	97.56	-	188.44	10.54
			12/8/2016[$]	548[$]	13.16	740.66	289.77	-	289.54	25.93
			6/8/2017	730	13.66	1,003.04	426.20	-	413.12	40.60
			12/8/2017	913	13.67	1,087.05	447.96	-	498.61	46.04
			Solid sampling and terminated							

- Below detection limit; [$]Altered glass removed from one of the triplicate vessels; [#] Measured at room temperature

Table 3.3. Long-Term PCT-B Results at 90 °C and S/V of 20,000 m^{-1} (Tests ILHC and ILHD) (continued).

Glass ID	Test	Immersion Date	Sampling Date	Period	pH#	Normalized Release [g/L]				
						B	K	Li	Na	Si
IDF15-A57CCC	ILHC	6/9/2015	6/16/2015	7	12.04	2.05	1.74	-	3.85	0.60
			7/7/2015	28	12.33	3.63	2.31	-	5.86	0.97
			8/4/2015	56	12.45	4.71	2.80	-	6.45	1.14
			10/6/2015	119	12.51	6.29	3.10	-	7.80	1.04
			12/8/2015	182	12.74	9.28	4.00	-	9.15	1.36
			3/8/2016	273	12.81	23.67	8.15	-	16.29	2.42
			6/7/2016	364	12.86	58.46	16.48	-	46.18	5.07
			12/8/2016	548	13.16	140.46	48.64	-	76.18	11.07
			6/8/2017	730	13.68	244.16	85.55	-	132.40	25.82
			12/8/2017	913	13.68	293.00	96.98	-	165.63	20.69
			5/31/2018	1087	13.21	265.95	73.67	-	126.36	15.02
			2/13/2019	1345	13.33	270.61	99.32	-	121.37	15.70
			5/28/2019	1449	13.46	286.09	67.33	-	142.17	15.18
			5/27/2020	1814	12.78	312.40	105.30	-	142.99	15.24
IDF16-A58CCC	ILHD	6/10/2015	6/17/2015	7	12.17	3.76	1.55	-	4.00	0.58
			7/8/2015	28	12.32	7.64	2.84	-	6.57	0.79
			8/5/2015	56	12.44	8.75	3.11	-	7.24	0.93
			10/7/2015	119	12.51	10.46	3.39	-	8.29	1.05
			12/9/2015	182	12.65	12.71	4.02	-	9.89	1.24
			3/9/2016	273	12.71	16.38	5.11	-	12.12	1.70
			6/9/2016	365	12.74	18.68	5.46	-	14.16	2.00
			12/8/2016	547	12.84	23.69	8.21	-	15.47	2.27
			6/9/2017	730	12.93	41.06	11.85	-	21.68	3.49
			12/11/2017	915	12.96	109.28	30.86	-	57.13	5.05
			2/14/2019	1345	12.85	165.19	47.85	-	74.65	6.57
			5/29/2019	1449	12.93	173.21	47.78	-	109.15	7.21
			5/27/2020	1813	12.89	433.81	146.70	-	214.52	13.75
IDF17-A60CCC	ILHD	6/10/2015	6/17/2015	7	12.26	4.30	2.46	-	5.43	0.95
			7/8/2015	28	12.42	6.77	4.07	-	8.46	1.42
			8/5/2015	56	12.48	7.31	4.37	-	8.91	1.58
			10/7/2015	119	12.54	7.69	4.67	-	9.94	1.74
			12/9/2015	182	12.74	11.07	5.86	-	12.58	2.48
			3/9/2016	273	12.81	16.15	9.66	-	15.44	3.64
			6/9/2016	365	12.84	24.79	12.59	-	24.65	5.19
			12/8/2016	547	12.94	38.48	21.01	-	27.50	6.62
			6/9/2017	730	12.98	46.84	23.63	-	32.46	8.38
			12/11/2017	915	13.02	49.86	31.64	-	44.07	8.27
			5/31/2018	1086	12.91	59.76	16.65	-	38.50	5.13
			2/14/2019	1345	12.91	60.24	30.93	-	38.47	9.29
			5/29/2019	1449	12.98	60.39	25.74	-	50.87	9.22
			5/27/2020	1813	12.57	63.20	35.84	-	43.28	9.26
IDF18-A161CCC	ILHD	6/10/2015	6/17/2015	7	11.53	7.30	3.17	-	6.28	0.50
			7/8/2015	28	11.87	8.77	4.48	-	7.66	0.65
			8/5/2015	56	11.98	9.23	4.76	-	8.16	0.87
			10/7/2015	119	12.22	14.84	7.82	-	12.17	1.24
			12/9/2015	182	12.33	210.83	112.87	-	139.43	1.40
			3/9/2016	273	12.41	394.29	196.67	-	225.99	1.87
			6/9/2016	365	12.43	544.32	227.03	-	340.78	1.93
			12/8/2016	547	12.77	684.90	343.36	-	376.92	2.64
			6/9/2017	730	12.88	564.15	288.33	-	401.11	2.89
			12/11/2017	915	12.92	676.30	341.62	-	435.99	3.77
			2/14/2019	1345	11.67	602.02	288.77	-	314.48	2.91
			5/29/2019	1449	11.68	463.69	262.52	-	345.44	2.69
			Solid sampling and Test terminated							

- Below detection limit; # Measured at room temperature

Table 3.3. Long-Term PCT-B Results at 90 °C and S/V of 20,000 m^{-1} (Tests ILHC and ILHD) (continued).

Glass ID	Test	Immersion Date	Sampling Date	Period	pH[#]	B Norm. Release [g/L]	K Norm. Release [g/L]	Li Norm. Release [g/L]	Na Norm. Release [g/L]	Si Norm. Release [g/L]
IDF19-C100CCC	ILHD	6/10/2015	6/17/2015	7	11.58	5.81	4.17	-	4.88	0.43
			7/8/2015	28	11.92	7.85	5.09	-	6.85	0.61
			8/5/2015	56	12.03	8.69	5.75	-	7.22	0.80
			10/7/2015	119	12.32	10.67	6.02	-	8.94	0.96
			12/9/2015	182	12.43	71.58	47.17	-	49.32	1.39
			3/9/2016	273	12.52	419.94	328.34	-	241.22	2.27
			6/9/2016	365	12.55	420.48	272.00	-	284.94	2.13
			12/8/2016	547	11.86	485.63	318.15	-	331.13	2.60
			6/9/2017	730	11.93	454.48	307.74	-	348.67	2.92
			12/11/2017	915	11.92	544.33	391.16	-	379.52	2.91
			2/14/2019	1345	11.62	510.20	348.87	-	285.44	3.43
			5/29/2019	1449	11.66	439.42	353.43	-	366.07	2.50
			Solid sampling and Test terminated							
IDF20-F6CCC	ILHD	6/10/2015	6/17/2015	7	11.54	1.60	1.37	2.35	2.26	0.47
			7/8/2015	28	11.85	1.94	1.53	3.08	3.22	0.65
			8/5/2015	56	11.94	2.04	1.67	3.35	3.52	0.74
			10/7/2015	119	12.15	2.44	1.66	3.99	4.51	0.82
			12/9/2015	182	12.26	3.74	2.38	5.57	5.73	1.04
			3/9/2016	273	12.32	11.35	6.59	10.99	11.08	1.59
			6/9/2016	365	12.35	337.31	107.88	196.55	233.60	2.63
			12/8/2016	547	11.66	459.43	192.73	232.94	299.54	3.37
			6/9/2017	730	11.86	641.69	212.38	276.99	378.30	4.95
			12/11/2017	915	11.81	701.72	297.35	295.66	401.25	5.10
			5/31/2018	1086	11.93	554.24	249.81	291.02	361.61	4.49
			2/14/2019	1345	11.96	558.38	249.42	228.10	307.15	4.08
			5/29/2019	1449	12.05	569.10	264.50	235.56	459.46	4.12
			Solid sampling and Test terminated							
ANL-LRM-2	ILHC	6/9/2015	6/16/2015	7	12.02	6.60	2.07	-	5.83	0.88
			7/7/2015	28	12.31	13.34	3.35	-	11.13	1.28
			8/4/2015	56	12.42	17.06	3.93	-	11.72	1.36
			10/6/2015	119	12.47	22.76	4.79	3.12	18.44	2.50
			12/8/2015	182	12.57	41.77	10.40	7.30	27.94	8.61
			3/8/2016	273	12.61	143.10	28.47	74.81	96.66	27.56
			6/7/2016	364	12.66	699.96	125.34	404.69	496.12	9.61
			12/8/2016[$]	548	12.43	918.89	169.37	599.61	710.94	205.39
			6/8/2017	730	12.47	729.60	157.64	605.12	527.29	18.20
			Solid sampling and Test terminated							
ANL-LRM-2	ILHD	6/10/2015	6/17/2015	7	12.03	6.80	1.90	-	5.88	0.91
			7/8/2015	28	12.31	13.22	3.40	-	11.00	1.28
			8/5/2015	56	12.43	17.22	3.99	-	12.02	1.37
			10/7/2015	119	12.47	23.12	5.11	2.54	18.55	2.12
			12/9/2015	182	12.54	47.98	10.61	11.30	30.81	9.73
			3/9/2016	273	12.61	119.70	22.95	61.66	75.74	22.92
			6/9/2016	365	12.66	581.49	106.92	354.90	453.58	8.17
			12/8/2016[$]	547	12.45	1000.19	191.78	594.14	767.94	177.58
			6/9/2017	730	12.48	789.10	173.24	589.47	580.22	46.24
			Solid sampling and Test terminated							

- Below detection limit; [#] Measured at room temperature; [$]Altered glass removed from one of the triplicate vessels

Table 3.4. Long-Term PCT-B Results at 90 °C and S/V of 2,000 m^{-1} (Tests ILHA and ILHB).

Glass name	Temp. (°C)	Test Name	S/V (m^{-1})	Immersion date	Sampling date	Elapsed time	pH#	Normalized release (g-glass/L)				
								B	K	Li	Na	Si
IDF1B2CCC	90	ILHA	2000	6/16/2010	6/23/2010	7	11.58	1.03	0.00	-	1.26	0.43
IDF1B2CCC	90	ILHA	2000	6/16/2010	7/14/2010	28	11.72	1.92	0.00	-	1.80	0.51
IDF1B2CCC	90	ILHA	2000	6/16/2010	8/11/2010	56	11.81	2.36	0.00	-	2.14	0.55
IDF1B2CCC	90	ILHA	2000	6/16/2010	10/14/2010	120	11.96	2.98	0.00	-	2.78	0.67
IDF1B2CCC	90	ILHA	2000	6/16/2010	12/13/2010	180	12.07	3.49	0.00	-	3.19	0.68
IDF1B2CCC	90	ILHA	2000	6/16/2010	12/2/2014	1630	12.48	5.63	2.41	-	5.51	0.90
IDF1B2CCC	90	ILHA	2000	6/16/2010	6/2/2015	1812	12.53	6.39	2.60	-	5.58	1.04
IDF1B2CCC	90	ILHA	2000	6/16/2010	6/1/2016	2177	12.57	7.71	3.39	-	6.29	1.14
IDF1B2CCC	90	ILHA	2000	6/16/2010	6/5/2017	2546	12.61	14.82	3.14	-	8.89	1.66
IDF1B2CCC	90	ILHA	2000	6/16/2010	6/6/2018	2912	12.53	33.52	9.85	-	19.36	2.59
IDF1B2CCC	90	ILHA	2000	6/16/2010	6/3/2019	3274	12.81	58.32	15.54	-	36.46	4.17
IDF1B2CCC	90	ILHA	2000	6/16/2010	5/28/2020	3634	12.22	55.45	24.07	-	33.22	4.42
IDF2G9CCC	90	ILHA	2000	6/16/2010	6/23/2010	7	11.66	1.42	0.91	-	1.60	0.43
IDF2G9CCC	90	ILHA	2000	6/16/2010	7/14/2010	28	11.81	2.37	1.41	-	2.28	0.54
IDF2G9CCC	90	ILHA	2000	6/16/2010	8/11/2010	56	11.92	2.70	1.56	-	2.67	0.57
IDF2G9CCC	90	ILHA	2000	6/16/2010	10/14/2010	120	12.04	3.12	2.38	-	3.45	0.62
IDF2G9CCC	90	ILHA	2000	6/16/2010	12/13/2010	180	12.11	3.51	2.23	-	3.82	0.70
IDF2G9CCC	90	ILHA	2000	6/16/2010	12/2/2014	1630	12.57	4.37	2.90	-	5.98	1.05
IDF2G9CCC	90	ILHA	2000	6/16/2010	6/2/2015	1812	12.63	4.54	3.09	-	6.27	1.15
IDF2G9CCC	90	ILHA	2000	6/16/2010	6/1/2016	2177	12.66	5.88	3.64	-	7.40	1.39
IDF2G9CCC	90	ILHA	2000	6/16/2010	6/5/2017	2546	12.68	7.94	4.11	-	8.06	1.82
IDF2G9CCC	90	ILHA	2000	6/16/2010	6/6/2018	2912	12.58	7.17	4.00	-	8.50	1.76
IDF2G9CCC	90	ILHA	2000	6/16/2010	6/3/2019	3274	12.61	9.53	4.60	-	9.23	2.41
IDF2G9CCC	90	ILHA	2000	6/16/2010	5/28/2020	3634	12.05	9.98	7.07	-	9.54	2.68
IDF3F7CCC	90	ILHA	2000	6/16/2010	6/23/2010	7	11.05	0.26	-	0.86	0.77	0.22
IDF3F7CCC	90	ILHA	2000	6/16/2010	7/14/2010	28	11.18	0.46	0.55	0.86	0.77	0.22
IDF3F7CCC	90	ILHA	2000	6/16/2010	8/11/2010	56	11.27	0.48	0.47	0.97	0.93	0.25
IDF3F7CCC	90	ILHA	2000	6/16/2010	10/14/2010	120	11.43	0.54	-	1.24	1.12	0.33
IDF3F7CCC	90	ILHA	2000	6/16/2010	12/13/2010	180	11.54	0.45	-	1.10	1.22	0.27
IDF3F7CCC	90	ILHA	2000	6/16/2010	12/2/2014	1630	11.97	2.82	2.07	3.23	3.41	0.95
IDF3F7CCC	90	ILHA	2000	6/16/2010	6/2/2015	1812	12.03	4.20	2.34	4.85	4.46	1.06
IDF3F7CCC	90	ILHA	2000	6/16/2010	9/2/2015	1904	12.15	17.67	6.14	13.91	11.30	1.29
IDF3F7CCC	90	ILHA	2000	6/16/2010	6/1/2016	2177	12.17	47.61	18.38	32.13	32.36	1.36
IDF3F7CCC	90	ILHA	2000	6/16/2010	6/5/2017	2546	12.33	87.82	28.31	55.99	49.02	1.40
IDF3F7CCC	90	ILHA	2000	6/16/2010	6/6/2018	2912	12.31	85.45	30.18	49.96	54.79	1.61
						TERMINATED						

- Below detection limit; # Measured at room temperature

Table 3.4. Long-Term PCT-B Results at 90 °C and S/V of 2,000 m^{-1} (Tests ILHA and ILHB) (continued).

Glass name	Temp. (°C)	Test Name	S/V (m^{-1})	Immersion date	Sampling date	Elapsed time	pH[#]	Normalized release (g-glass/L)				
								B	K	Li	Na	Si
IDF4A15CCC	90	ILHB	2000	7/13/2010	7/20/2010	7	11.52	0.95	0.56	-	1.10	0.35
IDF4A15CCC	90	ILHB	2000	7/13/2010	8/10/2010	28	11.66	1.54	0.72	-	1.53	0.43
IDF4A15CCC	90	ILHB	2000	7/13/2010	9/7/2010	56	11.81	1.86	0.85	-	1.83	0.45
IDF4A15CCC	90	ILHB	2000	7/13/2010	11/10/2010	120	12.03	2.16	0.00	-	2.46	0.50
IDF4A15CCC	90	ILHB	2000	7/13/2010	1/10/2011	181	12.11	2.56	1.50	-	2.53	0.56
IDF4A15CCC	90	ILHB	2000	7/13/2010	12/8/2014	1609	12.71	19.47	5.83	-	14.33	2.00
IDF4A15CCC	90	ILHB	2000	7/13/2010	6/22/2015	1805	12.66	33.17	13.27	-	23.64	2.86
IDF4A15CCC	90	ILHB	2000	7/13/2010	6/27/2016	2176	12.61	62.70	24.07	-	39.94	4.25
IDF4A15CCC	90	ILHB	2000	7/13/2010	6/12/2017	2526	12.81	71.16	25.43	-	43.41	4.84
IDF4A15CCC	90	ILHB	2000	7/13/2010	6/7/2018	2886	12.93	80.23	37.02	-	44.69	5.53
						TERMINATED						
IDF5A20CCC	90	ILHB	2000	7/13/2010	7/20/2010	7	11.58	0.99	0.60	-	1.10	0.40
IDF5A20CCC	90	ILHB	2000	7/13/2010	8/10/2010	28	11.68	1.79	0.82	-	1.69	0.54
IDF5A20CCC	90	ILHB	2000	7/13/2010	9/7/2010	56	11.88	2.06	0.91	-	1.98	0.57
IDF5A20CCC	90	ILHB	2000	7/13/2010	11/10/2010	120	12.08	2.34	0.57	-	2.73	0.62
IDF5A20CCC	90	ILHB	2000	7/13/2010	1/10/2011	181	12.26	2.84	2.05	-	2.81	0.71
IDF5A20CCC	90	ILHB	2000	7/13/2010	12/8/2014	1609	12.74	5.83	2.46	-	6.35	1.51
IDF5A20CCC	90	ILHB	2000	7/13/2010	6/22/2015	1805	12.68	8.24	3.05	-	6.79	1.79
IDF5A20CCC	90	ILHB	2000	7/13/2010	6/27/2016	2176	12.65	14.47	5.41	-	12.93	2.59
IDF5A20CCC	90	ILHB	2000	7/13/2010	6/12/2017	2526	12.86	23.52	7.76	-	17.20	3.49
IDF5A20CCC	90	ILHB	2000	7/13/2010	6/7/2018	2886	12.67	24.11	9.79	-	17.45	3.92
IDF5A20CCC	90	ILHB	2000	7/13/2010	6/4/2019	3248	12.91	24.06	6.12	-	17.98	4.41
IDF5A20CCC	90	ILHB	2000	7/13/2010	5/29/2020	3608	12.01	23.93	11.59	-	18.19	4.05
IDF6D6CCC	90	ILHB	2000	7/13/2010	7/20/2010	7	11.15	0.69	0.00	-	1.00	0.23
IDF6D6CCC	90	ILHB	2000	7/13/2010	8/10/2010	28	11.54	1.07	0.00	-	1.34	0.30
IDF6D6CCC	90	ILHB	2000	7/13/2010	9/7/2010	56	11.65	1.16	0.00	-	1.50	0.32
IDF6D6CCC	90	ILHB	2000	7/13/2010	11/10/2010	120	11.86	1.26	0.00	-	2.12	0.38
IDF6D6CCC	90	ILHB	2000	7/13/2010	1/10/2011	181	12.04	1.66	2.00	-	2.19	0.45
IDF6D6CCC	90	ILHB	2000	7/13/2010	12/8/2014	1609	12.62	66.95	31.59	-	45.18	1.39
IDF6D6CCC	90	ILHB	2000	7/13/2010	6/22/2015	1805	12.61	80.25	44.32	-	50.31	1.70
IDF6D6CCC	90	ILHB	2000	7/13/2010	9/2/2015	1877	12.66	77.90	43.08	-	50.23	1.81
						TERMINATED						
IDF7E12CCC	90	ILHA	2000	6/16/2010	6/23/2010	7	10.95	0.15	-	0.40	0.59	0.17
IDF7E12CCC	90	ILHA	2000	6/16/2010	7/14/2010	28	11.08	0.33	0.47	0.61	0.80	0.21
IDF7E12CCC	90	ILHA	2000	6/16/2010	8/11/2010	56	11.21	0.37	0.44	0.69	0.91	0.22
IDF7E12CCC	90	ILHA	2000	6/16/2010	10/14/2010	120	11.40	0.42	0.00	0.86	1.09	0.32
IDF7E12CCC	90	ILHA	2000	6/16/2010	12/13/2010	180	11.51	0.35	0.00	0.71	1.32	0.27
IDF7E12CCC	90	ILHA	2000	6/16/2010	12/2/2014	1630	11.97	82.54	35.79	47.67	55.26	2.00
IDF7E12CCC	90	ILHA	2000	6/16/2010	6/2/2015	1812	12.02	90.79	47.16	52.12	66.18	2.04
IDF7E12CCC	90	ILHA	2000	6/16/2010	6/1/2016	2177	12.23	87.30	39.61	50.75	59.38	1.63
IDF7E12CCC	90	ILHA	2000	6/16/2010	6/5/2017	2546	12.43	80.59	34.03	49.68	62.99	1.74
IDF7E12CCC	90	ILHA	2000	6/16/2010	6/6/2018	2912	12.43	83.64	35.87	44.99	60.73	1.74
						TERMINATED						

- Below detection limit; [#] Measured at room temperature

Table 3.4. Long-Term PCT-B Results at 90 °C and S/V of 2,000 m^{-1} (Tests ILHA and ILHB) (continued).

Glass name	Temp. (°C)	Test Name	S/V (m^{-1})	Immersion date	Sampling date	Elapsed time	pH[#]	Normalized release (g-glass/L)				
								B	K	Li	Na	Si
IDF8A125CCC	90	ILHA	2000	6/16/2010	6/23/2010	7	11.28	2.02	0.93	-	1.72	0.50
IDF8A125CCC	90	ILHA	2000	6/16/2010	7/14/2010	28	11.45	3.30	1.39	-	2.51	0.63
IDF8A125CCC	90	ILHA	2000	6/16/2010	8/11/2010	56	11.61	4.05	1.68	-	3.18	0.69
IDF8A125CCC	90	ILHA	2000	6/16/2010	10/14/2010	120	11.75	5.37	2.52	-	3.97	0.59
IDF8A125CCC	90	ILHA	2000	6/16/2010	12/13/2010	180	11.88	5.43	2.22	-	4.48	0.81
IDF8A125CCC	90	ILHA	2000	6/16/2010	12/2/2014	1630	12.45	49.97	14.77	-	37.68	6.68
IDF8A125CCC	90	ILHA	2000	6/16/2010	6/2/2015	1812	12.52	62.63	18.82	-	51.88	7.57
IDF8A125CCC	90	ILHA	2000	6/16/2010	6/1/2016	2177	12.66	56.38	19.75	-	45.76	6.06
IDF8A125CCC	90	ILHA	2000	6/16/2010	6/5/2017	2546	12.67	76.59	24.29	-	49.41	8.16
IDF8A125CCC	90	ILHA	2000	6/16/2010	6/6/2018	2912	12.65	85.93	24.58	-	56.05	8.86
						TERMINATED						
IDF9A187CCC	90	ILHB	2000	7/13/2010	7/20/2010	7	11.65	2.17	1.47	-	1.75	0.39
IDF9A187CCC	90	ILHB	2000	7/13/2010	8/10/2010	28	11.83	2.50	1.63	-	1.99	0.48
IDF9A187CCC	90	ILHB	2000	7/13/2010	9/7/2010	56	11.93	2.46	1.68	-	2.09	0.48
IDF9A187CCC	90	ILHB	2000	7/13/2010	11/10/2010	120	12.11	2.52	1.39	-	2.69	0.51
IDF9A187CCC	90	ILHB	2000	7/13/2010	1/10/2011	181	12.32	3.01	3.77	-	2.57	0.60
IDF9A187CCC	90	ILHB	2000	7/13/2010	12/8/2014	1609	12.94	75.20	41.27	-	52.25	1.34
IDF9A187CCC	90	ILHB	2000	7/13/2010	6/22/2015	1805	12.92	69.03	44.91	-	43.82	1.36
IDF9A187CCC	90	ILHB	2000	7/13/2010	9/2/2015	1877	12.94	72.24	46.89	-	41.44	1.74
						TERMINATED						
IDF10Zr6CCC	90	ILHB	2000	7/13/2010	7/20/2010	7	10.88	1.58	0.78	-	1.20	0.30
IDF10Zr6CCC	90	ILHB	2000	7/13/2010	8/10/2010	28	11.33	2.94	1.00	-	1.87	0.37
IDF10Zr6CCC	90	ILHB	2000	7/13/2010	9/7/2010	56	11.46	3.49	1.08	-	2.26	0.38
IDF10Zr6CCC	90	ILHB	2000	7/13/2010	11/10/2010	120	11.66	3.86	1.11	-	3.02	0.37
IDF10Zr6CCC	90	ILHB	2000	7/13/2010	1/10/2011	181	11.86	5.21	3.50	-	3.21	0.47
IDF10Zr6CCC	90	ILHB	2000	7/13/2010	12/8/2014	1609	12.53	5.89	1.75	-	5.66	0.60
IDF10Zr6CCC	90	ILHB	2000	7/13/2010	6/22/2015	1805	12.51	5.80	1.66	-	4.02	0.57
IDF10Zr6CCC	90	ILHB	2000	7/13/2010	6/27/2016	2176	12.51	5.85	1.72	-	5.18	0.62
IDF10Zr6CCC	90	ILHB	2000	7/13/2010	6/12/2017	2526	12.66	5.91	1.64	-	5.17	0.62
IDF10Zr6CCC	90	ILHB	2000	7/13/2010	6/7/2018	2886	11.93	6.05	1.77	-	5.13	0.67
IDF10Zr6CCC	90	ILHB	2000	7/13/2010	6/4/2019	3248	11.46	4.27	0.65	-	3.34	0.54
IDF10Zr6CCC	90	ILHB	2000	40372	5/29/2020	3608	11.46	5.80	2.24	-	4.94	0.75

- Below detection limit; [#] Measured at room temperature

Table 3.4. Long-Term PCT-B Results at 90 °C and S/V of 2,000 m^{-1} (Tests ILHA and ILHB) (continued).

Glass name	Temp. (°C)	Test Name	S/V (m^{-1})	Immersion date	Sampling date	Elapsed time	pH[#]	Normalized release (g-glass/L)				
								B	K	Li	Na	Si
ANL-LRM-2	90	ILHB	2000	7/13/2010	7/20/2010	7	11.03	1.23	0.41	-	1.10	0.33
ANL-LRM-2	90	ILHA	2000	6/16/2010	7/14/2010	28	11.22	2.79	0.82	-	2.10	0.45
ANL-LRM-2	90	ILHA	2000	6/16/2010	8/11/2010	56	11.53	4.07	1.05	-	3.07	0.52
ANL-LRM-2	90	ILHA	2000	6/16/2010	10/14/2010	120	11.71	5.80	1.54	-	4.39	0.43
ANL-LRM-2	90	ILHA	2000	6/16/2010	12/13/2010	180	11.92	6.86	1.03	-	5.14	0.66
ANL-LRM-2	90	ILHA	2000	6/16/2010	12/2/2014	1630	12.37	17.43	3.86	3.68	14.44	3.52
ANL-LRM-2	90	ILHA	2000	6/16/2010	6/2/2015	1812	12.42	19.01	5.54	4.39	15.30	3.79
ANL-LRM-2	90	ILHA	2000	6/16/2010	6/1/2016	2177	12.46	19.46	5.16	5.98	18.12	4.19
ANL-LRM-2	90	ILHA	2000	6/16/2010	6/5/2017	2546	12.51	24.79	5.30	8.18	24.75	5.38
ANL-LRM-2	90	ILHA	2000	6/16/2010	6/6/2018	2912	11.91	31.34	7.85	11.17	25.52	6.92
ANL-LRM-2	90	ILHA	2000	6/16/2010	6/3/2019	3274	11.96	39.40	9.21	NA	30.63	8.32
ANL-LRM-2	90	ILHA	2000	6/16/2010	5/28/2020	3634	11.58	50.49	16.44	31.07	38.25	9.65
ANL-LRM-2	90	ILHB	2000	7/13/2010	7/20/2010	7	11.01	1.21	0.44	-	1.06	0.32
ANL-LRM-2	90	ILHB	2000	7/13/2010	8/10/2010	28	11.24	2.75	0.73	-	1.99	0.46
ANL-LRM-2	90	ILHB	2000	7/13/2010	9/7/2010	56	11.54	3.70	0.93	-	2.63	0.49
ANL-LRM-2	90	ILHB	2000	7/13/2010	11/10/2010	120	11.75	5.04	0.34	-	3.86	0.58
ANL-LRM-2	90	ILHB	2000	7/13/2010	1/10/2011	181	11.92	6.88	2.47	4.28	4.29	0.67
ANL-LRM-2	90	ILHB	2000	7/13/2010	12/8/2014	1609	12.45	18.80	4.32	5.38	15.80	4.23
ANL-LRM-2	90	ILHB	2000	7/13/2010	6/22/2015	1805	12.42	20.03	4.61	5.21	15.16	4.31
ANL-LRM-2	90	ILHB	2000	7/13/2010	6/27/2016	2176	12.41	20.85	5.31	7.17	20.93	4.67
ANL-LRM-2	90	ILHB	2000	7/13/2010	6/12/2017	2526	12.45	28.08	5.84	10.16	23.01	6.05
ANL-LRM-2	90	ILHB	2000	7/13/2010	6/7/2018	2886	11.91	34.44	8.91	14.45	25.13	7.20
ANL-LRM-2	90	ILHB	2000	7/13/2010	6/4/2019	3248	11.97	41.66	9.21	NA	31.01	8.60
ANL-LRM-2	90	ILHB	2000	7/13/2010	5/29/2020	3608	11.76	49.47	15.93	28.33	42.36	9.43

- Below detection limit; [#] Measured at room temperature

Table 3.5. Long-Term PCT-B Results at 40 °C and S/V of 2,000 m^{-1} (Tests ILLA and ILLB).

Glass name	Temp. (°C)	Test Name	S/V (m^{-1})	Immersion date	Sampling date	Elapsed time	pH#	Normalized release (g-glass/L)				
								B	K	Li	Na	Si
IDF1B2CCC	40	ILLA	2000	6/22/2010	6/29/2010	7	10.58	0.21	-	-	0.25	0.08
IDF1B2CCC	40	ILLA	2000	6/22/2010	7/20/2010	28	10.67	0.24	-	-	0.35	0.14
IDF1B2CCC	40	ILLA	2000	6/22/2010	8/17/2010	56	10.77	0.24	-	-	0.45	0.16
IDF1B2CCC	40	ILLA	2000	6/22/2010	10/20/2010	120	10.85	0.32	-	-	0.56	0.19
IDF1B2CCC	40	ILLA	2000	6/22/2010	12/20/2010	181	11.06	0.42	-	-	0.56	0.22
IDF1B2CCC	40	ILLA	2000	6/22/2010	6/3/2015	1807	11.46	0.96	2.29	-	1.03	0.31
IDF1B2CCC	40	ILLA	2000	6/22/2010	6/2/2016	2172	11.41	1.17	9.44	-	1.15	0.34
IDF1B2CCC	40	ILLA	2000	6/22/2010	6/6/2017	2541	11.46	0.85	2.16	-	1.00	0.30
IDF1B2CCC	40	ILLA	2000	6/22/2010	6/8/2018	2908	11.22	0.86	0.00	-	1.00	0.30
IDF1B2CCC	40	ILLA	2000	6/22/2010	6/5/2019	3270	11.28	0.63	0.53	-	1.10	0.31
IDF1B2CCC	40	ILLA	2000	6/22/2010	6/1/2020	3632	9.68	0.90	0.00	-	1.05	0.31
IDF2G9CCC	40	ILLA	2000	6/22/2010	6/29/2010	7	10.66	0.16	0.12	-	0.26	0.08
IDF2G9CCC	40	ILLA	2000	6/22/2010	7/20/2010	28	10.75	0.21	0.19	-	0.37	0.12
IDF2G9CCC	40	ILLA	2000	6/22/2010	8/17/2010	56	10.81	0.24	0.22	-	0.48	0.14
IDF2G9CCC	40	ILLA	2000	6/22/2010	10/20/2010	120	10.88	0.35	0.05	-	0.60	0.18
IDF2G9CCC	40	ILLA	2000	6/22/2010	12/20/2010	181	11.10	0.44	0.25	-	0.67	0.21
IDF2G9CCC	40	ILLA	2000	6/22/2010	12/4/2014	1626	11.48	1.85	0.82	-	1.73	0.45
IDF2G9CCC	40	ILLA	2000	6/22/2010	6/3/2015	1807	11.48	1.85	0.81	-	1.73	0.45
IDF2G9CCC	40	ILLA	2000	6/22/2010	6/2/2016	2172	11.43	1.79	0.81	-	1.88	0.45
IDF2G9CCC	40	ILLA	2000	6/22/2010	6/6/2017	2541	11.48	2.02	0.96	-	1.95	0.46
IDF2G9CCC	40	ILLA	2000	6/22/2010	6/8/2018	2908	11.33	2.20	0.95	-	1.94	0.50
IDF2G9CCC	40	ILLA	2000	6/22/2010	6/5/2019	3270	11.54	1.91	0.86	-	2.16	0.51
IDF2G9CCC	40	ILLA	2000	6/22/2010	6/1/2020	3632	10.65	2.35	1.07	-	2.07	0.54
IDF3F7CCC	40	ILLA	2000	6/22/2010	6/29/2010	7	10.15	0.00	-	0.15	0.14	0.05
IDF3F7CCC	40	ILLA	2000	6/22/2010	7/20/2010	28	10.23	0.00	-	0.22	0.20	0.07
IDF3F7CCC	40	ILLA	2000	6/22/2010	8/17/2010	56	10.32	0.18	-	0.29	0.27	0.10
IDF3F7CCC	40	ILLA	2000	6/22/2010	10/20/2010	120	10.42	0.39	-	0.42	0.53	0.14
IDF3F7CCC	40	ILLA	2000	6/22/2010	12/20/2010	181	10.66	0.63	-	0.67	0.70	0.21
IDF3F7CCC	40	ILLA	2000	6/22/2010	12/4/2014	1626	11.27	0.87	1.01	1.04	1.06	0.26
IDF3F7CCC	40	ILLA	2000	6/22/2010	6/3/2015	1807	11.32	0.87	1.18	1.01	1.05	0.26
IDF3F7CCC	40	ILLA	2000	6/22/2010	6/2/2016	2172	11.28	0.91	1.41	1.00	1.18	0.28
IDF3F7CCC	40	ILLA	2000	6/22/2010	6/6/2017	2541	11.33	0.77	1.00	0.95	0.99	0.22
IDF3F7CCC	40	ILLA	2000	6/22/2010	6/8/2018	2908	11.15	0.80	0.55	0.96	0.93	0.25
IDF3F7CCC	40	ILLA	2000	6/22/2010	6/5/2019	3270	10.65	0.52	0.38	0.95	0.92	0.22
IDF3F7CCC	40	ILLA	2000	6/22/2010	6/1/2020	3632	9.63	0.78	0.65	0.93	0.95	0.24
IDF4A15CCC	40	ILLB	2000	7/14/2010	7/21/2010	7	10.52	0.00	-	-	0.19	0.06
IDF4A15CCC	40	ILLB	2000	7/14/2010	8/11/2010	28	10.61	0.17	-	-	0.31	0.09
IDF4A15CCC	40	ILLB	2000	7/14/2010	9/8/2010	56	10.81	0.19	-	-	0.33	0.11
IDF4A15CCC	40	ILLB	2000	7/14/2010	11/11/2010	120	10.87	0.15	-	-	0.42	0.13
IDF4A15CCC	40	ILLB	2000	7/14/2010	1/10/2011	180	11.05	0.39	-	-	0.49	0.17
IDF4A15CCC	40	ILLB	2000	7/14/2010	12/11/2014	1611	11.32	0.66	0.39	-	0.76	0.17
IDF4A15CCC	40	ILLB	2000	7/14/2010	6/23/2015	1805	11.31	0.70	0.58	-	0.78	0.16
IDF4A15CCC	40	ILLB	2000	7/14/2010	6/28/2016	2176	11.30	0.71	0.55	-	0.81	0.18
IDF4A15CCC	40	ILLB	2000	7/14/2010	6/13/2017	2526	11.32	0.69	0.00	-	0.97	0.18
IDF4A15CCC	40	ILLB	2000	7/14/2010	6/8/2018	2886	11.16	0.79	0.39	-	0.93	0.18
IDF4A15CCC	40	ILLB	2000	7/14/2010	6/6/2019	3249	11.21	0.72	0.29	-	1.01	0.18
IDF4A15CCC	40	ILLB	2000	7/14/2010	6/2/2020	3611	9.67	0.94	0.49	-	0.98	0.26

- Below detection limit; # Measured at room temperature.

Table 3.5. Long-Term PCT-B Results at 40 °C and S/V of 2,000 m^{-1} (Tests ILLA and ILLB) (continued).

Glass name	Temp. (°C)	Test Name	S/V (m^{-1})	Immersion date	Sampling date	Elapsed time	pH#	Normalized release (g-glass/L)				
								B	K	Li	Na	Si
IDF5A20CCC	40	ILLB	2000	7/14/2010	7/21/2010	7	10.58	0.00	-	-	0.28	0.09
IDF5A20CCC	40	ILLB	2000	7/14/2010	8/11/2010	28	10.68	0.25	-	-	0.41	0.13
IDF5A20CCC	40	ILLB	2000	7/14/2010	9/8/2010	56	10.92	0.30	-	-	0.46	0.15
IDF5A20CCC	40	ILLB	2000	7/14/2010	11/11/2010	120	11.11	0.28	-	-	0.59	0.19
IDF5A20CCC	40	ILLB	2000	7/14/2010	1/10/2011	180	11.22	0.45	-	-	0.67	0.24
IDF5A20CCC	40	ILLB	2000	7/14/2010	12/11/2014	1611	11.64	2.81	0.88	-	2.18	0.65
IDF5A20CCC	40	ILLB	2000	7/14/2010	6/23/2015	1805	11.61	3.04	1.06	-	2.21	0.68
IDF5A20CCC	40	ILLB	2000	7/14/2010	6/28/2016	2176	11.61	2.98	1.12	-	2.22	0.68
IDF5A20CCC	40	ILLB	2000	7/14/2010	6/13/2017	2526	11.65	2.97	0.89	-	2.55	0.70
IDF5A20CCC	40	ILLB	2000	7/14/2010	6/8/2018	2886	11.61	3.03	0.88	-	2.41	0.70
IDF5A20CCC	40	ILLB	2000	7/14/2010	6/6/2019	3249	11.68	2.88	0.79	-	2.65	0.73
IDF5A20CCC	40	ILLB	2000	7/14/2010	6/2/2020	3611	10.41	3.05	0.99	-	2.39	0.74
IDF6D6CCC	40	ILLB	2000	7/14/2010	7/21/2010	7	10.37	0.14	-	-	0.23	0.07
IDF6D6CCC	40	ILLB	2000	7/14/2010	8/11/2010	28	10.47	0.23	-	-	0.35	0.08
IDF6D6CCC	40	ILLB	2000	7/14/2010	9/8/2010	56	10.57	0.34	-	-	0.38	0.10
IDF6D6CCC	40	ILLB	2000	7/14/2010	11/11/2010	120	10.77	0.45	-	-	0.62	0.14
IDF6D6CCC	40	ILLB	2000	7/14/2010	1/10/2011	180	10.85	0.69	-	-	0.65	0.19
IDF6D6CCC	40	ILLB	2000	7/14/2010	12/11/2014	1611	11.42	1.09	1.47	-	1.03	0.23
IDF6D6CCC	40	ILLB	2000	7/14/2010	6/23/2015	1805	11.40	1.06	1.89	-	0.96	0.21
IDF6D6CCC	40	ILLB	2000	7/14/2010	6/28/2016	2176	11.46	1.05	1.67	-	0.95	0.20
IDF6D6CCC	40	ILLB	2000	7/14/2010	6/13/2017	2526	11.52	1.01	1.35	-	1.12	0.21
IDF6D6CCC	40	ILLB	2000	7/14/2010	6/8/2018	2886	11.43	1.27	1.24	-	1.17	0.23
IDF6D6CCC	40	ILLB	2000	7/14/2010	6/6/2019	3249	11.44	1.14	0.74	-	1.30	0.24
IDF6D6CCC	40	ILLB	2000	7/14/2010	6/2/2020	3611	9.92	1.36	1.26	-	1.23	0.25
IDF7E12CCC	40	ILLA	2000	6/22/2010	6/29/2010	7	10.11	0.00	-	0.16	0.16	0.06
IDF7E12CCC	40	ILLA	2000	6/22/2010	7/20/2010	28	10.17	0.00	-	0.20	0.23	0.08
IDF7E12CCC	40	ILLA	2000	6/22/2010	8/17/2010	56	10.22	0.19	-	0.29	0.32	0.11
IDF7E12CCC	40	ILLA	2000	6/22/2010	10/20/2010	120	10.32	0.37	-	0.27	0.45	0.13
IDF7E12CCC	40	ILLA	2000	6/22/2010	12/20/2010	181	10.58	0.47	-	0.44	0.53	0.17
IDF7E12CCC	40	ILLA	2000	6/22/2010	12/4/2014	1626	11.28	0.57	0.53	0.66	0.72	0.19
IDF7E12CCC	40	ILLA	2000	6/22/2010	6/3/2015	1807	11.33	0.55	0.53	0.63	0.70	0.18
IDF7E12CCC	40	ILLA	2000	6/22/2010	6/2/2016	2172	11.27	0.60	1.00	0.67	0.78	0.18
IDF7E12CCC	40	ILLA	2000	6/22/2010	6/6/2017	2541	11.37	0.55	0.99	0.58	0.70	0.15
IDF7E12CCC	40	ILLA	2000	6/22/2010	6/8/2018	2908	11.17	0.56	0.51	0.59	0.68	0.17
IDF7E12CCC	40	ILLA	2000	6/22/2010	6/5/2019	3270	10.54	0.32	0.32	0.58	0.72	0.16
IDF7E12CCC	40	ILLA	2000	6/22/2010	6/1/2020	3632	9.27	0.56	0.61	0.57	0.73	0.17
IDF8A125CCC	40	ILLA	2000	6/22/2010	6/29/2010	7	10.37	0.21	0.15	-	0.26	0.10
IDF8A125CCC	40	ILLA	2000	6/22/2010	7/20/2010	28	10.45	0.32	0.22	-	0.39	0.17
IDF8A125CCC	40	ILLA	2000	6/22/2010	8/17/2010	56	10.54	0.38	0.26	-	0.51	0.19
IDF8A125CCC	40	ILLA	2000	6/22/2010	10/20/2010	120	10.61	0.67	0.05	-	0.69	0.25
IDF8A125CCC	40	ILLA	2000	6/22/2010	12/20/2010	181	10.88	1.24	0.41	-	0.97	0.41
IDF8A125CCC	40	ILLA	2000	6/22/2010	12/4/2014	1626	11.56	10.91	3.58	-	8.01	1.67
IDF8A125CCC	40	ILLA	2000	6/22/2010	6/3/2015	1807	11.63	10.95	3.48	-	8.35	1.70
IDF8A125CCC	40	ILLA	2000	6/22/2010	6/2/2016	2172	11.84	10.71	3.60	-	9.02	1.63
IDF8A125CCC	40	ILLA	2000	6/22/2010	6/6/2017	2541	11.94	10.56	3.52	-	9.23	1.66
IDF8A125CCC	40	ILLA	2000	6/22/2010	6/8/2018	2908	11.91	10.39	3.51	-	8.86	1.67
IDF8A125CCC	40	ILLA	2000	6/22/2010	6/5/2019	3270	11.98	10.61	2.92	-	8.14	1.76
IDF8A125CCC	40	ILLA	2000	6/22/2010	6/1/2020	3632	11.14	10.28	3.50	-	8.47	1.61

- Below detection limit; # Measured at room temperature.

Table 3.5. Long-Term PCT-B Results at 40 °C and S/V of 2,000 m^{-1} (Tests ILLA and ILLB) (continued).

Glass name	Temp. (°C)	Test Name	S/V (m^{-1})	Immersion date	Sampling date	Elapsed time	pH[#]	Normalized release (g-glass/L)				
								B	K	Li	Na	Si
IDF9A187CCC	40	ILLB	2000	7/14/2010	7/21/2010	7	10.62	0.39	0.00	-	0.35	0.09
IDF9A187CCC	40	ILLB	2000	7/14/2010	8/11/2010	28	10.75	0.65	0.57	-	0.59	0.12
IDF9A187CCC	40	ILLB	2000	7/14/2010	9/8/2010	56	10.85	0.79	0.54	-	0.67	0.15
IDF9A187CCC	40	ILLB	2000	7/14/2010	11/11/2010	120	11.17	1.80	0.52	-	1.31	0.31
IDF9A187CCC	40	ILLB	2000	7/14/2010	1/10/2011	180	11.23	2.47	0.00	-	1.74	0.42
IDF9A187CCC	40	ILLB	2000	7/14/2010	12/11/2014	1611	11.83	2.80	1.47	-	2.16	0.41
IDF9A187CCC	40	ILLB	2000	7/14/2010	6/23/2015	1805	11.81	2.79	1.68	-	2.01	0.41
IDF9A187CCC	40	ILLB	2000	7/14/2010	6/28/2016	2176	11.85	2.72	1.61	-	1.98	0.41
IDF9A187CCC	40	ILLB	2000	7/14/2010	6/13/2017	2526	11.87	2.67	1.36	-	2.19	0.40
IDF9A187CCC	40	ILLB	2000	7/14/2010	6/8/2018	2886	11.54	2.74	1.40	-	2.11	0.40
IDF9A187CCC	40	ILLB	2000	7/14/2010	6/6/2019	3249	11.51	2.56	1.15	-	2.25	0.40
IDF9A187CCC	40	ILLB	2000	7/14/2010	6/2/2020	3611	10.20	2.69	1.39	-	1.98	0.38
IDF10Zr6CCC	40	ILLB	2000	7/14/2010	7/21/2010	7	10.11	0.15	0.00	-	0.20	0.07
IDF10Zr6CCC	40	ILLB	2000	7/14/2010	8/11/2010	28	10.28	0.32	0.00	-	0.36	0.10
IDF10Zr6CCC	40	ILLB	2000	7/14/2010	9/8/2010	56	10.41	0.39	0.00	-	0.36	0.10
IDF10Zr6CCC	40	ILLB	2000	7/14/2010	11/11/2010	120	10.62	0.32	0.00	-	0.45	0.12
IDF10Zr6CCC	40	ILLB	2000	7/14/2010	1/10/2011	180	10.71	0.49	0.00	-	0.44	0.16
IDF10Zr6CCC	40	ILLB	2000	7/14/2010	12/11/2014	1611	11.21	0.68	0.00	-	0.65	0.16
IDF10Zr6CCC	40	ILLB	2000	7/14/2010	6/23/2015	1805	11.17	0.71	0.00	-	0.66	0.17
IDF10Zr6CCC	40	ILLB	2000	7/14/2010	6/28/2016	2176	11.15	0.68	0.00	-	0.62	0.14
IDF10Zr6CCC	40	ILLB	2000	7/14/2010	6/13/2017	2526	11.17	0.66	0.00	-	0.68	0.15
IDF10Zr6CCC	40	ILLB	2000	7/14/2010	6/8/2018	2886	11.01	0.79	0.00	-	0.73	0.15
IDF10Zr6CCC	40	ILLB	2000	7/14/2010	6/6/2019	3249	11.01	0.78	0.26	-	0.76	0.15
IDF10Zr6CCC	40	ILLB	2000	7/14/2010	6/2/2020	3611	9.35	1.02	0.54	-	0.89	0.16
ANL-LRM-2	40	ILLA	2000	6/22/2010	6/29/2010	7	9.78	-	-	-	0.15	0.06
ANL-LRM-2	40	ILLA	2000	6/22/2010	7/20/2010	28	10.88	-	-	-	0.24	0.10
ANL-LRM-2	40	ILLA	2000	6/22/2010	8/17/2010	56	10.08	0.21	-	-	0.31	0.12
ANL-LRM-2	40	ILLA	2000	6/22/2010	10/20/2010	120	10.15	0.32	-	-	0.38	0.14
ANL-LRM-2	40	ILLA	2000	6/22/2010	12/20/2010	181	10.42	0.51	-	-	0.47	0.19
ANL-LRM-2	40	ILLA	2000	6/22/2010	12/4/2014	1626	11.08	0.89	0.21	-	0.83	0.23
ANL-LRM-2	40	ILLA	2000	6/22/2010	6/3/2015	1807	11.11	0.88	0.21	-	0.84	0.23
ANL-LRM-2	40	ILLA	2000	6/22/2010	6/2/2016	2172	11.15	0.90	0.30	-	0.92	0.24
ANL-LRM-2	40	ILLA	2000	6/22/2010	6/6/2017	2541	11.26	1.00	0.28	-	0.92	0.23
ANL-LRM-2	40	ILLA	2000	6/22/2010	6/8/2018	2908	11.06	1.05	0.27	-	0.95	0.24
ANL-LRM-2	40	ILLA	2000	6/22/2010	6/5/2019	3270	11.08	0.95	0.19	-	1.10	0.25
ANL-LRM-2	40	ILLA	2000	6/22/2010	6/1/2020	3632	9.70	1.20	0.27	-	1.04	0.24
ANL-LRM-2	40	ILLB	2000	7/14/2010	7/21/2010	7	9.76	-	-	-	0.13	0.05
ANL-LRM-2	40	ILLB	2000	7/14/2010	8/11/2010	28	9.87	-	-	-	0.23	0.09
ANL-LRM-2	40	ILLB	2000	7/14/2010	9/8/2010	56	10.08	0.20	-	-	0.25	0.09
ANL-LRM-2	40	ILLB	2000	7/14/2010	11/11/2010	120	10.17	0.00	-	-	0.35	0.12
ANL-LRM-2	40	ILLB	2000	7/14/2010	1/10/2011	180	10.27	0.28	-	-	0.34	0.16
ANL-LRM-2	40	ILLB	2000	7/14/2010	12/11/2014	1611	11.03	0.77	0.18	-	0.75	0.21
ANL-LRM-2	40	ILLB	2000	7/14/2010	6/23/2015	1805	11.02	0.73	0.22	-	0.69	0.20
ANL-LRM-2	40	ILLB	2000	7/14/2010	6/28/2016	2176	11.08	0.82	0.21	-	0.73	0.20
ANL-LRM-2	40	ILLB	2000	7/14/2010	6/13/2017	2526	11.08	0.75	0.17	-	0.85	0.21
ANL-LRM-2	40	ILLB	2000	7/14/2010	6/8/2018	2886	11.04	0.93	0.18	-	0.84	0.21
ANL-LRM-2	40	ILLB	2000	7/14/2010	6/6/2019	3249	11.07	0.89	0.18	-	0.92	0.22
ANL-LRM-2	40	ILLB	2000	7/14/2010	6/2/2020	3611	9.56	1.10	0.21	-	0.97	0.23

- Below detection limit; [#] Measured at room temperature.

Table 3.6. Long-Term PCT-B Results at 90 °C and Various S/V (Tests ILHE, ILHF and ILHG).

Glass ID	Sample ID	Test	S/V (m^{-1})	Start Date	Sampling Date	Period	pH#	Normalized Release [g/L]				
								B*	K*	Li*	Na*	Si*
IDF22 EC46CCC	22EC46	ILHE	20000	6/4/2018	6/11/2018	7	11.78	3.61	1.88	2.86	4.29	0.91
					7/2/2018	28	11.85	4.02	2.38	3.26	5.07	1.06
					7/30/2018	56	11.92	4.88	3.28	3.51	6.50	1.17
					10/2/2018	120	12.07	67.05$	33.11$	46.48$	45.12$	3.53$
					11/30/2018	179	11.82	486.72	241.88	262.49	275.67	6.80
					3/1/2019	270	11.81	712.21	371.47	280.30	411.39	9.32
					6/4/2019	365	11.86	714.50	278.54	264.44	464.99	8.13
					9/18/2019	471	11.65	658.03	284.46	212.26	348.82	7.03
					12/10/2019	554	11.62	527.53	260.94	189.55	317.22	6.29
					3/16/2020	651	12.00	481.48	244.61	143.79	310.29	5.70
IDF25 EC34CCC	25EC34				6/11/2018	7	11.91	8.10	2.66	-	6.68	1.10
					7/2/2018	28	11.93	8.66	3.05	-	7.61	1.11
					7/30/2018	56	12.00	9.76	4.44	-	8.20	1.10
					10/2/2018	120	12.04	35.03	43.25	-	33.21	3.62
					11/30/2018	179	12.22	158.78	70.22	-	86.77	6.45
					3/1/2019	270	11.82	518.54	184.75	-	233.80	13.72
					6/4/2019	365	11.88	592.30	149.76	-	347.44	18.07
					9/18/2019	471	11.83	548.47	198.21	-	271.96	17.89
					12/10/2019	554	11.85	508.09	184.96	-	289.71	17.40
					3/16/2020	651	12.17	547.85	175.56	-	290.71	17.25
IDF26 EC44CCC	26EC44				6/11/2018	7	11.82	5.09	2.22	2.75	5.01	1.07
					7/2/2018	28	11.86	5.45	2.71	2.69	5.69	1.19
					7/30/2018	56	11.96	5.42	3.49	2.52	6.41	1.19
					10/2/2018	120	12.02	35.06	14.73	26.75	25.18	3.37
					11/30/2018	179	12.10	315.96	154.98	187.70	192.26	8.64
					3/1/2019	270	11.82	687.89	327.12	273.13	391.23	16.55
					6/4/2019	365	11.88	774.53	258.90	244.37	489.01	17.72
					9/18/2019	471	11.81	652.42	282.88	159.14	328.66	14.70
					12/10/2019	554	11.79	568.61	252.11	135.01	328.05	12.90
					3/16/2020	651	12.13	572.78	239.56	106.83	321.94	12.26
IDF27 EC48CCC	27EC48				6/11/2018	7	11.70	2.42	1.59	2.69	3.44	0.78
					7/2/2018	28	11.84	2.66	2.03	3.13	4.11	0.89
					7/30/2018	56	11.91	2.87	2.49	3.27	4.43	0.95
					10/2/2018	120	11.97	6.92	3.86	7.64	7.92	1.63
					11/30/2018	179	12.10	77.12	34.12	49.03	100.86	1.63
					3/1/2019	270	11.59	652.16	260.76	277.14	329.05	5.35
					6/4/2019	365	11.55	806.51	297.04	314.75	584.67	5.79
					9/18/2019	471	11.47	655.86	287.92	285.78	344.48	5.26
					12/10/2019	554	11.41	544.47	276.47	265.75	356.97	4.67
					3/16/2020	651	11.70	564.31	247.63	218.91	343.29	4.74
IDF28 EC50CCC	28EC50				6/11/2018	7	12.01	8.25	2.77	-	6.04	0.62
					7/2/2018	28	12.13	11.25	3.59	-	8.36	0.79
					7/30/2018	56	12.17	13.06	6.03	-	8.95	0.91
					10/2/2018	120	12.24	13.53	4.67	-	9.81	0.89
					11/30/2018	179	12.32	14.60	5.05	-	10.02	0.85
					3/1/2019	270	12.32	16.27	5.65	-	12.54	0.98
					6/4/2019	365	12.45	24.44	5.87	-	17.98	1.45
					9/18/2019	471	12.45	34.58	10.45	-	20.09	1.92
					12/10/2019	554	12.40	40.32	13.47	-	24.00	2.18
					3/16/2020	651	12.60	43.83	14.27	-	27.41	2.34
					6/15/2020	742	12.57	41.29	15.41	-	25.37	2.10

- Empty data field; # Measured at room temperature.

Table 3.6. Long-Term PCT-B Results at 90 °C and Various S/V (Tests ILHE, ILHF and ILHG) (continued).

Glass ID	Sample ID	Test	S/V (m^{-1})	Start Date	Sampling Date	Period	pH#	B* Norm. Release [g/L]	K* Norm. Release [g/L]	Na* Norm. Release [g/L]	Si* Norm. Release [g/L]
IDF23 EC52CCC	1K23 EC52	ILHF	1000	6/5/2018	6/12/2018	7	10.48	0.58	0.00	0.57	0.23
					7/3/2018	28	10.90	1.85	0.64	1.39	0.34
					7/31/2018	56	11.38	2.14	0.90	1.49	0.35
					10/3/2018	120	11.13	2.60	0.85	1.81	0.40
					12/3/2018	181	11.35	2.60	1.04	1.84	0.42
					3/4/2019	272	11.39	2.54	0.88	1.97	0.42
					6/5/2019	365	11.46	2.84	1.03	2.32	0.47
					9/19/2019	471	11.55	2.83	0.90	2.04	0.48
					12/12/2019	555	11.58	2.85	0.83	2.08	0.46
					3/17/2020	651	11.52	2.77	1.17	2.32	0.49
					6/17/2020	743	11.61	2.84	1.01	2.28	0.49
	2K23 EC52		2000		6/12/2018	7	11.26	1.85	0.54	1.30	0.32
					7/3/2018	28	11.31	3.13	0.94	2.09	0.41
					7/31/2018	56	11.29	3.40	1.40	2.23	0.41
					10/3/2018	120	11.47	3.75	1.18	2.58	0.43
					12/3/2018	181	11.68	4.01	1.51	2.77	0.47
					3/4/2019	272	11.66	3.98	1.27	2.96	0.48
					6/5/2019	365	11.78	4.42	1.42	3.65	0.54
					9/19/2019	471	11.86	4.59	1.52	3.55	0.56
					12/12/2019	555	11.84	4.51	1.31	3.49	0.53
					3/17/2020	651	11.80	4.38	1.82	3.73	0.54
					6/17/2020	743	11.92	4.47	1.52	3.50	0.57
	5K23 EC52		5000		6/12/2018	7	11.58	3.49	0.98	2.33	0.38
					7/3/2018	28	11.65	5.72	1.78	3.57	0.52
					7/31/2018	56	11.80	6.38	2.48	4.35	0.57
					10/3/2018	120	11.79	6.65	1.98	4.59	0.57
					12/3/2018	181	11.98	6.56	2.35	4.50	0.57
					3/4/2019	272	11.92	6.34	2.04	4.88	0.57
					6/5/2019	365	11.99	6.78	1.99	5.68	0.64
					9/19/2019	471	12.09	7.73	2.22	5.40	0.66
					12/12/2019	555	12.08	6.70	2.06	5.34	0.63
					3/17/2020	651	12.01	6.73	2.73	6.09	0.66
					6/17/2020	743	12.18	7.18	2.48	5.75	0.69
	10K23 EC52		10000		6/12/2018	7	11.88	6.06	1.71	4.07	0.48
					7/3/2018	28	11.82	8.53	2.41	5.22	0.60
					7/31/2018	56	11.95	8.84	3.20	6.04	0.64
					10/3/2018	120	11.95	9.34	2.60	6.72	0.65
					12/3/2018	181	12.12	9.57	3.21	7.71	0.68
					3/4/2019	272	12.10	9.82	2.85	7.55	0.68
					6/5/2019	365	12.11	9.64	2.74	8.05	0.79
					9/19/2019	471	12.25	12.30	3.50	8.09	0.80
					12/12/2019	555	12.28	12.22	3.64	9.18	0.91
					3/17/2020	651	12.19	14.16	4.62	10.31	1.01
					6/17/2020	743	12.33	18.27	5.52	12.11	1.23
	20K23 EC52		20000		6/12/2018	7	12.07	9.99	2.99	6.70	0.63
					7/3/2018	28	12.01	12.36	3.56	7.84	0.70
					7/31/2018	56	12.13	13.22	4.68	8.68	0.75
					10/3/2018	120	12.13	15.60	4.35	10.82	0.82
					12/3/2018	181	12.33	15.67	5.57	10.54	0.87
					3/4/2019	272	12.25	15.84	4.76	11.10	0.92
					6/5/2019	365	12.30	21.38	5.38	15.21	1.59
					9/19/2019	471	12.46	57.92	13.90	30.24	2.46
					12/12/2019	555	12.46	90.66	35.30	48.79	3.09
					3/17/2020	651	12.55	132.39	56.71	91.49	3.75
					6/17/2020	743	12.69	156.88	78.09	98.19	3.68

- Empty data field; # Measured at room temperature.

Table 3.6. Long-Term PCT-B Results at 90 °C and Various S/V (Tests ILHE, ILHF and ILHG) (continued).

Glass ID	Sample ID	Test	S/V (m^{-1})	Immersion Date	Sampling Date	Period	pH#	B* Norm. Release [g/L]	K* Norm. Release [g/L]	Na* Norm. Release [g/L]	Si* Norm. Release [g/L]
IDF24 EC28CCC	1K24 EC28	ILHG	1000	6/5/2018	6/12/2018	7	10.98	0.67	0.45	0.74	0.25
					7/3/2018	28	11.11	1.47	0.75	1.24	0.36
					7/31/2018	56	11.20	1.83	0.86	1.43	0.39
					10/3/2018	120	11.30	1.96	0.98	1.73	0.41
					12/4/2018	182	11.47	2.19	1.09	1.81	0.47
					3/5/2019	273	11.52	2.17	1.12	1.91	0.47
					6/6/2019	366	11.57	2.27	1.11	2.33	0.51
					9/20/2019	472	11.72	2.29	1.13	2.07	0.49
					12/13/2019	556	11.63	2.18	1.11	2.02	0.48
					3/18/2020	652	11.85	2.29	1.27	2.13	0.51
					6/18/2020	744	11.73	2.18	1.26	2.08	0.50
	2K24 EC28		2000		6/12/2018	7	11.32	1.12	0.68	1.12	0.28
					7/3/2018	28	11.41	2.32	1.10	1.78	0.39
					7/31/2018	56	11.58	2.98	1.34	2.37	0.47
					10/3/2018	120	11.62	3.26	1.50	2.70	0.48
					12/4/2018	182	11.66	3.59	1.68	2.82	0.54
					3/5/2019	273	11.78	3.49	1.68	2.83	0.54
					6/6/2019	366	11.84	3.65	1.65	3.57	0.59
					9/20/2019	472	11.95	3.88	1.90	3.43	0.60
					12/13/2019	556	11.94	3.65	1.84	3.43	0.58
					3/18/2021	652	12.04	3.94	2.07	3.73	0.61
					6/18/2020	744	11.96	3.70	2.01	3.54	0.58
	5K24 EC28		5000		6/12/2018	7	11.69	2.45	1.32	2.31	0.37
					7/3/2018	28	11.74	4.45	2.12	3.32	0.53
					7/31/2018	56	11.86	4.90	2.23	3.84	0.54
					10/3/2018	120	11.92	5.70	2.72	4.80	0.60
					12/4/2018	182	12.03	6.05	2.91	4.83	0.63
					3/5/2019	273	12.12	6.28	2.94	4.97	0.65
					6/6/2019	366	12.08	6.12	2.65	5.91	0.67
					9/20/2019	472	12.22	6.83	3.34	5.70	0.71
					12/13/2019	556	12.16	6.83	3.14	5.78	0.69
					3/18/2021	652	12.20	7.31	3.73	6.26	0.73
					6/18/2020	744	12.19	7.00	3.45	6.03	0.70
	10K24 EC28		10000		6/12/2018	7	11.90	3.99	2.02	3.57	0.44
					7/3/2018	28	11.90	6.34	2.73	4.45	0.60
					7/31/2018	56	12.04	7.22	3.27	5.76	0.62
					10/3/2018	120	12.09	8.47	3.81	7.13	0.65
					12/4/2018	182	12.19	9.12	4.18	8.40	0.73
					3/5/2019	273	12.19	8.90	4.16	7.70	0.73
					6/6/2019	366	12.24	9.81	3.68	8.61	0.80
					9/20/2019	472	12.36	9.99	4.56	7.99	0.82
					12/13/2019	556	12.32	10.85	4.42	8.49	0.78
					3/18/2021	652	12.37	9.95	4.57	8.72	0.83
					6/18/2020	744	12.32	11.28	4.73	8.87	0.86
	20K24 EC28		20000		6/12/2018	7	12.08	5.97	3.31	5.72	0.51
					7/3/2018	28	12.11	9.47	4.21	7.39	0.67
					7/31/2018	56	12.25	11.20	5.60	9.01	0.77
					10/3/2018	120	12.27	12.78	6.31	10.92	0.78
					12/4/2018	182	12.41	13.66	6.93	10.72	0.90
					3/5/2019	273	12.37	13.54	6.65	10.80	0.90
					6/6/2019	366	12.43	15.80	6.21	13.97	1.04
					9/20/2019	472	12.55	17.10	8.12	13.92	1.08
					12/13/2019	556	12.50	16.43	6.87	13.07	0.97
					3/18/2021	652	12.55	24.74	9.77	18.70	1.45
					6/18/2020	744	12.63	42.88	15.29	27.24	2.02

- Empty data field; # Measured at room temperature.

Table 3.7. Long-Term PCT-B Results for Reference Glass ANL-LRM at 90 °C and S/V of 2,000 m^{-1} (Tests ILHE, ILHF, and ILHG).

Glass ID	Test	S/V (m^{-1})	Immersion Date	Sampling Date	Period	pH[#]	B* Norm. Release [g/L]	K* Norm. Release [g/L]	Li* Norm. Release [g/L]	Na* Norm. Release [g/L]	Si* Norm. Release [g/L]
ANL-LRM-2	ILHE	2000	6/4/2018	6/11/2018	7	10.64	1.09	0.29	0.00	1.01	0.33
				7/2/2018	28	11.19	2.66	0.57	3.55	2.06	0.46
				7/30/2018	56	11.49	3.74	0.95	4.39	2.72	0.54
				10/2/2018	120	11.47	4.97	0.84	6.11	3.33	0.57
				11/30/2018	179	11.56	5.04	1.03	5.64	3.40	0.61
				3/1/2019	270	11.67	5.74	1.17	4.97	4.44	0.64
				6/4/2019	365	11.82	6.65	1.22	5.22	5.84	0.83
				9/18/2019	471	11.71	6.69	1.24	5.32	4.65	0.89
				12/10/2019	554	11.62	6.89	1.40	4.80	5.08	1.14
				3/16/2020	651	11.78	7.16	1.48	4.74	5.71	1.23
				6/15/2020	742	11.73	6.53	1.43	4.82	5.31	1.14
	ILHF		6/5/2018	6/12/2018	7	10.83	1.33	0.30	0.00	1.12	0.35
				7/3/2018	28	10.93	2.34	0.52	3.12	1.76	0.43
				7/31/2018	56	11.16	3.34	0.75	4.39	2.39	0.50
				10/3/2018	120	11.35	4.59	0.83	5.34	3.29	0.58
				12/3/2018	181	11.59	4.97	1.00	6.26	3.34	0.62
				3/4/2019	272	11.61	5.18	1.00	6.03	3.88	0.63
				6/5/2019	365	11.58	5.84	0.99	6.00	4.41	0.74
				9/19/2019	471	11.72	6.39	1.11	7.54	4.51	0.89
				12/12/2019	555	11.62	6.64	1.21	6.33	4.74	1.07
				3/17/2020	651	11.59	7.07	1.42	6.72	5.66	1.21
				6/17/2020	743	11.71	7.03	1.47	6.11	5.97	1.27
	ILHG		6/5/2018	6/12/2018	7	10.57	1.15	0.24	0.00	1.06	0.32
				7/3/2018	28	10.99	2.50	0.54	3.10	1.86	0.43
				7/31/2018	56	11.35	3.89	0.85	3.64	2.94	0.54
				10/3/2018	120	11.56	5.36	1.06	4.69	4.09	0.61
				12/4/2018	182	11.64	5.80	1.09	6.65	3.96	0.66
				3/5/2019	273	11.59	5.82	0.99	8.29	3.98	0.66
				6/6/2019	366	11.70	6.59	1.17	8.00	5.62	0.96
				9/20/2019	472	11.77	7.00	1.27	7.30	5.32	1.09
				12/13/2019	556	11.63	6.55	1.16	6.87	4.85	1.16
				3/18/2021	652	11.71	6.75	1.63	6.05	5.35	1.21
				6/18/2020	744	11.65	6.25	1.31	5.53	5.02	1.20

[#] Measured at room temperature

Table 4.1. Summary of Phases Identified on Solid Samples Taken from PCT Vessels of the Ten IDF Phase 1 Glasses [50, 56].

Sample ID	Resumption?	Phyllosilicates	Tecto- and Soro-silicates	Others
Sampled from PCT-B at 90°C and S/V 20,000 m^{-1}				
IDF1-B2CCC in IHHA-6-5	272 days	Saponite	Lazurite	-
IDF2-G9CCC in IHHA-6-8	No	None detected		
IDF3-F7CCC in IHHA-6-11	No	None detected		$^{\$}ZnCr_2O_4$
IDF4-A15CCC in IHHB-6-3	272 days	None detected	Phillipsite and Lazurite	-
IDF5-A20CCC in IHHB-6-8	No	None detected	Gehlenite	-
IDF6-D6CCC	56 to 120 days	Agglomeration– sampling not possible		
IDF7-E12CCC	180 days	Agglomeration– sampling not possible		
IDF8-A125CCC in IHHA-6-15	No	None detected	Analcime	-
IDF9-A187CCC	56 to 120 days	Agglomeration – sampling not possible		
IDF10-Zr6CCC in IHHB-6-17	No	None detected		
Sampled from PCT-B at 90°C and S/V 2,000 m^{-1}				
IDF1-B2CCC in ILHA-18-5	2546 days and on-going	Various possible phyllosilicates	Chabazite $Ca_2Al_4Si_8O_{24}(H_2O)_{12}$	
IDF2-G9CCC in ILHA-18-8	No	No crystallization detected in XRD but few detectable surface crystals in SEM		
IDF3-F7CCC (in ILHA-18-11	2546 days	Nontronite	$Na_{3.555}(Al_{3.6}Si_{12.4}O_{32})(H_2O)_{10.556}$ and analcime $NaAl(SiO_6)(H_2O)$	$^{\$}ZnCr_2O_4$
IDF4-A15CCC in ILHB-18-5	1445 days	Various possible phyllosilicates	Zeolite, gobbinsite at last sampling + Phillipsite and lazurite	-
IDF5-A20CCC in ILHB-18-8	2546 days and on-going	Various possible phyllosilicates	Analcime $NaAl(SiO_6)(H_2O)$	
IDF6-D6CCC in ILHB-15-(9,10,11) Terminated	545 to 727 days	Lizardite	Analcime and Gobbinsite	-
IDF7-E12CCC in ILHA-18-14	1266 days	Tobermorite and Kaolinite	Analcime + Phillipsite and Coesite	-
IDF8-A125CCC in ILHA-18-17	727 to 1630 days	None detectable	Analcime and chabazite	-
IDF9-A187CCC in ILHB-15-(12,13,14) & Terminated	364 to 727 days	Lizardite	Analcime and gobbinsite	-
IDF10-Zr6CCC in ILHB-18-17	No	No crystallization detected in XRD but few detectable surface crystals in SEM		

$^{\$}$Trace amount of zincochromite ($ZnCr_2O_4$) originally identified in the CCC glass prior to leach test; - Empty data field

Table 4.2. Summary of Phases Identified on Solid Samples Taken from PCT Vessels of the Ten IDF Phase 2 Glasses [57].

Sample ID	Resumption?	Phyllosilicates	Tecto- and Soro-silicates
Sampled from PCT-B at 90°C and S/V 20,000 m^{-1}			
IDF11-G27CCC in ILHC-11-3	No	No crystallization detected in XRD but few detectable surface crystals in SEM	
IDF12-A38CCC in ILHC-11-6	Incipient at 1814 days	No crystallization detected in XRD but few detectable surface crystals in SEM	
IDF13-A51CCC in ILHC-11-9	Slow rise at 1 yr and fully altered at 1345 days	Various possible phyllosilicates	Zeolite $Na_6(Al_6Si_{10}O_{32})(H_2O)_{12}$ Analcime $NaAl(SiO_6)(H_2O)$
IDF14-A59CCC in ILHC-12	273 days	None clearly identified	Zeolite $Na_6(Al_6Si_{10}O_{32})(H_2O)_{12}$ + in prior sampling Phillipsite $(K,Na)_2(Si,Al)_8O_{16}\cdot 4H_2O$ in XRD; $(Na_{6.7}K_{0.1}Mg_{0.4}Ca_{0.2}Ti_{0.8}Zn_{0.4})Al_2Si_7O_{24}$ in SEM
IDF15-A57CCC in ILHC-11-15	Slow rise at 1 yr and plateaued ~30% altered	Various possible phyllosilicates	Zeolite $Na_6(Al_6Si_{10}O_{32})(H_2O)_{12}$
IDF16-A58CCC in ILHD-11-3	1813 days	No crystallization detected in XRD but few detectable surface crystals in SEM	
IDF17-A60CCC in ILHD-11-6	No	No crystallization detected in XRD but phyllosilicate layer visible in SEM	
IDF18-A161CCC in ILHD-11-9	119 days	Aliettite $(Ca_{0.9}Mg_6(Si,Al)_8O_{22}(OH)_4\cdot 4H_2O)$ or beidellite $(Na_{0.3}Al_2(Si,Al)_4O_{10}(OH)_2\cdot 2H_2O)$ in XRD	Zeolite $Na_6(Al_6Si_{10}O_{32})(H_2O)_{12}$ + in prior sampling Phillipsite $(K,Na)_2(Si,Al)_8O_{16}\cdot 4H_2O$ in XRD; Multiple morphologies, phillipsite or albite in SEM: $Na_6CaFe_{0.1}Zn_{0.3}Zr)Al_3Si_{10}O_{24}$
IDF19-C100CCC in ILHD-11-12	119 days	Aliettite $(Ca_{0.9}Mg_6(Si,Al)_8O_{22}(OH)_4\cdot 4H_2O)$ or beidellite $(Na_{0.3}Al_2(Si,Al)_4O_{10}(OH)_2\cdot 2H_2O)$ in XRD	Zeolite $Na_6(Al_6Si_{10}O_{32})(H_2O)_{12}$ + in prior sampling Phillipsite $(K,Na)_2(Si,Al)_8O_{16}\cdot 4H_2O$ in XRD; Multiple morphologies, phillipsite or albite in SEM: $Na_6CaFe_{0.1}Zn_{0.3}Zr)Al_3Si_{10}O_{24}$
IDF20-F6CCC in ILHD-11-15	365 days	Swinefordite $(Ca_{0.1}(Li,Al)_3Si_4O_{10}(OH)_2\cdot 2(H_2O)$ in XRD; Possibly cavansite $Ca(VO)Si_4O_{10}(H_2O)_4$ in SEM	Zeolite $Na_6(Al_6Si_{10}O_{32})(H_2O)_{12}$ + in prior sampling Phillipsite $(K,Na)_2(Si,Al)_8O_{16}\cdot 4H_2O$ smaller in XRD Possibly hemimorphite $Zn_4Si_2O_7(OH)_2\cdot H_2O$ in SEM
ANL-LRM2 in ILHC-11-18 and ILHD-11-18 & Terminated	272 days	None detected	Phillipsite $(K,Na)_2(Si,Al)_8O_{16}\cdot 4H_2O$ and possibly analcime in XRD; Multiple morphologies, generally small in SEM: $(Na_{3.7}K_{0.1}Mg_{0.2}Ca_{0.6}Fe_{0.1}Zn_{0.41}Zr_{0.3})Al_{1.5}Si_{4.8}O_{16}$

Table 4.3. EDS Analyses of Phyllosilicate Crystals Observed on IDF Phase 3 Altered Glasses.

Elemental at%	Na	Mg	Al	Si	K	Ca	Cr	Fe	Ti	Zn	Zr	Sn	O	Si/Al
23EC52-15-11														
Inner layer* (Fig. 4.7)	5.1	0.9	4.1	22.5	0.3	1.8	–	–	–	1.0	2.1	0.2	62.1	5.5
Outer layer (Fig. 4.7)	5.3	1.5	4.4	22.5	–	0.8	–	–	–	1.5	1.8	–	61.5	5.2
28EC50-16-11														
Inner layer (Fig. 4.9)	5.7	1.1	4.9	20.5	0.3	1.9	0.2	0.2	0.2	1.1	2.4	0.2	61.4	4.2
Outer layer (Fig. 4.9)	4.5	1.8	4.6	20.9	–	1.5	0.2	0.3	0.2	1.5	2.5	0.2	61.8	4.6
24EC28-15-11														
Inner layer (Fig. 4.11)	4.9	0.6	4.9	21.6	1.2	1.3	0.1	0.2	0.2	0.8	1.9	0.6	61.9	4.5
Inner layer (Fig. 4.12)	6.7	–	5.6	21.0	1.4	0.9	–	0.2	0.2	0.7	1.8	0.5	61.0	3.8
Outer layer (Fig. 4.11)	5.2	0.3	5.3	21.6	1.2	1.0	0.1	0.2	0.2	0.8	1.7	0.5	61.7	4.1

*"Inner layer" is close to the unaltered glass; "Outer layer" is close to the solution; in between is called "Middle layer"
- Empty data field

Table 4.4. EDS Analyses of Zeolite Crystals Observed on IDF Phase 3 Altered Glasses.

Elemental at%	Na	Al	Si	K	Ca	Fe	Zn	O	Si/Al
25EC34-07-11									
Spectrum 64	6.9	9.3	21.9	0.1	–	0.1	0.2	61.5	2.3
Spectrum 65	6.7	9.2	21.9	0.1	–	0.1	0.4	61.6	2.4
Spectrum 102	7.0	9.3	21.8	0.2	–	–	0.2	61.4	2.4
26EC44-10-11									
Spectrum 151	6.9	9.4	22.0	0.1	–	–		61.6	2.3
Spectrum 152	6.9	9.5	21.6	0.2	–	–	0.5	61.4	2.3
Spectrum 153	6.7	9.5	21.9	0.2	–	–	0.2	61.6	2.3
Spectrum 154	7.0	9.4	21.8	0.2	–	–	0.2	61.4	2.3
Spectrum 155	7.4	9.2	21.5	0.2	–	–	0.7	61.1	2.3
Spectrum 156	6.9	9.3	21.7	0.1	–	–	0.6	61.4	2.3
22EC46-05-11									
Spectrum 16	7.4	10.3	20.7	0.2	0.2	–	0.3	61.0	2.0
Spectrum 17	7.6	9.9	20.7	0.2	0.1	–	0.3	61.0	2.1
27EC48-13-11									
Spectrum 170	7.5	10.5	20.8	–	–	–	0.1	61.2	2.0
Spectrum 171	7.6	10.7	20.3	0.1	0.1	–	0.2	60.9	1.9
Spectrum 172	7.2	10.2	21.2	0.1	–	–	–	61.3	2.1
Spectrum 173	7.3	10.7	20.5	0.1	0.1	–	0.3	61.1	1.9

- Empty data field

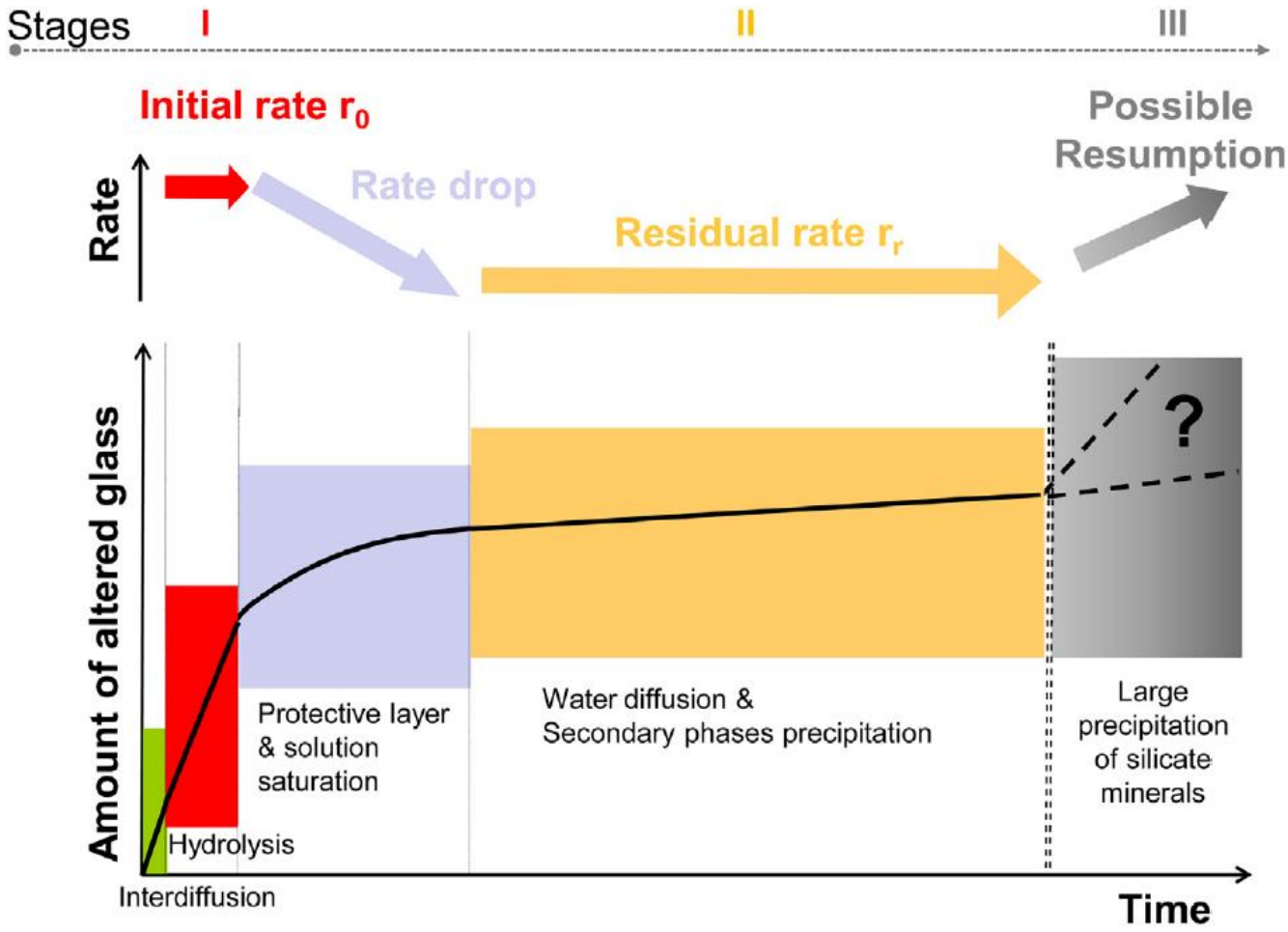

Figure 1.1. "Stages of nuclear glass corrosion and related potential rate-limiting mechanism", *after Gin. et al. [8].*

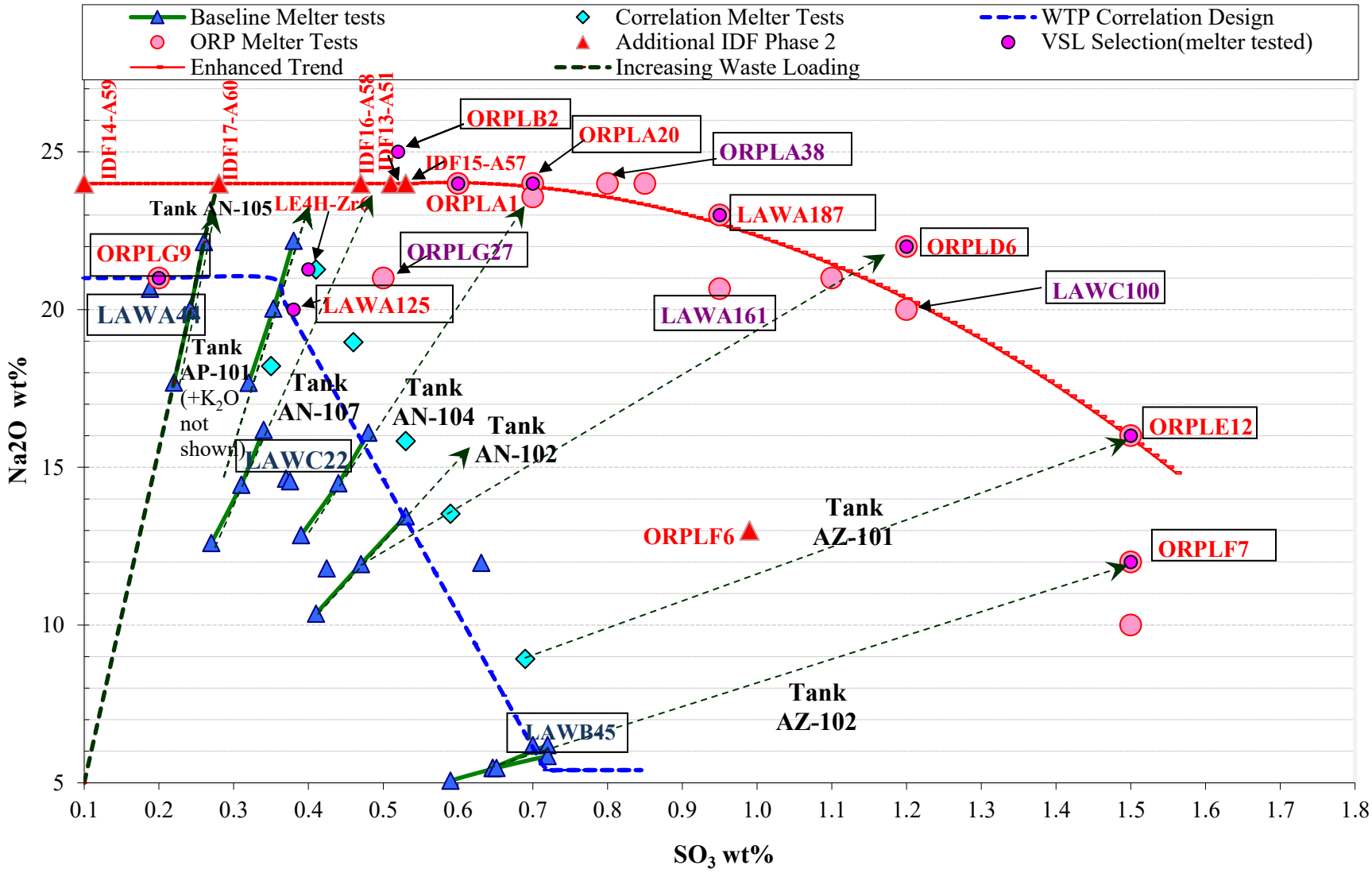

Figure 1.2. Overview of Na_2O and SO_3 loadings for WTP, ORP, and selected IDF glasses.

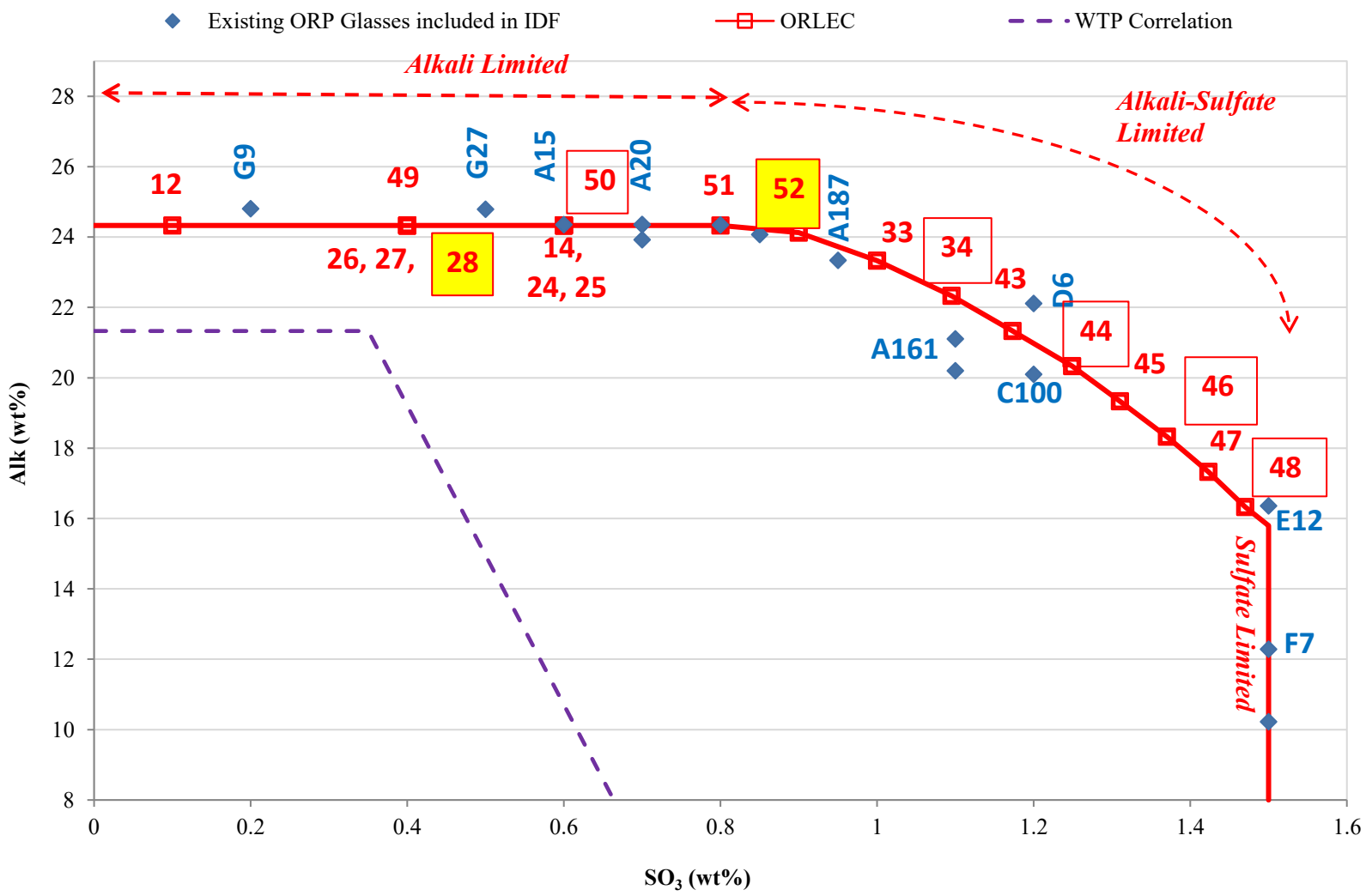

Figure 2.1. ALK ($Na_2O + 0.66 \times K_2O$) and SO_3 concentrations for the IDF glasses (blue diamonds) and the Enhanced LAW Correlation glasses (red squares); glasses selected for long-term PCT are labeled in red squares and the two glasses tested at various S/V are highlighted in yellow.

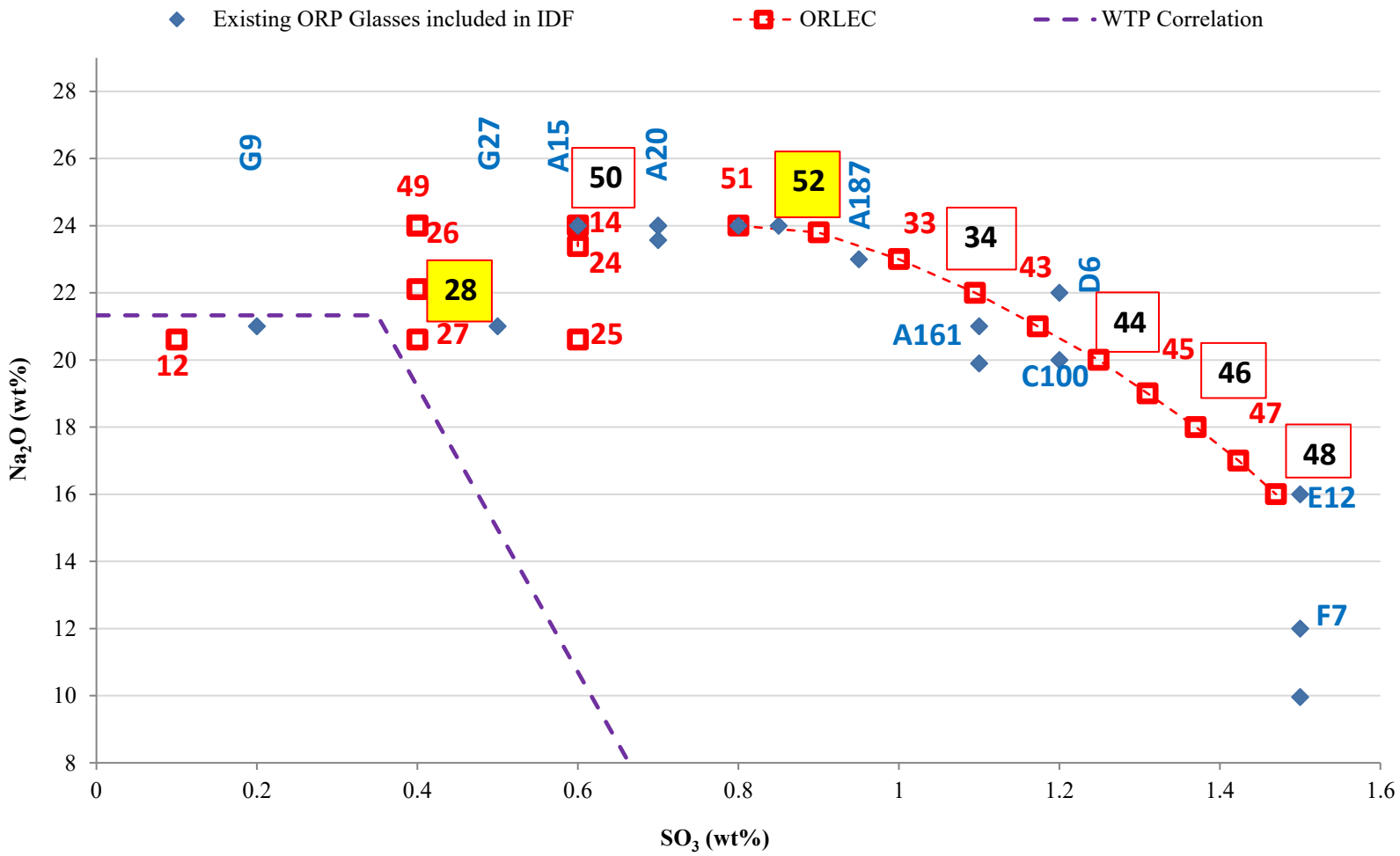

Figure 2.2. Na_2O and SO_3 concentrations for the IDF glasses (blue diamonds) and the ORLEC glasses (red squares); glasses tested in long-term PCT are labeled in red squares and the two glasses tested at various S/V are highlighted in yellow.

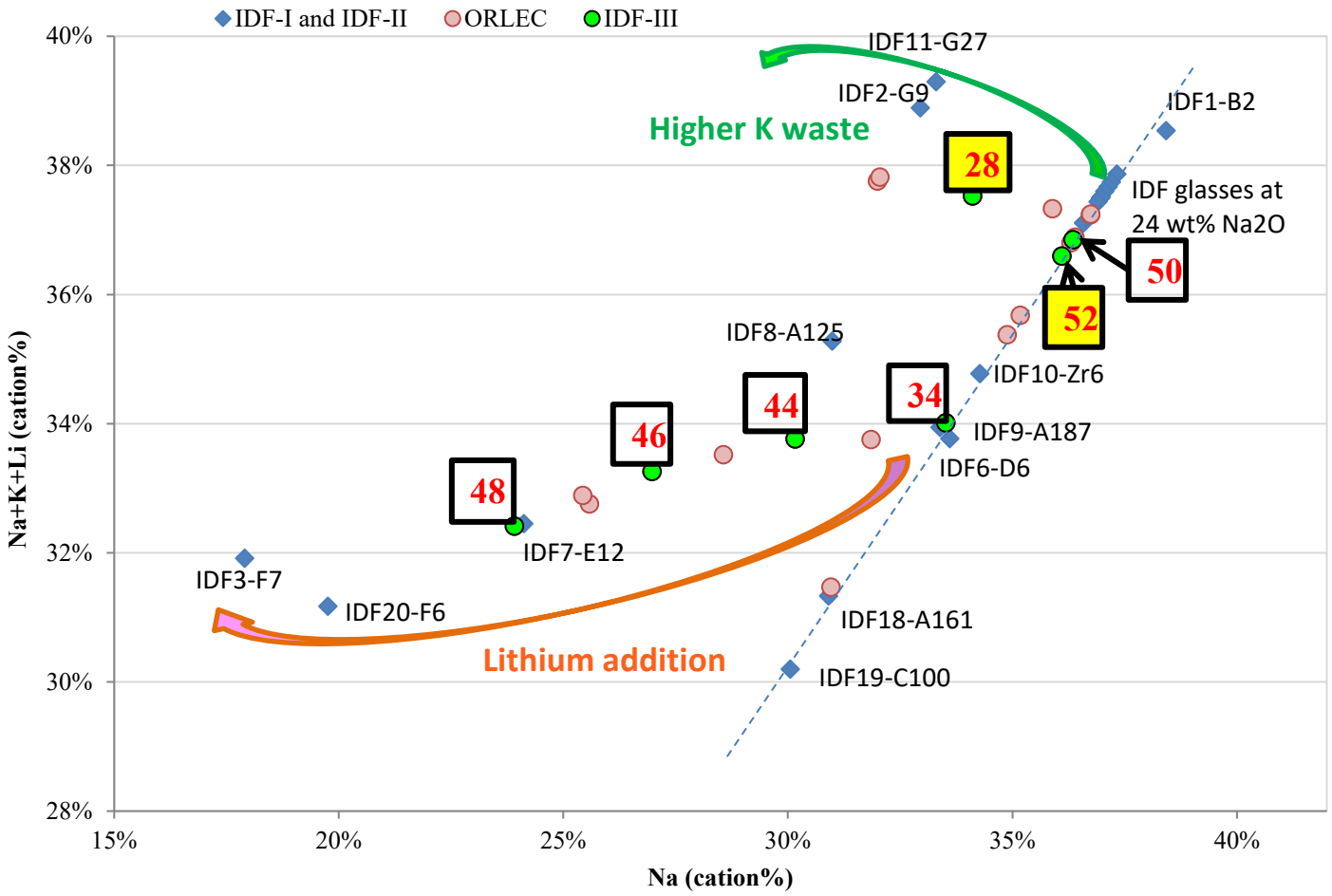

Figure 2.3. Sum of alkalis (Na, K, Li, in cation%) versus Na in the 20 IDF Phase 1 and Phase 2 glasses and the seven IDF Phase 3 glasses selected for long-term PCT.

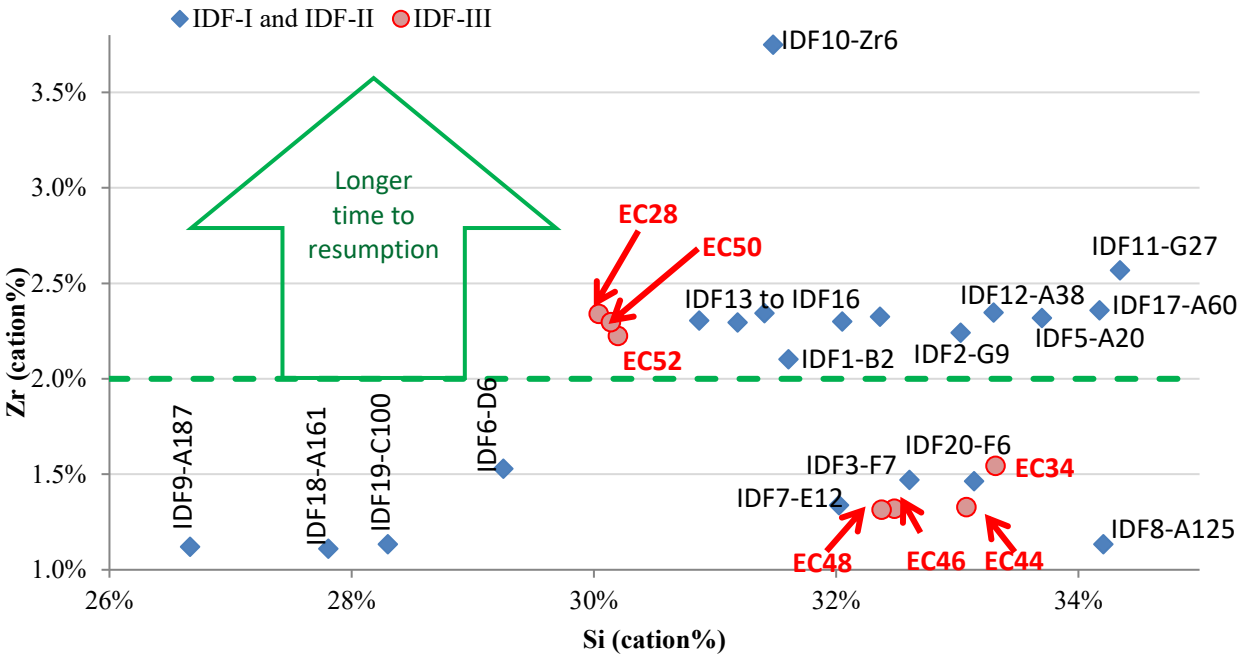

Figure 2.4. Zirconium versus silicon in the 27 IDF glasses (cation%).

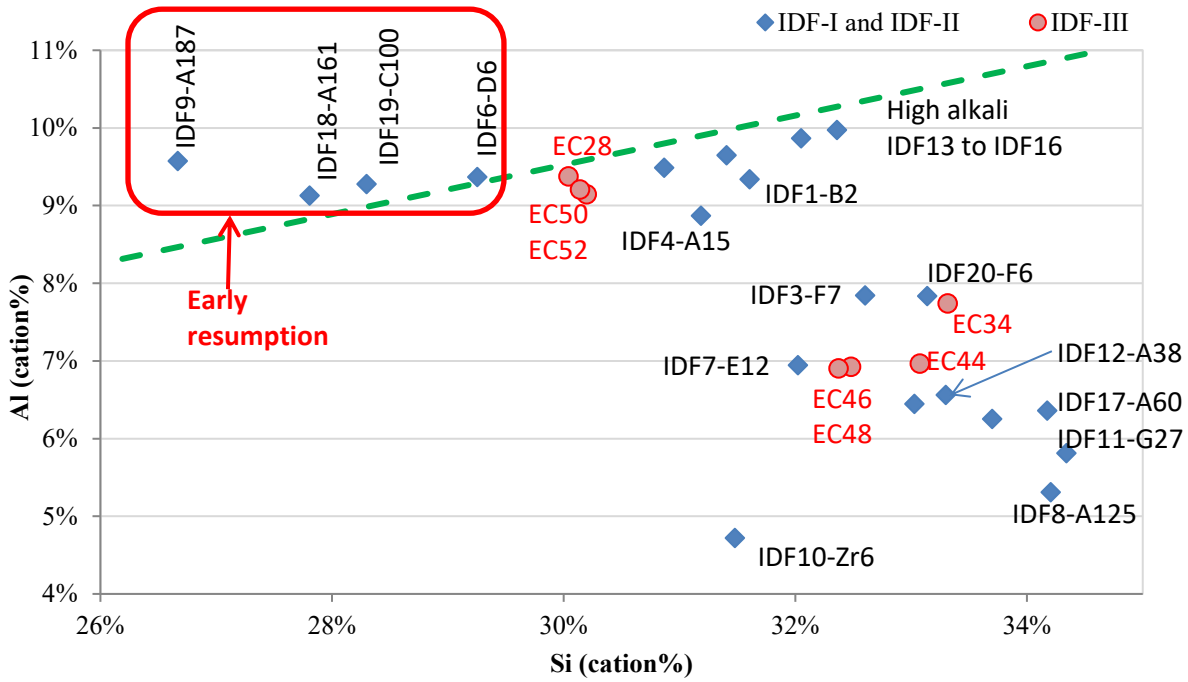

Figure 2.5. Aluminum versus silicon in the 27 IDF glasses (cation%).

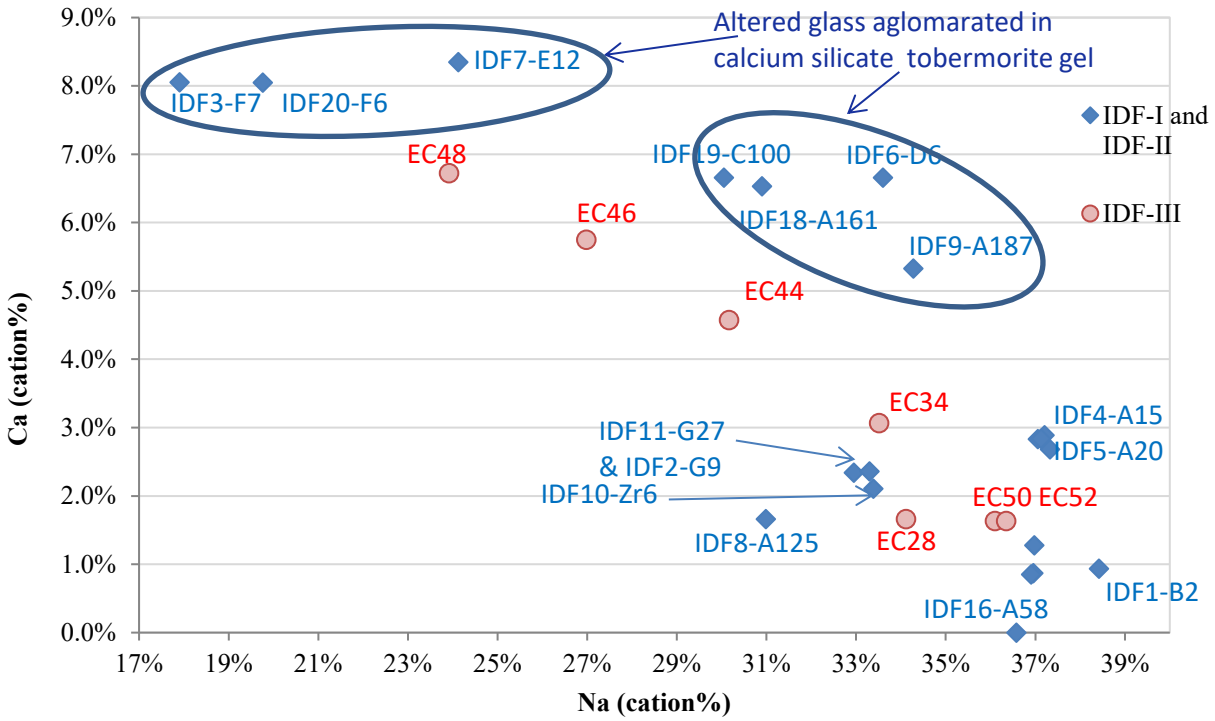

Figure 2.6. Calcium versus sodium in the 27 IDF glasses (cation%).

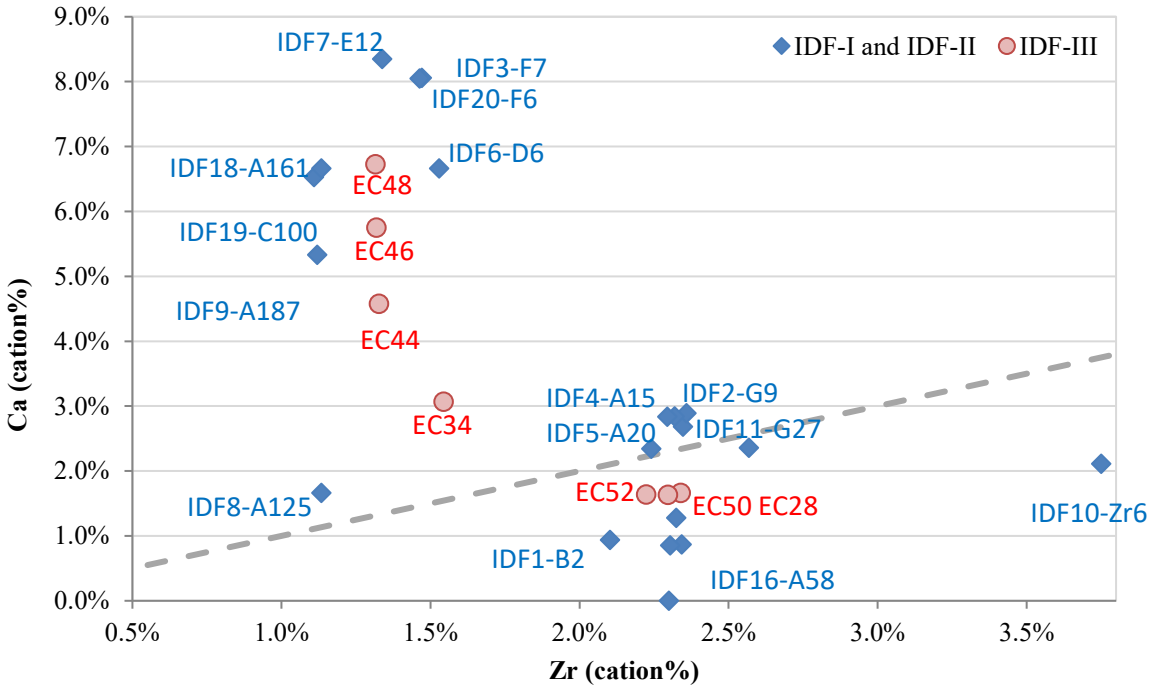

Figure 2.7. Calcium versus zirconium in the 27 IDF glasses (cation%). The dotted line shows equal amounts of Ca and Zr.

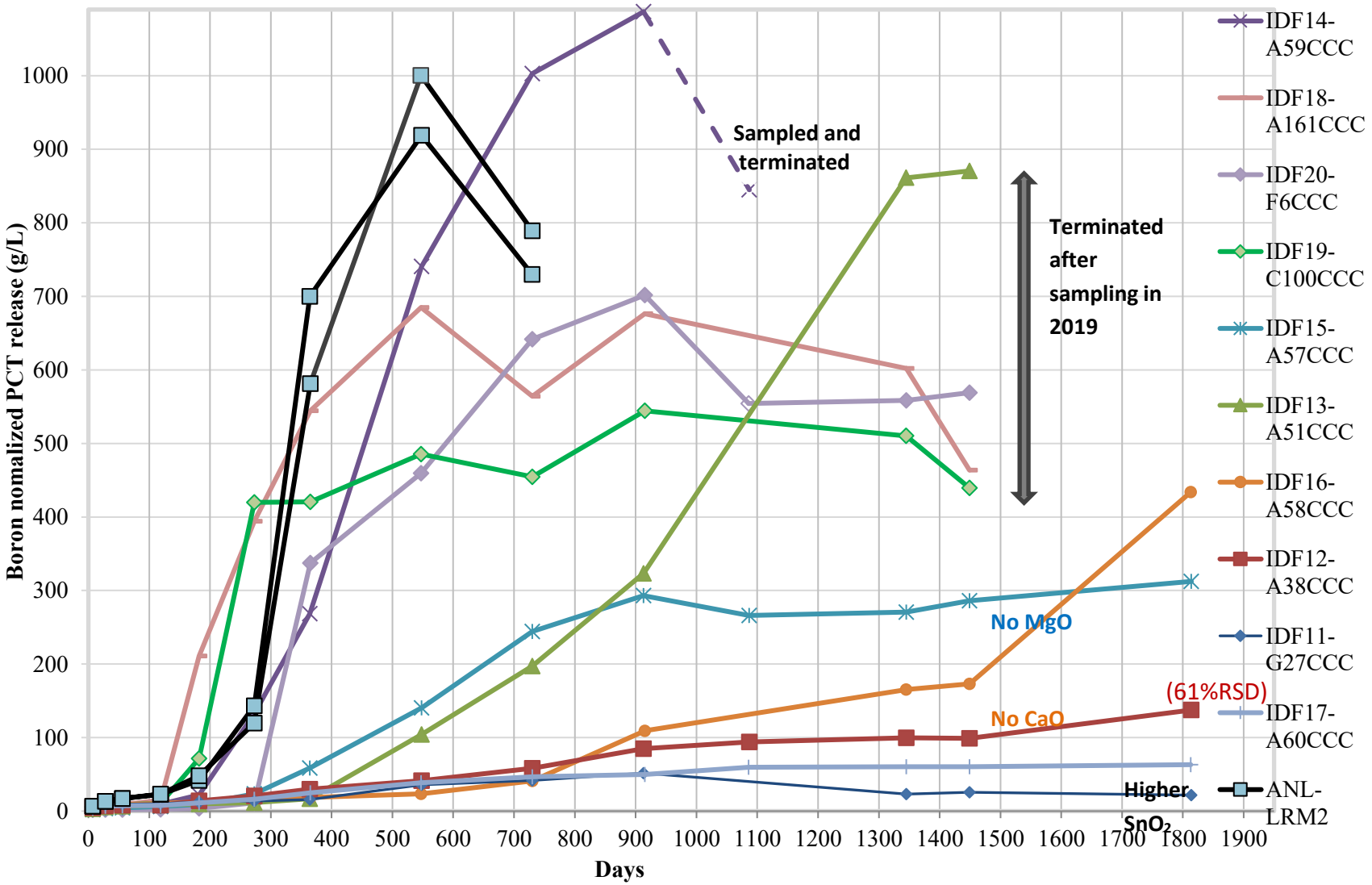

Figure 3.1. PCT-B results (90 °C and S/V of 20,000 m^{-1}) for the ten IDF Phase 2 glasses and the ANL-LRM2 reference glass. (Total available normalized boron release is 1000 g/l at S/V of 20,000 m^{-1})

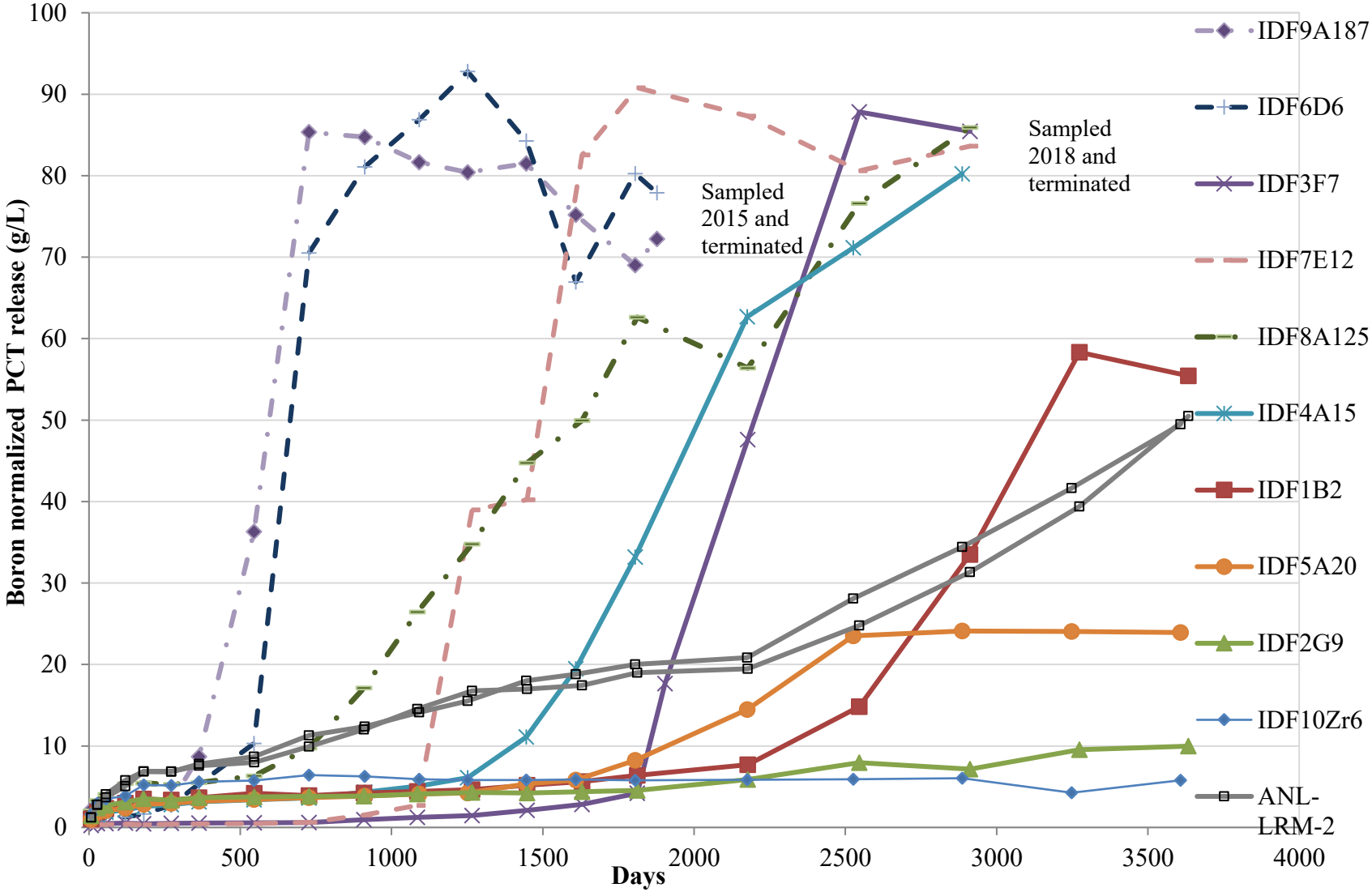

Figure 3.2. PCT-B results (90 °C and S/V of 2,000 m^{-1}) for the ten IDF Phase 1 glasses. (Total available normalized boron release is 100 g/l at S/V of 2,000 m^{-1})

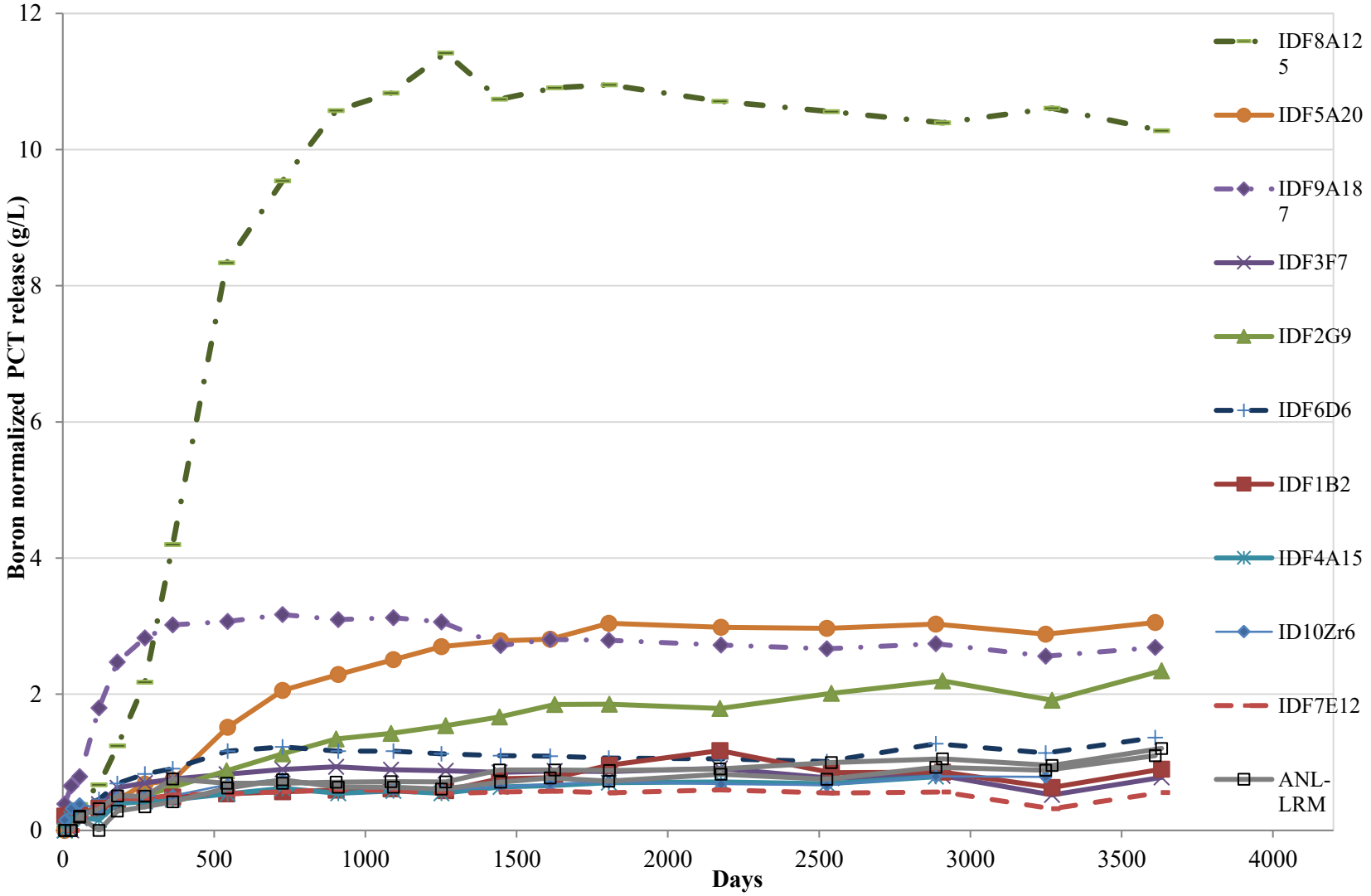

Figure 3.3. PCT-B results (40 °C and S/V of 2,000 m^{-1}) for the ten IDF Phase 1 glasses. (Total available normalized boron release is 100 g/l at S/V of 2,000 m^{-1})

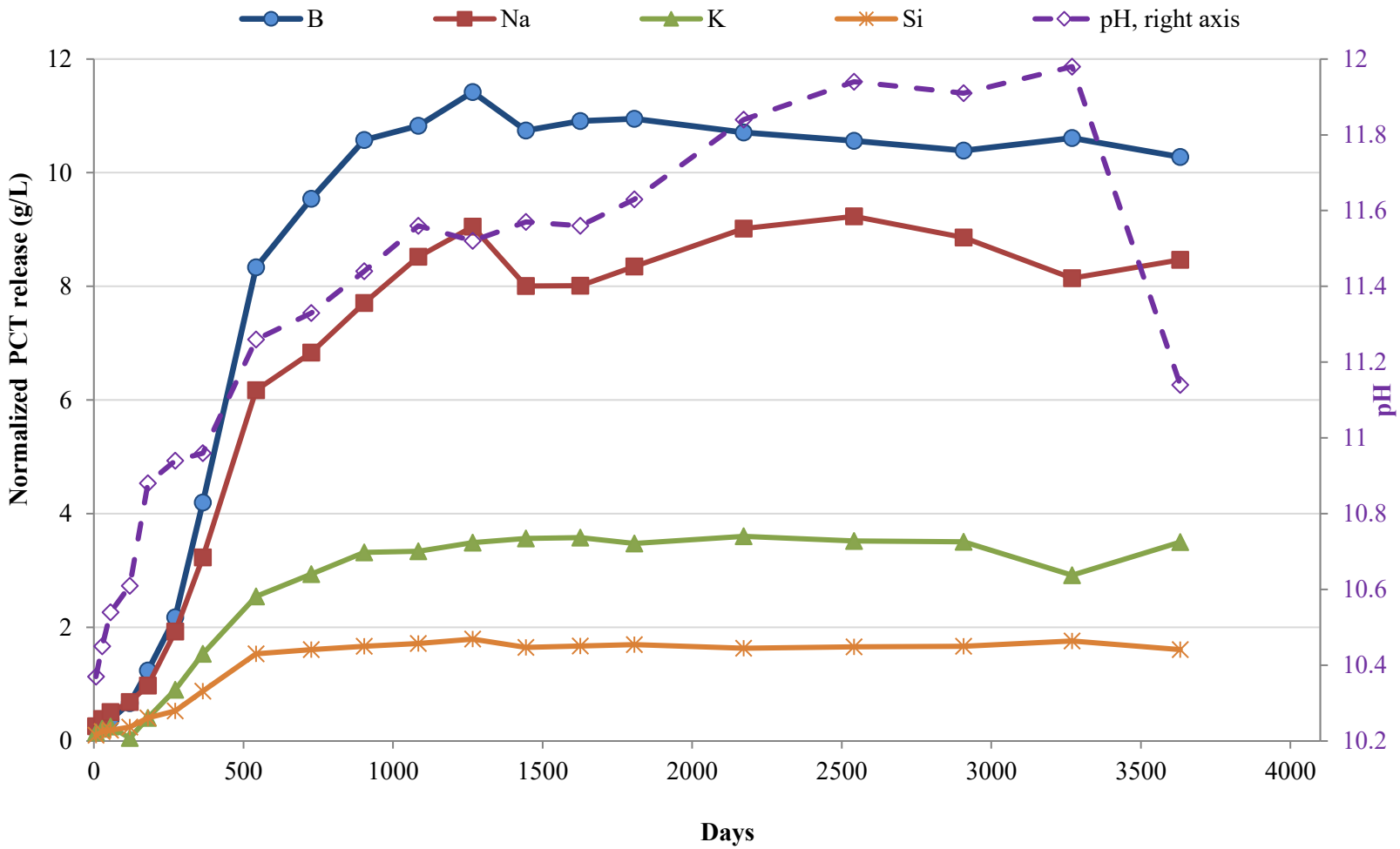

Figure 3.4. PCT-B results (40 °C and S/V of 2,000 m^{-1}) for glass IDF8-A125CCC. (Total available normalized boron release is 100 g/l at S/V of 2,000 m^{-1})

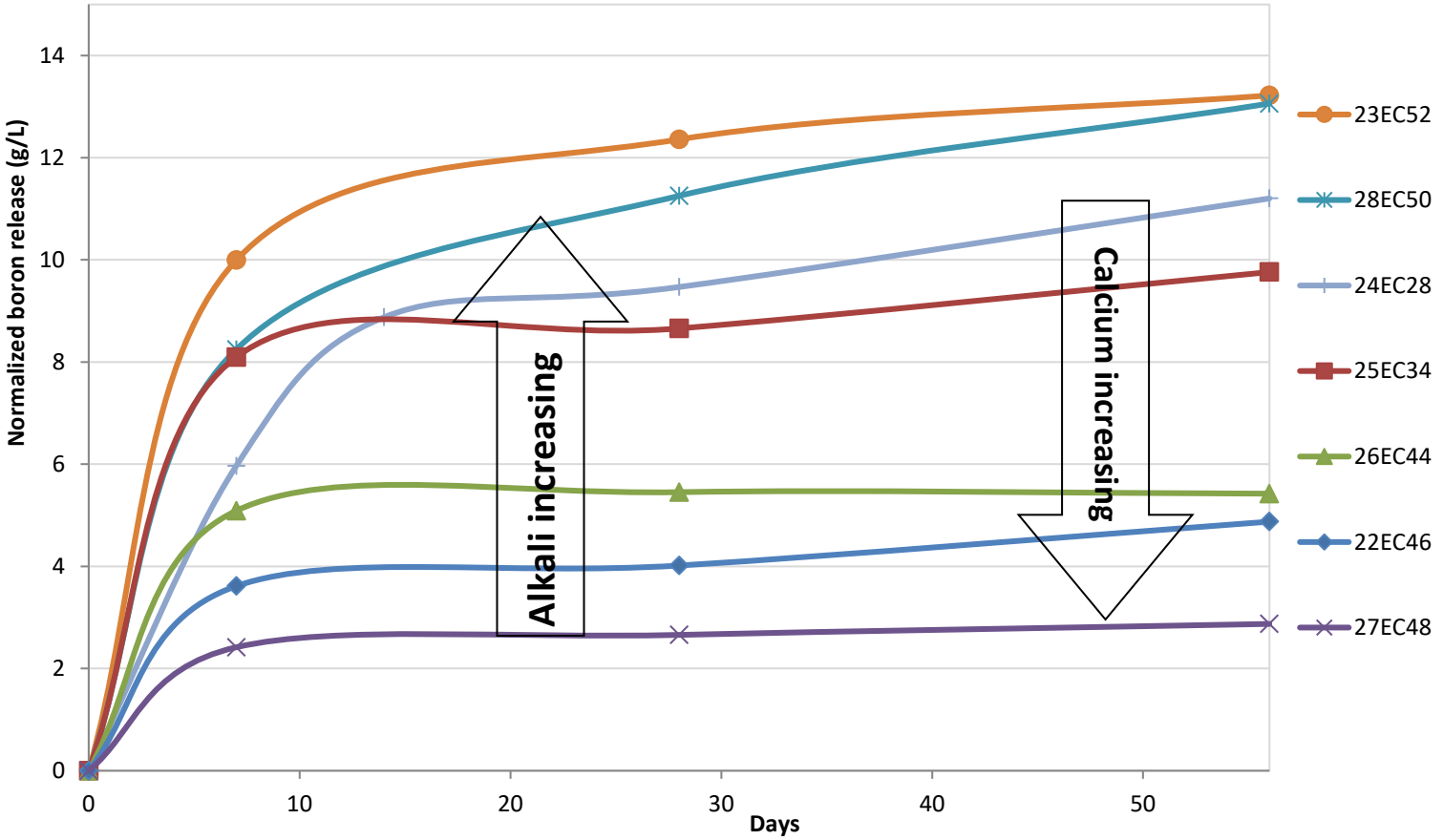

Figure 3.5. PCT normalized boron releases as a function of time during the first 56 days of PCT-B (residual rate regime) for the seven IDF Phase 3 glasses in tests ILHE, ILHF, and ILHG at 90 °C and S/V of 20,000 m^{-1}. (Total available normalized boron release is 1000 g/l at S/V of 20,000 m^{-1})

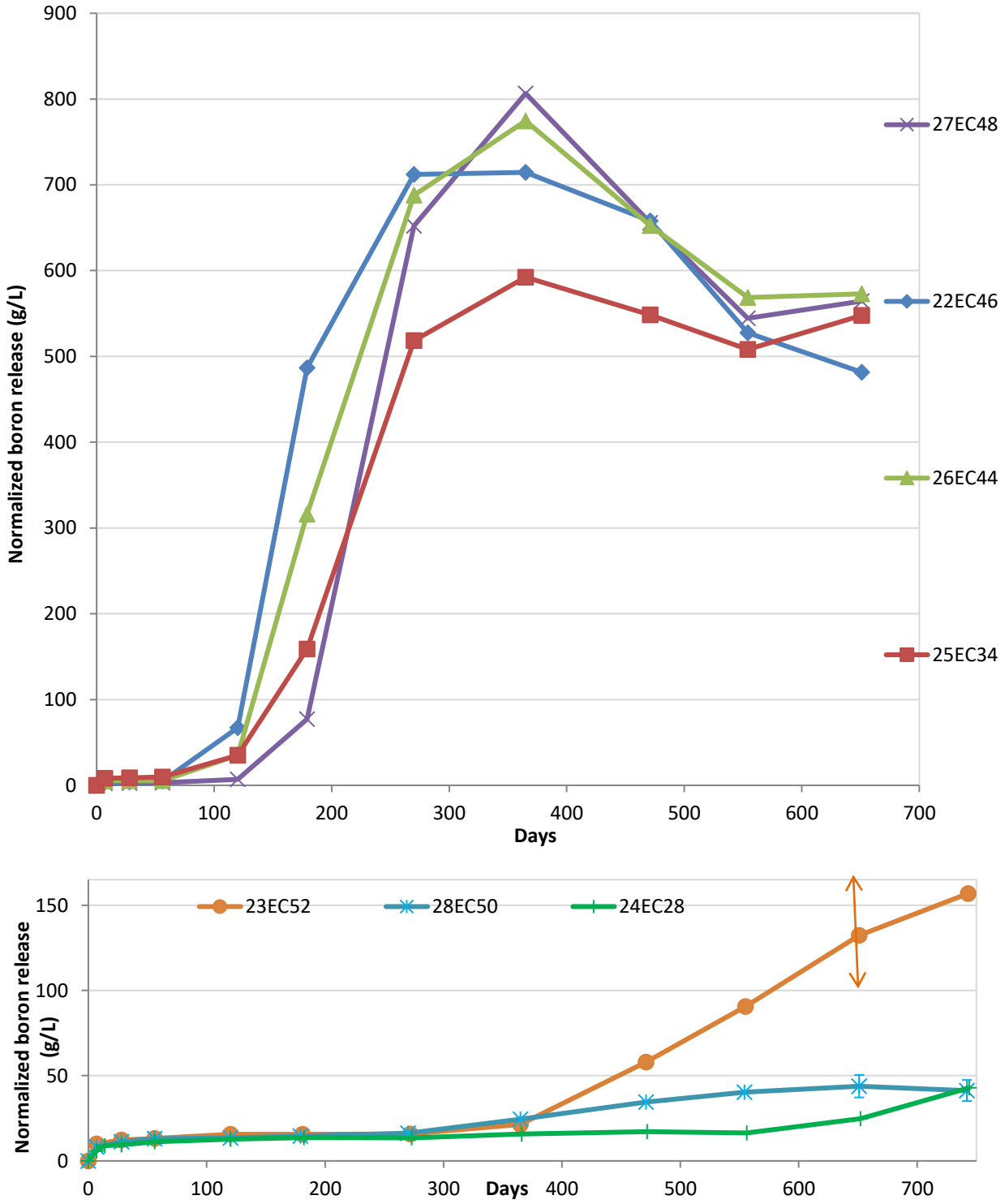

Figure 3.6. PCT normalized boron releases as a function of time during the first two years of PCT-B for the seven IDF Phase 3 glasses in tests ILHE, ILHF, and ILHG at 90 °C and S/V of 20,000 m^{-1} (arrows show variation in replicate tests).
(Total available normalized boron release is 1000 g/l at S/V of 20,000 m^{-1})

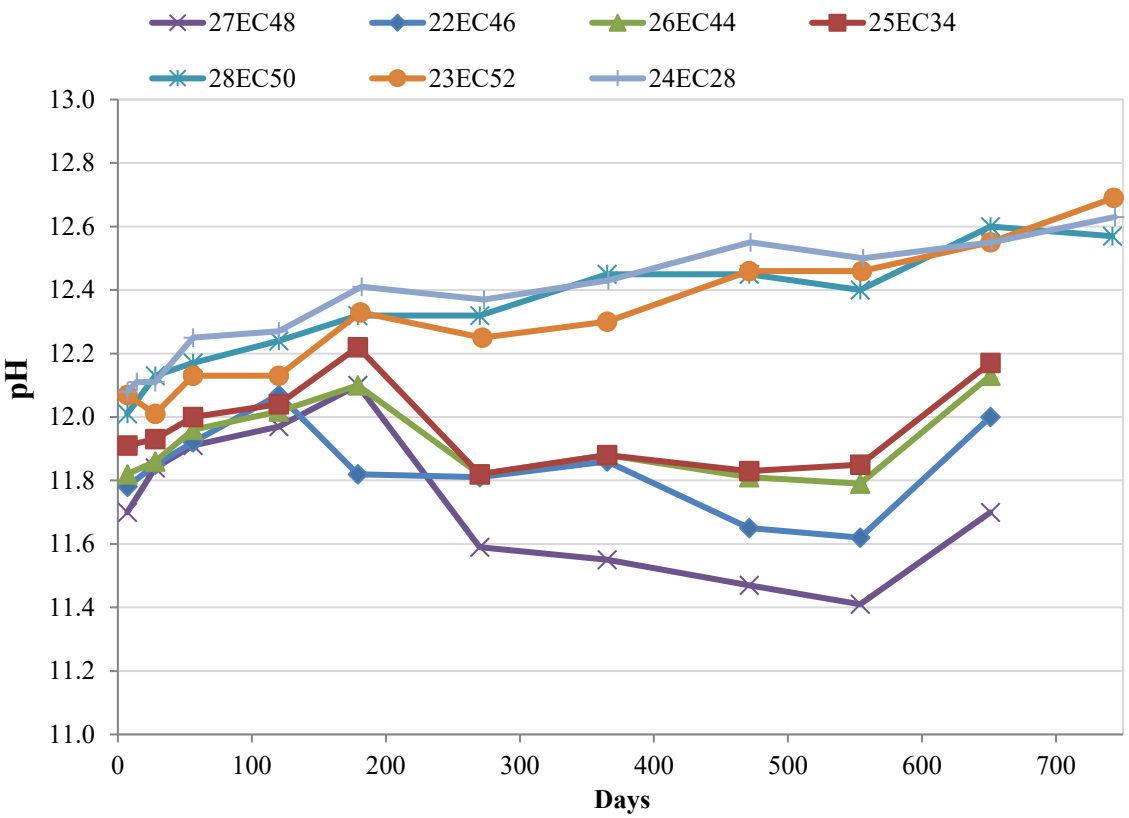

Figure 3.7. Leachate pH as a function of time during the first two years of PCT-B for the seven IDF Phase 3 glasses in tests ILHE, ILHF, and ILHG at 90 °C and S/V of 20,000 m^{-1}.

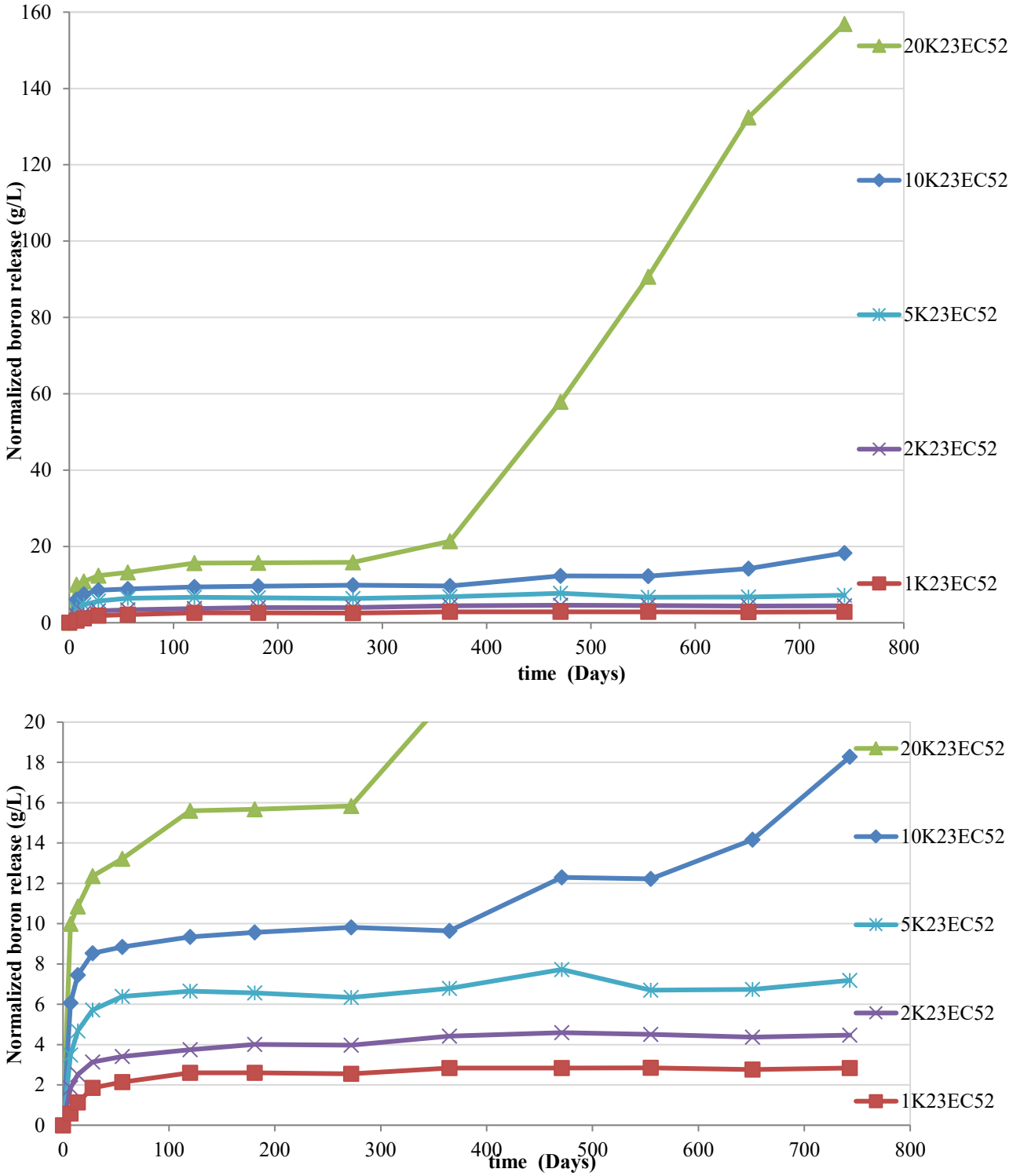

Figure 3.8. Normalized boron release from glass IDF23-EC52CCC in 90 °C PCT-B for two years at five S/V from 1000 m^{-1} to 20,000 m^{-1} (denoted as 1K to 20K) – lower graph expands the range of 0 to 20 g/L normalized boron release.

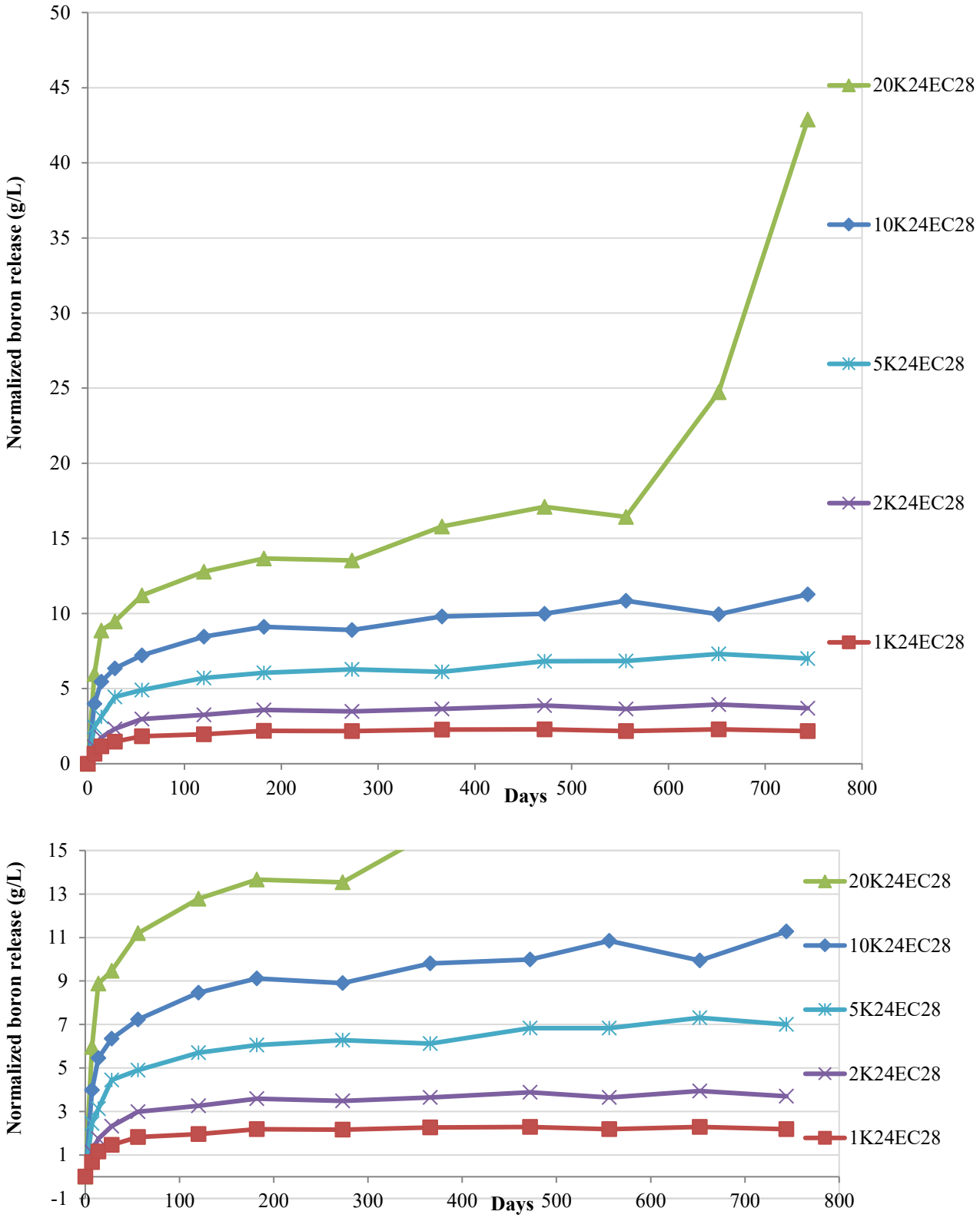

Figure 3.9. Normalized boron release from glass IDF24-EC28CCC in 90 °C PCT-B for two years at five S/V from 1000 m^{-1} to 20,000 m^{-1} (denoted as 1K to 20K) – lower graph expands the range of 0 to 15 g/L normalized boron release.

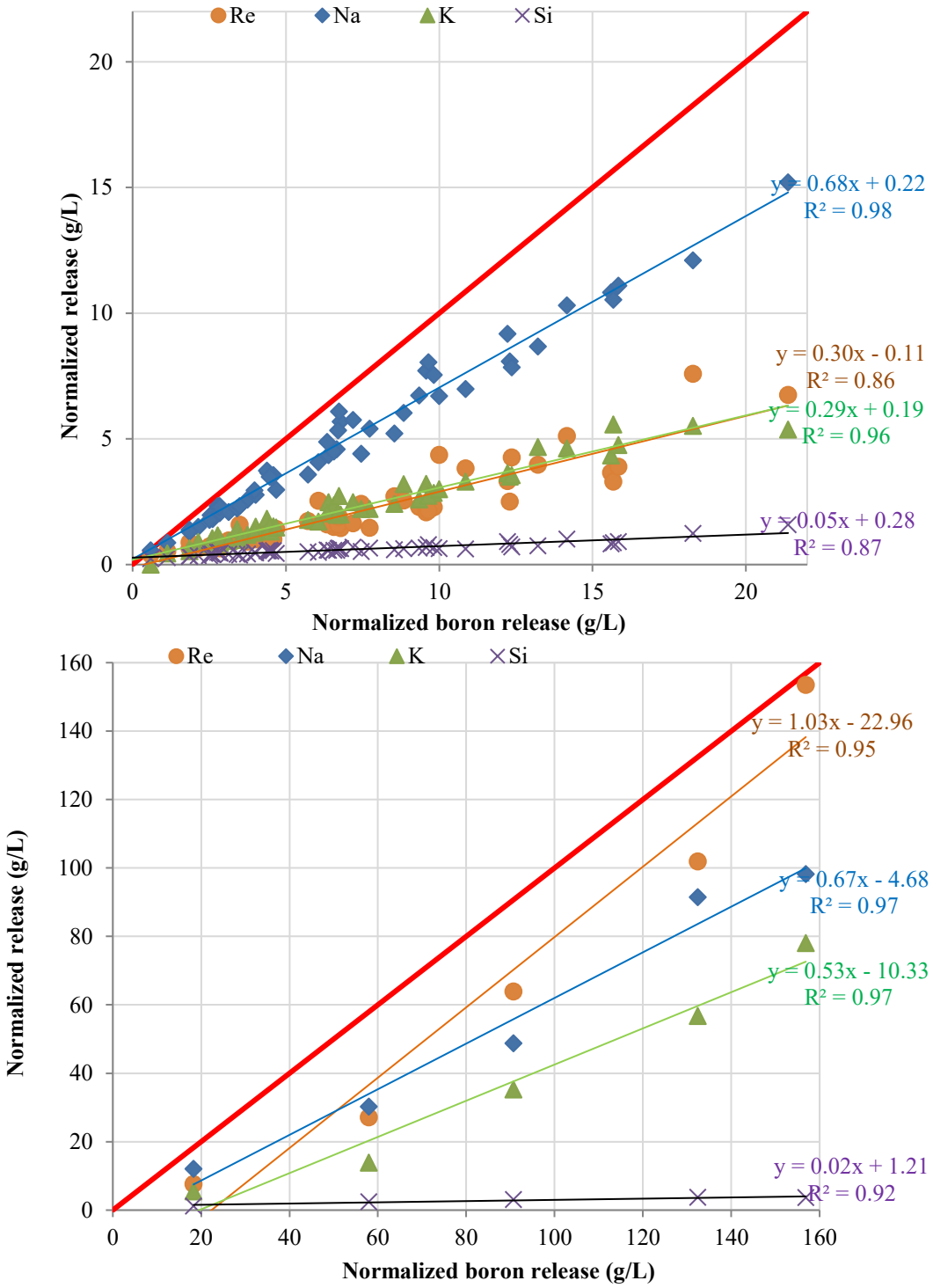

Figure 3.10. Display of deviation from congruence to boron (the red diagonal would be full congruence) for Re, Na, K, and Si in IDF23-EC52CCC up to 743 days of PCT-B data before resumption (top) and after resumption (lower graph, using data from 743-day sampling at S/V of 10,000 m^{-1} and at 471, 555, 651, and 743-day samplings at S/V of 20,000 m^{-1}).

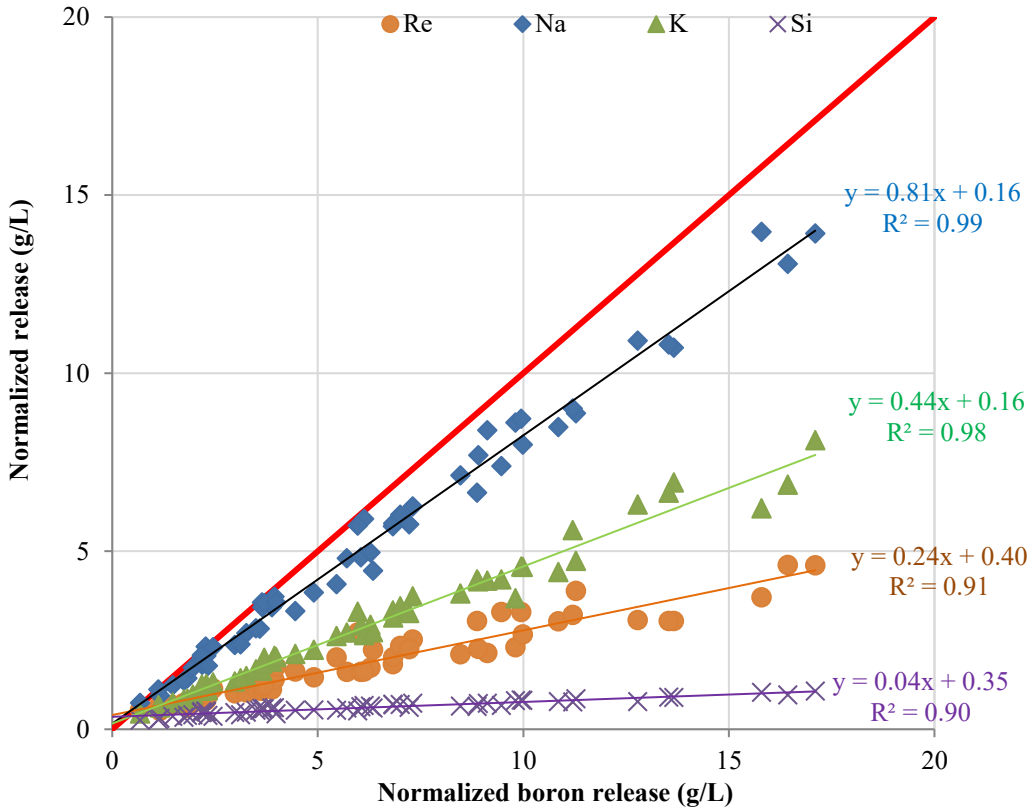

Figure 3.11. Display of deviation from congruence to boron (the red diagonal would be full congruence) for Re, K, Na, and Si in IDF24-EC28CCC over 744 days of PCT-B (652 and 744-day samplings not included at S/V of 20,000 m^{-1}).

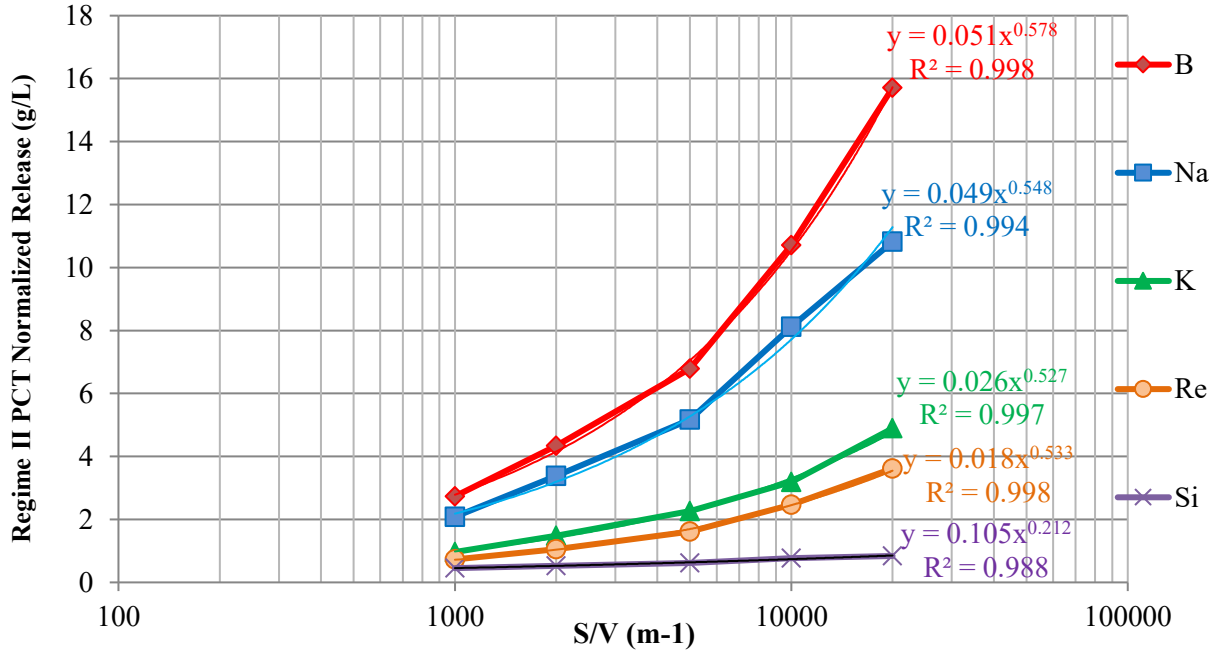

Figure 3.12. Effect of S/V on the residual rate region release of B, Na, K, Re, and Si from glass IDF23-EC52CCC in 90°C PCT-B (to 743-day sampling at S/V of 1000, 2000, and 5000 m^{-1}, to 555-day sampling at S/V of 10,000 m^{-1} and 272-day at S/V of 20,000 m^{-1}).

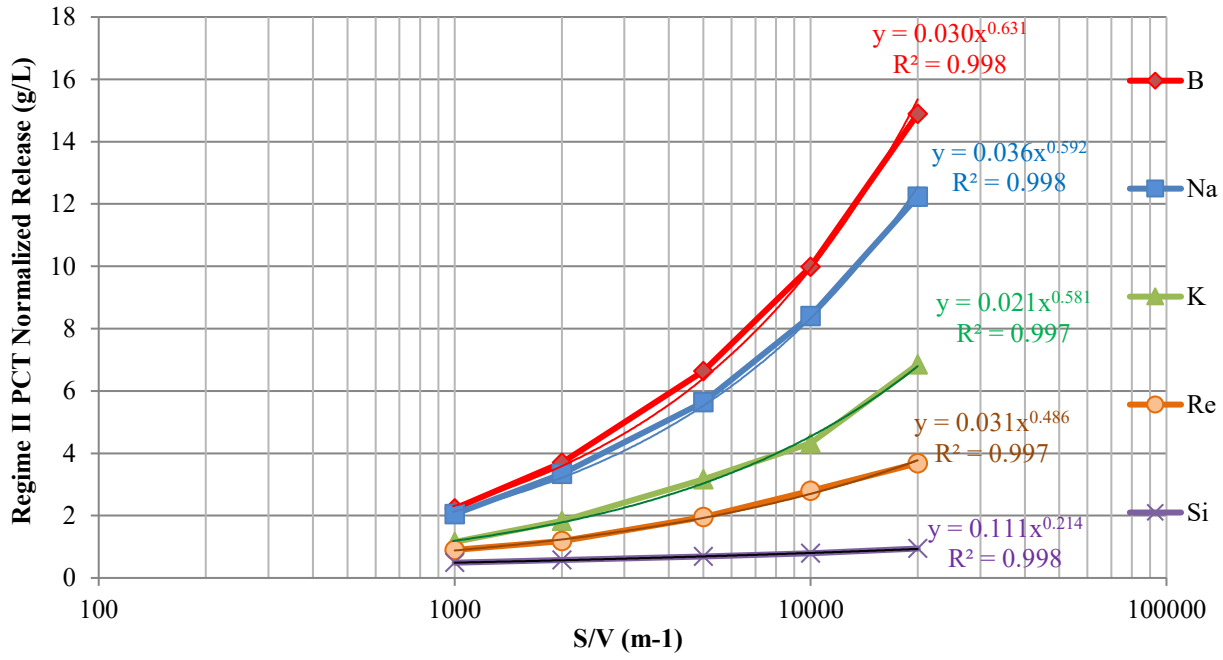

Figure 3.13. Effect of S/V on the residual rate region release of B, Na, K, Re, and Si from glass IDF24-EC28CCC in 90 °C PCT-B (to 743-day sampling at S/V of 1000, 2000, 5000 and 10,000 m^{-1}, and 556-day at S/V of 20,000 m^{-1}).

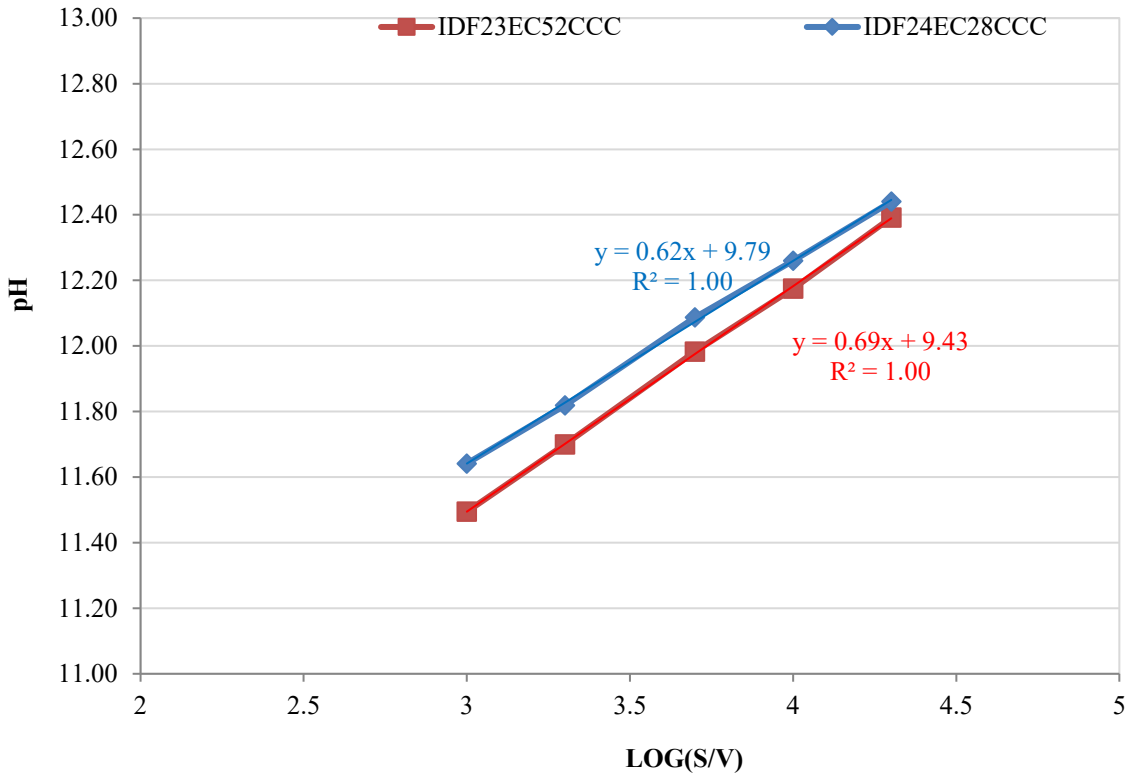

Figure 3.14. Effect of S/V on leachate solution pH from glasses IDF23-EC52CCC and IDF24-EC28CCC in 90 °C PCT-B (to 743-day sampling at S/V of 1000, 2000, and 5000 m^{-1}, to 555-day sampling at S/V of 10,000 m^{-1} and 272-day at S/V of 20,000 m^{-1}).

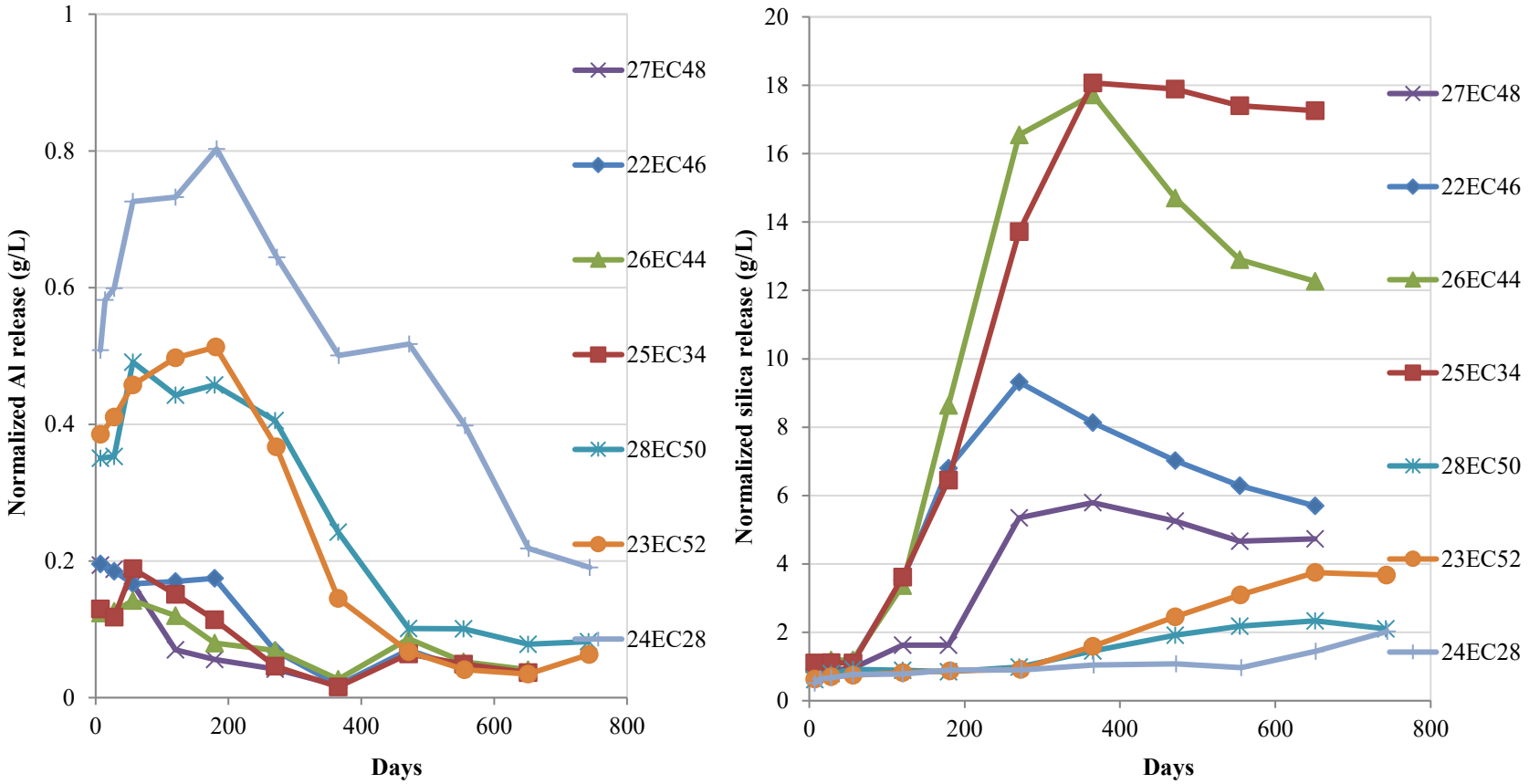

Figure 3.15. Al and Si normalized releases for the seven IDF Phase 3 glasses in PCT-B for two years at 90 °C and S/V of 20,000 m^{-1}.

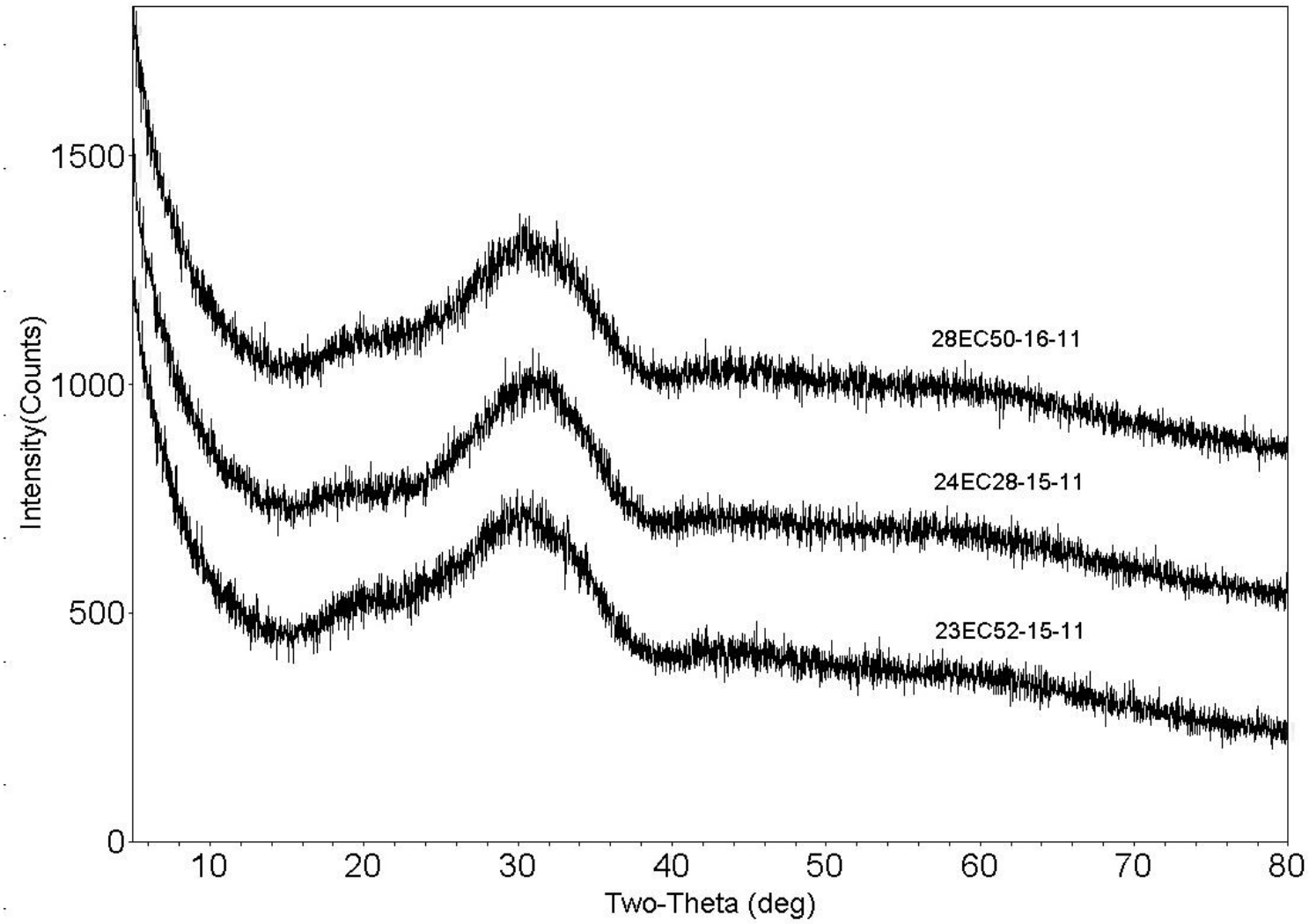

Figure 4.1. XRD powder patterns (raw data) for three low-alteration IDF Phase 3 glasses IDF28-EC50, IDF24-EC28, and IDF23-EC52, all subjected to PCT for 651 days at 90°C and S/V of 20,000 m^{-1}.

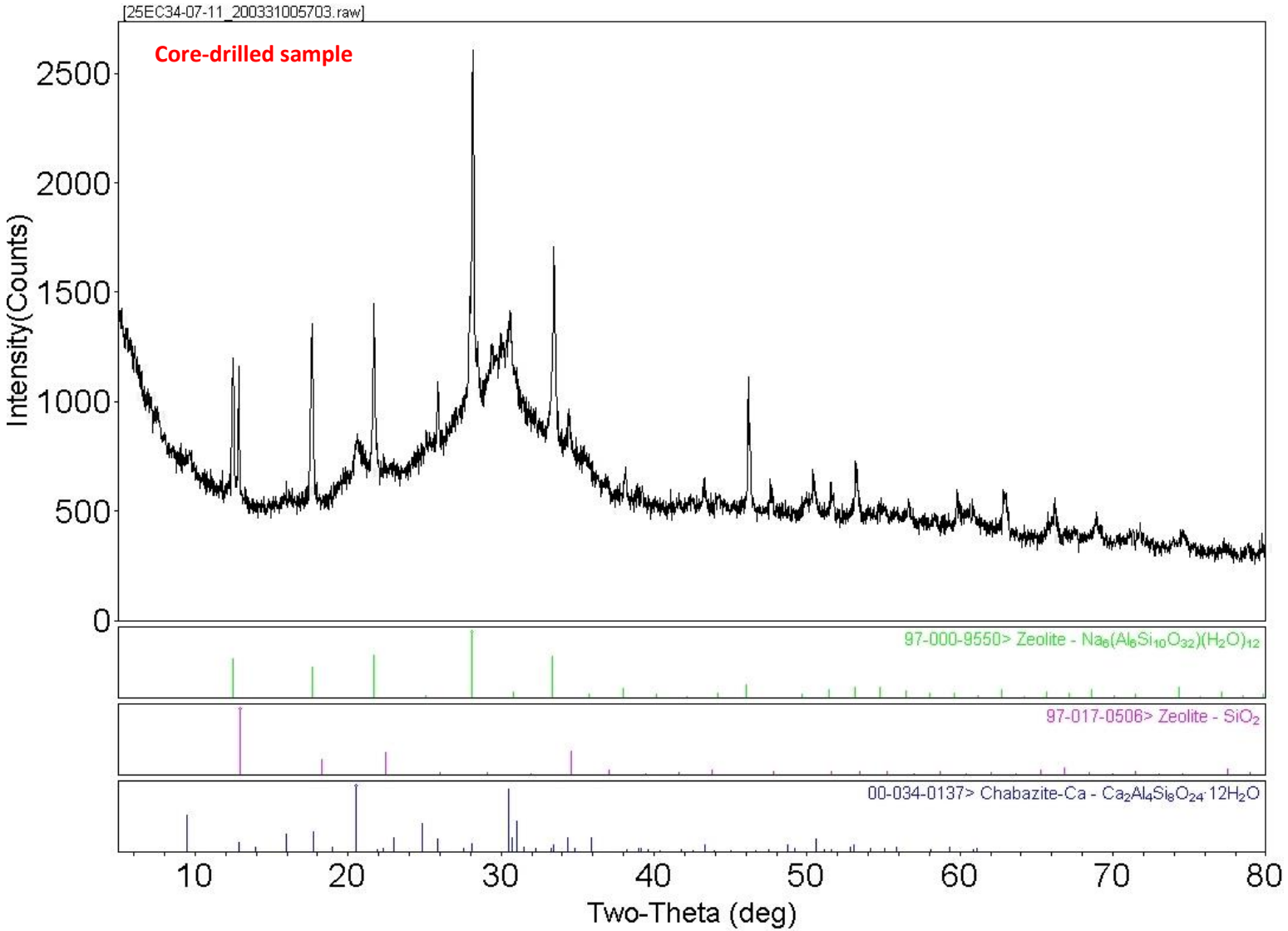

Figure 4.2. XRD powder patterns (raw data and best match) for altered IDF Phase 3 glass IDF25-EC34 subjected to PCT for 651 days at 90°C and S/V of 20,000 m^{-1}. Resumption was at ~179 days and normalized boron release rose sharply to 518 g/L.

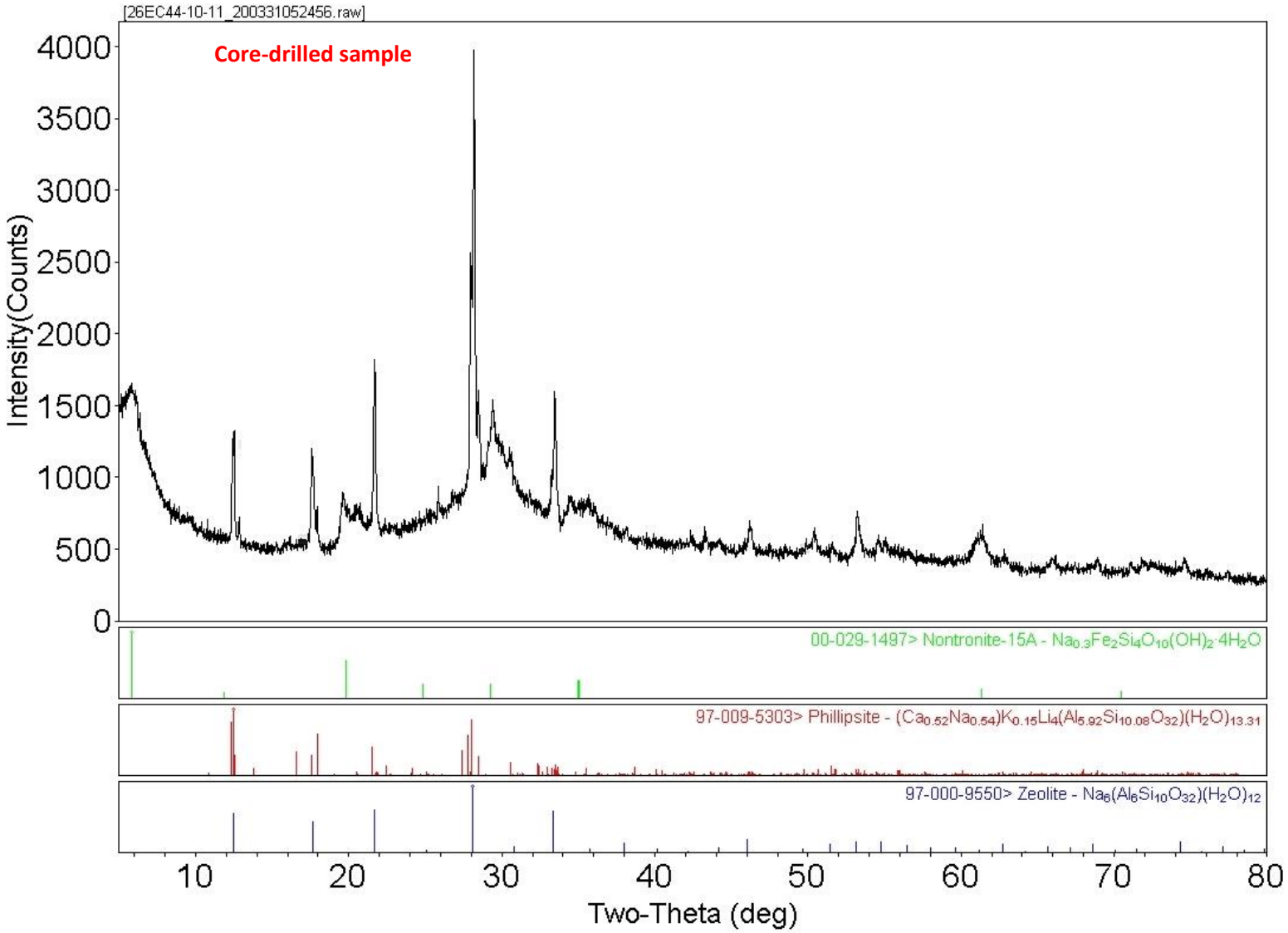

Figure 4.3. XRD powder patterns (raw data and best match) for altered IDF Phase 3 glass IDF26-EC44 subjected to PCT for 651 days at 90°C and S/V of 20,000 m^{-1}. Resumption was at ~200 days and normalized boron release rose sharply to 688 g/L.

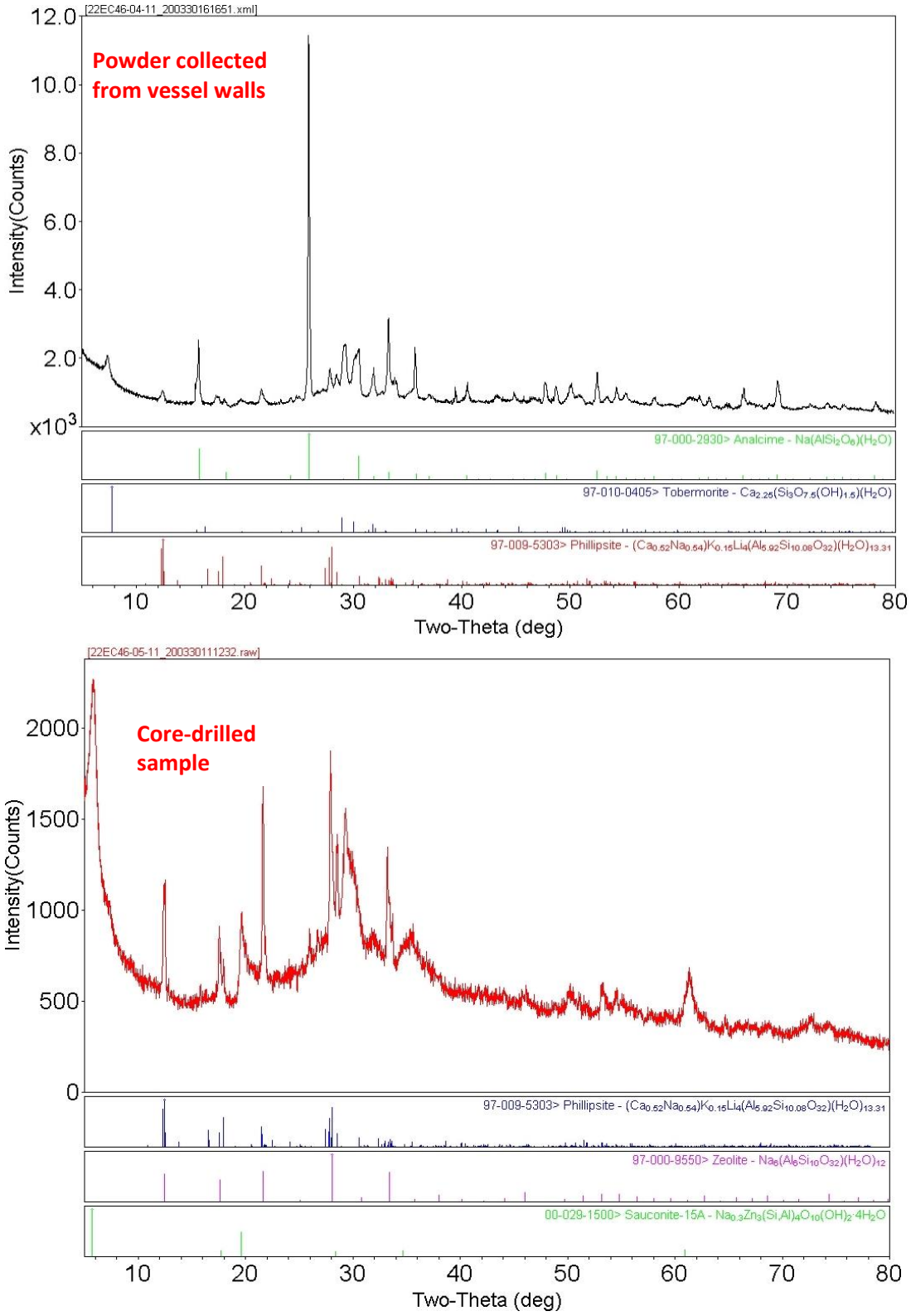

Figure 4.4. XRD powder patterns (raw data and best match) for altered IDF Phase 3 glass IDF22-EC46 subjected to PCT for 651 days at 90°C and S/V of 20,000 m^{-1}. Resumption was at ~179 days and normalized boron release rose sharply to 488 g/L.

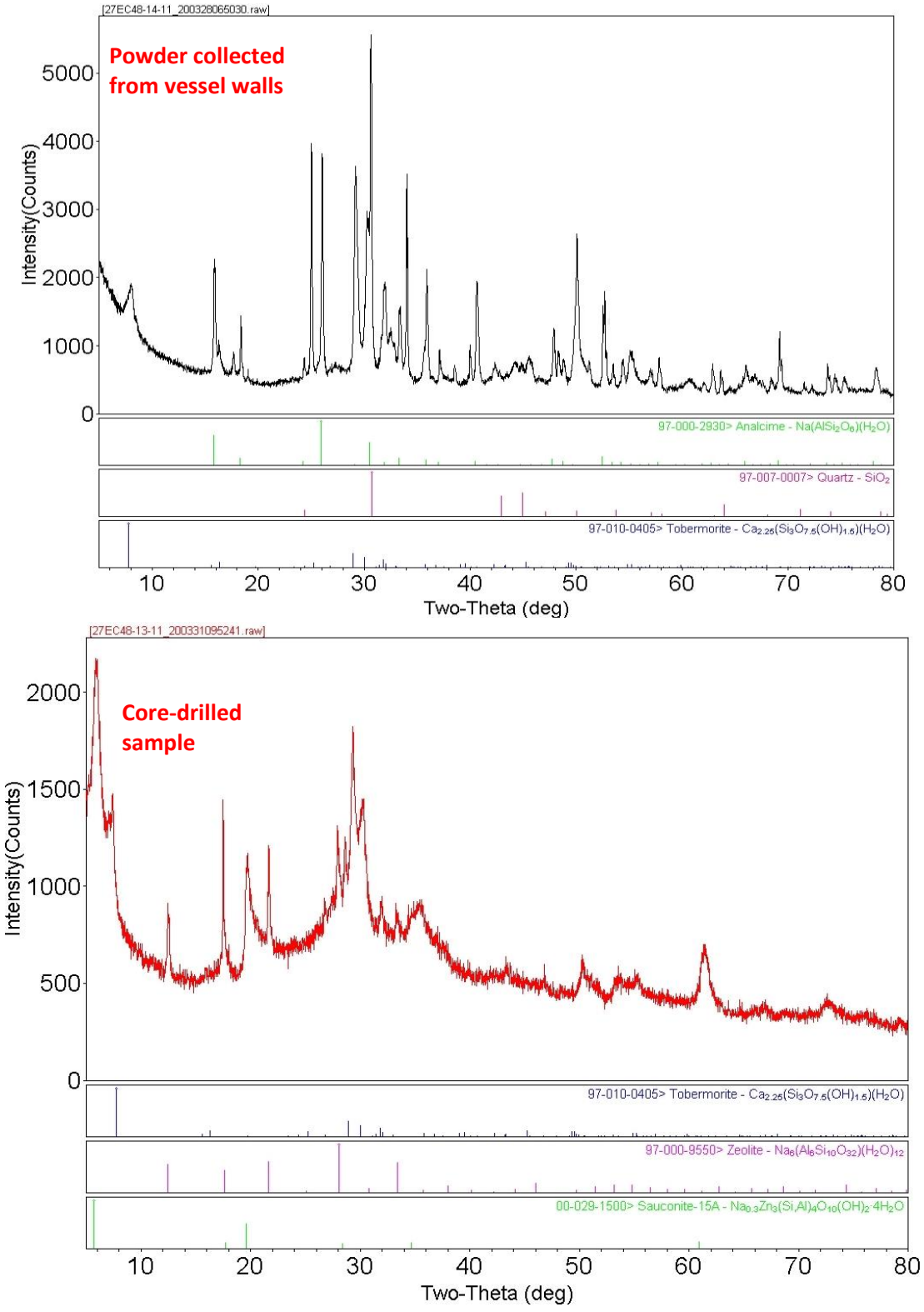

Figure 4.5. XRD powder patterns (raw data and best match) for altered IDF Phase 3 glass IDF27-EC48 subjected to PCT for 651 days at 90°C and S/V of 20,000 m^{-1}. Resumption was at ~270 days and normalized boron release rose sharply to 712 g/L.

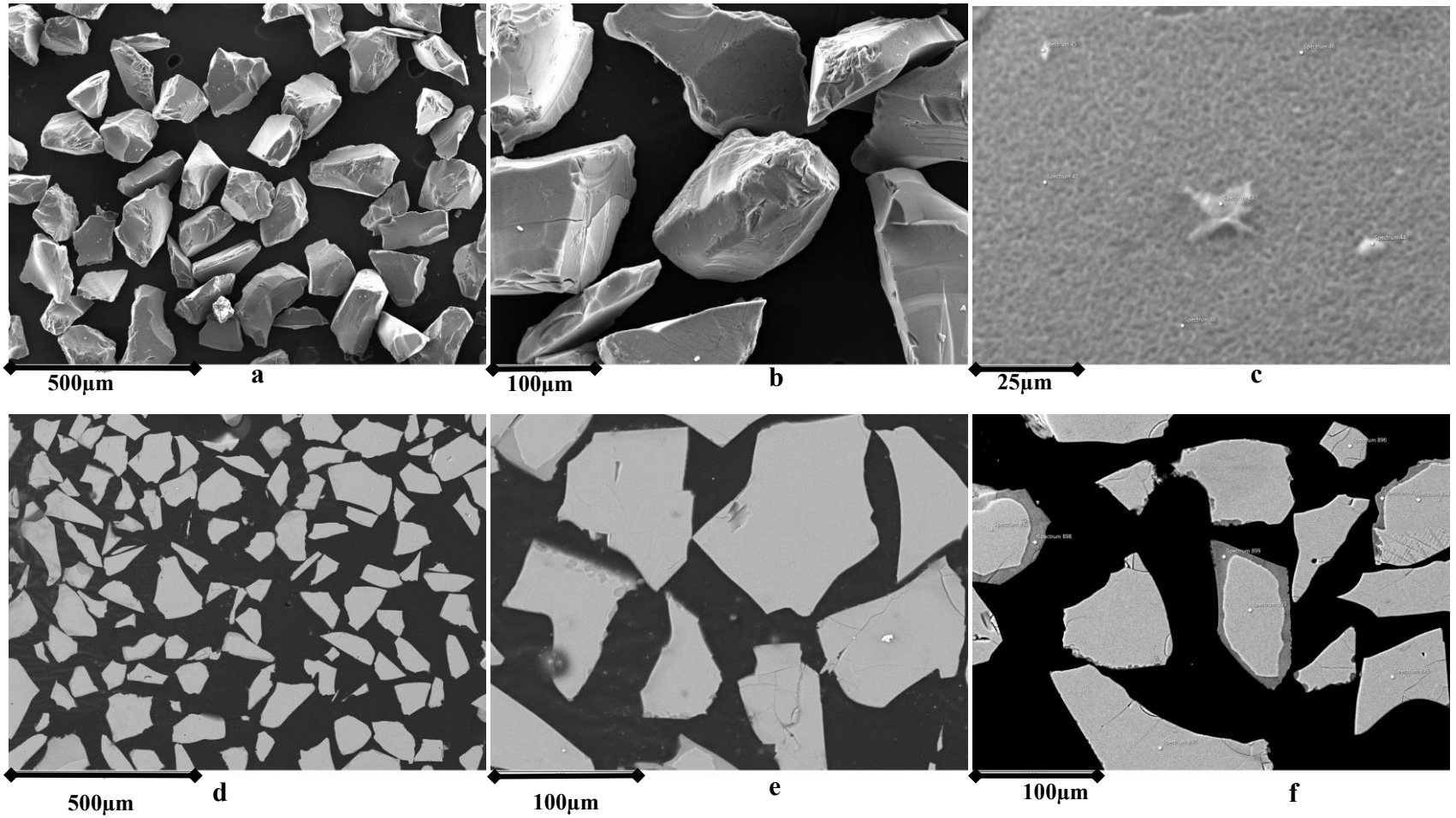

Figure 4.6. SEM micrographs from the surface (a-c) and cross-section (d-f) of altered IDF Phase 3 glass IDF23-EC52 subjected to PCT for two years at 90 °C and S/V of 20,000 m^{-1}. Resumption appears nascent and normalized boron release was 132 g/L (equivalent to ~13 % altered glass).

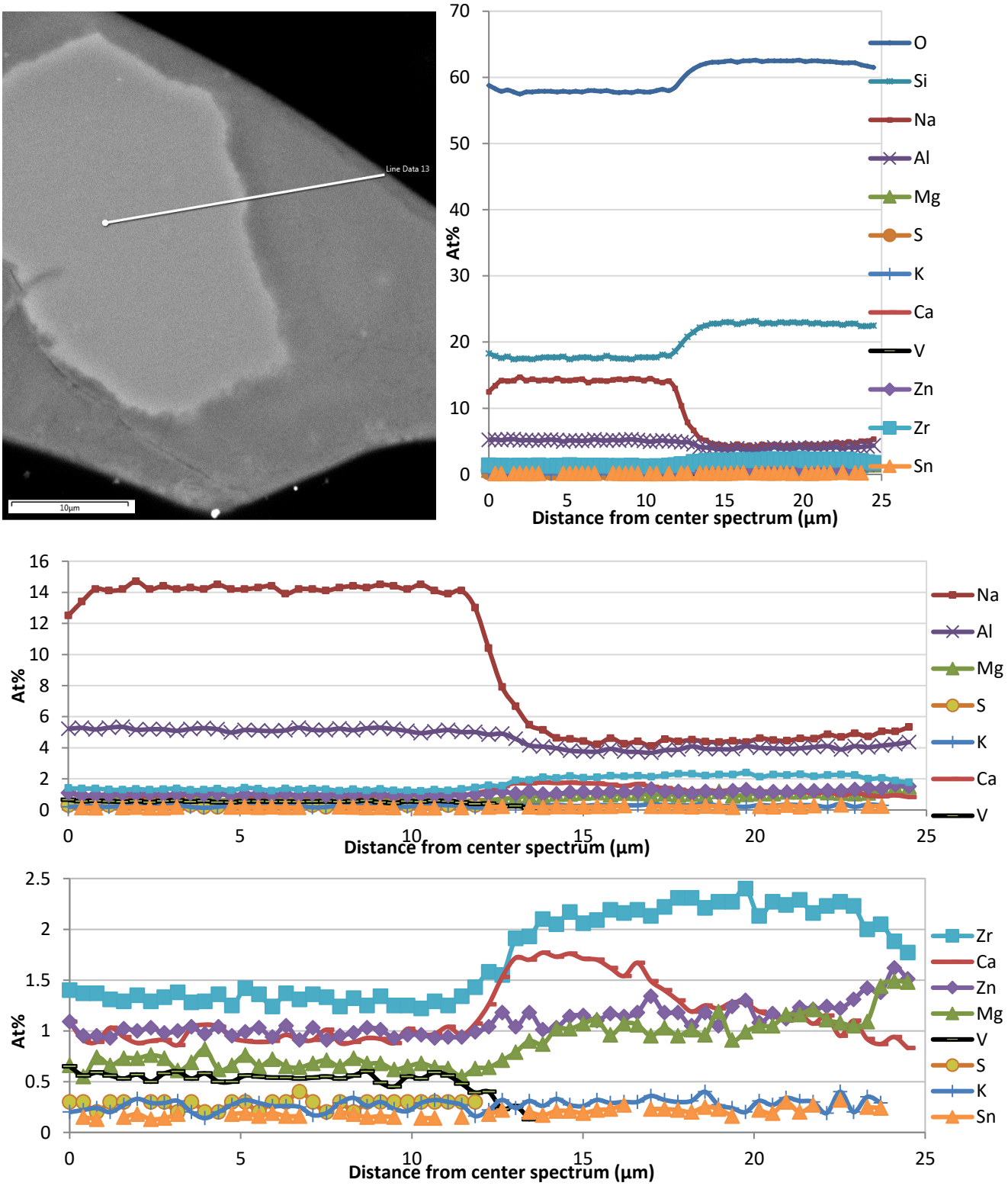

Figure 4.7. SEM micrographs and plots of EDS analyses from core to surface of altered IDF Phase 3 glass IDF23-EC52 subjected to PCT for two years at 90 °C and S/V of 20,000 m^{-1}.

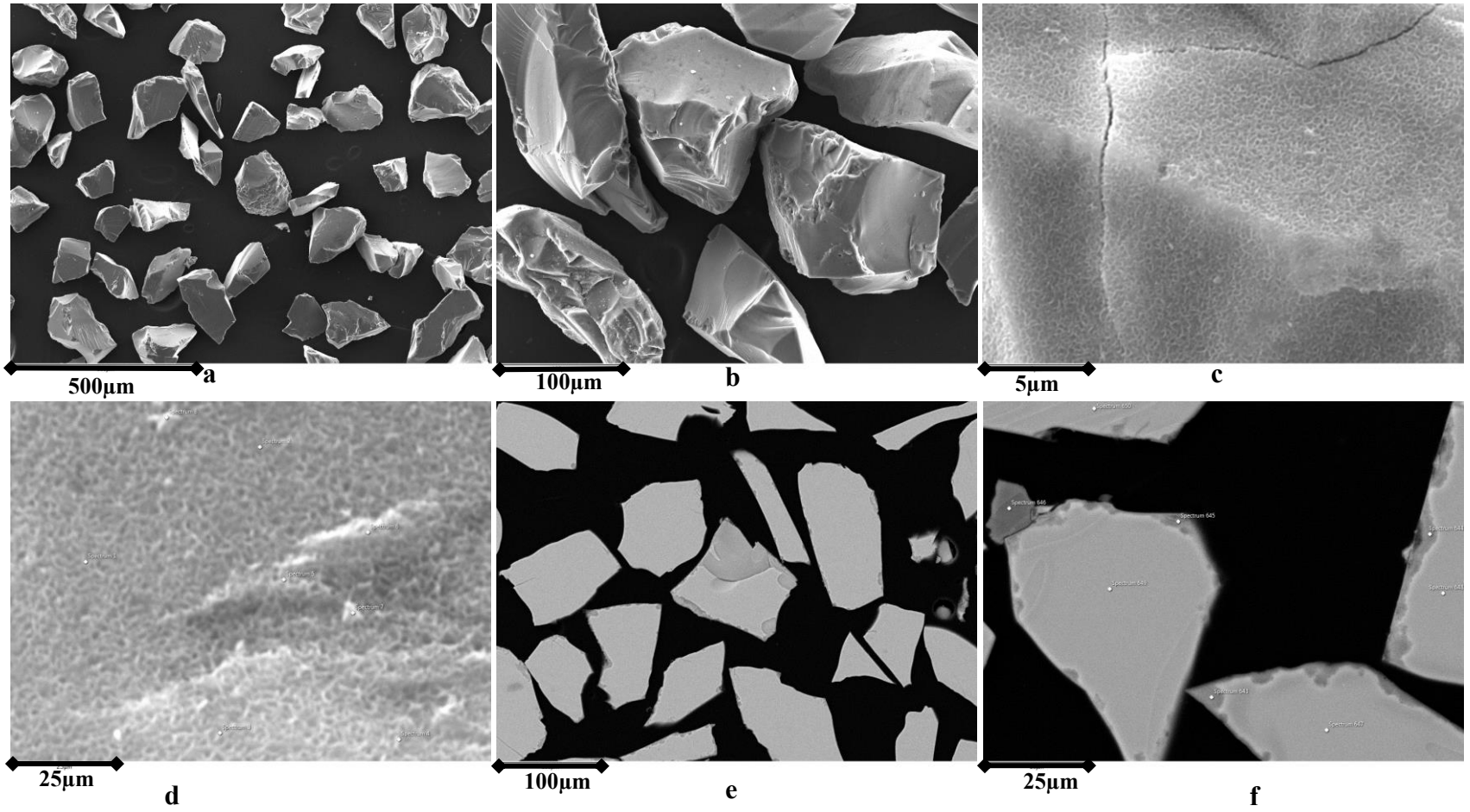

Figure 4.8. SEM micrographs from the surface (a-d) and cross-section (e-f) of altered IDF Phase 3 glass IDF28-EC50 subjected to PCT for two years at 90 °C and S/V of 20,000 m^{-1}. Resumption was not reached and normalized boron release was 44 g/L (equivalent to ~4 % altered glass).

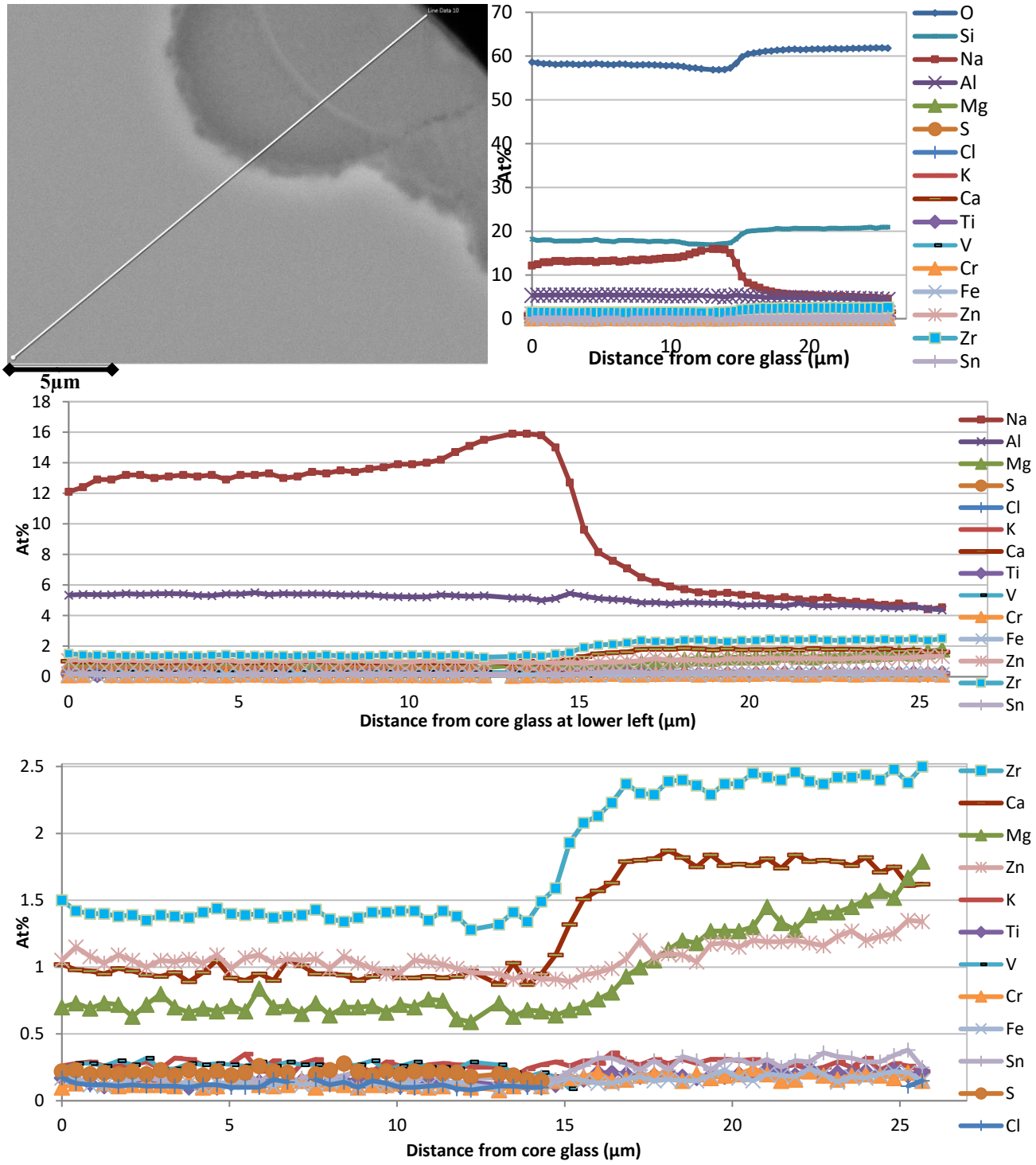

Figure 4.9. SEM micrograph and plots of EDS analyses (at three y-axis scales) from core to surface of altered IDF Phase 3 glass IDF28-EC50 subjected to PCT for two years at 90 °C and S/V of 20,000 m^{-1}.

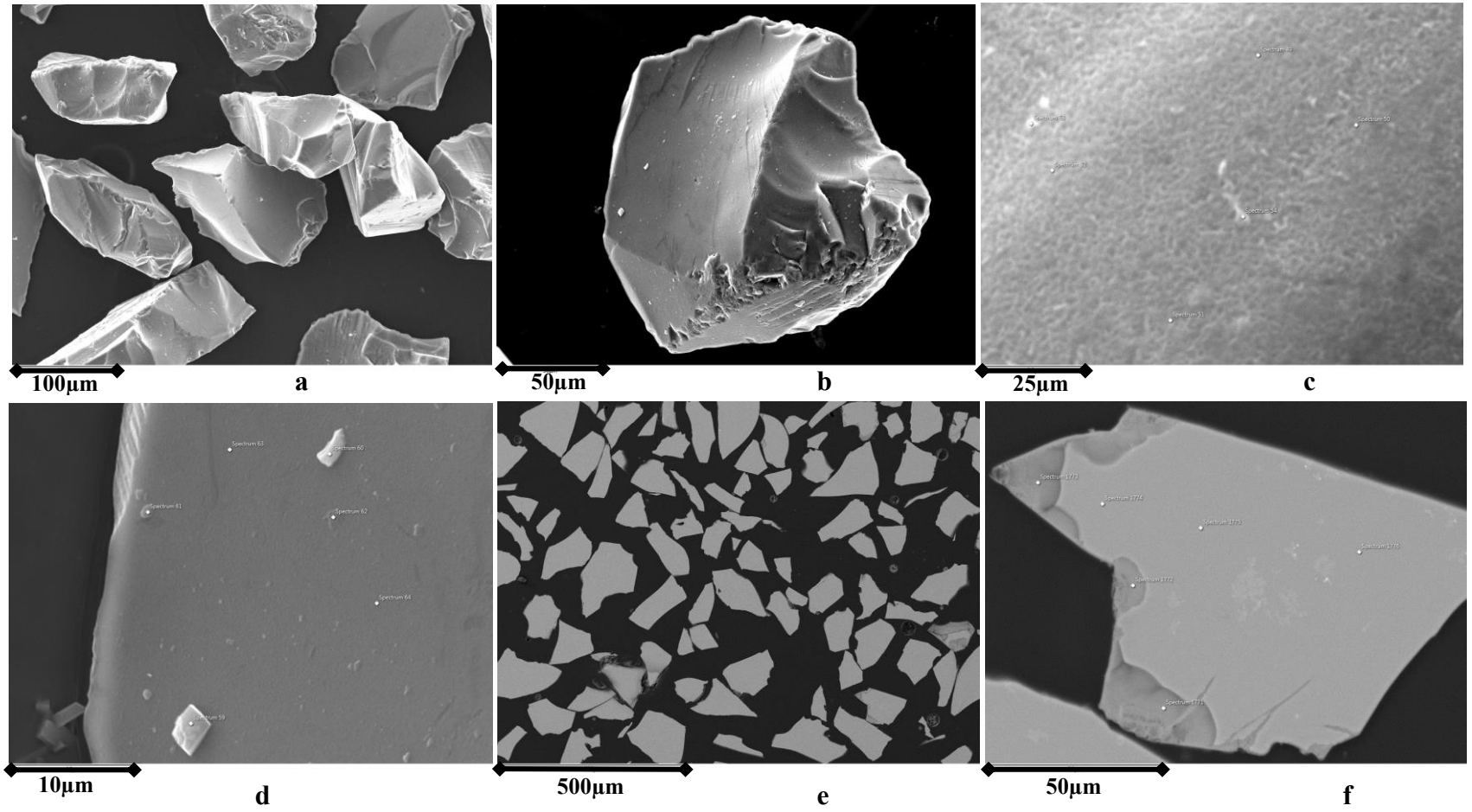

Figure 4.10. SEM micrographs from the surface (a-d) and cross-section (e-f) of altered IDF Phase 3 glass IDF24-EC28 subjected to PCT for two years at 90 °C and S/V of 20,000 m^{-1}. Resumption was not reached and normalized boron release was 25 g/L. (equivalent to ~2 % altered glass).

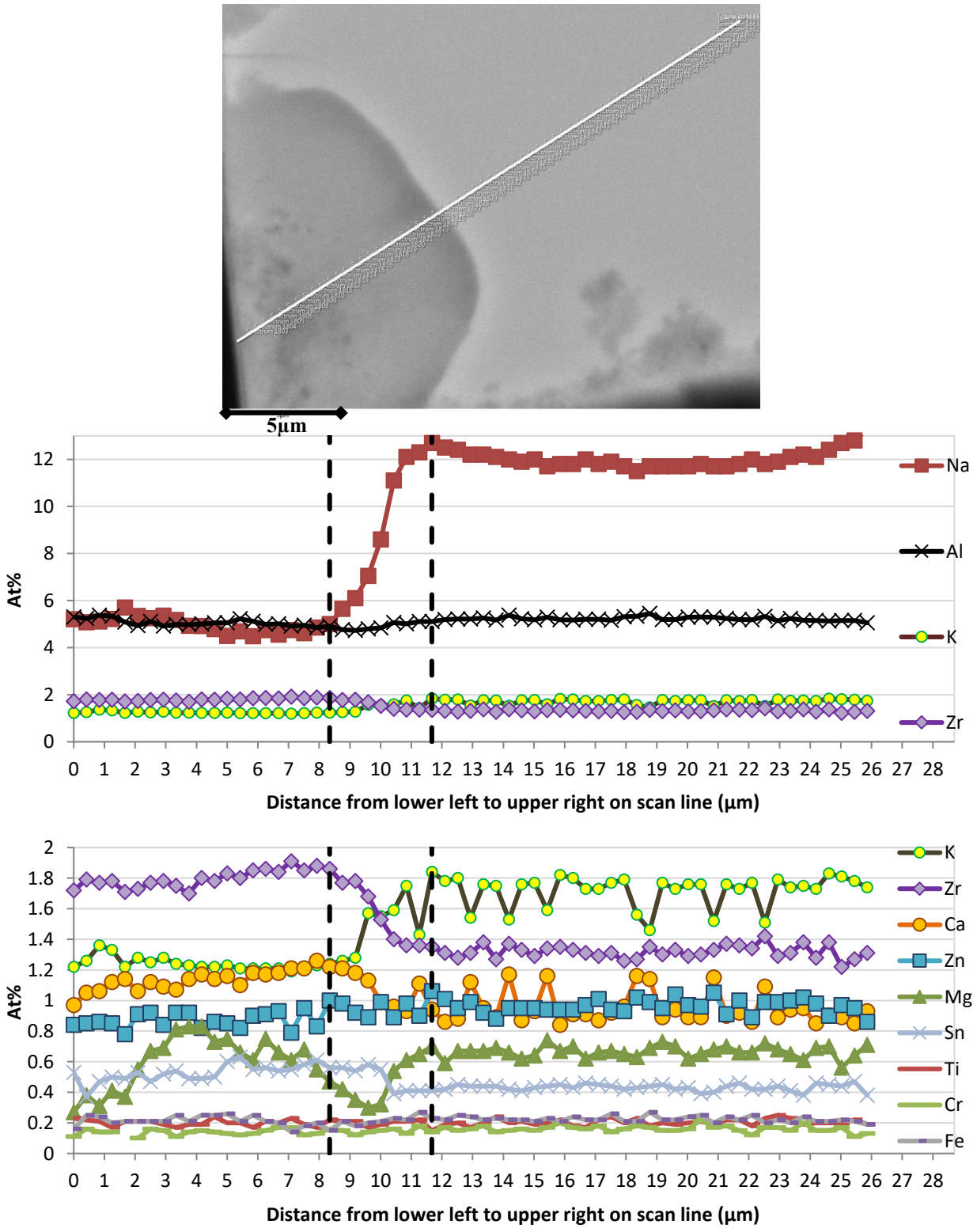

Figure 4.11. SEM micrographs and plot of EDS analyses (at two y-axis scales) from surface to core of altered IDF Phase 3 glass IDF24-EC28 subjected to PCT for two years at 90 °C and S/V of 20,000 m^{-1}.

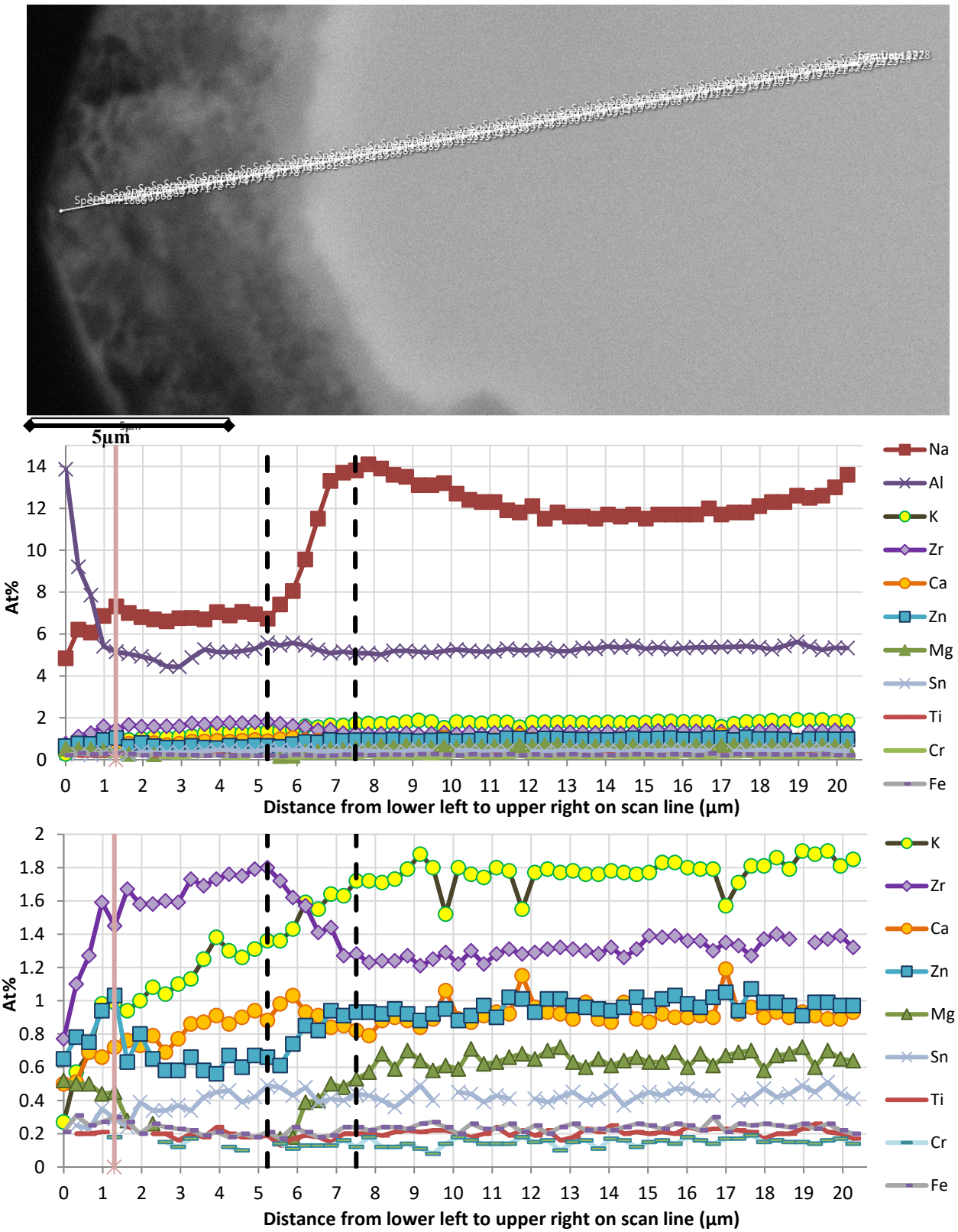

Figure 4.12. SEM micrograph and plots of EDS analyses (at two y-axis scales) from surface to core of a second, less-altered site from IDF Phase 3 glass IDF24-EC28 subjected to PCT for two years at 90 °C and S/V of 20,000 m^{-1}.

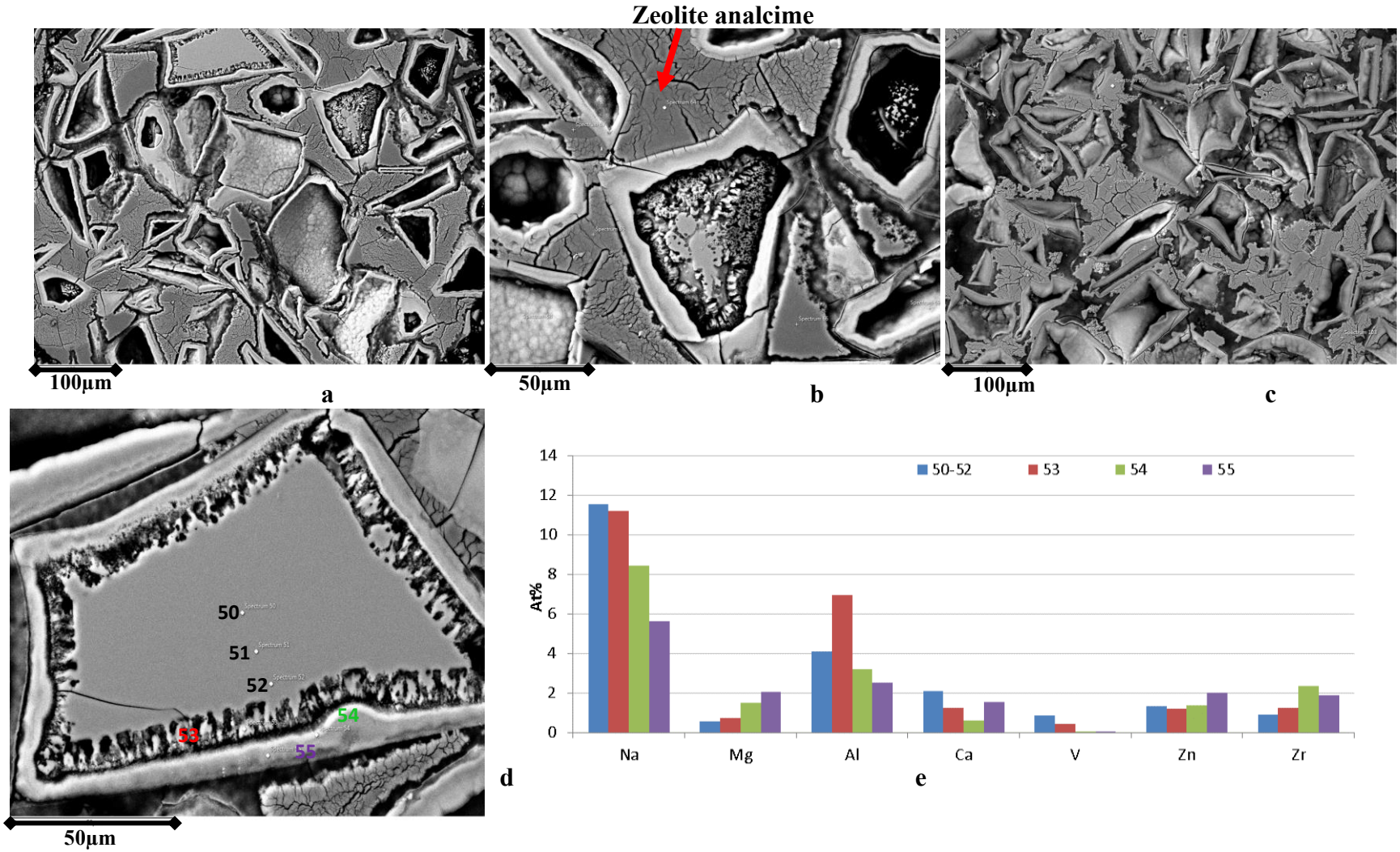

Figure 4.13. SEM micrographs of cross-section (a-d) and EDS analyses of altered IDF Phase 3 glass IDF25-EC34 subjected to PCT for 651 days at 90 °C and S/V of 20,000 m^{-1}. Resumption was at ~120 days and normalized boron release rose sharply to 600 g/L (~60% reacted glass). EDS analyses shown in the bar graph (e) compares the compositions of the phases shown in (d).

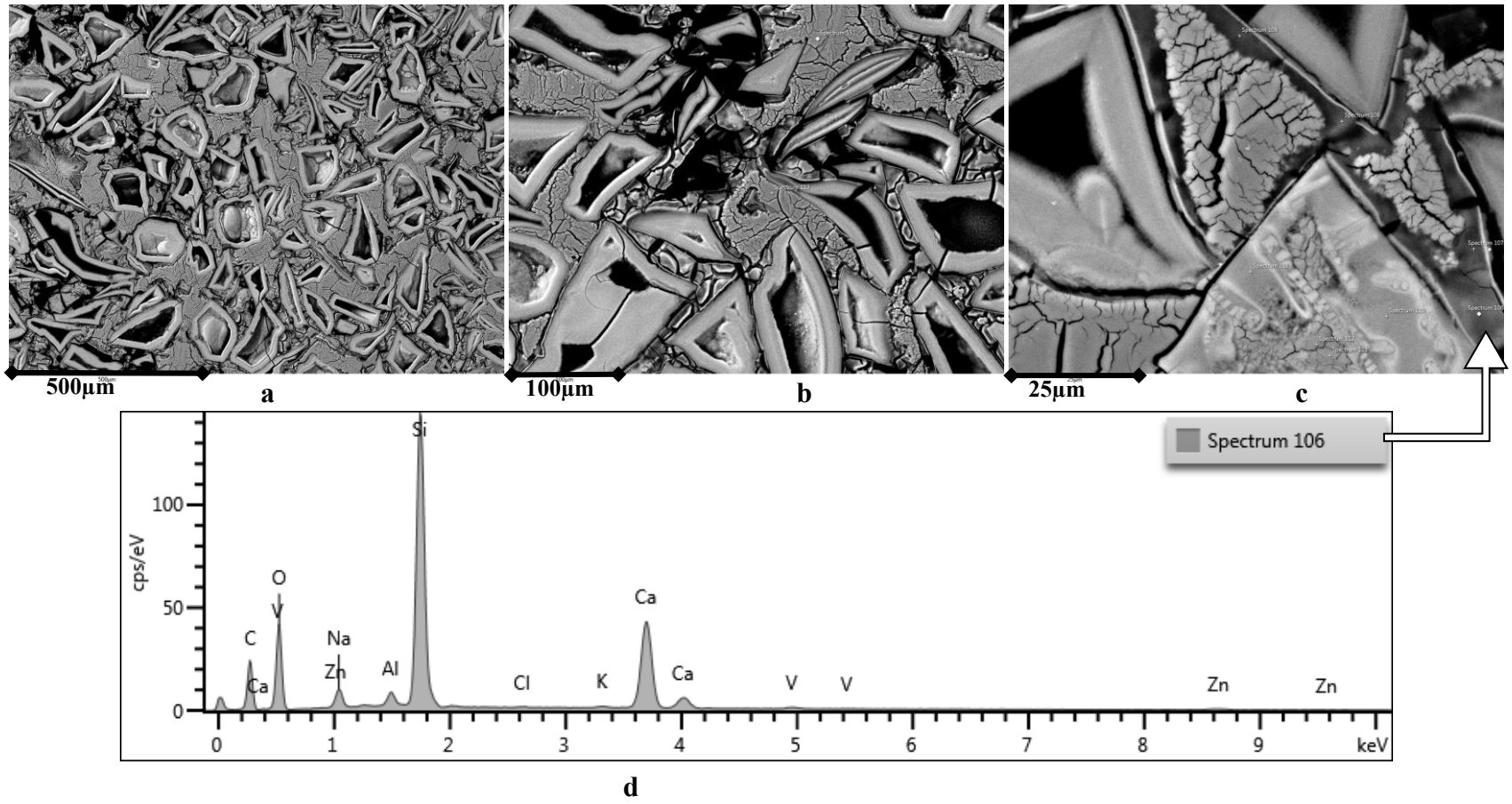

Figure 4.14. SEM micrographs of cross-section (a-c) and EDS spectrum of C-S-H in altered IDF Phase 3 glass IDF26-EC44 subjected to PCT for 651 days at 90 °C and S/V of 20,000 m^{-1}. Resumption was at ~120 days and normalized boron release rose sharply to 600 g/L.

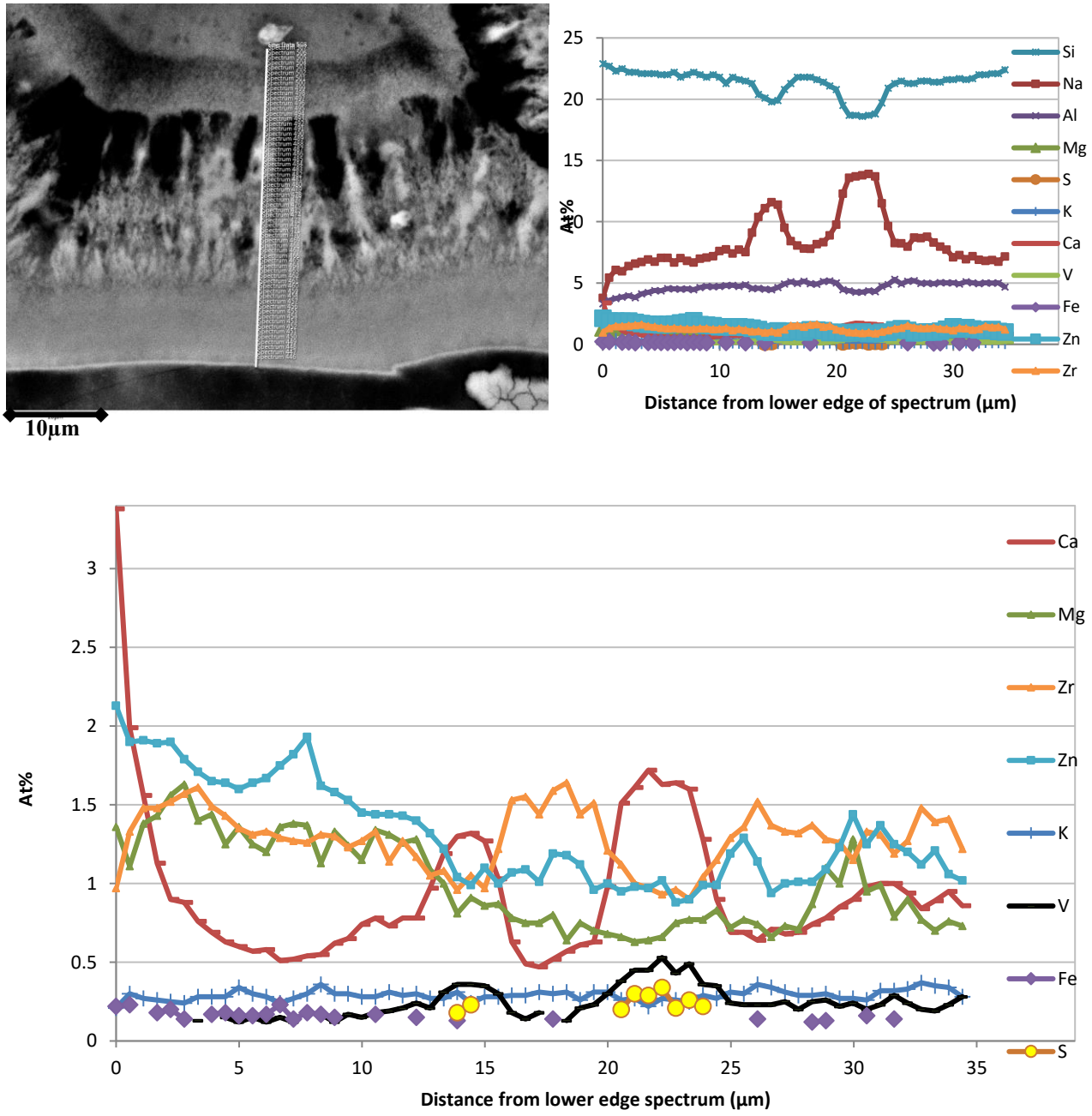

Figure 4.15. SEM micrograph and plots of EDS analyses (at two y-axis scales) from lower edge to core of altered IDF Phase 3 glass IDF26-EC44 subjected to PCT for 651 days at 90 °C and S/V of 20,000 m^{-1}.

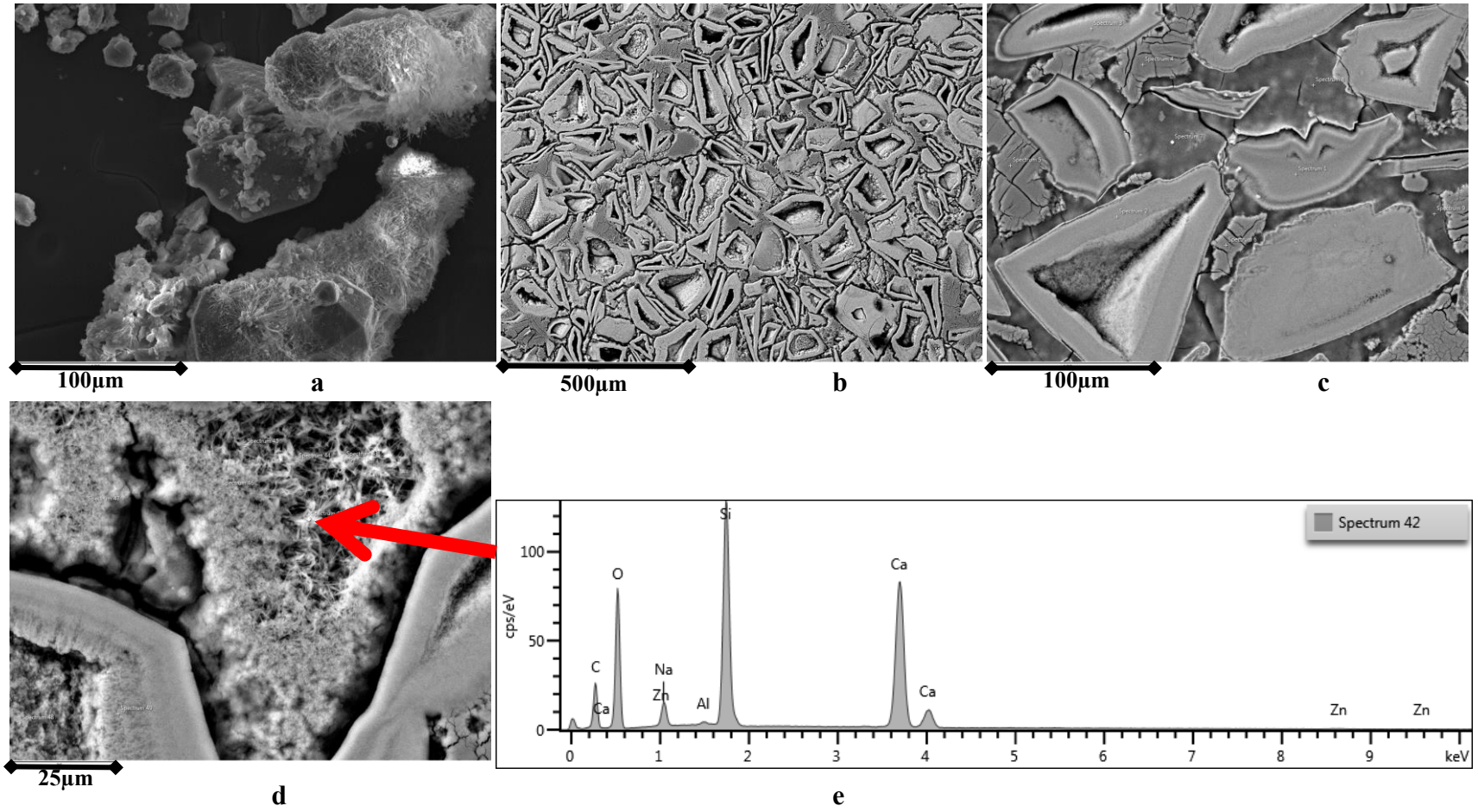

Figure 4.16. SEM micrographs from the surface of loose powder collected from the vessel wall (a) and cross-section of the core-drilled solid (b-d) taken from altered IDF Phase 3 glass IDF22-EC46 subjected to PCT for 651 days at 90 °C and S/V of 20,000 m^{-1}. The EDS spectrum (e) is from the interstitial phase shown in (d). Resumption was at ~120 days and normalized boron release rose sharply to 600 g/L.

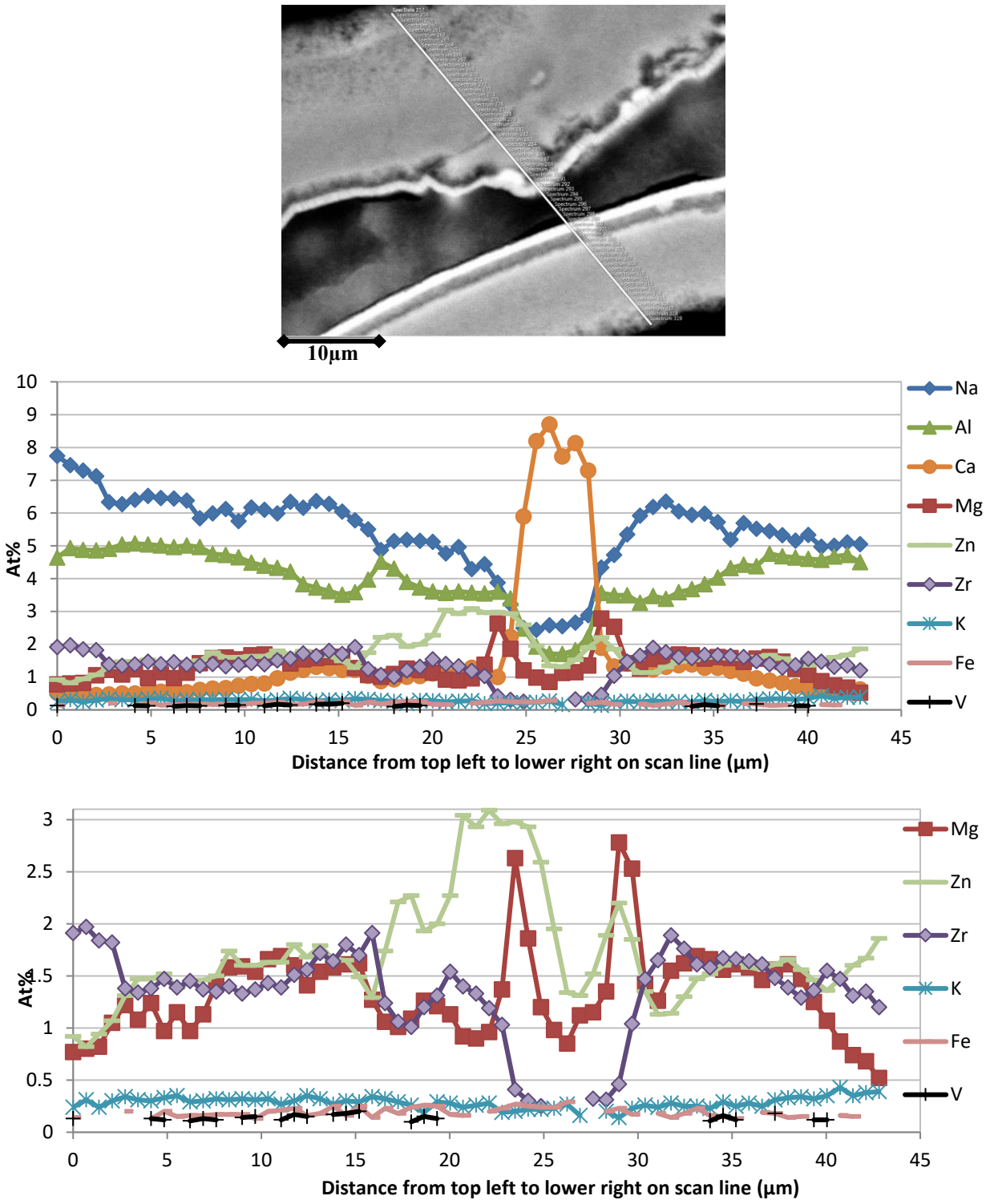

Figure 4.17. SEM micrograph and plots of EDS analyses (at two y-axis scales) from lower edge to core of altered IDF Phase 3 glass IDF22-EC46 subjected to PCT for 651 days at 90 °C and S/V of 20,000 m^{-1}. Not shown in the EDS spectra are Si and O, which show little variation across and in between the two grains (Si at 22.6 ±0.5 and O at 61.6 ±0.3 at %, respectively).

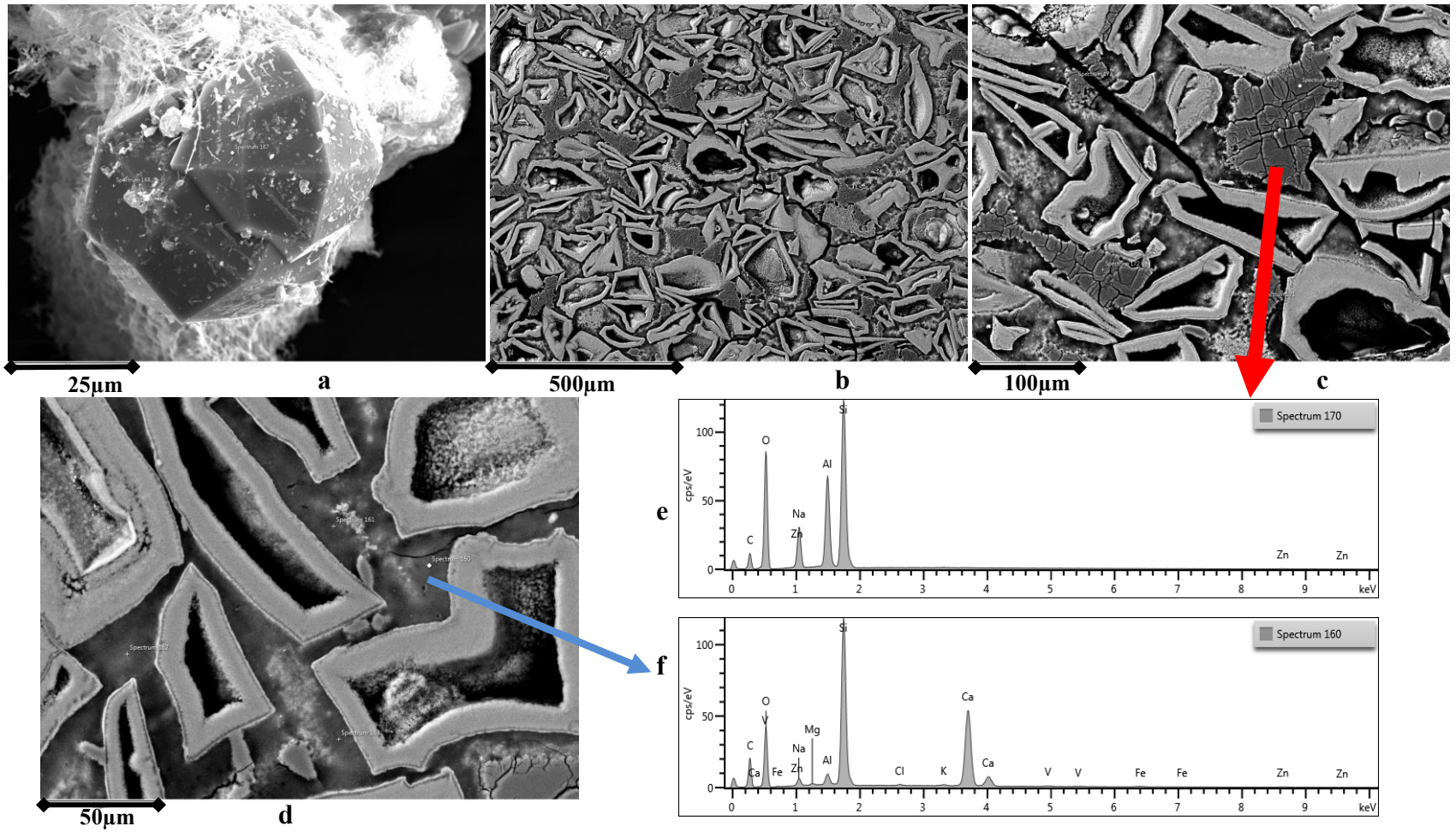

Figure 4.18. SEM micrographs from the surface of loose powder collected from the vessel wall (a) and cross-section of the core-drilled solid (b-d) taken from altered IDF Phase 3 glass IDF27-EC48 subjected to PCT for 651 days at 90 °C and S/V of 20,000 m^{-1}. The EDS spectra (e and f) are of the interstitial phases shown in (c) and (d), corresponding to analcime (e) and calcium silicate hydrate (f). Resumption was at ~120 days and normalized boron release rose sharply to 600 g/L.

Appendix A1. Percent Relative Standard Deviation of Triplicates in Long-Term PCT-B Results at 90 °C and S/V of 20,000 m^{-1} (Tests ILHC and ILHD).

Glass ID	Test	Immersion Date	Sampling Date	Period	%RSD measured on triplicate PCT results					
					pH	B	K	Li	Na	Si
IDF11-G27CCC	ILHC	6/9/2015	6/16/2015	7	0.1%	0.7%	1.2%	-	1.9%	0.9%
			7/7/2015	28	0.1%	0.4%	0.2%	-	2.4%	0.1%
			8/4/2015	56	0.1%	0.9%	0.6%	-	0.4%	0.6%
			10/6/2015	119	0.1%	0.9%	0.5%	-	0.8%	0.4%
			12/8/2015	182	0.1%	0.8%	0.2%	-	1.2%	0.1%
			3/8/2016	273	0.1%	0.9%	0.7%	-	1.3%	0.4%
			6/7/2016	364	0.1%	1.0%	0.6%	-	3.2%	0.6%
			12/8/2016	548	0.2%	2.2%	2.3%	-	0.7%	1.4%
			6/8/2017	730	0.1%	1.4%	0.4%	-	1.0%	2.1%
			12/8/2017	913	0.2%	2.1%	2.1%	-	0.7%	1.0%
			2/13/2019	1345	0.1%	2.5%	2.2%	-	2.8%	1.0%
			5/28/2019	1449	0.1%	0.5%	0.3%	-	5.1%	1.2%
			5/27/2020	1814	2.4%	1.1%	1.6%	-	0.8%	10%
IDF12-A38CCC	ILHC	6/9/2015	6/16/2015	7	0.1%	0.2%	0.4%	-	0.8%	0.3%
			7/7/2015	28	0.1%	0.4%	1.3%	-	0.9%	0.4%
			8/4/2015	56	0.1%	0.3%	1.2%	-	0.6%	0.3%
			10/6/2015	119	0.1%	0.6%	1.2%	-	0.4%	0.7%
			12/8/2015	182	0.1%	0.3%	2.3%	-	0.5%	0.2%
			3/8/2016	273	0.1%	0.5%	1.0%	-	1.3%	0.5%
			6/7/2016	364	0.1%	2.9%	2.2%	-	4.5%	2.3%
			12/8/2016	548	0.2%	1.4%	0.4%	-	0.7%	2.0%
			6/8/2017	730	0.2%	4.4%	0.8%	-	0.3%	1.7%
			12/8/2017	913	0.2%	1.0%	0.2%	-	4.1%	1.4%
			5/31/2018	1087	0.1%	0.3%	0.1%	-	3.6%	0.6%
			2/13/2019	1345	0.1%	1.7%	1.4%	-	3.7%	1.5%
			5/28/2019	1449	0.1%	2.3%	16.5%	-	1.0%	1.4%
			5/27/2020	1814	1.6%	61%	46%	-	49%	29%
IDF13-A51CCC	ILHC	6/9/2015	6/16/2015	7	0.1%	0.4%	0.4%	-	0.7%	0.8%
			7/7/2015	28	0.2%	0.3%	1.7%	-	0.4%	0.4%
			8/4/2015	56	0.2%	0.9%	1.5%	-	1.5%	0.3%
			10/6/2015	119	0.1%	0.6%	0.4%	-	1.6%	0.5%
			12/8/2015	182	0.2%	0.5%	0.9%	-	0.7%	0.6%
			3/8/2016	273	0.1%	0.5%	1.1%	-	1.3%	0.4%
			6/7/2016	364	0.2%	2.1%	2.3%	-	4.1%	1.1%
			12/8/2016	548	0.2%	2.7%	1.3%	-	1.4%	4.0%
			6/8/2017	730	0.1%	0.8%	0.4%	-	2.5%	1.2%
			12/8/2017	913	0.1%	0.5%	0.3%	-	0.6%	1.4%
			2/13/2019	1345	0.1%	2.0%	1.4%	-	2.1%	2.0%
			5/28/2019	1449	0.1%	2.3%	1.2%	-	1.0%	3.3%
IDF14-A59CCC	ILHC	6/9/2015	6/16/2015	7	0.1%	1.1%	1.2%	-	0.3%	0.5%
			7/7/2015	28	0.1%	0.6%	0.7%	-	0.3%	0.6%
			8/4/2015	56	0.1%	0.6%	1.7%	-	1.3%	0.7%
			10/6/2015	119	0.1%	0.4%	1.9%	-	1.5%	0.6%
			12/8/2015	182	0.2%	0.6%	1.1%	-	0.9%	0.9%
			3/8/2016	273	0.1%	5.1%	2.6%	-	4.7%	2.2%
			6/7/2016	364	0.1%	2.7%	2.2%	-	1.6%	2.3%
			12/8/2016[$]	548[$]	0.2%	0.2%	1.2%	-	0.8%	2.0%
			6/8/2017	730	0.1%	0.7%	1.6%	-	0.1%	0.8%
			12/8/2017	913	0.1%	1.7%	0.7%	-	1.3%	0.9%
			5/31/2018	Solid sampling and terminated						

- Release below detection limit as glass does not contain lithium.

Appendix A1. Percent Relative Standard Deviation of Triplicates in Long-Term PCT-B Results at 90 °C and S/V of 20,000 m^{-1} (Tests ILHC and ILHD) (continued).

Glass ID	Test	Immersion Date	Sampling Date	Period	%RSD measured on triplicate PCT results					
					pH	B	K	Li	Na	Si
IDF15-A57CCC	ILHC	6/9/2015	6/16/2015	7	0.1%	0.3%	0.3%	-	0.6%	0.7%
			7/7/2015	28	0.1%	0.6%	2.3%	-	1.7%	0.4%
			8/4/2015	56	0.1%	0.8%	0.8%	-	1.0%	0.4%
			10/6/2015	119	0.1%	1.4%	0.4%	-	0.3%	0.7%
			12/8/2015	182	0.2%	0.5%	0.4%	-	1.3%	0.7%
			3/8/2016	273	0.1%	0.8%	2.8%	-	2.9%	2.0%
			6/7/2016	364	0.1%	2.5%	3.4%	-	0.5%	3.2%
			12/8/2016	548	0.2%	2.2%	0.4%	-	3.2%	2.1%
			6/8/2017	730	0.1%	1.2%	0.9%	-	0.6%	0.6%
			12/8/2017	913	0.1%	0.7%	0.8%	-	1.6%	2.4%
			5/31/2018	1087	0.1%	0.6%	1.7%	-	1.6%	0.9%
			2/13/2019	1345	0.1%	0.4%	0.5%	-	1.1%	0.3%
			5/28/2019	1449	0.1%	1.1%	3.3%	-	2.1%	0.7%
			5/27/2020	1814	0.8%	2.5%	5.8%	-	7.4%	3.0%
IDF16-A58CCC	ILHD	6/10/2015	6/17/2015	7	0.1%	0.7%	1.2%	-	0.2%	0.2%
			7/8/2015	28	0.1%	0.4%	0.5%	-	1.6%	0.1%
			8/5/2015	56	0.1%	0.7%	0.8%	-	1.3%	0.5%
			10/7/2015	119	0.1%	0.5%	0.4%	-	1.1%	0.2%
			12/9/2015	182	0.1%	1.1%	1.3%	-	1.2%	1.1%
			3/9/2016	273	0.1%	0.8%	1.6%	-	1.7%	1.1%
			6/9/2016	365	0.2%	1.1%	3.5%	-	2.1%	1.7%
			12/8/2016	547	0.2%	0.3%	4.6%	-	1.3%	0.4%
			6/9/2017	730	0.1%	0.7%	2.0%	-	1.0%	0.2%
			12/11/2017	915	0.2%	0.7%	0.7%	-	2.1%	0.7%
			2/14/2019	1345	0.1%	2.3%	2.3%	-	2.2%	3.6%
			5/29/2019	1449	0.1%	1.1%	0.7%	-	9.3%	2.3%
			5/27/2020	1813	2.8%	16.4%	9.1%	-	14.7%	17.1%
IDF17-A60CCC	ILHD	6/10/2015	6/17/2015	7	0.1%	0.5%	0.9%	-	0.5%	0.1%
			7/8/2015	28	0.1%	0.4%	0.7%	-	0.5%	0.1%
			8/5/2015	56	0.1%	0.4%	1.1%	-	0.5%	0.3%
			10/7/2015	119	0.1%	0.1%	0.6%	-	0.3%	0.1%
			12/9/2015	182	0.2%	1.3%	1.0%	-	1.3%	0.5%
			3/9/2016	273	0.1%	0.2%	0.8%	-	1.5%	0.8%
			6/9/2016	365	0.2%	0.7%	1.2%	-	1.8%	1.9%
			12/8/2016	547	0.1%	1.2%	0.5%	-	0.9%	0.7%
			6/9/2017	730	0.1%	0.4%	0.9%	-	0.3%	1.0%
			12/11/2017	915	0.1%	0.8%	0.3%	-	0.6%	2.5%
			5/31/2018	1086	0.1%	1.9%	1.0%	-	0.4%	1.3%
			2/14/2019	1345	0.1%	0.2%	1.0%	-	0.7%	1.5%
			5/29/2019	1449	0.1%	1.4%	1.2%	-	6.0%	1.4%
			5/27/2020	1813	0.3%	21.0%	23.6%	-	16.8%	5.0%
IDF18-A161CCC	ILHD	6/10/2015	6/17/2015	7	0.1%	0.4%	0.9%	-	0.5%	0.3%
			7/8/2015	28	0.1%	0.3%	1.7%	-	1.6%	0.3%
			8/5/2015	56	0.1%	0.3%	1.0%	-	0.2%	0.3%
			10/7/2015	119	0.1%	0.0%	0.7%	-	1.4%	1.9%
			12/9/2015	182	0.2%	0.8%	0.2%	-	5.8%	0.6%
			3/9/2016	273	0.1%	1.4%	0.1%	-	1.0%	0.3%
			6/9/2016	365	0.2%	3.7%	0.9%	-	2.9%	0.2%
			12/8/2016	547	0.2%	2.8%	3.6%	-	1.5%	0.5%
			6/9/2017	730	0.1%	1.0%	1.8%	-	1.0%	0.4%
			12/11/2017	915	0.2%	1.9%	0.5%	-	1.8%	0.1%
			2/14/2019	1345	0.1%	0.8%	4.7%	-	0.2%	1.8%
			5/29/2019	1449	0.1%	1.9%	1.0%	-	3.0%	1.6%

- Release below detection limit as glass does not contain lithium.

Appendix A1. Percent Relative Standard Deviation of Triplicates in Long-Term PCT-B Results at 90 °C and S/V of 20,000 m^{-1} (Tests ILHC and ILHD) (continued).

Glass ID	Test	Immersion Date	Sampling Date	Period	%RSD measured on triplicate PCT results					
					pH	B	K	Li	Na	Si
IDF19-C100CCC	ILHD	6/10/2015	6/17/2015	7	0.1%	0.3%	0.8%	-	0.4%	0.5%
			7/8/2015	28	0.1%	0.0%	1.6%	-	0.6%	0.1%
			8/5/2015	56	0.2%	0.2%	1.4%	-	1.1%	0.8%
			10/7/2015	119	0.1%	0.2%	1.2%	-	0.4%	0.4%
			12/9/2015	182	0.2%	0.8%	0.4%	-	0.6%	0.7%
			3/9/2016	273	0.1%	0.6%	1.3%	-	0.4%	0.1%
			6/9/2016	365	0.2%	0.8%	0.3%	-	0.5%	0.9%
			12/8/2016	547	0.1%	2.1%	0.8%	-	1.4%	0.7%
			6/9/2017	730	0.1%	1.3%	0.5%	-	2.1%	0.3%
			12/11/2017	915	0.2%	2.7%	0.4%	-	1.4%	0.3%
			2/14/2019	1345	0.1%	1.4%	0.7%	-	1.3%	0.8%
			5/29/2019	1449	0.1%	1.1%	1.9%	-	7.0%	0.4%
IDF20-F6CCC	ILHD	6/10/2015	6/17/2015	7	0.1%	0.5%	1.0%	0.6%	0.5%	0.3%
			7/8/2015	28	0.2%	0.5%	1.0%	0.7%	0.5%	0.5%
			8/5/2015	56	0.2%	0.7%	0.7%	0.5%	0.2%	0.4%
			10/7/2015	119	0.1%	0.6%	2.0%	1.0%	0.5%	0.5%
			12/9/2015	182	0.1%	1.2%	2.6%	0.8%	0.3%	0.9%
			3/9/2016	273	0.1%	2.6%	2.0%	1.3%	4.2%	1.6%
			6/9/2016	365	0.2%	1.7%	2.9%	3.5%	1.7%	1.2%
			12/8/2016	547	0.1%	3.4%	0.9%	1.1%	2.9%	0.2%
			6/9/2017	730	0.1%	0.8%	0.6%	0.5%	1.7%	1.8%
			12/11/2017	915	0.1%	2.4%	1.0%	0.8%	1.1%	0.9%
			5/31/2018	1086	0.1%	0.7%	1.7%	0.8%	1.5%	0.1%
			2/14/2019	1345	0.1%	0.7%	0.8%	0.8%	0.9%	0.5%
			5/29/2019	1449	0.1%	1.6%	0.8%	0.5%	4.2%	0.1%
ANL-LRM-2	ILHC	6/9/2015	6/16/2015	7	0.1%	0.5%	0.3%	-	0.8%	0.4%
			7/7/2015	28	0.1%	0.3%	0.5%	-	1.4%	0.2%
			8/4/2015	56	0.1%	0.6%	1.6%	-	0.5%	0.2%
			10/6/2015	119	0.1%	1.2%	0.7%	2.8%	0.6%	1.4%
			12/8/2015	182	0.2%	1.6%	0.5%	1.5%	0.8%	0.9%
			3/8/2016	273	0.1%	1.2%	0.4%	1.4%	2.6%	0.7%
			6/7/2016	364	0.1%	3.0%	2.3%	4.8%	2.9%	2.4%
			12/8/2016[$]	548	0.2%	2.6%	1.9%	0.4%	4.1%	1.7%
			6/8/2017	730	0.1%	0.4%	1.0%	0.3%	0.3%	1.0%
			Test terminated							
ANL-LRM-2	ILHD	6/10/2015	6/17/2015	7	0.1%	0.2%	1.1%	-	0.3%	0.1%
			7/8/2015	28	0.2%	0.4%	1.4%	-	0.8%	0.2%
			8/5/2015	56	0.1%	0.5%	0.6%	-	0.5%	0.1%
			10/7/2015	119	0.1%	0.5%	0.5%	1.7%	1.2%	0.1%
			12/9/2015	182	0.1%	0.6%	0.2%	0.8%	0.5%	0.1%
			3/9/2016	273	0.1%	0.8%	0.3%	1.4%	1.5%	0.1%
			6/9/2016	365	0.2%	2.2%	2.9%	2.3%	1.8%	0.2%
			12/8/2016[$]	547	0.2%	0.8%	0.5%	0.8%	4.1%	0.2%
			6/9/2017	730	0.1%	1.9%	1.7%	2.2%	2.0%	0.1%
			Test terminated							

- Below detection limit; *Normalized release calculated from average of triplicate tests with less than 10% RSD (median 0.6%RSD); [#] Measured at room temperature; [$]Altered glass removed from one of the triplicate vessels

Appendix A2. Percent Relative Standard Deviation of Triplicates in Long-Term PCT-B Results at 90 °C and Various S/V (Tests ILHE, ILHF, and ILHG).

Glass ID	Sample ID	Test	S/V (m^{-1})	Immersion Date	Sampling Date	Period	%RSD measured on triplicate PCT results					
							pH	B	K	Li	Na	Si
IDF22 EC46CCC	22EC46	ILHE	20000	6/4/2018	6/11/2018	7	0.5%	1.3%	4.5%	0.0%	3.9%	1.4%
					7/2/2018	28	0.2%	2.4%	0.9%	1.5%	2.1%	3.8%
					7/30/2018	56	0.3%	1.8%	2.9%	1.4%	0.4%	1.7%
					11/30/2018	179	0.3%	16.8%	13.9%	4.3%	13.6%	9.9%
					3/1/2019	270	0.3%	3.6%	5.0%	3.4%	2.5%	6.4%
					6/4/2019	365	0.2%	0.3%	6.1%	0.0%	4.5%	7.1%
					9/18/2019	471	0.1%	2.7%	1.1%	0.4%	1.1%	1.4%
					12/10/2019	554	0.1%	0.1%	0.3%	2.5%	1.2%	1.7%
					3/16/2020	651	0.4%	0.5%	0.2%	2.4%	1.4%	1.2%
IDF25 EC34CCC	25EC34				6/11/2018	7	0.3%	3.6%	10.7%	-	3.2%	1.8%
					7/2/2018	28	0.2%	0.5%	2.3%	-	0.7%	2.2%
					7/30/2018	56	0.1%	1.5%	2.7%	-	2.6%	0.7%
					11/30/2018	179*	0.0%	7.6%	10.9%	-	7.5%	2.3%
					3/1/2019	270	0.2%	10.9%	8.8%	-	7.8%	13.2%
					6/4/2019	365	0.1%	2.6%	9.2%	-	13.2%	6.5%
					9/18/2019	471	0.4%	3.3%	0.9%	-	1.1%	1.6%
					12/10/2019	554	0.1%	2.1%	4.2%	-	0.9%	1.3%
					3/16/2020	651	0.5%	1.5%	3.2%	-	0.5%	0.8%
IDF26 EC44CCC	26EC44				6/11/2018	7	0.3%	2.3%	3.2%	2.5%	1.7%	3.1%
					7/2/2018	28	0.3%	2.7%	2.3%	2.9%	0.8%	1.2%
					7/30/2018	56	0.0%	1.8%	2.8%	3.6%	1.0%	2.5%
					11/30/2018	179*	0.0%	63.9%	62.7%	46.8%	61.9%	0.0%
					3/1/2019	270	0.1%	1.5%	1.0%	2.9%	2.0%	2.5%
					6/4/2019	365	0.2%	3.3%	4.2%	0.0%	5.1%	1.5%
					9/18/2019	471	0.1%	1.1%	1.9%	2.3%	1.4%	1.5%
					12/10/2019	554	0.2%	2.6%	3.9%	2.4%	6.1%	4.8%
					3/16/2020	651	0.1%	2.3%	0.5%	1.4%	5.2%	6.4%

*Triplicates are not in agreement – a manual average is estimated and used in the report.

Appendix A2. Percent Relative Standard Deviation of Triplicates in Long-Term PCT-B Results at 90 °C and Various S/V (Tests ILHE, ILHF, and ILHG) (continued).

Glass ID	Sample ID	Test	S/V (m^{-1})	Immersion Date	Sampling Date	Period	%RSD measured on triplicate PCT results					
							pH	B	K	Li	Na	Si
IDF27 EC48CCC	27EC48	ILHE	20000	6/4/2018	6/11/2018	7	0.2%	1.1%	0.6%	1.1%	1.2%	1.1%
					7/2/2018	28	0.3%	0.5%	3.2%	1.1%	2.7%	1.7%
					7/30/2018	56	0.1%	0.4%	1.3%	0.4%	0.5%	0.1%
					10/2/2018	120	0.2%	11.8%	5.1%	7.4%	5.2%	5.4%
					11/30/2018	179				4.7%		
					3/1/2019	270	0.1%	6.4%	7.1%	5.1%	6.5%	4.6%
					6/4/2019	365	0.2%	2.0%	1.2%	0.0%	9.3%	2.1%
					9/18/2019	471	0.3%	2.1%	0.6%	0.4%	0.5%	0.8%
					12/10/2019	554	0.1%	2.7%	2.5%	2.9%	1.0%	6.0%
					3/16/2020	651	0.1%	2.7%	1.0%	2.4%	1.3%	3.4%
IDF28 EC50CCC	28EC50				6/11/2018	7	0.2%	11.7%	13.6%	-	12.3%	6.4%
					7/2/2018	28	0.2%	1.5%	5.0%	-	5.0%	3.6%
					7/30/2018	56	0.3%	3.4%	3.4%	-	2.8%	1.0%
					10/2/2018	120	0.1%	1.7%	1.7%	-	1.9%	0.4%
					11/30/2018	179	0.1%	1.7%	0.1%	-	0.5%	11.6%
					3/1/2019	270	0.1%	1.4%	1.5%	-	1.1%	0.2%
					6/4/2019	365	0.2%	3.1%	7.1%	-	6.2%	0.8%
					9/18/2019	471	0.0%	1.9%	3.8%	-	1.8%	0.7%
					12/10/2019	554	0.1%	4.3%	8.9%	-	1.4%	2.4%
					3/16/2020	651	0.5%	14.2%	16.1%	-	9.6%	8.3%
					6/15/2020	742	0.1%	16.5%	14.9%	-	14.2%	7.9%

- Release below detection limit as glass does not contain lithium.

Appendix A2. Percent Relative Standard Deviation of Triplicates in Long-Term PCT-B Results at 90 °C and Various S/V (Tests ILHE, ILHF, and ILHG) (continued).

Glass ID	Sample ID	Test	S/V (m^{-1})	Immersion Date	Sampling Date	Period	%RSD measured on triplicate PCT results				
							pH	B	K	Na	Si
IDF23 EC52CCC	1K23 EC52	ILHF	1000	6/5/2018	6/12/2018	7	0.6%	6.3%	-	5.4%	1.3%
					7/3/2018	28	1.0%	4.2%	2.3%	2.8%	1.7%
					7/31/2018	56	4.0%	0.8%	2.9%	0.3%	0.6%
					10/3/2018	120	0.5%	0.6%	2.0%	2.1%	1.3%
					12/3/2018	181	0.4%	1.1%	0.9%	0.8%	1.2%
					3/4/2019	272	0.3%	1.1%	1.6%	0.6%	0.1%
					6/5/2019	365	0.8%	1.8%	2.6%	2.7%	2.5%
					9/19/2019	471	0.3%	3.0%	1.9%	1.9%	3.9%
					12/12/2019	555	0.9%	3.2%	7.3%	1.5%	0.5%
					3/17/2020	651	0.1%	1.1%	2.5%	2.2%	1.4%
					6/17/2020	743	0.4%	1.5%	3.1%	0.3%	2.2%
	2K23 EC52		2000		6/12/2018	7	0.4%	6.3%	15.7%	3.9%	4.4%
					7/3/2018	28	0.2%	2.1%	2.8%	1.1%	1.5%
					7/31/2018	56	0.5%	1.3%	4.1%	1.0%	1.5%
					10/3/2018	120	0.2%	0.5%	1.8%	0.3%	0.7%
					12/3/2018	181	0.2%	0.9%	1.4%	0.4%	0.7%
					3/4/2019	272	0.1%	0.1%	1.3%	1.2%	0.7%
					6/5/2019	365	0.3%	2.2%	2.0%	3.5%	1.4%
					9/19/2019	471	0.3%	0.1%	2.2%	0.9%	0.4%
					12/12/2019	555	0.2%	3.9%	7.9%	2.8%	2.2%
					3/17/2020	651	0.1%	2.2%	2.6%	1.3%	0.8%
					6/17/2020	743	0.3%	1.6%	4.0%	1.3%	1.3%
	5K23 EC52		5000		6/12/2018	7	0.6%	5.7%	3.9%	4.6%	3.1%
					7/3/2018	28	0.2%	1.3%	4.1%	1.3%	0.2%
					7/31/2018	56	0.2%	0.8%	2.2%	1.9%	0.7%
					10/3/2018	120	0.1%	1.8%	1.1%	1.0%	1.0%
					12/3/2018	181	0.1%	0.8%	1.1%	0.2%	1.1%
					3/4/2019	272	0.3%	1.1%	1.1%	0.3%	1.4%
					6/5/2019	365	0.2%	1.6%	4.0%	4.2%	2.2%
					9/19/2019	471	0.1%	2.4%	1.0%	4.7%	0.9%
					12/12/2019	555	0.1%	3.1%	4.4%	0.9%	3.0%
					3/17/2020	651	0.2%	2.0%	2.6%	0.4%	1.9%
					6/17/2020	743	0.2%	1.6%	0.5%	1.5%	1.3%
	10K23 EC52		10000		6/12/2018	7	0.4%	6.6%	4.9%	7.2%	3.4%
					7/3/2018	28	0.1%	1.9%	2.6%	0.9%	1.8%
					7/31/2018	56	0.2%	0.5%	1.1%	2.2%	2.5%
					10/3/2018	120	0.1%	2.7%	6.4%	3.2%	1.4%
					12/3/2018	181	0.1%	1.7%	2.0%	2.3%	1.4%
					3/4/2019	272	0.2%	1.7%	1.8%	3.5%	2.7%
					6/5/2019	365	0.6%	9.5%	0.6%	4.1%	0.9%
					9/19/2019	471	0.2%	7.0%	2.8%	5.9%	8.9%
					12/12/2019	555	0.2%	7.6%	6.9%	4.5%	6.5%
					3/17/2020	651	0.2%	2.9%	3.7%	4.7%	3.9%
					6/17/2020	743	0.3%	0.7%	0.6%	1.0%	0.5%
	20K23 EC52		20000		6/12/2018	7	0.3%	0.5%	2.7%	1.6%	0.6%
					7/3/2018	28	0.1%	1.5%	2.0%	4.5%	2.2%
					7/31/2018	56	0.2%	2.4%	2.4%	3.3%	2.5%
					10/3/2018	120	0.2%	4.5%	6.5%	4.5%	0.9%
					12/3/2018	181	0.2%	2.7%	5.2%	2.3%	1.3%
					3/4/2019	272	0.1%	3.4%	1.9%	2.6%	7.4%
					6/5/2019	365	0.1%	8.3%	5.5%	9.1%	5.7%
					9/19/2019	471	0.3%	13.4%	3.3%	13.0%	6.7%
					12/12/2019	555	0.3%	3.6%	19.0%	8.5%	0.7%
					3/17/2020	651	0.1%	2.2%	2.4%	3.1%	0.8%
					6/17/2020	743	0.1%	0.9%	1.6%	2.8%	6.9%

- Empty data field; *Normalized release calculated from average of triplicate tests with less than 10% RSD
[#] Measured at room temperature

Appendix A2. Percent Relative Standard Deviation of Triplicates in Long-Term PCT-B Results at 90 °C and Various S/V (Tests ILHE, ILHF, and ILHG) (continued).

Glass ID	Sample ID	Test	S/V (m^{-1})	Immersion Date	Sampling Date	Period	%RSD measured on triplicate PCT results				
							pH	B	K	Na	Si
IDF24 EC28CCC	1K24 EC28	ILHG	1000	6/5/2018	6/12/2018	7	1.1%	4.2%	7.1%	4.6%	1.1%
					7/3/2018	28	0.2%	2.0%	3.8%	1.8%	2.4%
					7/31/2018	56	1.2%	1.8%	2.7%	0.4%	1.0%
					10/3/2018	120	0.4%	0.8%	1.7%	1.5%	1.2%
					12/4/2018	182	1.5%	1.1%	1.0%	0.6%	1.6%
					3/5/2019	273	0.2%	2.4%	4.1%	1.9%	2.6%
					6/6/2019	366	0.8%	3.1%	3.8%	3.1%	3.8%
					9/20/2019	472	0.2%	1.6%	4.4%	2.2%	1.6%
					12/13/2019	556	0.3%	4.3%	3.6%	2.5%	2.1%
					3/18/2020	652	0.3%	4.9%	3.8%	3.0%	0.9%
					6/18/2020	744	0.3%	2.0%	2.8%	0.2%	1.3%
	2K24 EC28		2000		6/12/2018	7	0.1%	1.2%	2.9%	2.9%	1.2%
					7/3/2018	28	0.1%	0.9%	1.2%	0.7%	0.7%
					7/31/2018	56	0.3%	0.9%	1.9%	0.2%	1.2%
					10/3/2018	120	0.3%	1.2%	2.2%	1.6%	1.9%
					12/4/2018	182	0.2%	0.8%	1.0%	4.8%	0.8%
					3/5/2019	273	0.3%	2.1%	0.8%	0.8%	0.4%
					6/6/2019	366	0.2%	1.9%	2.8%	2.2%	2.0%
					9/20/2019	472	0.2%	2.8%	1.9%	1.9%	1.4%
					12/13/2019	556	0.3%	3.0%	3.2%	0.7%	2.0%
					3/18/2021	652	0.1%	3.0%	2.4%	0.1%	1.1%
					6/18/2020	744	0.1%	1.2%	2.0%	1.4%	1.7%
	5K24 EC28		5000		6/12/2018	7	0.2%	0.5%	2.1%	2.5%	0.5%
					7/3/2018	28	0.2%	1.0%	0.8%	4.0%	0.9%
					7/31/2018	56	0.1%	0.4%	0.4%	0.5%	0.7%
					10/3/2018	120	0.2%	1.3%	2.6%	0.7%	1.2%
					12/4/2018	182	0.1%	1.0%	1.9%	0.6%	1.5%
					3/5/2019	273	0.4%	0.7%	1.0%	0.4%	0.8%
					6/6/2019	366	0.3%	2.5%	3.3%	2.3%	1.9%
					9/20/2019	472	0.2%	1.1%	0.4%	1.4%	1.0%
					12/13/2019	556	0.2%	0.8%	1.6%	0.3%	2.2%
					3/18/2021	652	0.2%	0.3%	0.9%	1.1%	1.6%
					6/18/2020	744	0.2%	0.6%	0.7%	0.4%	0.5%
	10K24 EC28		10000		6/12/2018	7	0.2%	1.6%	2.0%	0.4%	2.7%
					7/3/2018	28	0.2%	2.0%	4.0%	0.4%	2.0%
					7/31/2018	56	0.2%	0.3%	0.7%	0.5%	0.8%
					10/3/2018	120	0.1%	0.1%	1.2%	0.9%	1.0%
					12/4/2018	182	0.1%	0.9%	1.5%	1.8%	1.1%
					3/5/2019	273	0.2%	2.4%	5.1%	3.6%	1.7%
					6/6/2019	366	0.2%	1.7%	0.3%	1.4%	1.2%
					9/20/2019	472	0.3%	2.8%	1.9%	3.8%	3.4%
					12/13/2019	556	0.2%	5.1%	6.6%	5.5%	1.3%
					3/18/2021	652	0.2%	2.3%	2.7%	2.3%	1.7%
					6/18/2020	744	0.1%	5.7%	6.0%	5.1%	4.1%
	20K24 EC28		20000		6/12/2018	7	0.2%	7.1%	6.7%	8.0%	4.2%
					7/3/2018	28	0.1%	0.2%	0.6%	0.9%	0.9%
					7/31/2018	56	0.1%	0.2%	0.9%	1.4%	0.7%
					10/3/2018	120	0.2%	0.6%	4.7%	3.6%	1.8%
					12/4/2018	182	0.2%	0.9%	1.5%	2.2%	0.9%
					3/5/2019	273	0.2%	2.2%	2.6%	3.5%	1.4%
					6/6/2019	366	0.1%	4.8%	1.5%	3.8%	0.8%
					9/20/2019	472	0.3%	6.9%	7.0%	10.5%	4.8%
					12/13/2019	556	0.0%	6.8%	6.2%	2.4%	3.4%
					3/18/2021	652	0.1%	10.4%	6.0%	13.2%	7.2%
					6/18/2020	744	0.2%	2.3%	1.5%	3.0%	2.4%

- Empty data field; *Normalized release calculated from average of triplicate tests with less than 10% RSD.
Measured at room temperature

Appendix A3. Percent Relative Standard Deviation of Triplicates in Long-Term PCT-B Results for Reference Glass ANL-LRM at 90 °C and S/V of 2,000 m^{-1} (Tests ILHE, ILHF, and ILHG).

Glass ID	Test	S/V (m^{-1})	Immersion Date	Sampling Date	Period	%RSD measured on triplicate PCT results					
						pH	B	K	Li	Na	Si
ANL-LRM-2	ILHE	2000	6/4/2018	6/11/2018	7	0.8%	2.4%	5.3%	-	3.2%	2.0%
				7/2/2018	28	0.4%	1.9%	0.6%	1.8%	1.3%	1.1%
				7/30/2018	56	0.1%	0.7%	2.0%	2.0%	0.7%	0.7%
				10/2/2018	120	0.4%	3.3%	4.3%	3.2%	1.1%	2.2%
				11/30/2018	179	0.5%	2.0%	0.6%	3.1%	0.6%	1.0%
				3/1/2019	270	0.1%	0.5%	2.1%	0.4%	0.1%	0.4%
				6/4/2019	365	0.3%	1.2%	1.6%	0.0%	2.2%	4.0%
				9/18/2019	471	0.4%	1.8%	3.0%	4.9%	1.3%	0.6%
				12/10/2019	554	0.2%	0.4%	2.5%	8.1%	1.0%	2.2%
				3/16/2020	651	0.3%	1.4%	2.1%	5.0%	1.3%	2.7%
				6/15/2020	742	0.4%	0.7%	1.2%	5.8%	1.1%	3.8%
	ILHF		6/5/2018	6/12/2018	7	0.4%	2.9%	3.8%	-	2.0%	0.9%
				7/3/2018	28	0.9%	1.5%	2.5%	2.8%	1.6%	0.4%
				7/31/2018	56	1.1%	0.4%	1.4%	1.0%	1.9%	0.9%
				10/3/2018	120	0.4%	2.3%	4.4%	1.6%	1.5%	1.4%
				12/3/2018	181	0.1%	2.9%	1.5%	2.1%	0.8%	2.6%
				3/4/2019	272	0.2%	1.4%	2.9%	3.9%	0.6%	1.2%
				6/5/2019	365	0.6%	0.6%	2.1%	3.3%	2.5%	6.8%
				9/19/2019	471	0.3%	1.0%	0.9%	0.3%	0.9%	1.5%
				12/12/2019	555	0.3%	4.0%	13.8%	10.9%	3.2%	13.0%
				3/17/2020	651	0.4%	3.4%	6.6%	3.2%	2.9%	10.6%
				6/17/2020	743	0.3%	4.4%	10.9%	3.2%	6.1%	9.1%
	ILHG		6/5/2018	6/12/2018	7	3.2%	1.2%	17.3%	-	4.7%	3.8%
				7/3/2018	28	0.5%	1.9%	2.4%	2.8%	2.4%	2.0%
				7/31/2018	56	0.4%	1.3%	0.9%	3.6%	0.9%	0.8%
				10/3/2018	120	0.3%	1.8%	1.9%	3.2%	1.0%	0.2%
				12/4/2018	182	0.2%	2.1%	2.4%	1.9%	1.6%	0.9%
				3/5/2019	273	0.3%	1.6%	2.2%	1.6%	1.6%	1.6%
				6/6/2019	366	0.3%	2.1%	4.3%	1.6%	2.6%	5.4%
				9/20/2019	472	0.8%	1.6%	1.9%	14.7%	0.9%	2.2%
				12/13/2019	556	0.3%	0.3%	5.6%	14.1%	2.0%	2.9%
				3/18/2021	652	0.5%	0.2%	18.6%	17.1%	0.5%	1.5%
				6/18/2020	744	0.3%	1.6%	0.2%	9.3%	0.5%	1.0%

- Release below detection limit.

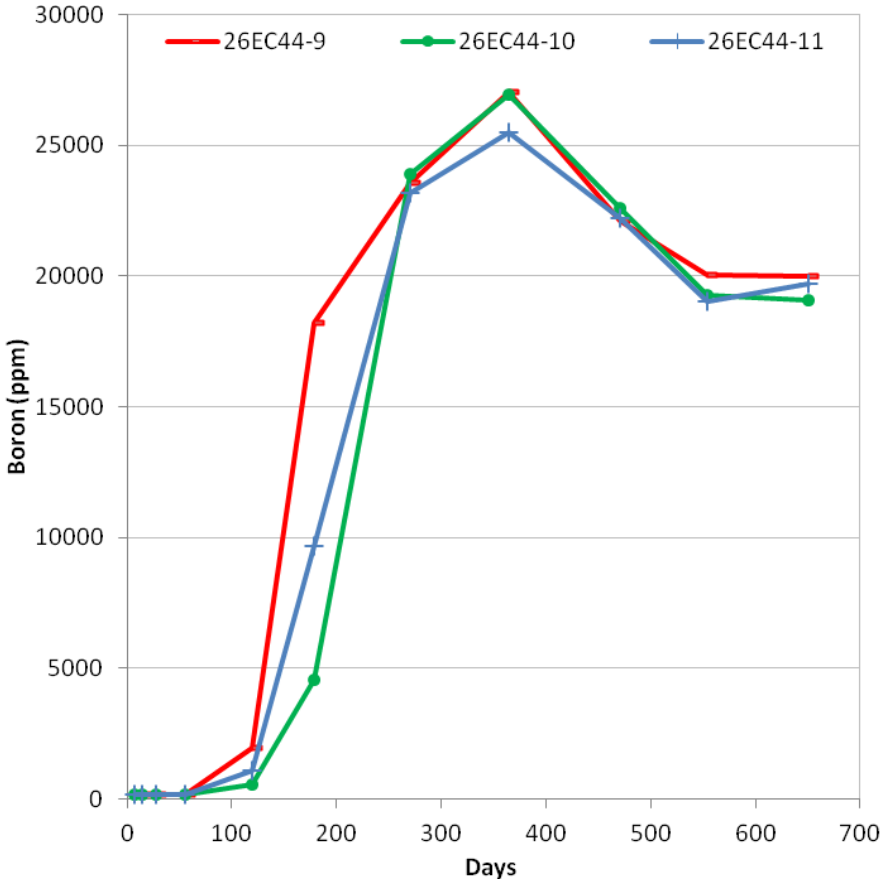

Figure A.1. Example of boron analyses for triplicates during resumption. Data are from test ILHE on IDF26-EC44 for the three vessels 9, 10, and 11.